MASTER THESIS

SPIT QUANTIFICATION AT THE MARKER WADDEN

Niels van Kouwen

18 August 2022

Committee:
Prof. dr. ir. S.G.J. Aarninkhof
Prof. dr. ir. A.J.H.M. Reniers
Ir. A.M. Ton
Ir. T. Vijverberg
Dr. S.E. Vos

TU Delft

Spit quantification
at the Marker Wadden

A case study of the southern and northern spits at the Marker Wadden Islands, Lake Markermeer in the Netherlands

By

Niels Casper van Kouwen

Department of Hydraulic Engineering
Section: Coastal Engineering

In partial fulfilment of the requirements for the degree of

Master of Science
in Civil Engineering

at the Delft University of Technology
to be defended publicly on the 18th of August 2022

Thesis committee:	Prof. dr. ir. S.G.J. Aarninkhof	Delft
	Prof. dr. ir. A.J.H.M. Reniers	Delft
	Ir. A.M. Ton	Delft
	Ir. T. Vijverberg	Boskalis
	Dr. S.E. Vos	Delft

TU Delft Delft University of Technology

Preface

This thesis is the final conclusion of my master in Hydraulic engineering at the Delft University of Technology. Although I tried long enough to maintain being a civil engineering student in Delft, it is finally time for me to make the next step.

At the start of this academic year, the thesis was the only part of my Master that I still had to fulfil. However, I had no idea what I wanted to research and what methods I wanted to use. After a quick search on Brightspace I found a subject about the Marker Wadden and drones that immediately caught my eye. After a quick chat with Anne, we decided that this would be the focus for my thesis the coming year. So, I went from no clue to a thesis subject in about a week, which must be some kind of record.

I always like 'carte blanche' projects like this and I very much enjoyed the experimenting and figuring out I had to do with the Marker Wadden data. However without my thesis committee I never would have been able to make chocolate from all the data and possibilities surrounding this research (not being able to make chocolate from something is a Dutch saying meaning you can't wrap your head around something). Therefore, I would like to thank my chair, Stefan Aarninkhof for pushing this research to higher levels than I thought possible at the start and his constructive feedback along the way. Also I would like to thank Ad Reniers for encouraging me to try and make this thesis as much of an addition to literature as possible. I would like to thank Thomas Vijverberg for his time and refreshing insights, including his views on what would be interesting for the Marker Wadden project and Sander Vos for his help on all the ins and outs that are important when working with this kind of data. I especially would like to thank Anne Ton for all the time and energy she invested into this thesis. Our weekly brainstorming sessions were extremely fruitful and helped me find my way in the labyrinth of strange ideas I often had. Most of all I had a blast working with you and for me our discussions were the highlight of my week (weekends not included).

Personally, this thesis had everything. There was a certain framework surrounding this subject I could work in but there was certainly enough room for me to come up with my own ideas. I could experiment with drones, go into the field, learn all the possibilities of python and still got a good look behind the scenes in the whole organisation behind the Marker Wadden. I had loved the variety and this thesis was therefore the perfect conclusion of my time as a student, here in Delft.

Finally I would like to thank all my friends and family. Especially Britt, Jasper, Laura and Suus who volunteered to be my study partner when everyone else decided to go on holiday. I was afraid that graduating would mean a nine months long labour of a brainchild, but actually I will look back on my last year as time in which I got to do a fun and interesting research, where friends were there for me every time I needed to blow of some steam.

Niels van Kouwen
Delft, August 2022

Thesis build-up

For this thesis it was decided by the author and thesis committee to write the main findings in the form of a paper. The paper presents (almost) all results that were found during this thesis. However, because this is a Master Thesis, it may be desirable to obtain more in-depth knowledge behind certain results. That is why this paper is accompanied by a list of appendices. Each appendix elaborates a chapter in the results or methods. It is not necessary to read all appendices in order to understand the thesis findings, but they provide additional information to support the paper. Some appendices also present extra research that has been done during the thesis but has not been presented in the paper.

Because the structure of this thesis is not in the traditional format, the presentation and answering of research (sub)questions that have been stated at the start of this thesis are dispersed over both the paper and appendices. That is why they are also presented here, together with a short version of their goal/research aim and a brief summary of their final answers. Also the locations in the paper and appendices where these research questions are elaborated are indicated here. A morphodynamic conceptual model has been made for both spits based on literature and case studies, that can be considered as a form of a hypothesis for the morphological development of both spits and their drivers. These models are mentioned in the paper (Chapter: case studies) and shown in figure 1 and 2.

Many observations and forms of analysis were done for the southern spit to develop an efficient method of spit quantification. After that the northern spit was quantified with the same method to test the practicality of the quantification method. The northern spit (which has other properties than the southern spit) was quantified with the same method and scripts, and only afterwards it was investigated if these results made sense. This gave an idea of how efficient and effective the quantification method actually is. It is because of this that the results presented for the southern spit are more detailed than the results for the northern spit (in the appendices at least).

Summary, based on research questions

During this thesis the scope of research has been widened, which results in two main research questions. One focussing more on spits in low-energy lake environments and the other more directed towards the method for spit analysis.

Main research questions

Research question: What main processes drive and influence a spit in a low-energy, lake environment and what is the effect of morphological spit development on the surroundings? *Using the Marker Wadden as a case study.*

Goal: To give a nuanced picture that explains the development of both spits, using quantified results.

Summary of findings: Both spits do not grow towards a curve, but propagate (in length) towards a clear direction. For both spits the submerged spit-platform part grows during high energy periods and the emerged part only grows during lower energy periods.

The northern spit indeed develops as a simple spit, because of the lake circulation that approaches from both ends. However most of the sediment comes from the Noordstrand and scarp at the northern side of the spit. This material is delivered by currents from SW and W winds and is reorganised by currents from S winds. The growth rate of this spit is double of what is projected because the sediment supply to the spit is more than three times of what is expected by van Santen (2016).

In the hypothesis the contribution of waves is overestimated for the southern spit. The waves do have a significant effect on the emerged part of the spit but because the spit-platform has such an important role to play in the development of the emerged part and the general spit development, the propagation direction of the southern spit is at the location where currents pass over the platform boundary. The growth rate of the southern spit is around 40 m/year in its propagation direction as the sediment supply towards the spit is almost seven times as high as expected (van Santen, 2016).

Spits in low-energy lake environments are affected by lake circulation currents in addition to wave-driven longshore currents, propagate in a distinct direction and need an alternation between high energy periods and lower energy periods in order to grow both above and below the waterline.

Research question: How can morphodynamic spit developments and its hydrodynamic drivers be efficiently linked and quantified? *Using the Marker Wadden as a case study.*

Goal: The morphodynamic developments of spits are hard to link to hydrodynamic drivers due to the complexity of both the spit morphodynamics and hydrodynamics. This method uses polar coordinates and simplified elevation levels to make it easier to simplify and analyse morphodynamic trends and hydrodynamic processes. This enables us to link the two.

Summary of findings: The method described in this paper, allows for the quantification of morphodynamic and hydrodynamic relations around spits and is an efficient way of data analysis of these complex three-dimensional landforms. This simplification in polar coordinates makes it possible to efficiently describe and quantify processes around the spit in a detailed fashion. Thus, making it possible to objectively pinpoint the case-specific drivers behind different forms of spit growth.

Subquestion 1

Research question: What is the best method to capture (spit) morphodynamics using drone imaging and Structure-from-motion?

Goal: Many different parameters in the drone set-up are of influence on the accuracy and the efficiency of the DEM (Digital Elevation Model) construction. The contribution of each parameter to the accuracy needs to be known in order to reason what parameters should be set on a less accurate setting in order to keep the drone measurement process efficient.

Summary of findings: Because of time and material issues the experiment for finding the ultimate settings and set-up is not executed during this thesis, in accordance with the thesis committee. However, a method to obtain these settings has been developed in this thesis. The parameters that can be varied for drone imaging on coastal environments are reduced to four: height of flight, frontal overlap, lateral overlap and amount of ground control points (GCPs). The contribution of each of these parameters to the accuracy can be calculated in nine test flights with the Taguchi method.

Subquestion 2

Research question: What morphodynamic changes can be observed in the spits over time and (wind)conditions?

Goal: Find trends in the morphology that eventually could be linked to hydrodynamic processes.

Summary of findings: A distribution of sediment around both spits was found. Both spits have a clear propagation

direction. It was found that the submerged spit-platform and the emerged spit part do not grow simultaneously but thrive under different conditions.

Subquestion 3

Research question: Which hydrodynamic processes in the Markermeer could affect spit development of the Marker Wadden spits?

Goal: Analyse the magnitude and change of flow directions and velocities around the spit.

Summary of findings: For both the waves and the lake circulations, combined current directions and flow velocities for all wind conditions can be approximated. Current directions do not change significantly when wind velocity increases. Flow velocities also follow the same pattern of increase and decline around the spit for different wind velocities. It was found that lake circulation currents do change direction around the spit because of small scale circulation cells around the beaches and sediment extraction pits.

Subquestion 4

Research question: Can the main trends and developments of spits be attributed to certain hydrodynamic processes and sediment supply?

Goal: Use the findings of subquestion 3 to explain the trends found in subquestion 2.

Summary of findings: Based on the effect of the different current patterns (current directions around the spit) on sedimentation around the spit, several current patterns can be discarded as they are not important for spit growth. The other currents can be averaged as a single sedimentation current pattern that is responsible for all spit growth. The location of most sedimentation is the location where the sedimentation current passes over the platform boundary, where there is suddenly abundant room for the flow to dissipate. This results in the growth of the submerged spit-platform which is found to be very important for the propagation direction of the spit.

It was also found that the growth of the emerged spit part is dependent on the incoming flow velocity and the size of the platform. This means that the growth of the emerged spit part is affected by the growth of the submerged spit-platform and vice versa. Also the emerged spit and submerged spit-platform thrive under different conditions.

Subquestion 5

Research question: How can the found morphodynamic and hydrodynamic relations help evaluate and predict spit developments and what are the possibilities and constraints of the used analysis method for spit quantification?

Goal: With this method of data analysis it becomes possible to show and quantify the link between spit morphology and its hydrodynamic drivers in a detailed manner.

Summary of findings: The used method makes it possible to discard certain spit parameters when looking for important relations for spit development. The empirical relations that are found are accurate enough to use them for the prediction of spit developments. The method can most likely be applied on other spit types in other environments. However, a lot of data and prior knowledge is necessary to analyse a spit in a detailed fashion.

Location of findings

Research question	Paper	Appendix	Other
Main questions	Overall	Overall	
Subquestion 1		A	B: focusses on post-processing of DEMs.
Subquestion 2	Results, *spit growth quantification*	C	
Subquestion 3	Results, *Flow around the spit*	D	
Subquestion 4	Results, *Growth orientation linked to flow & Sedimentation on elevation levels*	E & F	
Subquestion 5	Results, *Predictive potential of found relations* / Discussion	G	The success of the analysis of the northern spit indicates that this method can be applied on multiple spit types.
Extra: Sediment balance Zuidstrand		H	This has been done to bolster the findings of sediment supply around the spit.

Table 1. Location of research topics in the paper and appendices

Time

Begin

Start of spit formation

Clear spit has been formed

DOMINANT

Only waves

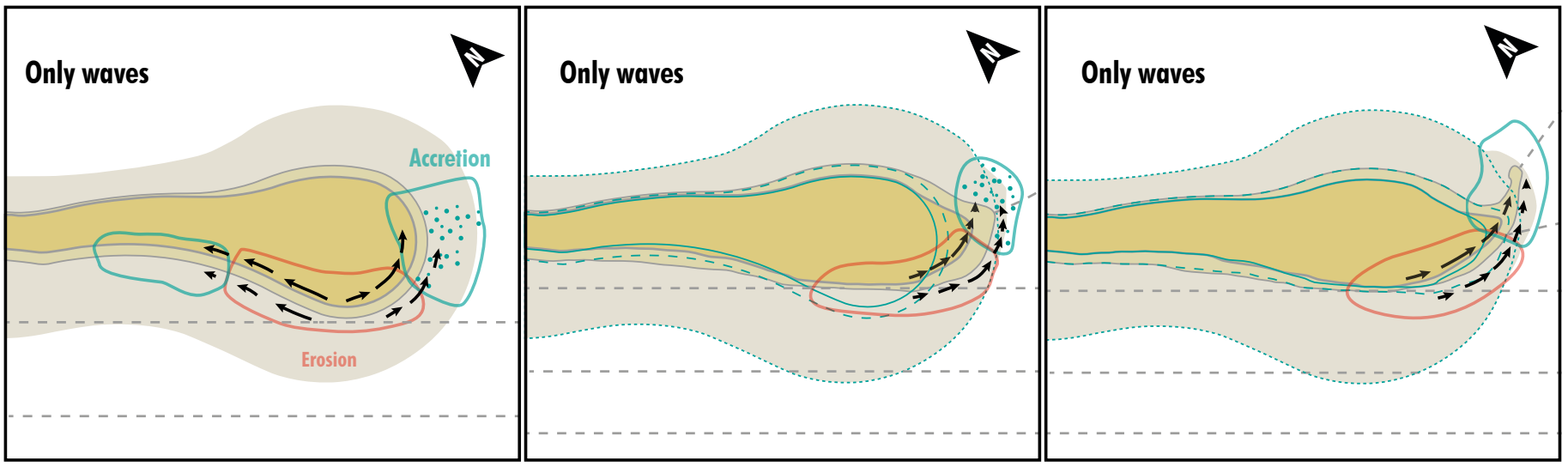

Waves approach the beach almost perpendicular resulting in little to no longshore currents. Except on the head where the curves of the coastline can cause fast currents, reshaping the head to be more aligned with the beach and to grow in a curve on the distal end side. This results in a very curved spit.

Only lake circulation

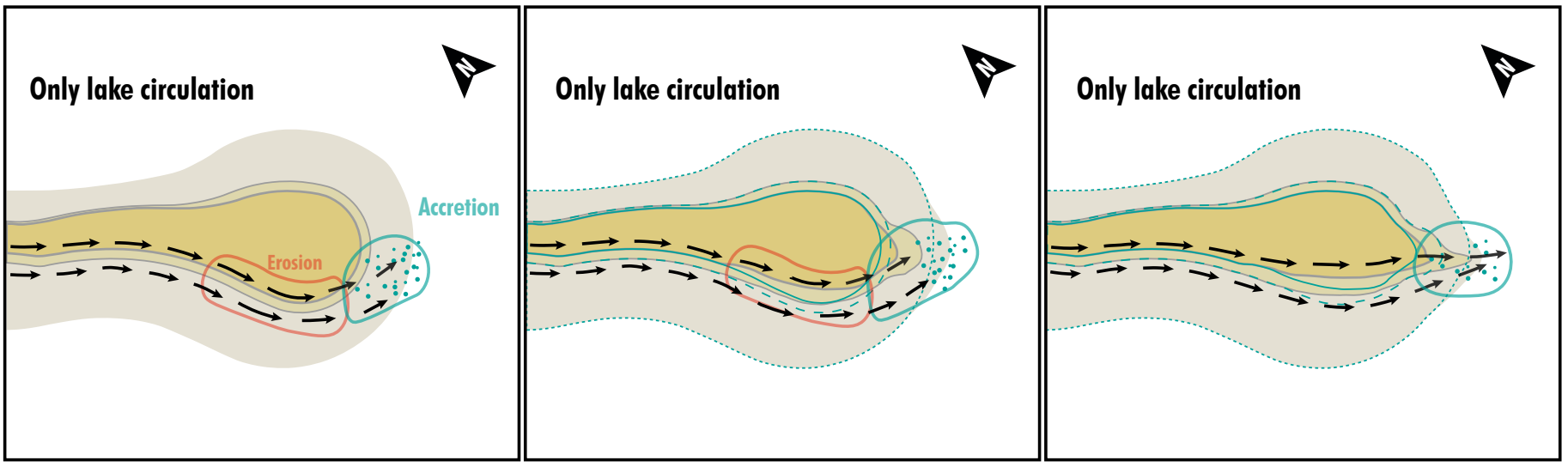

In the scenario where lake circulation currents approach the head from the north the currents are converged near the protrusion of the head creating local erosion. The more the erosion has taken place, the less this convergence occurs. The material from the head and beach is transported beyond the head and the platform resulting in a relatively straight spit.

Legend

- Land above set-up level
- Land below set-up level
- Submerged platform
- previous contour lines
- Magnitude of longshore current
- Incoming wave crests
- Important area of erosion
- Important area of accretion
- Magnitude of accretion

Prediction from all process combined

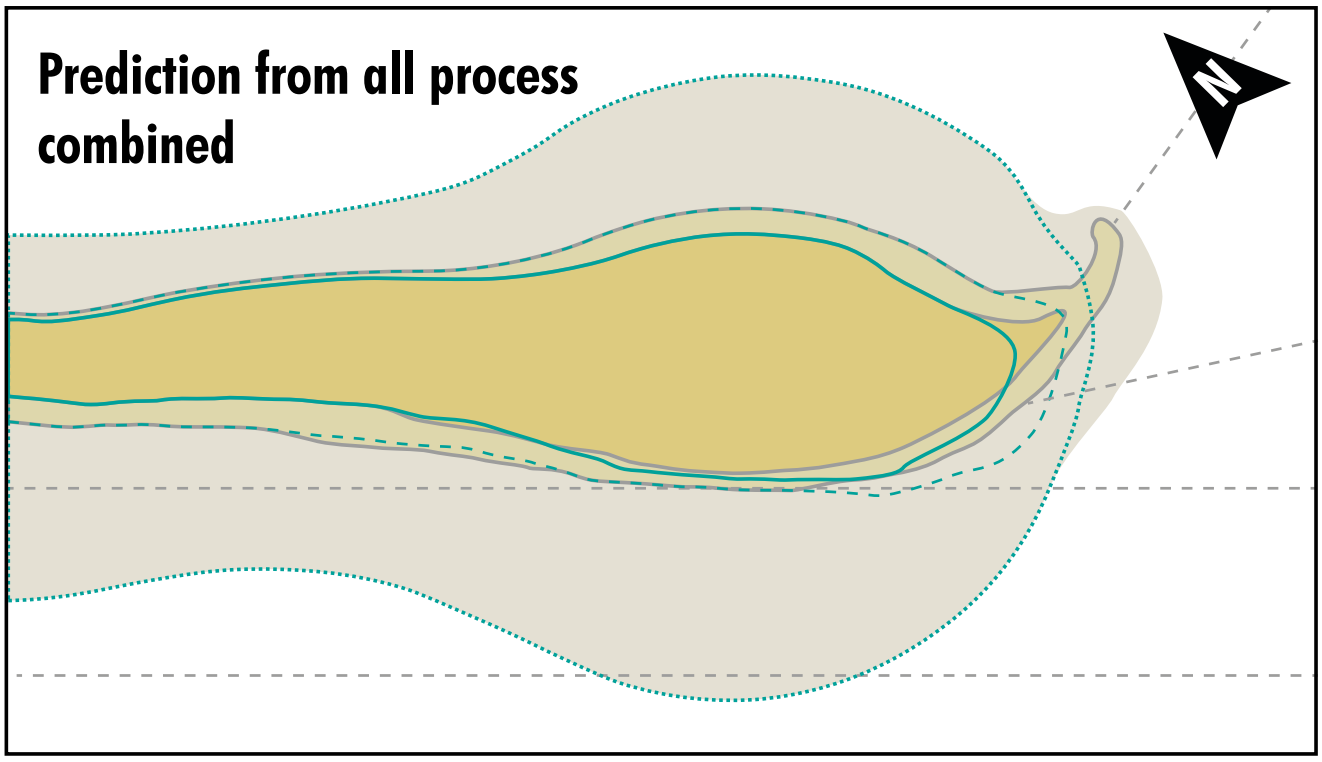

The contribution of lake circulation is hard to tell in this case but the effect of incoming waves around the head, and the accompanying erosion is easier to tell. Therefore is it likely that some form of a curved spit will grow.

Figure 1. Southern spit: morphodynamic and hydrodynamic hypothesis

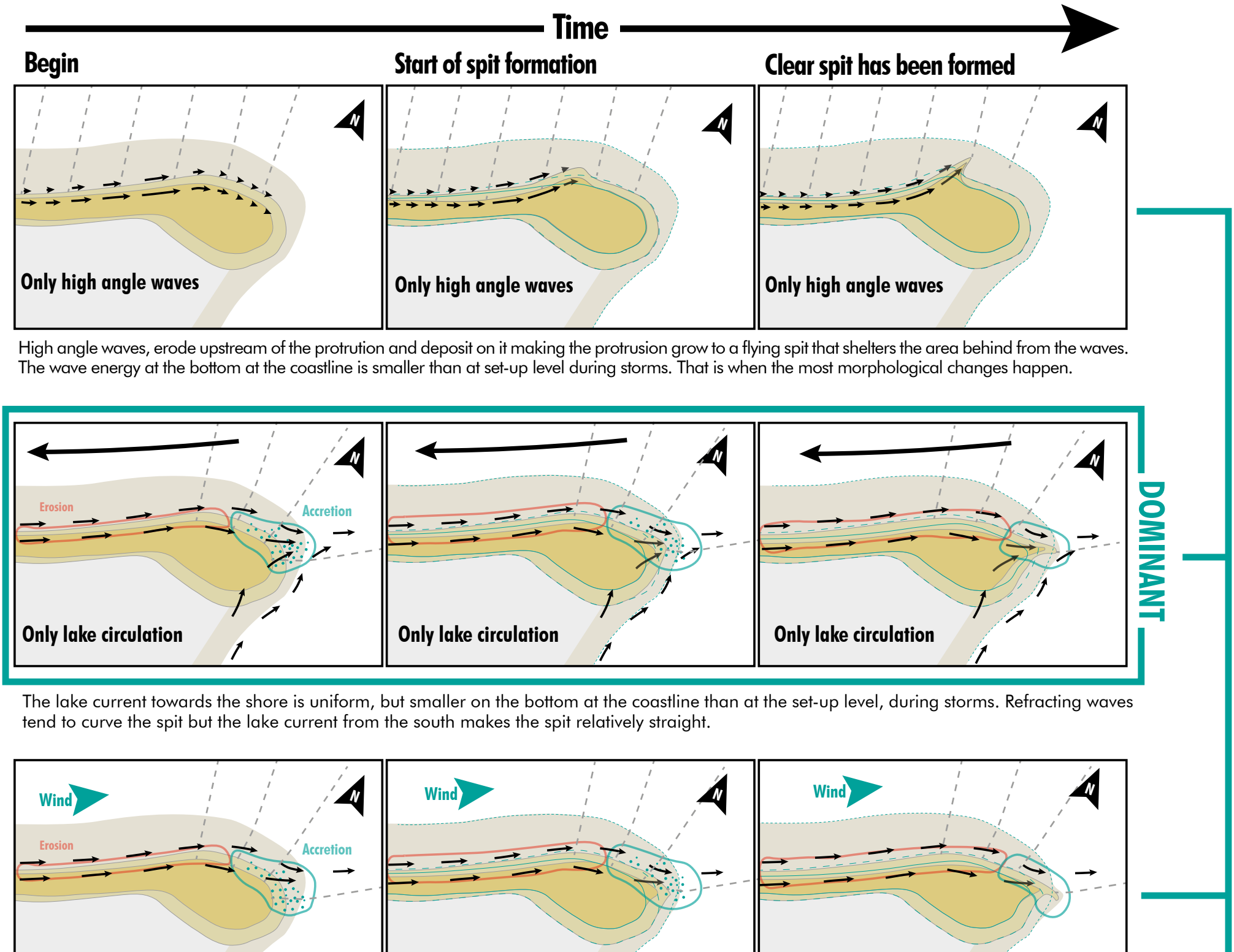

Figure 2. Northern spit: morphodynamic and hydrodynamic hypothesis

PAPER

SPIT EVOLUTION AT THE MARKER WADDEN

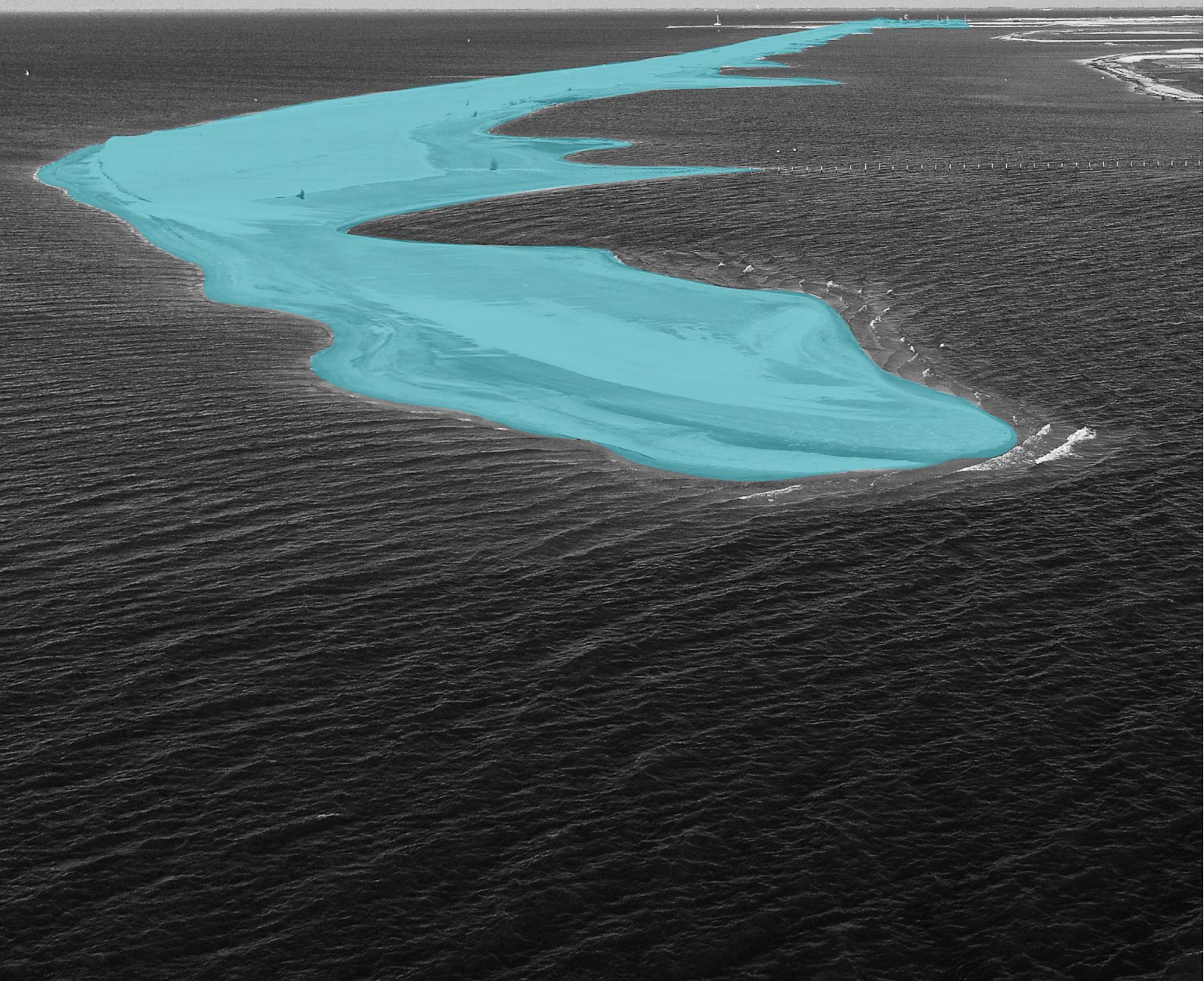

Quantifying complex relations between spit growth and its hydrodynamic drivers, in non-tidal, wind-dominated lake environments. Application to the Marker Wadden (Lake Markermeer, The Netherlands).

Abstract

Many sand spits are morphodynamically complex cases that are hard to quantify. Therefore, most case studies on sand spits in a specific type of environment, are descriptive or even non-existent. As is the case for spits in low-energy lake environments, like the two spits at the Marker Wadden islands. Because quantification is necessary for spits in such complex environments, sedimentation was quantified around both spits using polar coordinates and morphologically simplified elevation levels around the spit-platform. It was found that, sediment rich currents that pass over the spit-platform boundary at a certain direction drive spit-platform growth in that direction. The spit-platform growth in turn dictates the growth of the emerged spit. Spit growth quantification enables a detailed understanding of the Marker Wadden spits, which gives insights in spit behaviour in low-energy lake environments. The quantification of spits in other environments could be a powerful tool for the understanding of spit behaviour.

Introduction

Along our coasts, different types of coastal systems and landforms can be defined. One of these coastal systems are sand spits, which often have complex morphodynamics (Allard et al., 2008). Spits can be defined as a partly subaerial ridge or embankment of sediment attached to the land at one end and terminating in open water at the other, which needs to be fed by longshore processes (Allen, 1982; Evans, 1942).

Spits often occur at places where the coastline changes its longshore uniform direction, as this gives the longshore current more room to disperse and lose its transport capacity, resulting in sedimentation (Uda, 2018). Meistrell (1966) showed that the growth of the subaerial ridge of the spit is preceded by a submerged spit-platform. The interaction between the emerged part and the platform is often important for the spit shape and its growth.

Kraus & Asce (1999) continued the research of Meistrell by stating that with unrestricted spit growth all the material that is transported towards the distal end accretes partially in the subaerial spit and partially on the spit-platform (for definitions, see Figure 1). They assume that the ratio with which the spit and its platform grow is always the same, although Meistrell's experiments showed that spit and platform growth are inversely related.

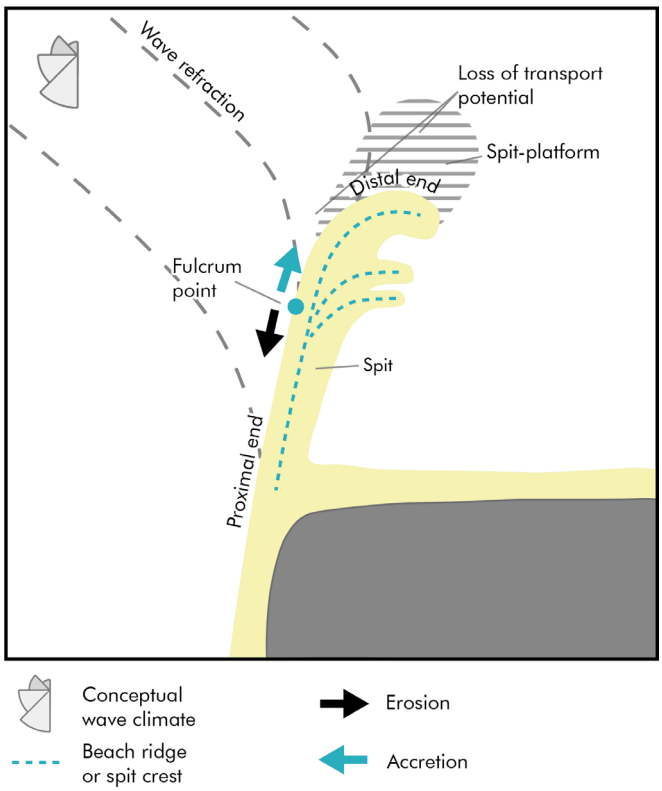

Figure 1. A schematic representation of a recurved spit. Illustration based on Rossel & Westh (2020)

The growth of a spit in a certain environment can be beneficial for the environment. Besides the societal functions spits may have, like recreation and flood protection, they are also valuable and unique coastal habitats for a wide range of flora and fauna (Allard et al., 2008; Rossel & Westh, 2020). Spits are highly dynamic, and their shape and size can change in very short timespans depending on various complex drivers (Randazzo et al., 2015). Therefore research of a spit also means research of its environment. Different drivers on different locations results in an abundance of spits with different types and shapes all around the world, of which several different categories can be distinguished (Robin et al., 2020; Uda, 2018). Several categories of spits are:

- Recurved spit:

These are the most common kind of spits. Recurved spits occur mostly on places where wave-driven longshore transport occurs on one side of the spit. This creates a hook, or possibly multiple hooks (Allen, 1982). The most important driver in the formation of this shape is the changing angle of incidence of the waves that passes the optimum angle of 45 degrees at the fulcrum point (Figure 1) (Ashton et al., 2016). Typical recurved spits, with hooks formed by originally low angle or even perpendicular waves are the Arçay spit (Allard et al., 2008), the Buctouche spit (R. Davidson-Arnott et al., 1995) and the spit on Hagemeister Island (Ashton et al., 2016) (Figure 2a).

- Simple spit:

Simple spits have a relatively linear shape, caused by two longshore currents coming from both sides of the spit. Each current effectively erases the hook caused by the current on the other side (Rossel & Westh, 2020). Examples of simple spits are Skagens Odde in Denmark (Bruun, 1993; Rossel & Westh, 2020) and the spit in Cape Helopen in the USA (Kraft et al., 1978) (Figure 2b).

- Flying spit:

According to Ashton & Murray (2006), spits in regions with predominantly high angle waves tend to protrude from the beach. These, so called, flying spits originate from the principle that high angle waves result in higher wave-driven transport at the sides of a protrusion than at the top. Examples of flying spits can be found in lake Mega-Chad in Central Africa, the Azov Sea in Ukraine (Bouchette et al., 2010) and Lake Erie in Canada (R. G. D. Davidson-Arnott & van Heyningen, 2003) (Figure 2c).

- Non-wave dominated spit:

Not only wave induced transport can influence spit growth (Evans, 1942) as tides and lake circulations can also create significant longshore currents (Nutz et al., 2018). These spits tend to be more linear as the waves that are essential in shaping the hook (Ashton et al., 2016) are not present. Examples where tides play an important role in spit morphodynamics are the Lubec spit in the USA (Randazzo et al., 2015) and the 'El Punital' spit in Spain (Losada et al., 1991)(Figure 2d).

However, in practice it is not always clear in which class a spit belongs. There can often be multiple hydrodynamic drivers attributed to a spit. For each of these drivers the effect on the morphodynamics can be completely different. Therefore, in practice it becomes necessary to find the role of each of these relations between spit morphology and hydrodynamics to be able to describe and predict the eventual spit development. Quantification of observed processes is therefore an important step in the research of spit cases.

There is much that is already known about spits, especially from a schematic perspective. In principle the relation between morphological developments of spits, and its hydrodynamic drivers have been shown by authors like Ashton et al. (2016). However, few have managed to quantify, or even link, spit morphology and its drivers in case studies of a spit (Allard et al., 2008; Héquette & Ruz, 1991). As a result, most research on spits is descriptive. For example, spits can be classified as a recurved spit because of its hook but explaining why the curve of the hook is sharp or gentle seems troublesome. Linking the sensitive morphological behaviour of spits to hydrodynamic processes can become even more difficult in environments that have multiple hydrodynamic components, and typical morphodynamic behaviour themselves. Low-energy lake environments are environments that possess these properties.

Since low-energy lake environments have multiple hydrodynamic components, little is known about spits in these systems. These environments have limited wave energy. They are therefore dependent on high-energy events for large scale morphodynamic developments, without receiving sediment replenishments during low-energy periods. Additionally, lakes are subjected to lake circulation currents due to set-up differences across the lake at

high winds (Ton et al., 2021; Wellen, 2021). Both hydrodynamic processes can have a pronounced effect on spit development. Also, beach profiles in low-energy lake environments typically have a long platform in front of the coast, at a depth around the depth-of-closure (Brideau et al., 2022; Ton et al., 2021; Vila-Concejo et al., 2020). This can be of large influence on spits as platforms have proven to be of essence for spit development.

All in all, spits in low-energy lake environments are too complex to research descriptively and therefore its morphodynamics are relatively unknown. To objectively understand spits in complex environments like this, the link between spit morphology and hydrodynamics needs to be quantified, despite the problematic sensitivity of the spit morphodynamics. Thus, to fill this knowledge gap a novel method for spit analysis and quantification is developed and applied in this paper.

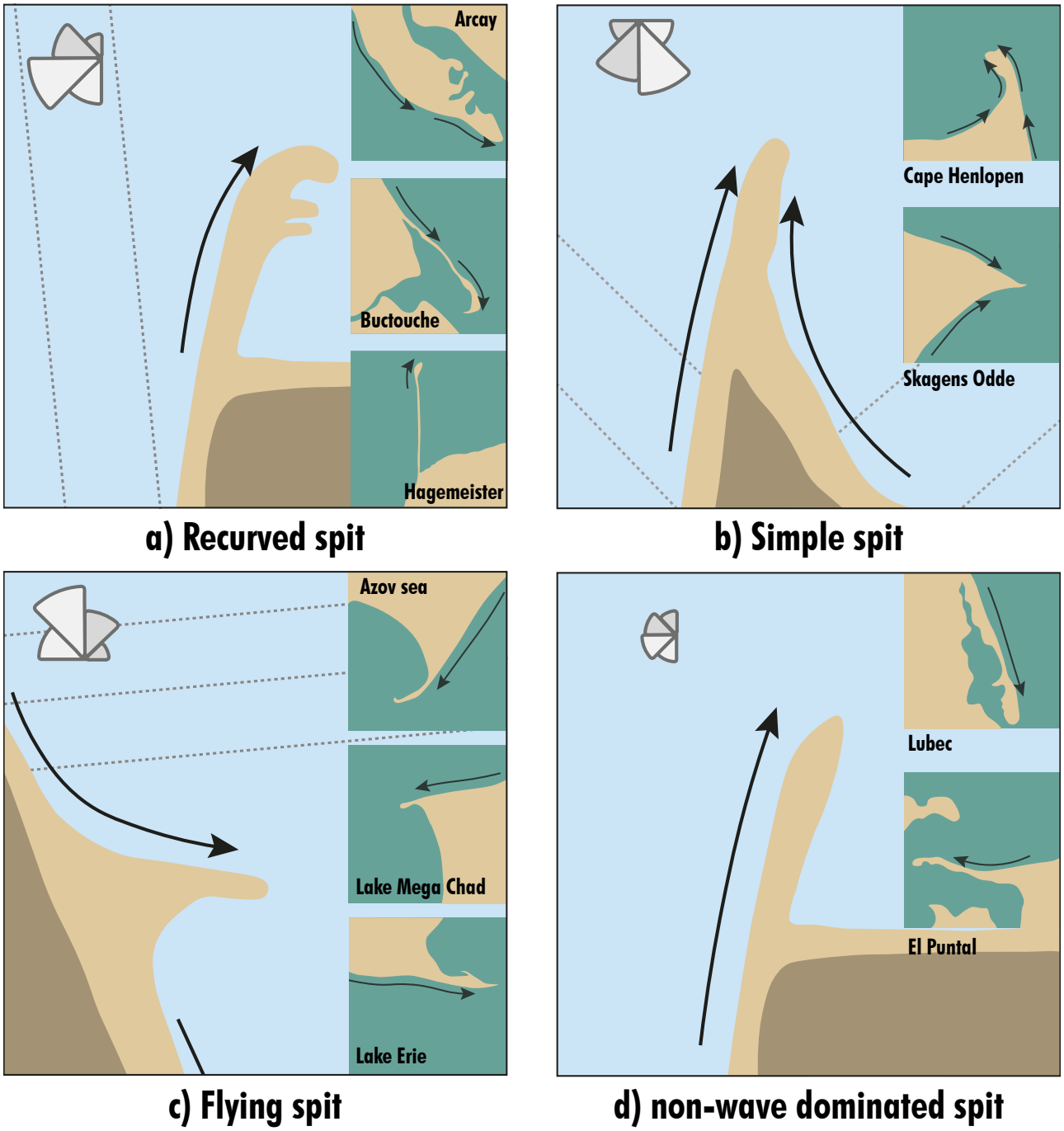

Figure 2. The different classes of spits, recurved spits, simple spits, flying spits and non-wave dominated spits respectively. For every spit the main figure is a schematic representation of the spit type, with on the right the examples referred to in the introduction. The wave rose on the upper left indicates the schematic wave climate, the dashed lines indicate the incoming wave crests, and the black arrows the sediment transport along the spit.

Study sites

To research spit behaviour in a typical low-energy lake environment, the Marker Wadden islands in the Netherlands are used as a case. This artificial archipelago is constructed in 2016 to improve the ecological value of lake Markermeer as a whole (Jin et al., 2022). Lake Markermeer is a closed-off lake that can be classified as a low-energy, non-tidal environment. Moreover, this shallow lake (~4m) can be subject to significant lake circulation currents due to set-up differences in the lake. Al these factors make this a complex case to link morphological developments with certain hydrodynamic drivers and/or wind conditions (Ton et al., 2021; Vila-Concejo et al., 2020; Wellen, 2021).

The islands, which are mostly build of silt, are protected by two sandy beaches with dune rows (Figure 3, Figure 4). Each beach begins at a groyne and has an open ending or head. It is from these two heads that new, young spits start to develop. The most northern beach and spit is subject to high angle waves and lake circulation currents from both sides. Considering the different classes from the introduction it can be expected that this spit would be a combination of a simple spit and a flying spit. Meanwhile the southern beach and spit is mainly subjected to perpendicular and very low angle waves from one side. Based on the spit classes it can be expected that this spit would resemble a recurved spit (Boskalis Nederland, 2015; van Santen, 2016; Wellen, 2021).

Using similar case studies and the known schematic relations, a general idea about spit shape and development can be formed, as has just been done for the northern and southern spit. However, proving and nuancing this reasoning presents a challenge. To get the desired amount of insight into the developments of both spits and nuance the extent to which both spits can be attributed to a spit class, a novel method of quantifying spit morphodynamics and hydrodynamics has been developed and used.

Figure 3. Marker Wadden islands, seen from the tip of the southern spit. Picture made by N. van Kouwen and A. Ton (2022).

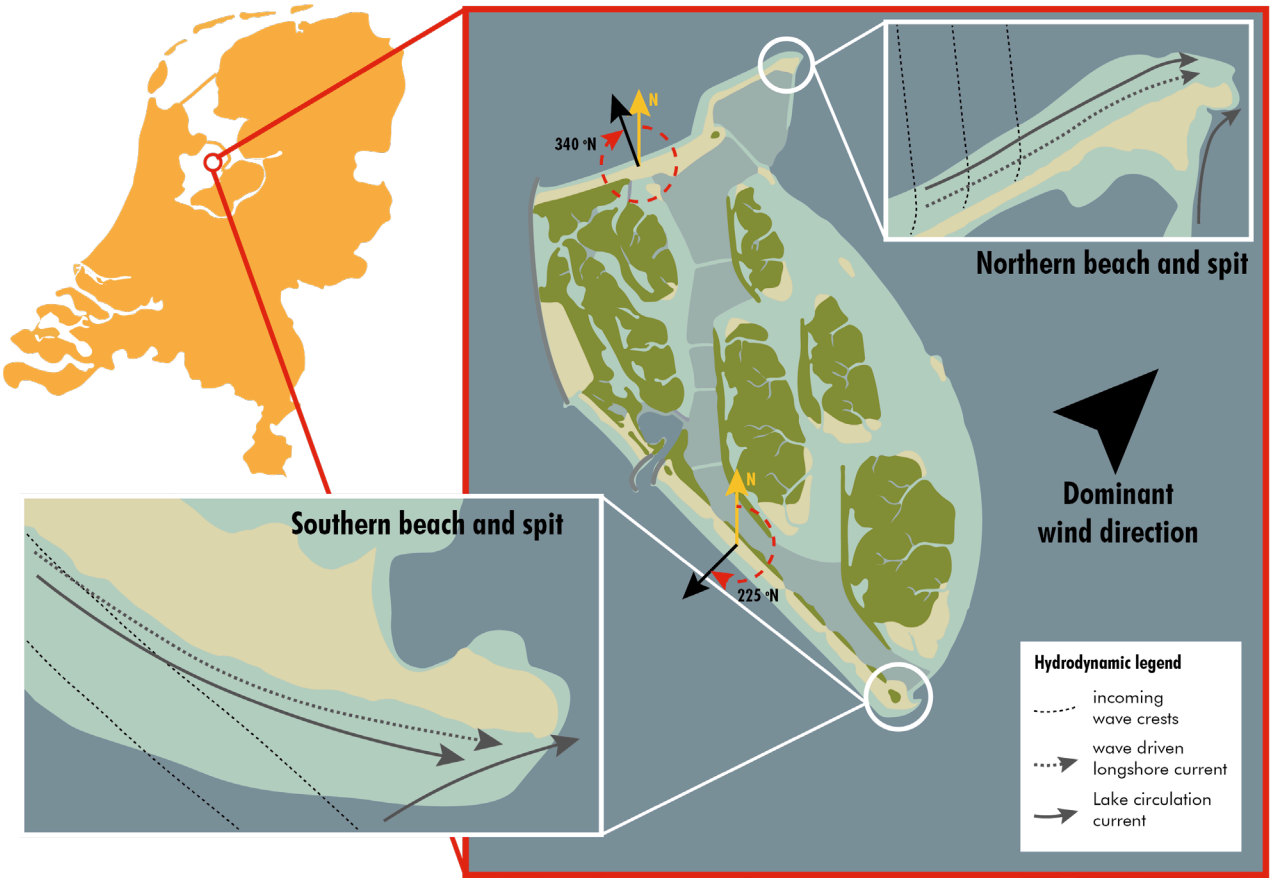

Figure 4. Location and situation of the Marker Wadden islands, in lake Markermeer in the Netherlands. The black and red arrow combination indicates the orientation of the beaches relative to the north. Drawing based on Boskalis Nederland (2015).

Method

To quantify the spit morphodynamics, a novel method is used with a polar coordinate system instead of X,Y coordinates. Also, elevations are simplified into three elevation classes.

Because of the dynamic nature and shape of spits, another orientation system can be more efficient to track developments over time than the traditional Cartesian or GPS-based coordinate system. Since most processes of spit growth take place around the distal end and the spit grows from a semi-circular head, a polar coordinate system is more suitable. It makes it easier to simplify the data analysis, to calculate only the most important parameters for spit formation and development. For the analysis of ebb-tidal deltas, polar coordinates were efficient as well (Pearson, 2021). Polar coordinates allow for continuity in the analysis as the length of the spit changes because besides distances, the orientation in degrees can be considered as well.

For this polar coordinate system, a centre point is chosen. All calculations will be done relative to this point. For the centre point it is important that it is subaerial during the entire period over which data is analysed and that between the centre point and a considered sedimentation location there is only one transition from land to water (Figure 5b). As long as the centre point meets these two requirements for most of the time (especially for the last requirement slight deviations are inevitable), a location for the centre point can be manually picked based on the expected growth patterns beforehand.

Currents and morphological changes will be quantified at degrees around the centre point. This way currents and sedimentation can be described around the spit. Because this paper aims to analyse spit growth in a practical manner, the boundaries of the 180 degrees that are analysed (chosen for convenience), are set around the diWstal end of the spit. Here almost all sedimentation is expected to occur as sedimentation occurs on the distal end and erosion on the proximal end (Ashton et al., 2016) (Figure 1, Figure 5). Because polar coordinates are used, the distance from the centre point to the concerned areas should be as small as possible to be the most accurate, without neglecting areas that experience important sedimentation for spit growth.

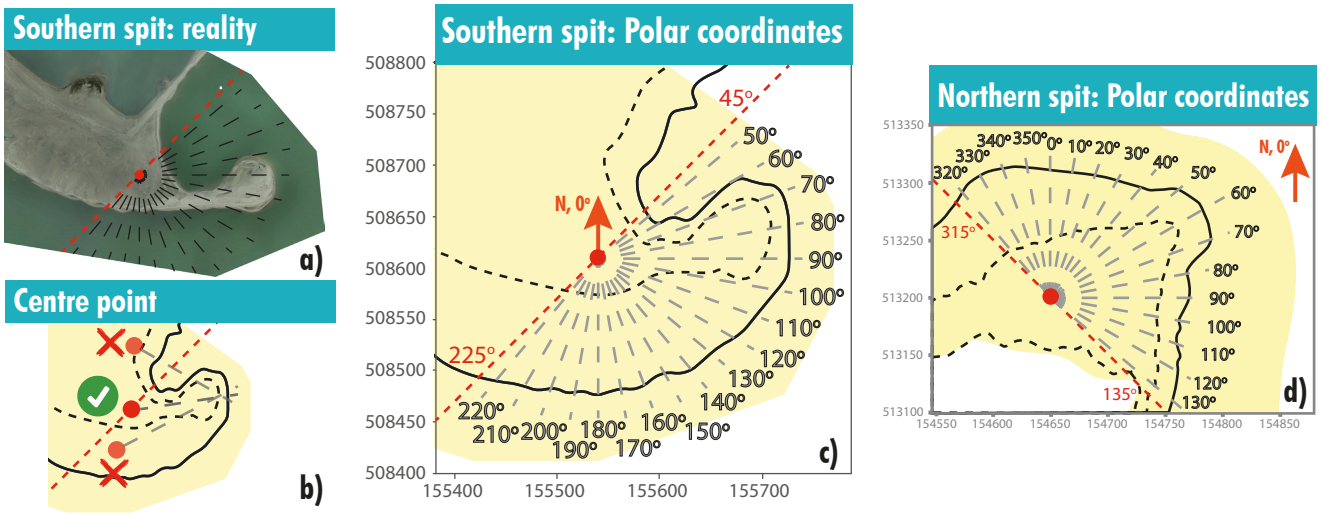

Figure 5. The polar coordinate system used for spit quantification. a) Represents how the schematic drawing of c is situated in reality. b) Here it is indicated how the centre point should be chosen. c) Gives the set-up of the polar co-ordinate system; here different directions in degrees are indicated around the centre point (red dot). All 180 degrees are relative to the north and the boundaries of the considered area are indicated by the red dashed lines. d) Gives the same information as figure c but for the northern spit.

To quantify changes in elevation, morphology will be simplified to three elevation classes, chosen based on different morphological properties:

- The subaerial level (above the waterline: -0.3 m NAP), sedimentation on this level is limited on the Marker Wadden islands and thus analysed in less detail in this paper. This level is emerged most of the time but partly submerged during storms.
- The platform level (below -0.3 m NAP and above -1.2 m NAP, generally -1 m NAP).
- The sub-platform level (below -1.2 m NAP), this is the level below/in front of the spit-platform. After a level boundary there is a steep drop towards the next elevation class (Rijkswaterstaat, 2018; Ton et al., 2021) (Figure 6).

These two boundaries divide the spit into two cross-sectional parts, the emerged part, and the submerged spit-platform part. The emerged part grows in length when sedimentation on the platform level takes place, and the submerged part grows in length when sedimentation on the sub-platform level takes place (Figure 6c). The location and magnitude of sedimentation and hydrodynamic properties (current directions and velocities) will be quantified based on the orientation (in degrees) around to the centre point, relative to the north, and the elevation class on which it occurs, which allows us to see trends without getting lost in small scale dynamics.

Flow around the spit

The hydrodynamic data comes from a Delft3D model of Lake Markermeer made and validated with field data by Ton et al. (2022). The hydrodynamics are completely dependent on the local wind conditions and therefore 32 wind scenarios are modelled based on 8 varying wind directions and 4 wind velocities (Table 1). For each scenario the flow directions and

Wind dir	Wind vel	Wind dir	Wind vel
N (North)	5 m/s	N	15 m/s
NE (Northeast)	5 m/s	NE	15 m/s
E (East)	5 m/s	E	15 m/s
SE (Southeast)	5 m/s	SE	15 m/s
S (South)	5 m/s	S	15 m/s
SW (Southwest)	5 m/s	SW	15 m/s
W (West)	5 m/s	W	15 m/s
NW (Northwest)	5 m/s	NW	15 m/s
N	10 m/s	N	20 m/s
NE	10 m/s	NE	20 m/s
E	10 m/s	E	20 m/s
SE	10 m/s	SE	20 m/s
S	10 m/s	S	20 m/s
SW	10 m/s	SW	20 m/s
W	10 m/s	W	20 m/s
NW	10 m/s	NW	20 m/s

Table 1. 32 scenarios consisting of different combinations of wind directions and wind velocities.

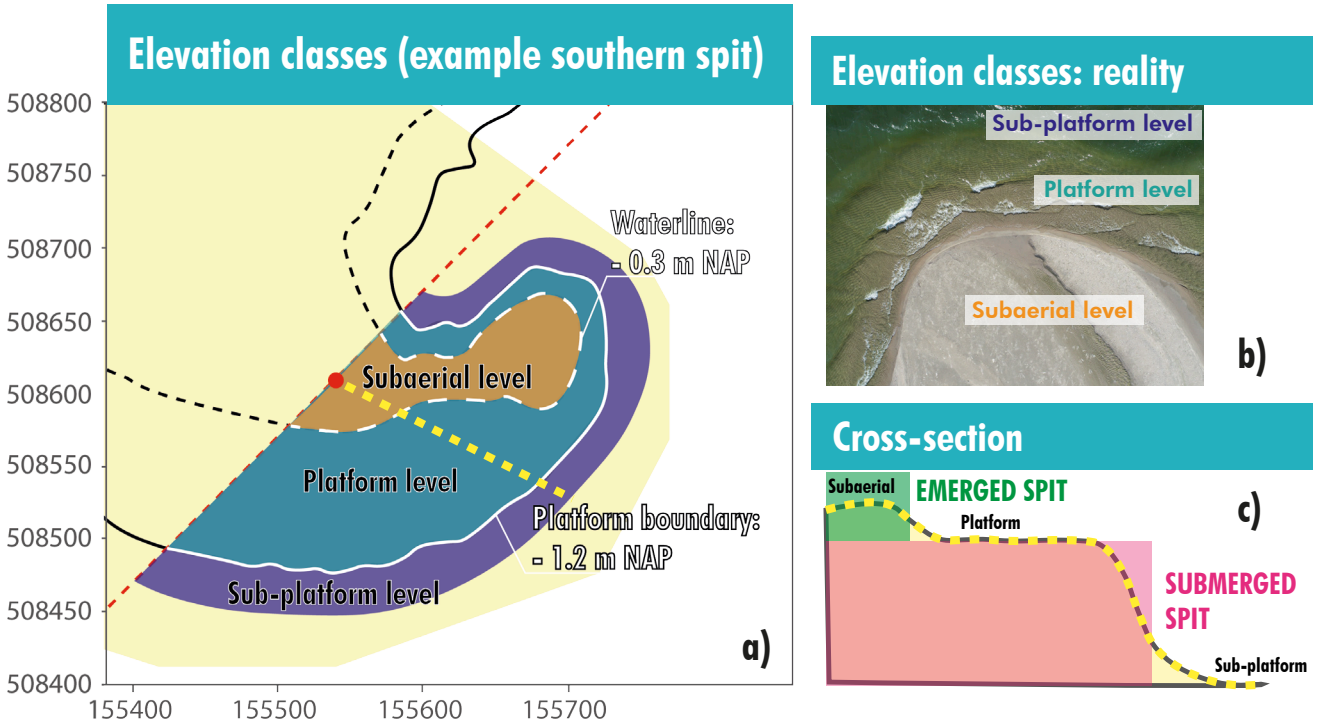

Figure 6. Three used elevation classes: subaerial level, above the waterline; the platform level, below the waterline and above the platform boundary; The sub-platform level, below the platform boundary. In the cross-section these boundaries split the spit into the emerged spit and the submerged spit-platform.

velocities can be computed in the polar coordinate system around the spit for the combined current, driven by both waves and lake circulations. The flow directions and velocities are computed for every degree around the spit by averaging over the one direction, ranging from the coastline to slightly past the platform boundary (indicated by the grey lines in Figure 5 c). Flow directions are weighted with the flow velocity in this averaging, as currents with larger flow velocities have a larger influence on sediment transport. Hereafter, these averaged flow directions can be fitted for the whole observed 180° degrees to link these currents to sedimentation patterns more easily. With these fits, it was evaluated for each of the 32 scenarios, how much each scenario occurred during a period.

Flow velocity is especially important to represent the transportation capacity of incoming flow. Therefore, the flow velocity at a degree in front of the spit tip (v_{in}) is computed as the most important spit growth behaviour is expected to occur around this location. Lake Markermeer is a low-energy environment and therefore the morphodynamics are mainly dependent on high-energy events (Ton et al., 2021; Vila-Concejo et al., 2020). Taking all wind scenarios in equal amount into account for the analysis of the spit morphodynamics, regardless of the wind speeds, is therefore not the best representation morphodynamically speaking. The flow velocity is strongly correlated with the wave height and intensity of lake circulations, which are in turn heavily dependent on the wind velocities.

For sedimentation in this low-energy environment, there should be a minimum threshold of transporting energy before large scale sedimentation takes place. Thus, for the analysis of historical wind conditions during a period, only wind conditions with velocities higher than 7,5 m/s are considered as very low energetic conditions have very little effect in a low-energy environment. Also, to get a representative incoming flow velocity for the energy conditions during the period (v_{in}) not the mean flow velocities during a measurement period are considered but the 97% quantile of the flow velocity during a period. This 97% quantile is the highest possible quantile for which the ratio between low-energy events and storm events still can be observed but also shows flow velocities that are more representative regarding their morphological effect.

Spit growth quantification

The spit growth of both spits is quantified by using topographical data of the Marker Wadden,

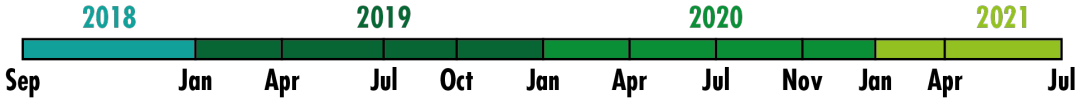

Figure 7. Timeline of measurements done by Boskalis. With the month of measurement indicated in black.

measured by Boskalis Nederland with in-field measurements. These measurements were done four times per year and the interval between measurements varies between 2,5 to 4,5 months (Figure 7). The measurements consist of drone photogrammetry and underwater multibeam measurements that can be interpolated in post processing, from which pointclouds can be created from measured data, that have a general vertical accuracy of around 5 cm. The difference between pointclouds, each measured at a certain date, shows the morphological changes during a period between the two dates. These elevation changes are interpolated over a grid to get a mesh with elevation changes. Changes in elevation of a single grid cell can be multiplied with the area of the square at specific locations to compute erosion and sedimentation volumes at these locations in a period.

Spit growth is quantified by computing the accreted volumes around the spit during a period. In most literature spit growth is evaluated by calculating changes in length. But this method can be very subjective as it depends on definitions, like the exact location of the spit tip for example. Also, growth in length is not suitable to quantify growth in multiple dimensions, which is important considering the curvature of spits. Quantifying deposited volumes at all degrees around the centre point allows for a more detailed and objective analysis.

Groups of adjacent degrees with above average sedimentation in a period between measurements, will be considered a deposit and its centre of mass the location of the deposit. This means that a deposit can be identified as a deposit if at a certain degree $s_{N=1st\ deg} \geq s_{mean}$, where $s_{N=1st\ deg}$ is the total accreted volume that is calculated at that particular degree and s_{mean} the mean accreted volume taken over the whole considered 180 degrees. The end boundary of a deposit can be identified if $s_{N=last\ deg} \leq s_{mean}$, where $s_{N=last\ deg}$ is the total accreted volume that is calculated at that degree. Then the centre of mass, and thus the location of the deposit is:

$$deg_{dep} = \frac{\sum_{deg_{N=last}}^{deg_{N=1st}} \deg * s_{deg}}{\sum_{deg_{N=last}}^{deg_{N=st}} s_{deg}}, \quad \textit{Equation 1.}$$

with deg_{dep} the degree at which the deposit is located, $deg_{N=1st}$ the degree at which the deposit starts (lowest degree), $deg_{N=last}$ the degree at which the deposit ends (highest degree), and s_{deg} the total accreted volume at a certain location.

Additionally, for spit growth it is important to consider sedimentation on the different elevation classes. The amount of sedimentation on an elevation class is dependent the potential of the energy of the flow to transport sediment. Thus, the sedimentation on a specific location is dependent on the incoming transport capacity of the flow, and the loss of transport capacity on the considered location/elevation class. The loss of transport capacity of the flow is from now on defined as flow dissipation. Flow dissipation occurs when flow enters an area with more space for the flow to disperse and lose its energy, which was used to transport sediment. Additionally, the change in the angle of incidence of the waves along the spit also results in wave-driven flow dissipation.

The increase in space for flow dissipation can occur if the path of the flow gets wider, for example where the spit gets smaller, or when the bathymetry gets deeper, for example, during flow over the platform boundary. The increase in space is limited on the platform level because of its depth. Thus, the potential of the energy of the flow to transport sediment needs to be low enough on the platform level for sedimentation to occur there. Otherwise, most material will accrete on the sub-platform level where space (in depth) for flow dissipation is sufficient (Figure 6).

So, the ratio between the accreted volumes on the platform level and accreted volumes the sub-platform level can be deduced from the incoming transport capacity of the flow, represented by the incoming flow velocity: v_{in}, and the dissipation of flow on the platform level. This ratio is in this paper defined as the sedimentation ratio,

$$r_{sed} = \frac{sed_{plat}}{sed_{sub-plat}}, \quad \textit{Equation 2.}$$

here r_{sed} is the sedimentation ratio, sed_{plat} the accreted volume on the platform level and $sed_{sub\text{-}plat}$ the volume on sub-platform level. For each gridpoint at each degree it was determined if the point was originally on the platform level or the sub-platform

level. With this the volumes accreted on the platform level, and the volumes accreted on the sub-platform level, can be calculated for each degree. The space for flow dissipation on the platform level can be expressed with the area of the platform, on which most sedimentation occurs. This is calculated by the sum of the area of every gridpoint on the platform, where generally more sedimentation occurs than erosion.

Results

Although the two Marker Wadden spits are located in the same region, the morphodynamic developments and hydrodynamic drivers differ substantially. The goal is to quantify the link between morphological spit behaviour and hydrodynamics for each of the two spits, to explain the spit growth processes.

Flow around the spit

For every direction around the spit the flow direction and velocity was computed (Figure 8a). Flow directions around both spits stay relatively constant as wind velocities increase. The direction of the current is mostly dependent on the wind direction and changes gradually when moving around the spit. Currents along the southern spit are caused by both lake circulations and waves, increasing both if wind velocities increase. The northern currents at the northern spit are both caused by lake circulations and waves while the current coming from the south and flowing to the north can only be caused by lake circulations as that area is sheltered from waves (Figure 8 b).

Because the consistency of current directions at

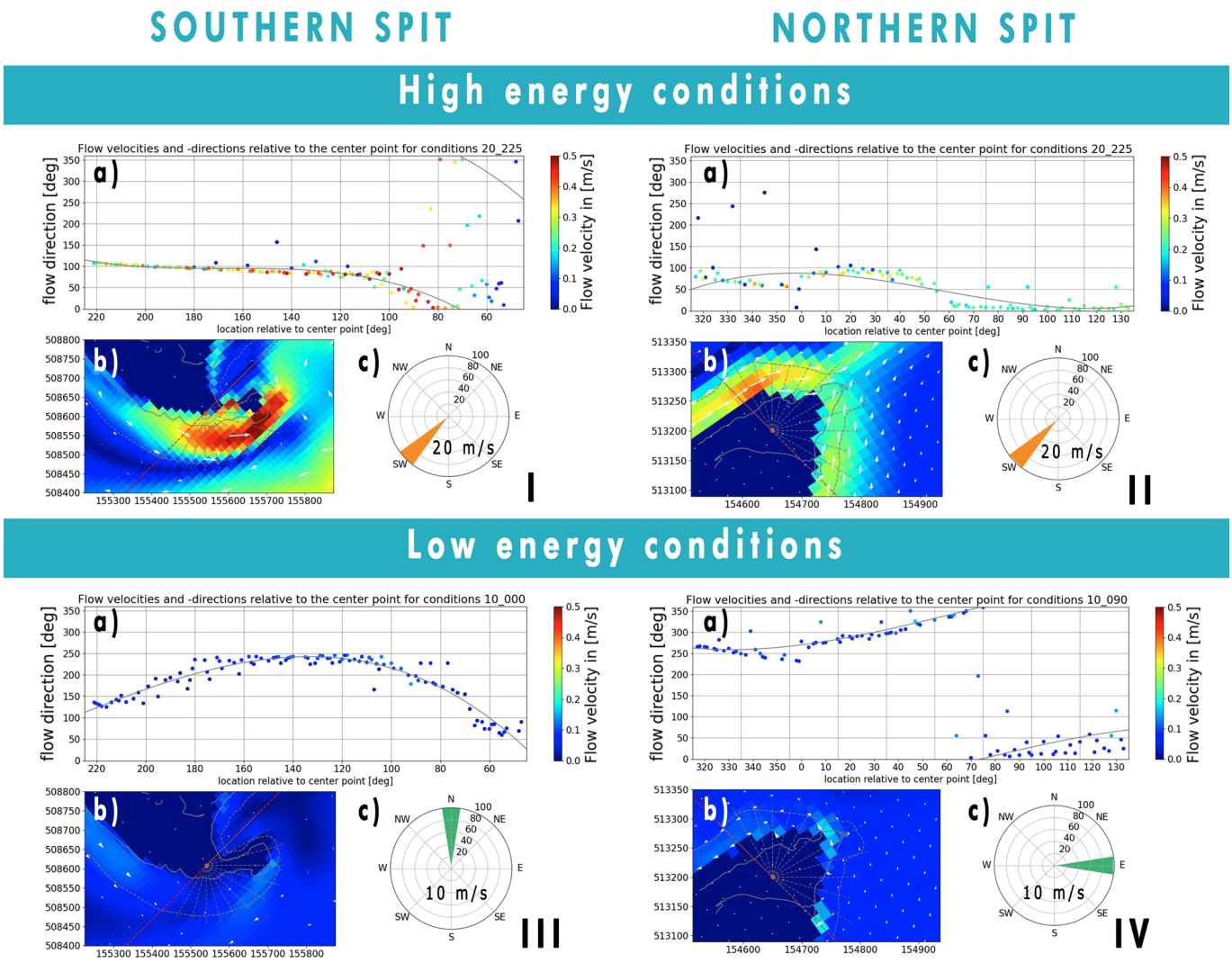

Figure 8. Examples of current patterns and velocities during different conditions. a) Fitted in grey to obtain a distribution of current directions and velocities along the spit for each of the 32 scenarios. Flow velocities are indicated by the colour scale. b) Visual current directions (arrows) and velocities (colours) around both spits. The grey polar lines indicate how far from the centre point the currents are concerned. c) The windrose gives the wind conditions that are modelled.

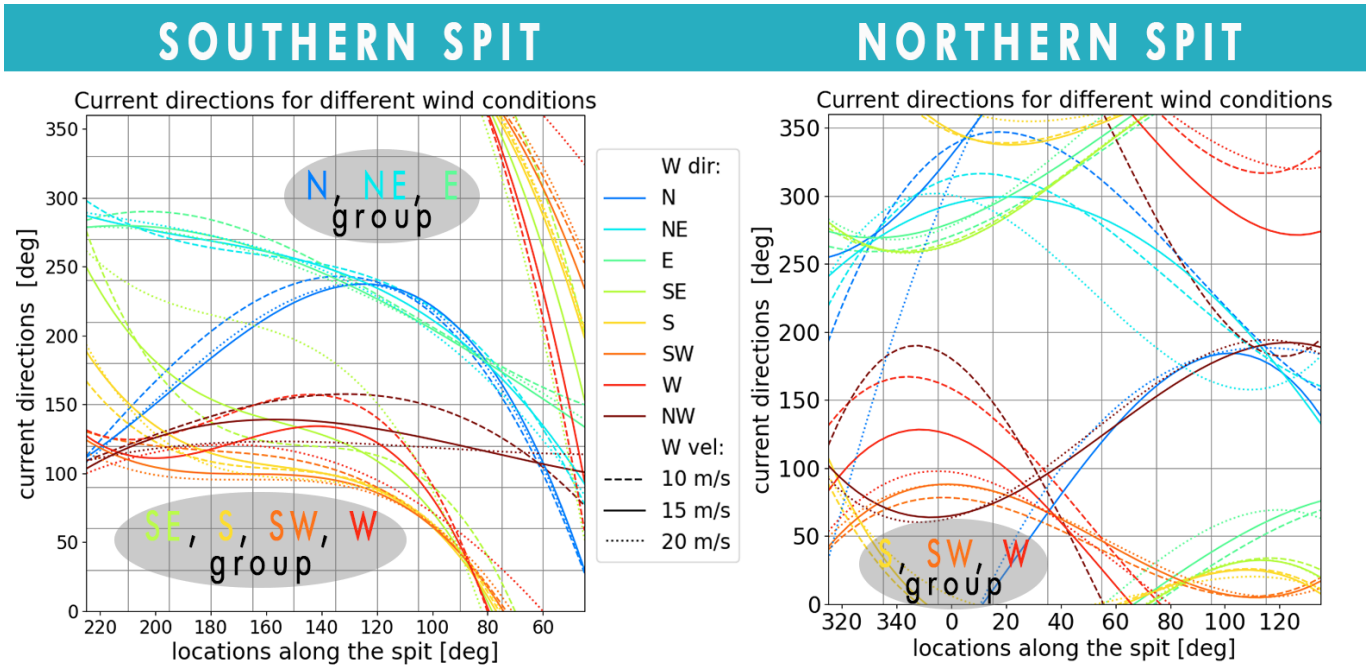

Figure 9. Current directions around both spits for different wind conditions. Currents that occur during different wind conditions can be grouped on similarity of the wind induced current directions. (This is further used in section: Growth orientation linked to flow).

increased winds velocities, different groups can be distinguished based on similarity. In the case of the southern spit winds from the SE, S, SW, and W all have similar current directions, especially near the spit tip. The same holds for the northern spit for winds from the S, SW, and W (Figure 9). Additionally, when wind velocities increase, flow velocities also increase, but distribution of the flow velocity around the spit remains constant. For instance, a location where flow velocities increase at slower winds is also a location where they increase for higher winds and vice versa.

Spit growth quantification

Spit growth can be quantified based on accreted volumes around the spit. For every direction (one degree) around the spit, sedimentation volumes are divided over the different elevation levels (Figure 10a and Figure 11a). This shows the locations where sedimentation is concentrated, thus significant spit growth occurs, and the locations where growth is limited. Erosion (red) occurs on the scarp, at the proximal end of the spit and sedimentation (blue) occurs on the distal end (Figure 10b and Figure 11b). If deposits are found at directions with gradually higher or lower degrees in succeeding periods, this can indicate that the spit grows towards a certain curvature. Deposits that occur constantly at a certain orientation relative to the centre point indicate a growth direction trend of the spit.

For both the northern spit and the southern spit there is a clear range of directions around the centre in which the sedimentation is multiple times higher than on other parts around the spit, especially on the sub-platform level (Figure 12). This range of directions with significantly higher accreted volumes indicates the propagation direction of the spit and is fairly constant over all different morphological periods, which can experience different wind conditions (Figure 10 and Figure 11).

The morphological behaviour is different for periods with high-energy conditions than for periods with lower energy conditions, which is indicated by the windroses (Figure 10 and Figure 11, Figure 10 c and Figure 11 c). In periods with faster wind velocities, thus faster flow velocities, more erosion occurs at the proximal end creating a scarp, more sedimentation occurs in general, and more sedimentation occurs on the sub-platform level, relative to the platform level (Figure 10 and Figure 11). This last observation indicates that when flow velocities are high, the transport capacity is too high on the platform level, and decreases insufficiently, for sedimentation on top of the spit-platform to occur.

Because the distribution of material around the spit is so similar between different periods, a general distribution of material was made based on all data. The distribution of material in volumes, that

have accreted at different degrees around the centre point for the whole measured timeseries, indicates the likely percentage of the total sedimentation that accretes on a location/degree around to the centre point (Figure 12). For example, for the southern spit at 100° degrees relative to the north, around 1,25% of the total sedimentation volume accretes. For the southern spit the main sedimentation direction, and thus propagation direction, is between 70° and 120° degrees orientated from the centre point, while for the northern spit this is between 45° and 70° degrees. Figure 10a, Figure 11a and Figure 12 denote that the sediment supply to the northern spit is less than half of the supply of the southern spit. This explains the smaller developments that are seen at the northern spit.

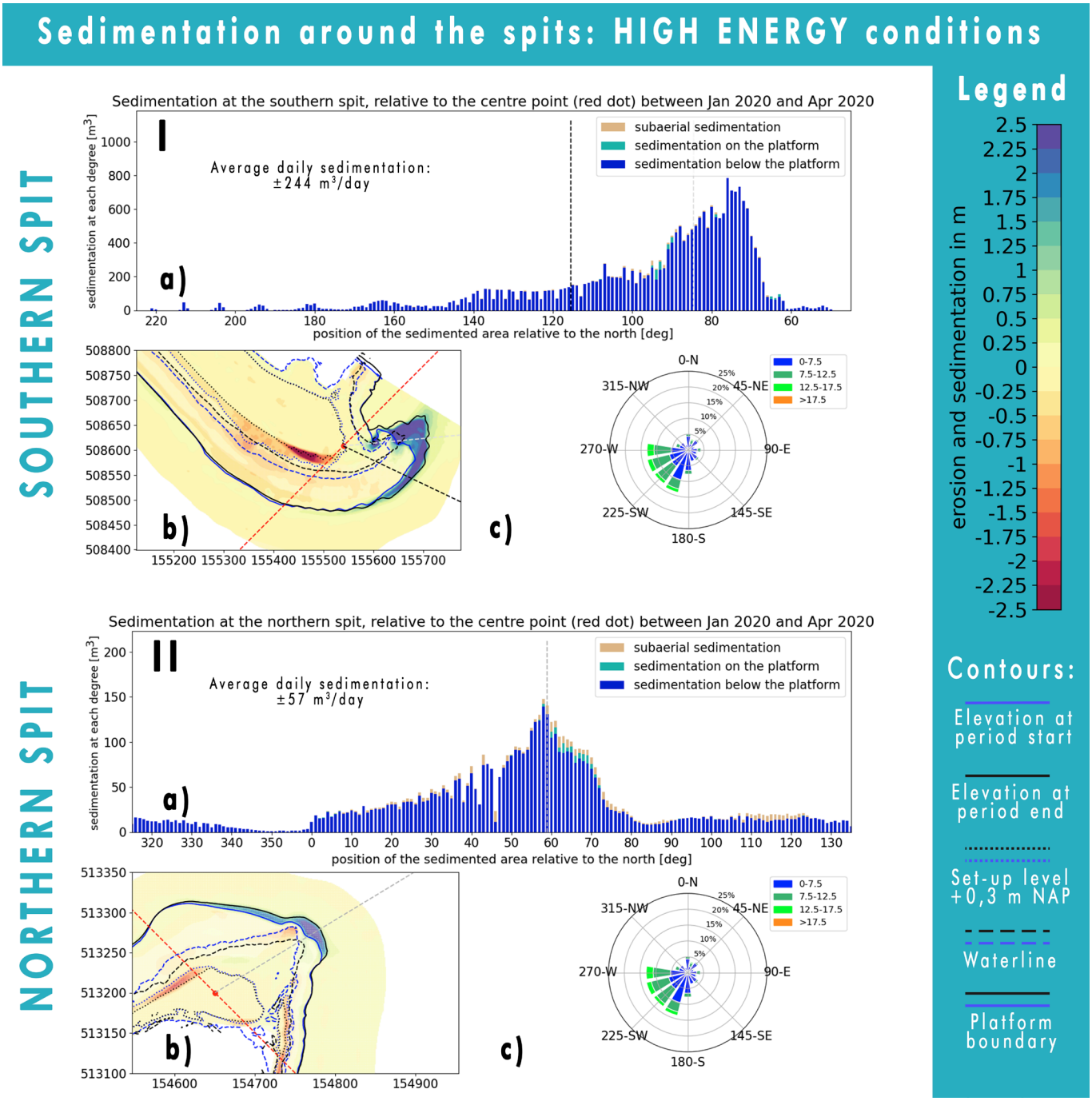

Figure 10. Examples of sedimentation patterns on both spits during high-energy periods. a) Each bar gives the sedimentation that occurred in the period on that particular direction. In the bar graphs the grey lines indicate the centre of mass of a distinguishable deposition. The difference in the elevation of sedimentation locations can be seen by the size difference between the sub-platform level (blue) and the platform level (turquoise). b) A visual representation of the location of sedimentation (blue) and erosion (red). c) The windrose gives the wind conditions during the period.

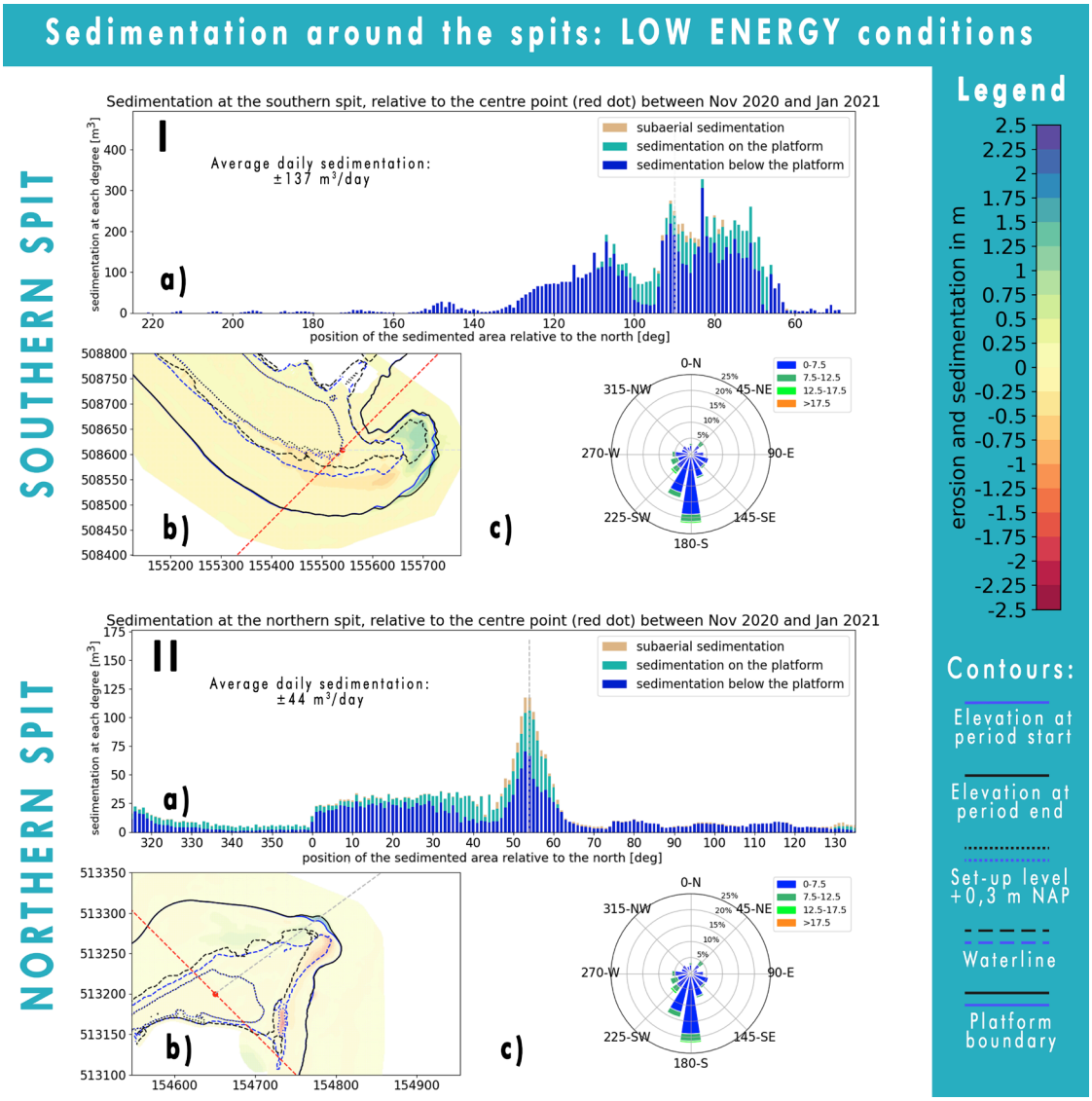

Figure 11. Examples of sedimentation patterns on both spits during low-energy periods. a) Each bar gives the sedimentation that occurred in the period on that particular direction. In the bar graphs the grey lines indicate the centre of mass of a distinguishable deposition. The difference in the elevation of sedimentation locations can be seen by the size difference between the sub-platform level (blue) and the platform level (turquoise). b) A visual representation of the location of sedimentation (blue) and erosion (red). c) The windrose gives the wind conditions during the period.

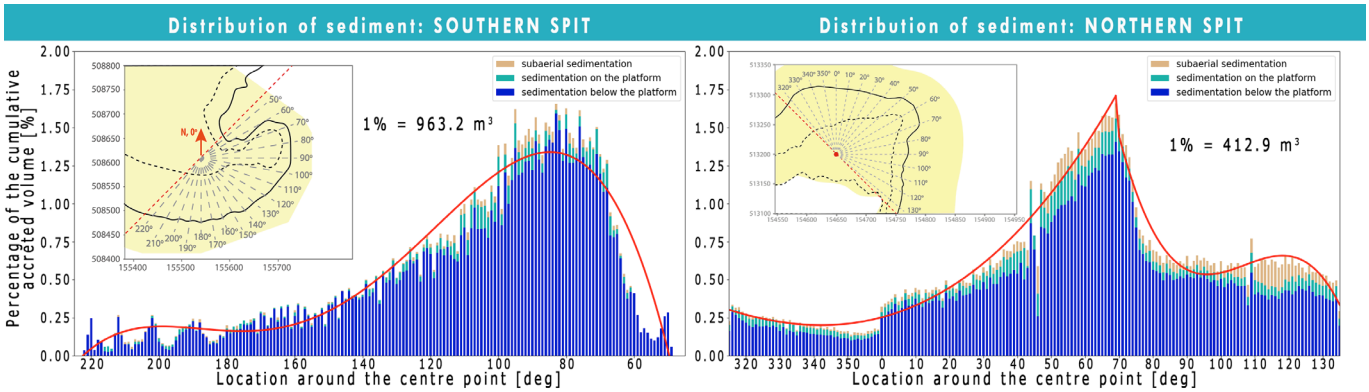

Figure 12. Distribution of sediment around both spits for the total measurement period (Sep 2018 - Jul 2021). Each bar gives the percentage of the total sedimentation that occurred on that particular degree. With a fitted non-linear relation for the distribution of total sediment in red. The distribution in the elevation of sedimentation locations can be seen by the size difference between the sub-platform level (blue) and the platform level (turquoise).

Growth orientation linked to flow

The exact location of an accreted deposit is dependent on the sediment transport by a current or multiple different currents from different wind conditions. A current is essential for large-scale sedimentation if it delivers sediment to the location that experiences most spit growth, thus flows from or by a sediment source to the sediment sink. In the case of the Marker Wadden this means that the current must flow from the areas with significant erosion (the scarp for example) to the location with the highest volumes of sedimentation, the propagation direction.

In the same manner of reasoning the current must flow to a location where flow dissipation can occur. For example, over the platform boundary and around the waterline where waves slowly lose energy. Also, currents that occur more frequent

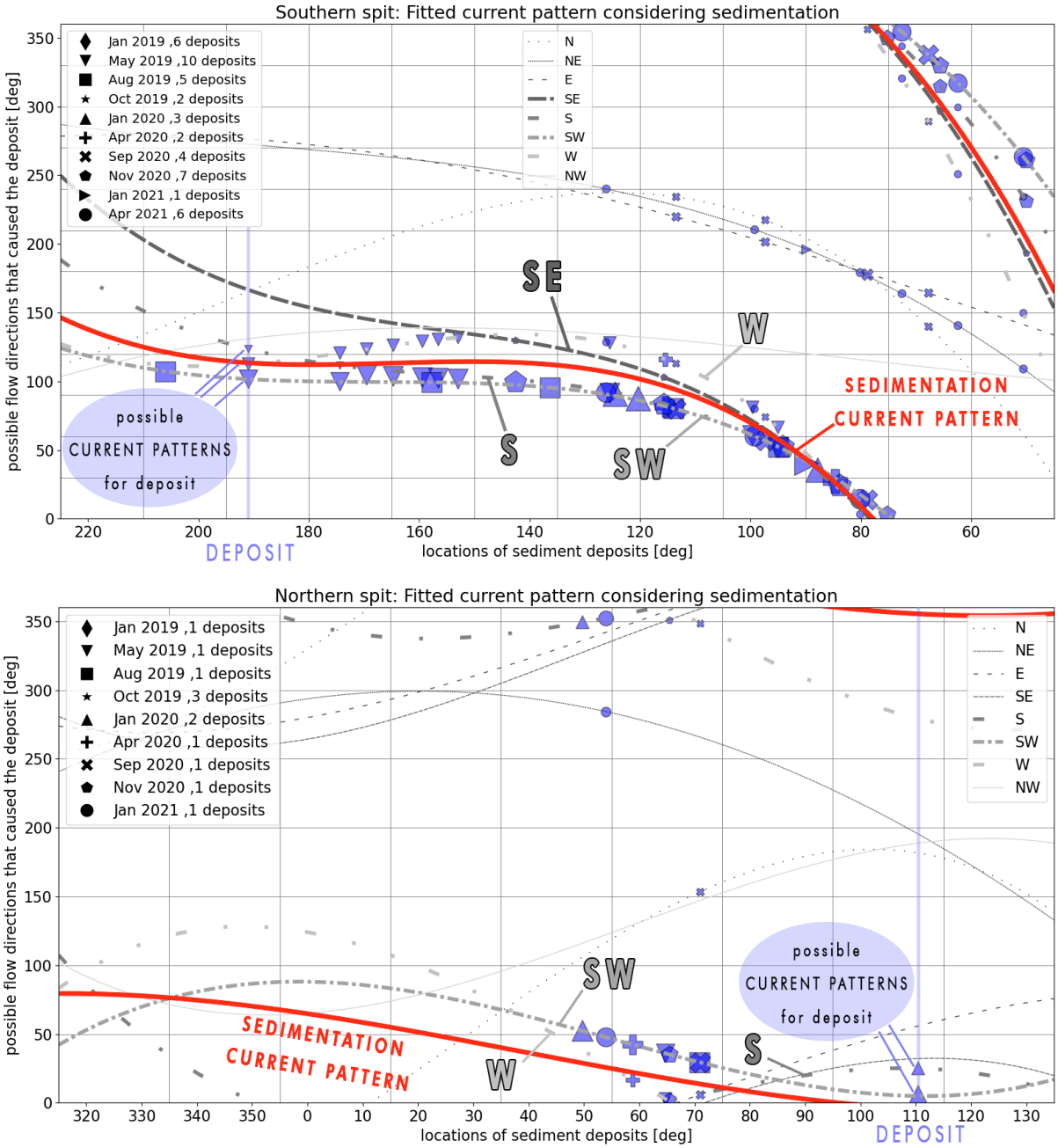

Figure 13. The sedimentation current pattern that is mainly responsible for sedimentation (red). The blue markers indicate a deposit during a morphological period. This deposit can be caused by a number of current patterns. When a current pattern occurs more than 5 percent of the time it becomes a possible current for this deposit and gets indicated by a marker. The size of the marker indicates the occurrence of the current and the more likely it is that it has caused the deposit (in this case only flows where considered, created by winds higher than 7,5 m/s). The currents that are the most likely driver of most deposits are indicated by thick lines.

can build up larger deposits at a certain location. Likewise, similar currents that lose energy at the same location also can build up larger deposits.

Considering these criteria there is a limited amount of currents, which occur during different conditions, that do have a large effect on the sedimentation that was observed during spit growth quantification. The 'sedimentation current pattern', as it is called from now on, is the averaged combination of these currents (Figure 13).

Currents that occur often have similar flow directions at the locations where most deposits are situated, indicating that there is an average current pattern that can be considered as the main driver for spit developments (Figure 13). For the southern spit this sedimentation current pattern is the combination of currents caused by SE, S, SW and W winds, while for the northern spit the S, SW and W winds are used.

This sedimentation current pattern can be combined with the distribution percentage of the total sedimentation, around the centre point, from Figure 12 (Figure 14,I and II), indicating the accreting current directions at the locations with most sedimentation. The flows closest to the beach transport the most sediment, from the beach and scarp at the proximal end. These flows eventually pass over the spit-platform boundary at the locations where most sedimentation takes place (Figure 14,III (b) and IV (b)). Thus, the flow dissipation that arises as the flows pass over the spit-platform boundary, is a very important mechanism for the growth direction of the spits.

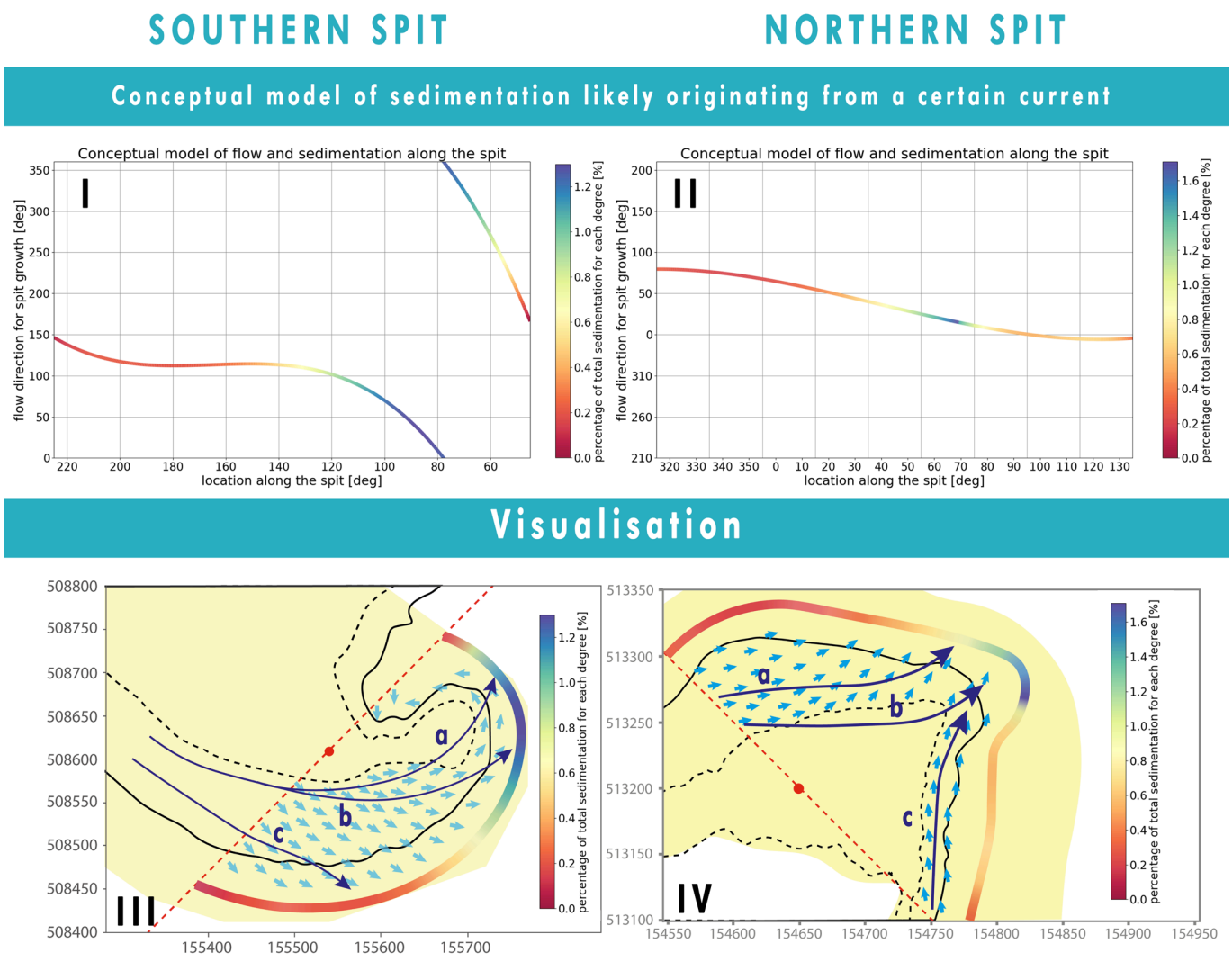

Figure 14. Representative sedimentation current pattern that is responsible for the observed spit growth directions, with distribution of sediment around the spit indicated by the colours, the sedimentation current pattern indicated with the line itself (I and II) and light blue arrows (III and IV) and the paths of sediment indicated by the dark blue arrows (III and IV).

The northern spit has a straight shape, which can be attributed to the lake circulation currents that result in longshore currents approaching from two sides (Figure 14 IV). These currents each transport sediment and erase the hook that is created by the opposite current, resulting in a simple spit (Rossel & Westh, 2020). The curved shape of the southern spit can partly be attributed to the change in wave angles, but also to the small circulation cell nearby caused by a sand mining pit to the south, that curves the current. The derived average sedimentation current pattern, indeed only starts to curve significantly when the circulation cell starts to affect the current coming from the beach (Figure 14 III (b)). This change in direction might be an important factor in the bend that is formed on this spit.

Sedimentation on elevation levels

During high-energy periods almost all sedimentation occurs on the sub-platform level while there is a more even distribution of material between the platform level and sub-platform level during lower energy periods (Figure 10a and Figure 11a). This indicates that the submerged and emerged growth of the spit is dependent on the energetic conditions during a period. The sedimentation ratio (r_{sed}, Equation 2) depends on the transport capacity of the flow on the platform level that should be low enough for sedimentation on this level.

The incoming transport capacity is represented by the incoming flow velocity (v_{in}) while the flow dissipation on the platform level is represented by the platform area on which sedimentation occurs. Also, the platform area takes into account that it is more likely that descending sand grains are 'caught' by the spit-platform if the platform is larger.

The elevation on which sedimentation occurs is dependent on wind energy. This indicates that the emerged spit and spit-platform do not grow simultaneously. When flow velocities are high, most sedimentation occurs on the sub-platform level. When the spit-platform is large, more sedimentation occurs on the platform level. And this also works the other way around. It means that the shape of the spit-platform is essential for the growth of the emerged spit. Both the spit-platform and emerged spit influence each other's growth.

The platform area and flow velocity (v_{in}) do not have an equal contribution when it comes to the sedimentation ratio (r_{sed}). Nor are they the only parameters of effect. By multiplying the platform area with the flow velocity on the x-axis (Figure 15), and by giving the flow velocity a negative weight (a

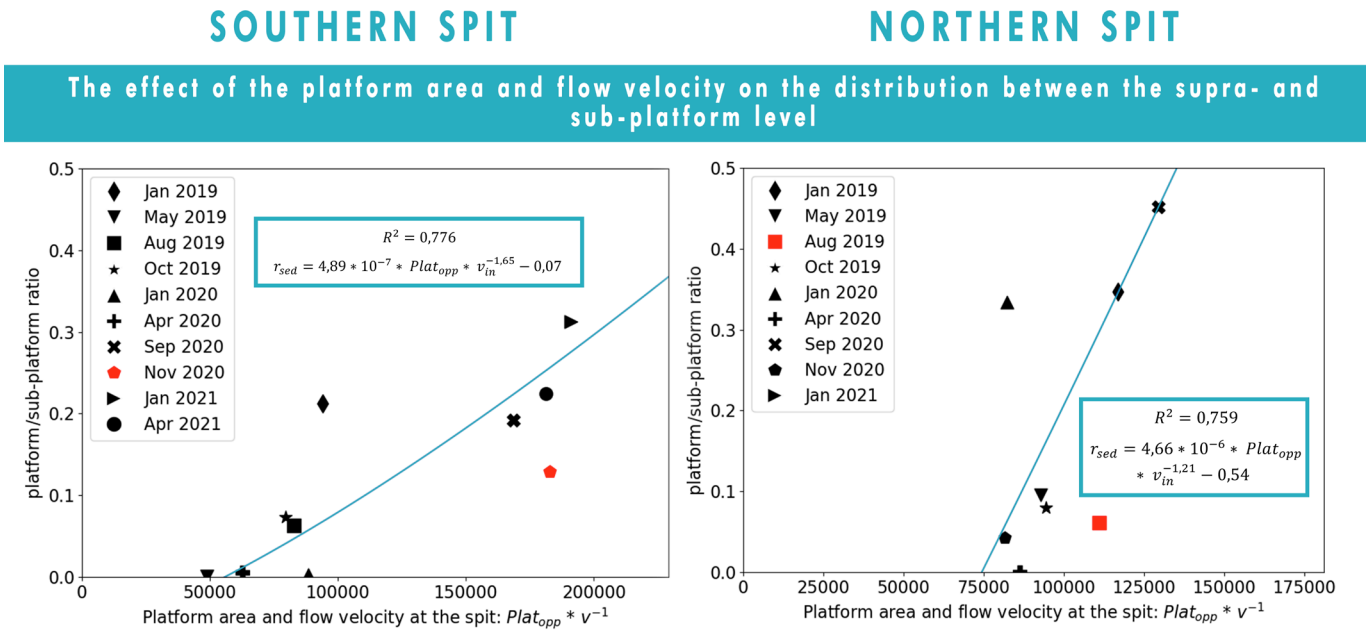

Figure 15. The relation (best fit) between the platform area and flow velocity and the sedimentation ratio. On the x-axis we find the size of the platform at the start of a period divided by the flow velocity during this period. The indicated date is the date on which the measurement is taken, thus the date at the end of the considered period. In red the outlier periods are indicated. These points where likely affected by an erosion event that eroded the sedimentation on the platform, resulting in a relative low ratio. The height of R^2 indicates the quality of the approximation.

large area and a small flow velocity have the same effect on the ratio), the best fit for the contribution of the platform area and flow velocity can be found. Thus, there is an empirical fitted relation, specific for every spit, that approaches the ratio of sedimentation (r_{sed}) on the platform level and the sub-platform level with the platform area and flow velocity (v_{in}) (Figure 15). These relations can indicate what main drivers were responsible for the observed emerged and submerged spit growth.

Both fits can approximate the sedimentation ratio (r_{sed}) relatively well with two parameters (Figure 15). The fits have roughly the same accuracy, which is relatively high but cannot be improved any further as the platform area and incoming flow velocity (v_{in}) are not the only parameters that can affect r_{sed} (equation 2). The exponent on v_{in} is the exponent for which the accuracy of the fit is highest and is purely a representation for the importance of v_{in} relative to the platform area for the sedimentation ratio. For both spits this exponent shows that the higher the incoming flow velocities are, the more important this parameter becomes for the sedimentation ratio. This effect is more severe for the southern spit than for the northern spit. The first number of the best fit represents the slope of the fit which is not the same for the southern and northern spit. All in all, the effect of the incoming transport capacity and the loss of this capacity at the platform level on the sedimentation ratio (r_{sed}) can be approximated well with the incoming flow velocity and platform area.

In Figure 15 outliers are present for both spits because they are periods that had relatively calm conditions with a very short moment of high flow velocities near the end of the period. It is likely that these events eroded away material on the platform level and therefore resulted in a relatively low r_{sed}. Other phenomena were also not incorporated in the approximation, like the different behaviour of the southern spit when it started to form (Jan 2019). But keeping in mind that v_{in} and the platform area are not the only important parameters for r_{sed} it was chosen to keep this data in the approximation. However, the erosion processes are not considered in this method of analysis and therefore excluded.

Predictive potential of found relations

The fitted empirical relations of the sediment distribution around the spit (Figure 12) and the fitted sedimentation ratio (r_{sed}) allow for a detailed approximation of the three-dimensional distribution of material around the spit as a result of different energetic conditions for each specific case. Therefore, an empirical relation of the sediment supply or total sum of sedimentation volumes around the spit, would make it possible to give an estimate of where, what volumes will accrete because of certain wind conditions. This gives the novel method a predictive potential and makes it possible to predict future shapes of both spits at the Marker Wadden.

The total amount of sedimentation can be approximated by the incoming transport capacity and therefore incoming flow velocity (v_{in}), because the accreted volumes are higher during higher energetic conditions (Figure 10a and Figure 11a). Also, large-scale sedimentation is caused by the currents that make up the sedimentation current pattern (SE, S, SW and W winds for the southern spit). Therefore, the probability of occurrence of these currents determines the amount of sediment that is supplied to the areas of largest growth. So, the sedimentation per day in a period can be approximated in the same manner as in Figure 15, but by using the flow velocity during a period and the percentage of occurrence of sediment supplying wind conditions, thus the occurrence of the sedimentation current pattern (Figure 16).

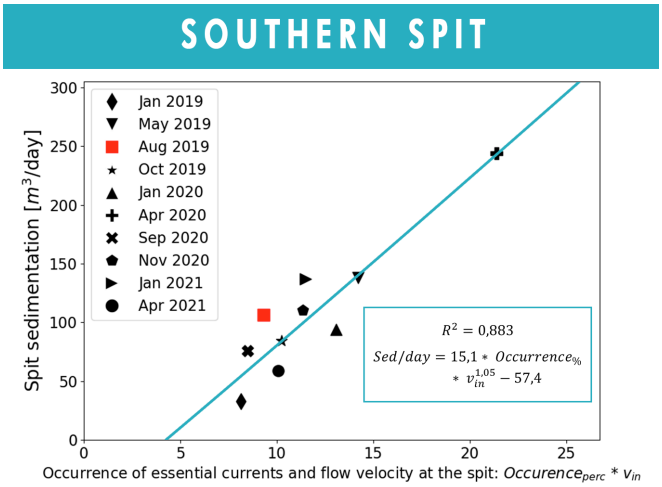

Figure 16. Sedimentation per day, dependent on the occurrence of wind conditions that drive sediment supplying currents, and the incoming flow velocity. On the x-axis we find the occurrence of wind conditions that make up the sedimentation current pattern during this period multiplied by the flow velocity during this period. The indicated date is the date on which the measurement is taken, thus the date at the end of the considered period. The height of R^2 indicates the quality of the approximation. The red outlier is not considered as a nourishment took place during that period.

This empirical relation does not pass through zero which bolsters the fact that morphodynamics in low-energy environments is dependent on higher energy events. So, indeed a minimum flow velocity is needed for large scale sedimentation. Also, the occurrence of the sedimentation current pattern and the incoming flow velocity (v_{in}) have almost the same relative importance (exponent of v_{in} is almost 1). This indicates that both flow directions and flow velocities are very important for the magnitude of sedimentation.

The accreted volumes on the platform level and the sub-platform level can be calculated for each direction around the spit, using the polar coordinate system, if the wind conditions of a period are known. By simplifying the topography to a schematic representation of an emerged part (which is filled by platform sedimentation) and a submerged spit-platform (which is filled by sub-platform sedimentation) predictions of the new locations of the coastline and platform boundary can be made for each degree around the spit, depending on the wind conditions of a period (Figure 17).

To investigate the predictive potential of the found empirical relations, a year of developments of the southern spit (Apr 2021 – Mar 2022) have been approximated. This year is a well-balanced representation of the diversity of conditions that can occur at the Marker Wadden islands, with large storms like Eunice and Franklin but also calm summer conditions. By using the wind conditions as input, predictions have been made for the new coastline and platform boundary. These predictions are compared to the actual morphological changes (Figure 18). Especially the predictions of the submerged spit-platform are very close. In general, the predictions for the emerged spit are also adequate, but the emerged spit has much more processes that can affect the three-dimensional shape and is therefore harder to fully predict.

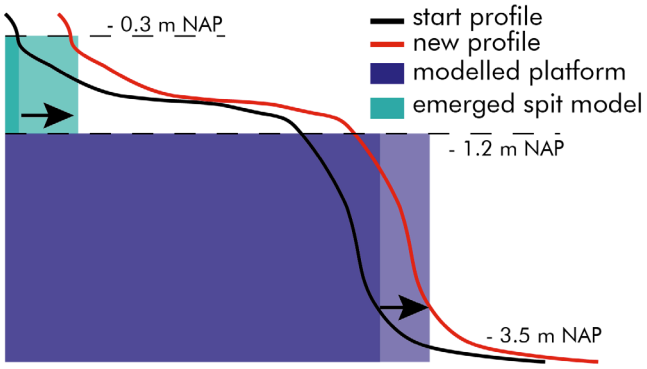

Figure 17. Schematic representation of how the cross-sectional growth of the spit is modelled. If the emerged part of the spit should grow in reality (start profile to new profile) at a certain degree relative to the centre point, the turqoise bar at that degree increases. The same holds for the spit-platform and the blue bar.

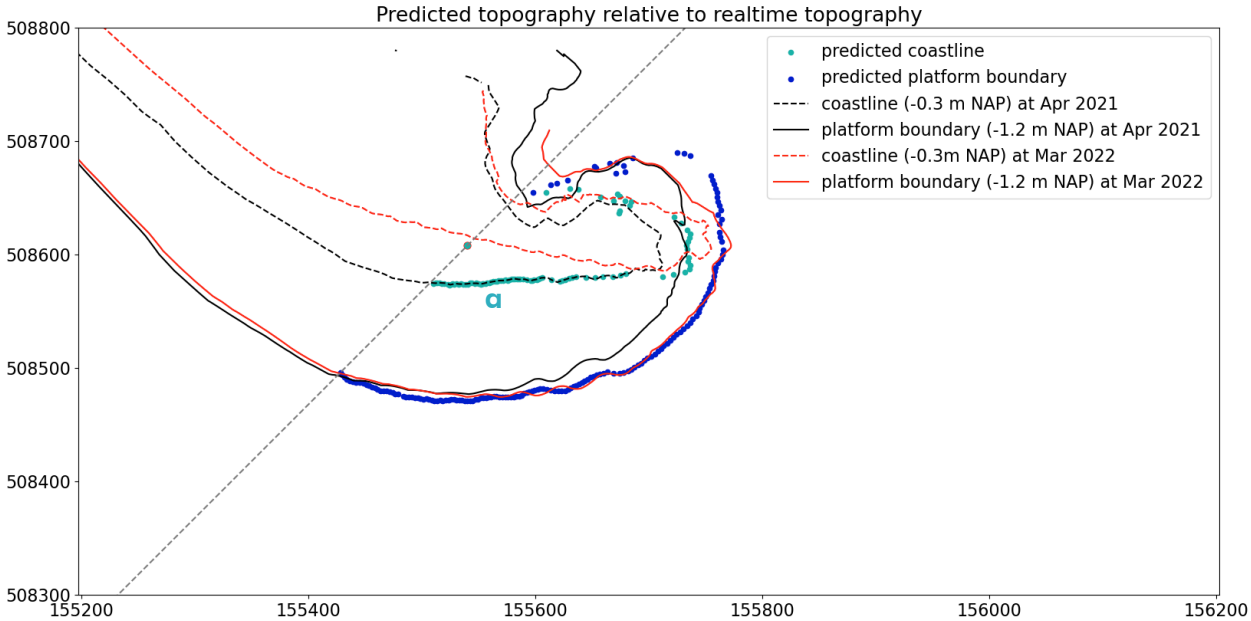

Figure 18. Predicted coastline and spit-platform boundaries for the year Apr 2021-Mar 2022, compared to the real spit developments in that year. The prediction is based on the found empirical distribution of sediment around the spit, the empirical ratio between platform sedimentation and sub-platform sedimentation and the empirical relation for the total sedimentation as a result of currents caused by certain wind conditions.

Discussion

Key drivers for spits in low-energy lakes

The loss of transport capacity of sediment rich currents at a location with immediate changes in shoreline orientation is designated as the key concept behind spit growth in literature. This loss of transport capacity can come in many forms, which can drive many forms of spit growth. Uda (2018) stated that spits grow because the flow enters a location where there is more space for the flow to disperse and lose energy, while others contributed the shape of a spit to the change in wave angle along a curving coastline, which results in a flying spit for high wave angles and a recurved spit for low wave angles (Ashton et al., 2016; Ashton & Murray, 2006). Quantification of spit processes and developments can be used to great effect to find the detailed form of these concepts around transport capacity loss, in complex environments like low-energy lakes.

The key process that dictates the spit growth of both spits in this low-energy lake environment are the sediment rich currents that make up the sedimentation current pattern, that transport material over the spit-platform boundary at a specific location (Figure 14 III, a/b and Figure 14 IV, b). At these locations flow gets dispersed because of the drastically increasing depth, sedimentation occurs at the sub-platform level and therefore the spit-platform increases in length. Thus, this makes the spit-platform grow in a certain direction (Figure 12). A larger platform means more flow dissipation on top of this platform, which results in sedimentation on the platform level, and therefore the emerged spit part grows in length (Figure 15) in roughly the same direction as the spit-platform (Figure 12).

Thus, for the absolute spit growth that is observed, the energy loss because of flow dispersion in expanding space and the resulting spit-platform growth is of more influence than the mechanism described by Ashton et al., (2016). For the Marker Wadden, the effect of waves on absolute spit growth is limited, which can be expected in an area where wave energy is limited (Ton et al., 2021). With the exception that the waves do have a large influence on the direction of the sedimentation current pattern and therefore influence the propagation direction of the spit-platform.

However, waves do have a significant effect on the shape of the emerged spit as that is above the depth-of-closure (Ton et al., 2021). The transport capacity does decrease on the platform level as the angle of incidence of incoming waves change. Waves are also important in the stirring-up of sediment around the coastline and emerged spit. This results in erosion near the proximal end, which is important for the complete shape of the emerged spit, and is important for the sediment supply towards the distal end.

The submerged spit-platform and the emerged spit do not grow simultaneously at the same pace. Meistrell (1966) stated that growth of the submerged spit-platform is essential for the development of the emerged part of the spit. The calculations indeed show clearly that a small spit-platform has negative effects for the longitudinal growth of the emerged spit. In analytical modelling of spits for example, the submerged part and the emerged part are assumed to grow with an equal pace (Kraus & Asce, 1999; Palalane et al., 2014). In this case however the submerged spit-platform and emerged spit almost work as two separate entities influencing each other and thriving under different wind conditions (Figure 15 and Figure 17).

Simplifications, assumptions and inaccuracies

The main source for inaccuracies in understanding the development of the spit shape, especially in the approximation of the sedimentation ratio (Figure 15), is the fact that erosion has barely been considered in the analysis. Erosion was left out because the main focus was finding the dominant drivers behind spit growth and the effect this specific growth has on the main shape. Taking erosion into account would have been possible, in the same way as has been done for sedimentation. However, this would have made the analysis more complex and less efficient. More parameters would have to be included and therefore, would have made discovered relations and simplifications less clear. Nevertheless, including erosion can give more insights into the complete spit morphology and therefore including or excluding erosion from the analysis should depend on the aim of the study.

The effect of the neglect of erosion can clearly be seen in the predictive model (Figure 18). This very simple model is used only to illustrate the

possibilities to do predictions with this quantifying method. The growth of the submerged spit-platform can be approximated very well, and the growth of the emerged part is close. However, the shape of the emerged spit does not resemble the shape in reality (Figure 18a). This is because only sedimentation is calculated, while in reality a large part of the sedimentation at the emerged spit is eroded away by waves. The reason for this erosion is that contrary to everything below the spit-platform boundary, the emerged spit is above the depth-of-closure (Ton et al., 2021). Also, a spatial distribution of the spit-platform ratio would have made the prediction more accurate. At least erosion and a spatial distribution need to be added to be able to fully predict the three-dimensional shape of spits but the potential of using the relations acquired by this method of quantification to do predictions for spit growth, is promising.

A large part of the empirical relations that resulted from this method of quantifications were found by linking the growth orientation of the spit to the flow directions. This made it possible to express the distribution of sediment around the spit as the result of a single sedimentation current pattern. This sedimentation current pattern is an average of currents that occur during different wind regimes, that are of importance for large scale sedimentation (Figure 13). This simplified representation of processes around the spit neglects hydrodynamic drivers that have a less pronounced role. For example, for the southern spit, currents caused by N to E wind regimes, do result in sedimentation around the spit, although this is eventually neglected in the sedimentation current pattern as sedimentation because of these wind regimes is relatively small due to their limited sediment supply and occurrence. However, the sedimentation current pattern (Figure 14) does represent reality well considering the accuracy of the predictive model (Figure 18). This is because only the currents that are important for large scale sedimentation have been considered for the averaged sedimentation current pattern. Only considering the hydrodynamics that are of essence for sedimentation can therefore be a fast method to examine the drivers behind spit growth as long as currents in the system that are important for sedimentation, are relatively similar and can be grouped in a limited number of groups (Figure 9).

The spit-platform area is a useful parameter to represent flow dissipation on the platform level. However, it does not represent loss of transport capacity one-on-one. For example, the parameter represents the increase in space, for the flow to disperse, well. But in this case the decrease in transport capacity because of the changing angle of incidence is underrepresented with this parameter. The fact that the incoming flow velocity and especially the platform area represent physical processes instead of being physical process by themselves, explains the differences between the two best fits for the sedimentation ratio (Figure 15). For example, the platform size is much smaller for the northern spit than for the southern spit, because the entire northern spit is smaller. Therefore it is not surprising that the slope of both fits is different. This could be mitigated to some extend by using a parameter like platform area divided by the area of the entire spit.

Also, the platform area does not seem to be the best parameter to symbolize platform bathymetry. When energy dissipates particles do not drop down immediately but slowly descend while going with the flow. The platform must be large enough to 'catch' this particle. So essentially, sediment particle path length, would be a better parameter but this is hard to quantify. However, this is possible by using a morphodynamically validated Delft 3D model for example. The spit-platform area on the other hand, is physically not the best parameter to use but it is a very efficient parameter to work with. Thus, a careful trade-off needs to be made between the efficiency and accuracy of the analysis before determining a parameter to represent flow dissipation on the platform level.

Sediment supply is an important parameter that can be affected by all sorts of phenomena, like storage of material in sand banks and aeolian transport. For the Marker Wadden islands, the occasional collapse of scarps at the proximal ends were of significant influence. But also sheltering behind the spit tip, debris, different grain sizes, vegetation, local sand mining, dredging and nourishment operations and wind forcing over the shallow platform are of influence, to name a few.

Lastly, the (model) simplifications and interpolations that are implemented in this paper inevitably result in inaccuracies, as well as the use of different coordinate systems. For example, the interpolation and preprossessing of the pointclouds is done with a Cartesian system while this data is then analysed with polar coordinates.

Possibilities and limitations of the novel method

First of all, the implemented method of quantifying spit relations and developments using polar coordinates and a simplification of the elevations, works well for the applications used in this paper. However, to be able to conclude if this novel method can be applied well for spits in general, instead of only for spits in low-energy environments, more research needs to be done. Other cases of spits also have to be analysed to get more insight into the applicability of the method. Nevertheless, it seems like this method is efficient and flexible enough to be promising for other spit cases.

While most literature focuses on the large-scale spit development, in space and time, this method proves itself effective for analysing spit developments on a small scale. This makes it possible to quantify and analyse young spits and spit tips in a timeframe of a couple of years, in a detailed fashion. The larger the spatial scale the less accurate this method becomes. For example, a deposit on a certain direction may be very close to the centre point but may also be a kilometre away. Increasing the temporal scale mitigates this problem to some extend as detailed sedimentation becomes less interesting and can be disregarded. Only, considering the main sedimentation locations and growth trends can filter out a lot of the mistakes that are made at a large spatial scale.

This method is also useful in locations with different kinds of hydrodynamic forcing. Complex currents, like in this low-energy lake environment, with eddies, lake circulations and an inconsistent wind climate, can be analysed well. The case of the northern spit is, hydrodynamically speaking, different from the case of the southern spit. However, still reliable results could be found, although these spits can be classified in completely different classes. This method is therefore likely also applicable in other environments and is very flexible to work with. It is relatively easy to tailor the method of analysis based on the parameters that are of interest for a specific spit case study. However, one must be wary of using too many hydrodynamic scenarios. In this case for example, only 32 scenarios where analysed which were only dependent on the wind conditions. Once there is a case where tides also play a role this number of scenarios increases significantly, making the analysis much more time consuming. In these cases, it is therefore advisable to see if certain scenarios can be discarded in advance, as they are not likely to be of importance to the spit developments that are of interest.

The largest drawback of this method is that a considerable amount of data needs to be available. Especially morphological data in the form of regular topographical measurements is important. Most spit case studies are executed based on aerial photographs for example which can lead to a subjective and more qualitative analysis of spit growth. To use this more objective analysis of quantifying volumes of material, a frequent series of accurate topographical data, above and below the waterline, is necessary. Although a less frequent series of measurements than used in this paper, will also suffice.

Drone photogrammetry can provide a cost-effective method to acquire this data for the subaerial topography (Casella et al., 2020; Rossel & Westh, 2020). However, as the spit-platform morphology proves essential to research spit developments, some form of accurate bathymetry measurements is also necessary. This bathymetry data can be harder to acquire. Therefore, spits that occur in large engineering projects are useful cases to analyse, as often a lot of data is collected around these projects.

For the hydrodynamic data a 3D model, or 2DH as used in this paper, is desirable but not necessary. Measurement stations, like an Acoustic Doppler Current Profiler for example, that measure flow directions and velocities and are dispersed at a few points around the spit orientated around the centre point, will suffice. For the locations of these stations especially data near the spit tip is key. Of course, using a Delft-3D or a similar model will give a lot more flexibility in exploring spit behaviour under different conditions.

Also, in order to explain and verify quantitative results a thorough understanding of the system is necessary. When setting up the quantification method by picking a centre point and elevation levels for example, the expected hydrodynamic drivers one would want to quantify influence the choices that are made in that stage. Assumptions that are evident for one spit, may be less relevant for the other. Considering the labour intensiveness of the method, it depends on the number of hydrodynamic drivers and the desired level of detail

one would want to analyse. If the centre point and elevation levels are picked well and the system behaviour is clear, this quantification method should take between a couple of weeks to months to apply and verify.

Conclusion

Spits form at places where the coastline drastically changes its orientation, which results in an increase in space for the flow to disperse and lose transport capacity. Schematically the drivers behind different types of spit growth are known. But during the study of a complex spit case, these schematic principles turn out to be difficult to implement. This results in mostly descriptive case studies. To the same extend, the exact mechanisms behind spit growth in non-tidal, wind-dominated, low-energy environments, especially in lakes, have been unknown so far. The specific bathymetry, with significant submerged platforms in front on the coast, and the complex hydrodynamics in these environments makes it necessary to quantify the morphodynamics around spits, like the ones on the Marker Wadden islands, to be able to describe spit growth and its drivers in detail. However, few have managed to link the hydrodynamics and morphology in cases like this (Allard et al., 2008; Héquette & Ruz, 1991).

By using a novel method for data analysis, which uses polar coordinates and simplified elevation classes based on morphodynamic properties, it becomes possible to quantify the spit morphodynamics. This simplification in polar coordinates makes it possible to efficiently describe and quantify processes around the spit in a detailed fashion. Thus, making it possible to objectively pinpoint the case-specific drivers behind different forms of spit growth. The quantification method allows for a detailed analysis of spits in low-energy lake environments by quantifying the spit growth trends and its hydrodynamic drivers in the case of the Marker Wadden. It is therefore recommended to experiment with the use of this method for spit data analysis, on spits in different types of systems.

The key mechanism behind spit growth in the system of the Marker Wadden islands, are the frequent, fast flowing and sediment rich currents that flow over the spit-platform boundary, transporting most material to a certain location. Sedimentation occurs because of the sudden increase in depth and the submerged spit-platform increases in length at this location. The larger the spit-platform the more transport capacity gets lost by the flow on top of this platform. This results in sedimentation on the platform level and growth of the emerged spit. For a large part the growth direction of the emerged spit is thus dictated by the growth direction of the submerged spit-platform. Waves play an important role in the eventual shape of the emerged spit by influencing transportation energy loss of the flow around the distal end and stirring-up the sediment around the proximal end. This makes waves very important for the sediment supply of the spit.

For spits, in the low-energy lake system of the Marker Wadden islands at least, the interaction between the emerged part of the spit and the submerged spit-platform is essential. These components influence each other's growth and do not grow simultaneously. They also grow under different energetic conditions. So, the spit growth in the Marker Wadden islands is for a very large part dependent on the currents that result in the growth of the submerged spit-platform. Lake circulation currents play an important role in the eventual location of sedimentation, especially of the spit-platform. Although the role of waves in the complete spit morphodynamics is also important in low-energy lake environments, it can easily be overestimated when only considering the schematic relations from literature (Ashton et al., 2016; Ashton & Murray, 2006). This should be considered when using computational models, that use LST bulk formula like ShorelineS, to model spit developments in similar environments. Because of the clear presence of a platform in the bathymetry of other low-energy environments and the limited wave energy in these environments (Ton et al., 2021; Vila-Concejo et al., 2020), it is likely that other spits in low-energy (lake) environments have a similar dependency on the growth of the submerged spit-platform for its entire propagation behaviour.

The understanding of spits in lake Markermeer is an important component in the understanding and maintenance of the whole Marker Wadden system. Because spits are such dynamic coastal features, knowing spit behaviour in low-energy environments can give more in-depth insights in the morphodynamics in low-energy (lake) systems. Also, while the contribution of the spit-platform to the complete growth of the spit is often underappreciated in other case studies, this paper

shows that the spit-platform can be a very important component for spit morphodynamics. Negligence of the spit-platform can lead to conclusions that eventually do not agree with the complete reality. During the modelling of spit morphodynamics, in environments like this, it is therefore advised to model the emerged spit and submerged spit-platform as two separate components.

In the end, the quantitative method of analysis turned out to be an elegant method to objectively link spit growth at the Marker Wadden islands to its hydrodynamic drivers in a detailed fashion. Using a similar approach for other environments can be promising but needs to be researched and validated first. As we start to divert more and more from the uniform coastlines and start to engineer our beaches towards, more natural, non-uniform coasts, spits will start to play a larger role on large scale coastal projects. Then a detailed understanding of spit morphodynamics is key in design and maintenance of these coasts. This is exactly what drove the need for this research of spits in the low-energy lake system that is the Marker Wadden and is possibly what will drive the need for a detailed understanding of other spits in the future.

Bibliography

Allard, J., Bertin, X., Chaumillon, E., & Pouget, F. (2008). Sand spit rhythmic development: A potential record of wave climate variations? Arçay Spit, western coast of France. *Marine Geology*, *253*(3–4), 107–131. https://doi.org/10.1016/j.margeo.2008.05.009

Allen, J. R. (1982). *Spits*. https://doi.org/10.1007/0-387-30843-1_432

Ashton, A. D., & Murray, A. B. (2006). High-angle wave instability and emergent shoreline shapes: 2. Wave climate analysis and comparisons to nature. *Journal of Geophysical Research: Earth Surface*, *111*(4). https://doi.org/10.1029/2005JF000423

Ashton, A. D., Nienhuis, J., & Ells, K. (2016). On a neck, on a spit: Controls on the shape of free spits. *Earth Surface Dynamics*, *4*(1), 193–210. https://doi.org/10.5194/esurf-4-193-2016

Boskalis Nederland. (2015). *EMVI 2-LANDSCHAPPELIJKE KWALITEIT VOGELPARADIJS INSCHRIJVING DEEL 2*.

Bouchette, F., Schuster, M., Ghienne, J. F., Denamiel, C., Roquin, C., Moussa, A., Marsaleix, P., & Duringer, P. (2010). Hydrodynamics in Holocene Lake Mega-Chad. *Quaternary Research*, *73*(2), 226–236. https://doi.org/10.1016/j.yqres.2009.10.010

Brideau, L. E., Mercaldi, B., Tait, J., & Vila-Concejo, A. (2022). *Dominant transport processes and beach replenishment on low-energy spits*. https://ssrn.com/abstract=4020787

Bruun, P. (1993). Relation between Growth of a Marine Foreland and Sea Level Rise Case: The Skagen Spit, North Jutland, Denmark. In *Source: Journal of Coastal Research* (Vol. 9, Issue 4). Autumn.

Casella, E., Drechsel, J., Winter, C., Benninghoff, M., & Rovere, A. (2020). Accuracy of sand beach topography surveying by drones and photogrammetry. *Geo-Marine Letters*, *40*(2), 255–268. https://doi.org/10.1007/s00367-020-00638-8

Davidson-Arnott, R. G. D., & van Heyningen, A. G. (2003). Migration and sedimentology of longshore sandwaves, Long Point, Lake Erie, Canada. *Sedimentology*, *50*(6), 1123–1137. https://doi.org/10.1046/j.1365-3091.2003.00597.x

Davidson-Arnott, R., Ollerhead, J., & Davidson-Arnott, R. C. D. (1995). *BUCTOUCHE SPIT, NEW BRUNSWICK*.

Evans, O. F. (1942). *The origin of spits, bars and related structures*. http://www.journals.uchicago.edu/t-and-c

Héquette, A., & Ruz, M.-H. (1991). Spit and Barrier Island Migration in the Southeastern Canadian Beaufort Sea. In *Source: Journal of Coastal Research* (Vol. 7, Issue 3).

Jin, H., van Leeuwen, C. H. A., van de Waal, D. B., & Bakker, E. S. (2022). Impacts of sediment resuspension on phytoplankton biomass production and trophic transfer: Implications for shallow lake restoration. *Science of the Total Environment*, *808*. https://doi.org/10.1016/j.scitotenv.2021.152156

Kraft, J. C., Allen, E. A., & Maurmeyer, E.

M. (1978). THE GEOLOGICAL AND PALEOGEOMORPHOLOGICAL EVOLUTION OF A SPIT SYSTEM AND ITS ASSOCIATED COASTAL ENVIRONMENTS: CAPE HENLOPEN SPIT, DELAWARE t. In *JOURNAL OF SEDIMENTARY PETROLOGY* (Vol. 48, Issue 1).

Kraus, N. C., & Asce, M. (1999). *ANALYTICAL MODEL OF SPIT EVOLUTION AT INLETS*. ASCE.

Losada, M. A., Medina, R., Vidal, C., & Roldán, A. (1991). *Historical Evolution and Morphological Analysis of "El Puntal" Spit, Santander (Spain)*.

Meistrell, F. J. (1966). *The spit-platform concept: Laboratory observation of spit development*.

Mudde, C. (2019). *Development and verification of ShorelineS on longshore sediment transport and spit formation A CASE STUDY OF LOBITO, ANGOLA C. Mudde*.

Nutz, A., Schuster, M., Ghienne, J. F., Roquin, C., & Bouchette, F. (2018). Wind-driven waterbodies: a new category of lake within an alternative sedimentologically-based lake classification. *Journal of Paleolimnology*, *59*(2), 189–199. https://doi.org/10.1007/s10933-016-9894-2

Palalane, J., Larson, M., & Hanson, H. (2014). ANALYTICAL MODEL OF SAND SPIT EVOLUTION. *Coastal Engineering Proceedings*, *1*(34), 72. https://doi.org/10.9753/icce.v34.sediment.72

Pearson, S. (2021). *Sediment pathways on ebb-tidal deltas*.

Randazzo, G., Jackson, D. W. T., & Cooper, J. A. G. (2015). *Sand and Gravel Spits*. http://www.springer.com/series/8795

Rijkswaterstaat. (2018). *Peilbesluit IJsselmeergebied*.

Robin, N., Levoy, F., Anthony, E. J., & Monfort, O. (2020). Sand spit dynamics in a large tidal-range environment: Insight from multiple LiDAR, UAV and hydrodynamic measurements on multiple spit hook development, breaching, reconstruction, and shoreline changes. *Earth Surface Processes and Landforms*, *45*(11), 2706–2726. https://doi.org/10.1002/esp.4924

Rossel, A., & Westh, S. (2020). *Tails of sand: a two-part study into morphological evolution of spits in Denmark*.

Ton, A. M., Vuik, V., & Aarninkhof, S. G. J. (2022). Longshore sediment transports by large-scale lake circulations at low-energy, non-tidal beaches: a field and model study.

Ton, A. M., Vuik, V., & Aarninkhof, S. G. J. (2021). Sandy beaches in low-energy, non-tidal environments: Linking morphological development to hydrodynamic forcing. *Geomorphology*, *374*. https://doi.org/10.1016/j.geomorph.2020.107522

Uda, T. (2018). *Spits* (pp. 1–5). https://doi.org/10.1007/978-3-319-48657-4_297-2

van Santen, R. (2016). *Marker Wadden - ontwerp en verificatie zachte randen*.

Vila-Concejo, A., Gallop, S. L., & Largier, J. L. (2020). Sandy beaches in estuaries and bays. In *Sandy Beach Morphodynamics* (pp. 343–362). Elsevier. https://doi.org/10.1016/b978-0-08-102927-5.00015-1

Wellen, F. W. (2021). *Development of a non-equilibrium beach in a low-energy lake environment Using the Noordstrand of the Marker Wadden as a case study*.

APPENDICES

SPIT EVOLUTION
AT THE MARKER WADDEN

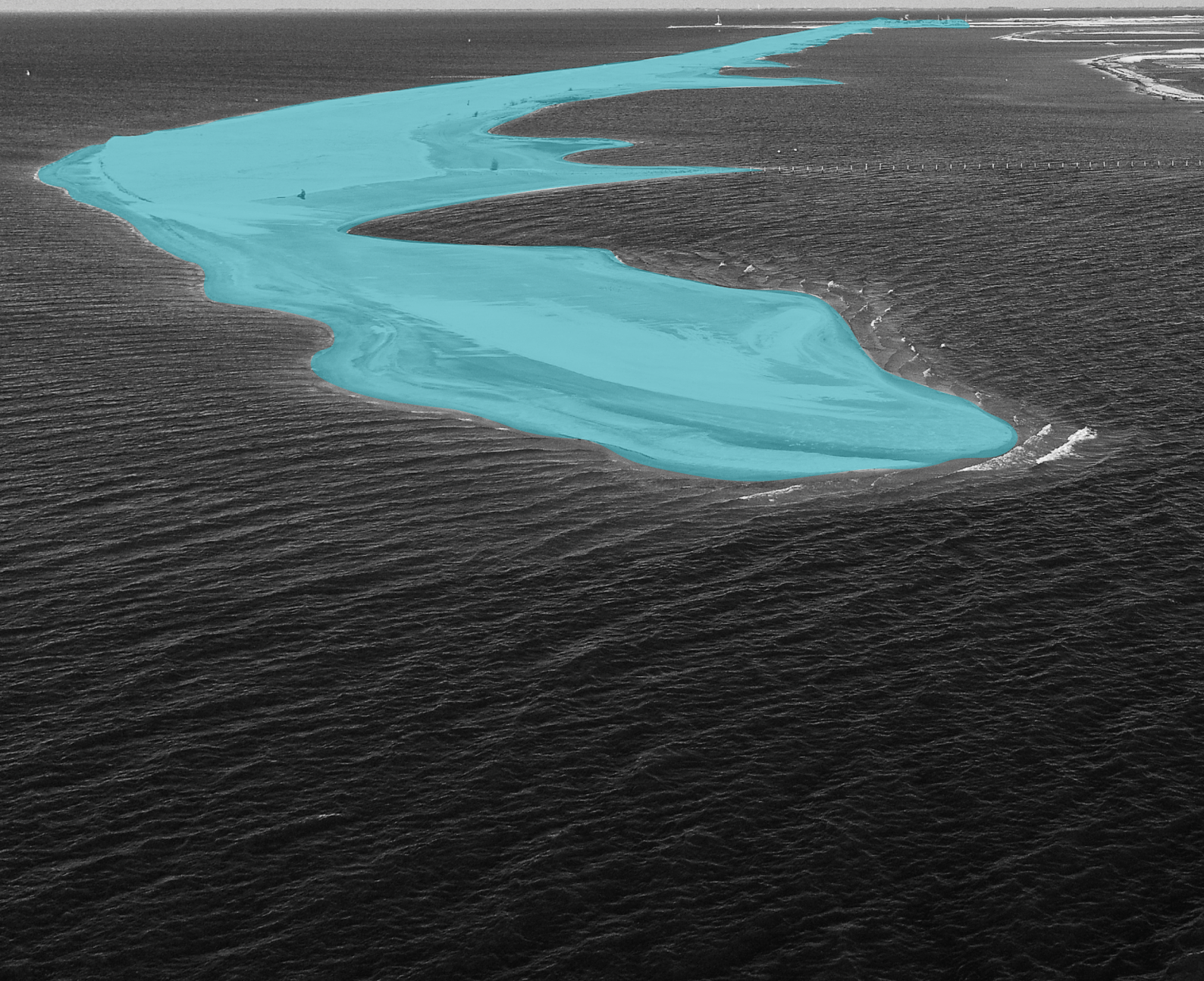

Complete table of contents

Appendix

A Extra Method

Determining drone accuracy and efficiency

Table of contents appendix A

The first subquestion of this thesis aims to obtain more insight in the accuracy and efficiency of the methodology for drone imaging. This appendix discusses the parameters (drone settings) of drone imaging that are of importance for the measurement of spits and coastal areas. Also, it provides an optimisation method to find the best set-up for drone measurements.

Theory of drone imaging

Drone imaging is one method to create a digital elevation model (DEM). Such a model allows to have a complex 3D model of a certain area. This model can be used for all kinds of measurements in all three dimensions. Two kinds of DEMs can be distinguished (Rossel & Westh, 2020):

- Digital Terrain Models (DTM): These models are for example made with LIDAR and are, among other things, used to get a high-resolution model of the earth's surface. It has the possibility to filter out features like vegetation or buildings.
- Digital Surface Models (DSM): These models model the surface with all its features on it. Additional filtering is much harder with these kinds of models. DEMs made with drones fall in this category.

Drone images can be converted into a DEM with a photogrammetric method called Structure-from-Motion (SfM). As is normal in all photogrammetry, SfM creates 3D-structures from overlapping, offset images (Westoby et al., 2012). The advantage of this method is that camera positions, -angles and surface geometry are solved automatically. This means that camera orientation and a network of known 3D control points are not necessary for the reconstruction of the scene geometry (Cullen et al., 2018). This has as a consequence that the 3D pointcloud is generated with its own image-based coordinate system. Therefore, a small number of ground control points (GCP's) is necessary to georeference the pointcloud in such a way that the coordinate system and the real-world coordinate system coincide (Westoby et al., 2012). These GCP's are recognisable points on the drone images, of which the GPS coordinates are manually measured. It is important for these GCP's to be situated on several diverse locations and angles in the concerned area. A way to make a SfM from drone images and implement GCP's is to use software like Pix4Dmapper or Agisoft (Casella et al., 2020; Rossel & Westh, 2020).

Casella et al., (2020) has analysed 28 drone accuracy studies from which it can be deduced that the range of accuracy of a DEM made with SfM has an accuracy typically between 0,05 and 0,11 m. If the drone measurements and DEM construction are executed carefully, the average RMSE of a DEM can be limited to 5 cm with a survey efficiency (complete process) of 3 m^2 per minute (e.g. a survey area of 1 ha needs 55 hours of measurements and DEM construction). An important source of inaccuracies in SfM reconstructions that are made by drone imaging is that they can't compensate for distortions of the lens of the camera. On the sides of an image, deformations always occur because of a specific type of lens, but also because of manufacturing errors. These distortions result in a deformation of the DEM and this is called the doming effect. Together with having an insufficient amount of GCP's, this is the most important source of inaccuracies in a DEM. De doming effect can be reduced by (Casella et al., 2020):

- Correcting the images with a special script.
- Adding images taken under an angle.
- A good distribution and amount of ground control points.
- For some lenses it appears to work to fly at higher altitudes.

Everything concerned, this makes Structure-from-Motion with drone images a cheap, fast, and accurate technique to create DEMs. Especially for highly dynamic surfaces, like the spits at the Marker Wadden (Rossel & Westh, 2020).

Of each drone and terrain type, a new measurement set-up needs to be made to get an accurate DEM in a time-efficient fashion. There are many different factors to consider in this set-up that affect the accuracy

and efficiency. That is why it is difficult to find the objective 'best' set-up of the drone and accompanying equipment. The method as described in this appendix will provide a way to find an accurate and efficient set-up of the drone parameters. Also, after this method is applied it will give insights into the parameters that should be altered first, if requirements for the measurement set-up, in terms of accuracy and efficiency, change.

Properties of a potential drone, suitable for measurements in coastal areas

The drone that is used to illustrate how an optimal set-up of the drone imaging method can be achieved, is the DJI Phantom 4 RTK. This is the most sophisticated, accurate, and professional drone available in the TU Delft Hydraulic Engineering department. The drone that was used by Boskalis Nederland to collect the data for this entire research is even more advanced. But because of the knowledge that is available of this DJI drone, and the applicability of this appendix for future research, the DJI Phantom 4 RTK is further used as example for this optimisation method. This method can also be used for other drones, but to illustrate the considerations that need to be made in this method, the Phantom 4 RTK was chosen.

Properties of the drone are:

- This RTK drone needs significantly less GCP's than regular drones because the drone is significantly more accurate in determining its own location. The drone is able to correct for the atmospheric error in its own GPS signal by being connected with an external RTK network.
- Maximum speed of 50 km/h.
- Flight time only for measuring is 20 minutes (excluding time to return to base and decreasing flight capacity due to high winds).
- Ground sample density (H/36,5) cm/pixel (H is flying height).
- Minimum interval between photos is 3 seconds.

The desired measured area for the southern spit has a size of around 10 ha and the northern spit around 4 ha.

Important parameters for a drone imaging set-up

Many parameters in the operating of drones can be distinguished that are of influence on the accuracy and efficiency measurement process:

- *Environmental constraints (for example, difficult terrain or atmospheric disturbances):*

  Particularly for the spits at the Marker Wadden the coastline can be hard to pin down because of run-up and backwash. These inaccuracies must be considered. Beaches are also hard to map because of the low textures and contracts in the beach surface, which makes it harder for the software to point out features (Casella et al., 2020).

- *Camera quality:*

  The camera quality is eventually important for the Ground Sample Density (GSD). This is the distance between the centre of two consecutive pixels. Thus, the larger this parameter, the lower the resolution of the images and the higher the inaccuracies in the eventual DEM. It is evident that camera properties like resolution and focal point are essential for the GSD. The quality of the camera, combined with the height of flight eventually determines the GSD. Often a specific minimum GSD is desired and therefore the type of camera, attached to the drone, determines the height of flight. Regularly the

GSD is between 1.5 and 2.5 cm/pixel (de Luis-Ruiz et al., 2021).

- *Number and dispersion of GCP's:*

  Ground control points need to be dispersed equally over the desired measured area at different angles and elevations for the best effect. The exact number of ground control points that is needed for a certain accuracy in measurements is difficult to determine from literature. This is because research on ground control points all use different drones and settings that also influence accuracy. However, there seems to be an optimum number of GCP's after which the accuracy does not increase any further. The number of GCP's should be as low as possible as a higher amount significantly increases the time needed for post-processing in the software (Oniga et al., 2018).

  The GCP density that is recommended also differs a lot in literature. For regular drones literature recommends a GCP density of 14 GCP's per ha or 1 GCP/700 m^2 (Casella et al., 2020; Oniga et al., 2018). In the hydraulic lab of the TU Delft there was already experience with a non-RTK version of the drone (DJI Phantom 4 Pro). Here a good GCP density for flat surfaces proved to be 1 GCP/3000 m^2. Especially considering the area of the southern spit, the number of GCP's that would be needed would be too high for the post-processing to be time efficient. Fortunately, RTK drones need less GCP's. It is likely that, for RTK drones, only GCP's as check points are needed to anchor the DEM, but that GCP's have very little effect on the accuracy (Teppati Losè et al., 2020). For this research a maximum number of GCP's will be used, which is half of what is needed for the non-RTK version.

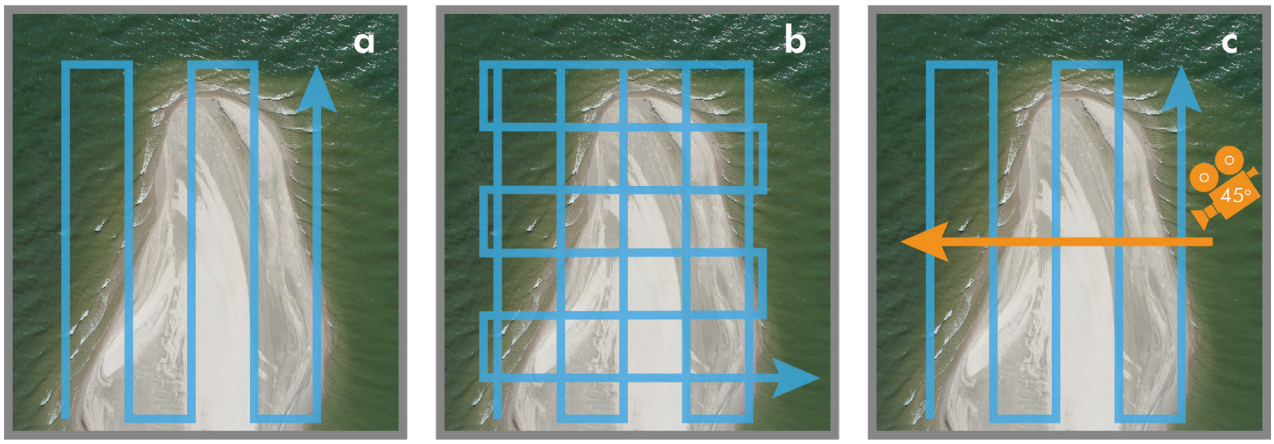

Figure 1. Possible flight grids

- *Geometry and direction of plane passes:*

  The pattern in which a flight is done is also of influence on the accuracy of the DEM, but also on the length and therefore efficiency of the flight. A simple grid is a flight in just one direction, efficient and sufficient for flat areas (Figure 1 a). A double grid provides more accuracy and is often used in more vertical varying areas (de Luis-Ruiz et al., 2021) (Figure 1 b). Boskalis Nederland, who have a lot of experience in UAV measurements on beaches, use a simple grid and then make one cross-sectional pass over the area with the camera tilted under an angle of 45 degrees. This pattern should get rid of the doming effect and is also used as the pattern for this research (Figure 1 c).

- *Speed of flight:*

  Speed of flight is mainly a limiting factor for efficiency. The drone can take a photo every 3 seconds. To get the desired overlap of pictures the drone must fly at a certain pace to fly from measurement point to measurement point in more than 3 seconds, otherwise measurement points are skipped. Therefore, flight height and overlap indirectly determine this parameter.

- *Height of flight:*

  The camera on the drone often stays the same (on the DJI Phantom 4 RTK the camera is fixed on the body). This means that the height of flight is the only important adjustable parameter for the ground sample density. The lower the flight, the lower the GSD and the more accurate the DEM. However, higher flights can cover larger areas and are therefore much more efficient. Also, lower flights result in more pictures increasing the data that needs to be processed dramatically.

- *Inclination of camera:*

  It is possible to tilt the camera of the drone while taking photographs. This might be beneficial for the accuracy for objects with altimetric features that are of interest. For beaches and spits these features are limited and therefore taking photographs perpendicular to the ground will be the most accurate (Casella et al., 2020; de Luis-Ruiz et al., 2021).

- *Forward overlap:*

  Forward overlap, as well as lateral overlap, is important for the SfM technique to work. Often a minimal forward overlap is 60% over the previous photo, and an 80%-90% overlap is often used for orthophotographs. A higher overlap means a more accurate DEM but more pictures have to be taken, the drone can fly slower and therefore the area that can be covered is much smaller. This has not only a negative impact on the area that can be covered but the data that needs to be processed also gets significantly higher with a larger overlap (de Luis-Ruiz et al., 2021) (Figure 2 a).

- *Lateral overlap:*

  The same holds for the lateral overlap as for the frontal overlap. A minimum lateral overlap is around 20% of the adjacent photographs and for orthophotos often a lateral overlap of 80% is used (de Luis-Ruiz et al., 2021) (Figure 2 b).

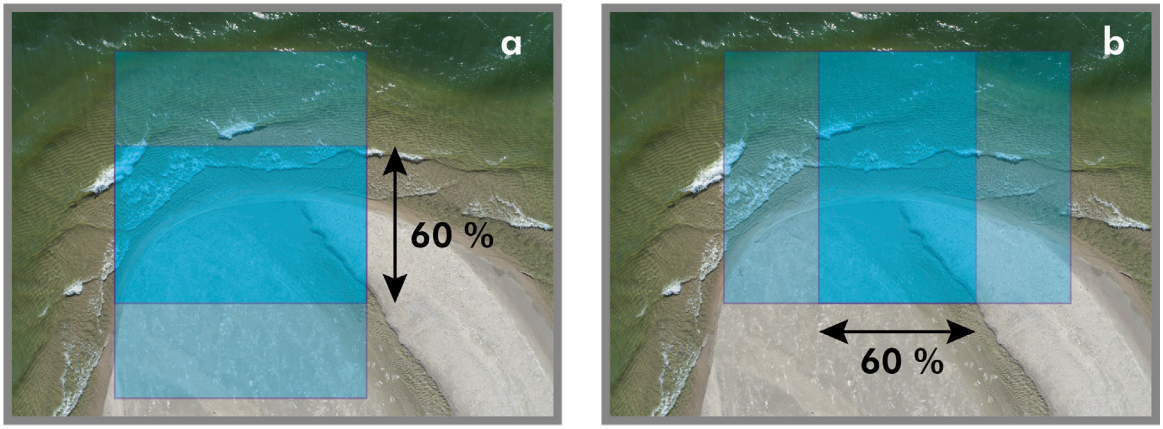

Figure 2. The difference between frontal and lateral overlap

Based on literature, experience, and the properties of the drone it seems that there are four remaining parameters that can affect the accuracy: the number of GCP's, frontal overlap, lateral overlap, and the ground sample density which is completely dependent on the flight height. Once the contribution of each of these parameters to the accuracy is known, choices can be made based on the accuracy and efficiency of this parameter. The effect of a parameter on the efficiency can be based on the time of flight, number of images, post-processing time, and measurement set-up time (setting up and measuring the GCP's in the field for example) (Table 1). Especially the processing time is of large effect on the time-efficiency. The number of images is the most important factor considering computation time and the time of flight needed to cover a certain area is the most important if a large area needs to be measured, preferably on one battery charge (20 min).

Parameter higher level	Time of flight	Amount of images	Processing time	Set-up time
Flight height	Less	Less	Less	-
Forward overlap	More	More	More	-
Lateral overlap	More	More	More	-
Number of GCP's	-	-	Substantially more	Substantially more

Table 1. Effect of a high level parameter on the efficiency

Determining the accuracy

If the effect of the four parameters on the accuracy would be investigated with test flights, with three levels (low, middle, high), 81 test flights need to be done. However, de Luis-Ruiz et al., (2021) used the Taguchi Design of Experiments Method to optimize the parameters in only nine flights. In that paper the calibration was done for an archaeological site. In this appendix, the approach of de Luis-Ruiz et al., (2021) is followed and slightly adjusted for the optimisation of coastal sites.

Each parameter will be given three levels, a low (1), middle (2), and high level (3). Nine flights will be done with different combinations of the parameter's levels (Table 2). Each level can be defined for the four remaining parameters (Table 3). This makes it possible to define the settings of each flight (Table 4).

Test (flight) nr.	Factor A	Factor B	Factor C	Factor D
1	1	1	1	1
2	1	2	2	2
3	1	3	3	3
4	2	1	2	3
5	2	2	3	1
6	2	3	1	2
7	3	1	3	2
8	3	2	1	3
9	3	3	2	1

Table 2. Different level combinations for each of the nine tests

Parameter	Low level (1)	Middle level (2)	High level (3)
GSD (flight height)	1,5 cm/pixel (50,5 m)	2 cm/pixel (67,3 m)	2,5 cm/pixel (84,2 m)
Forward overlap	60 %	70 %	80 %
Lateral overlap	40 %	60 %	80 %
GCP amount/density	± 3	1 GCP/ 1 ha	1 GCP/ 5000 m^2

Table 3. Different levels for each of the four drone parameters

Test flight nr.	GSD	Forward overlap	Lateral overlap	GCP amount/density
1	1,5 cm/pix (50,5 m)	60 %	40 %	± 3
2	1,5 cm/pix	70 %	60 %	1 GCP/ 1 ha
3	1,5 cm/pix	80 %	80 %	1 GCP/ 5000 m^2
4	2 cm/pix (67,3 m)	60 %	60 %	1 GCP/ 5000 m^2
5	2 cm/pix	70 %	80 %	± 3
6	2 cm/pix	80 %	40 %	1 GCP/ 1 ha
7	2,5 cm/pix (84,2 m)	60 %	80 %	1 GCP/ 1 ha
8	2,5 cm/pix	70 %	40 %	1 GCP/ 5000 m^2
9	2,5 cm/pix	80 %	60 %	± 3

Table 4. The setting for each of the nine flights, needed to determine the accuracy for drone photogrammetry on spits and beaches.

Each of these flights take images of the measurement area and for each of these flights a DEM is made of that area. All over the measurement area rulers or fluorescent beams of a standard length (for example 1 m) are dispersed. These beams need to be dispersed in the same manner as the GCP's but not necessarily on the same location (Figure 3). These beams eventually end up in the DEM. In the model the length of each beam can be measured. The deviation of the beams in the DEM relative to 1 m can provide the accuracy of that specific DEM.

For each flight the signal-to-noise ratio (S/N) can be determined. This can be done by squaring each of the deviances of the beams (the difference between the length of the beam in the DEM and the beam in reality). These square values should be averaged. Then the logarithm of this value should be multiplied with -10 to give the signal-to-noise ratio of a single test flight (formula 1).

$$1) \quad S/N = -10 \cdot log_{10} \frac{1}{n} \sum_{i=1}^{n} (y_{DEM} - y_{real})_i^2$$

For each level of each parameter also average signal-to-noise ratio can be calculated ($(S/N)_{ij}$). For the lowest level of the GSD (or flight height) this is the average of the signal-to-noise ratios of the first three test flights for example.

Now the sum of squares for each parameter, out of the three levels, can be calculated (SS_i) (formula 2) as well as the sum of squares for the variation with respect to the average (SS) (formula 3). With those figures the contribution of each parameter to the accuracy of a DEM can be computed (formula 4).

$$2) \quad SS_i = \sum_{i=1}^{3} \left[(S/N)_{ij} - \overline{S/N} \right]^2$$

$$3) \quad SS = \sum_{i=1}^{9} \left[S/N - \overline{S/N} \right]^2$$

$$4) \quad Contribution\ (\%) = \frac{SS_i}{SS} \cdot 100$$

Based on the Taguchi Design of Experiments Method the most accurate set-up of drone parameters can be achieved by choosing the level with the lowest average signal-to-noise ratio of a parameter ($(S/N)_{ij}$) out of the three. This set-up is not the most accurate set-up but still one of the most accurate combination of parameters that can be achieved.

Figure 3. Fluorescent beams in the aerial photograph

Combining accuracy and efficiency

It is known what the contribution is of each parameter to the total accuracy of a DEM. Now decisions can be made in such a way that accuracy gets sacrificed as little as possible to obtain the desired efficiency of the measurement process. If for example, the computational power, to convert the images to a DEM, is limited, a choice can be made between increasing the flight height and therefore the GSD, decreasing the frontal overlap or decreasing the lateral overlap. If the contribution of the flight height to the accuracy turns out to be low, it is possible to increase the flight height with limited concessions for the accuracy. If the area that needs to be measured is too large with the current drone set-up, the time of flight needs to be decreased. The same parameters as before can then be altered. By knowing the effect of the GCP's on the accuracy, the number of GCP's can be minimized to save time.

By knowing the contribution of each parameter to the accuracy, decisions concerning the settings of the drone parameters can easily be made in order to obtain an accurate set-up for the desired efficiency.

Bibliography

Casella, E., Drechsel, J., Winter, C., Benninghoff, M., & Rovere, A. (2020). Accuracy of sand beach topography surveying by drones and photogrammetry. *Geo-Marine Letters*, *40*(2), 255–268. https://doi.org/10.1007/s00367-020-00638-8

Cullen, N., Verma, A., & Bourke, M. (2018). A comparison of structure from motion photogrammetry and the traversing micro-erosion meter for measuring erosion on shore platforms. *Earth Surface Dynamics*, *6*(4), 1023–1039. https://doi.org/10.5194/esurf-6-1023-2018

de Luis-Ruiz, J. M., Sedano-Cibrián, J., Pereda-García, R., Pérez-álvarez, R., & Malagón-Picón, B. (2021). Optimization of photogrammetric flights with uavs for the metric virtualization of archaeological sites. Application to Juliobriga (Cantabria, Spain). *Applied Sciences (Switzerland)*, *11*(3), 1–21. https://doi.org/10.3390/app11031204

Oniga, V.-E., Breaban, A.-I., & Statescu, F. (2018). *Determining the Optimum Number of Ground Control Points for Obtaining High Precision Results Based on UAS Images*. 352. https://doi.org/10.3390/ecrs-2-05165

Rossel, A., & Westh, S. (2020). *Tails of sand: a two-part study into morphological evolution of spits in Denmark*.

Teppati Losè, L., Chiabrando, F., & Giulio Tonolo, F. (2020). Are measured ground control points still required in UAV based large scale mapping? assessing the positional accuracy of an RTK multi-rotor platform. *International Archives of the Photogrammetry, Remote Sensing and Spatial Information Sciences - ISPRS Archives*, *43*(B1), 507–514. https://doi.org/10.5194/isprs-archives-XLIII-B1-2020-507-2020

Westoby, M. J., Brasington, J., Glasser, N. F., Hambrey, M. J., & Reynolds, J. M. (2012). "Structure-from-Motion" photogrammetry: A low-cost, effective tool for geoscience applications. *Geomorphology*, *179*, 300–314. https://doi.org/10.1016/j.geomorph.2012.08.021

Appendix

B

Method

Pointcloud post-processing and volume calculations

Table of contents appendix B

Pointcloud build-up

For the morphological calculations of the Marker Wadden spits, pointclouds were used. These pointclouds are the result of measurements by Boskalis Nederland, taken four times per year. The pointcloud for every measurement moment is a combination of different topographical measurements, all done around a certain date. Everything above the waterline is measured by an RTK drone using photogrammetry. Everything below the spit-platform boundary, and the deeper parts of the spit-platform itself, is measured using a multibeam echosounder from a boat. The gap between the pointcloud of the drone and the pointcloud of the multibeam is filled with interpolation in post-processing. The interpolation is made by Boskalis Nederland using DredgeView 2. This interpolation is verified by the manually measured cross-shore paths over the spit-platform that are taken every 100 m by A. Ton et al., with a Viva GPS station (GS 10 and/or GS 14). It is likely that this interpolation between the separate pointclouds of the drone and multibeam data decreases the accuracy of the combined pointcloud for the whole spit (Figure 1).

Post-processing in CloudCompare

The CloudCompare software was used to post-processes the pointclouds to prepare them for calculations in python. Firstly, the three pointclouds from the different sources were merged to one pointcloud. Secondly, the pointclouds were cut to preserve only the data necessary for calculations. This eventually would save time when the scripts in python needed to be run. The cut was done at the point where the spit would transition onto the adjacent beach. So, at the location of the cut the angle of the coastline (relative to the north) would be the same as for the rest of the beach (Figure 1).

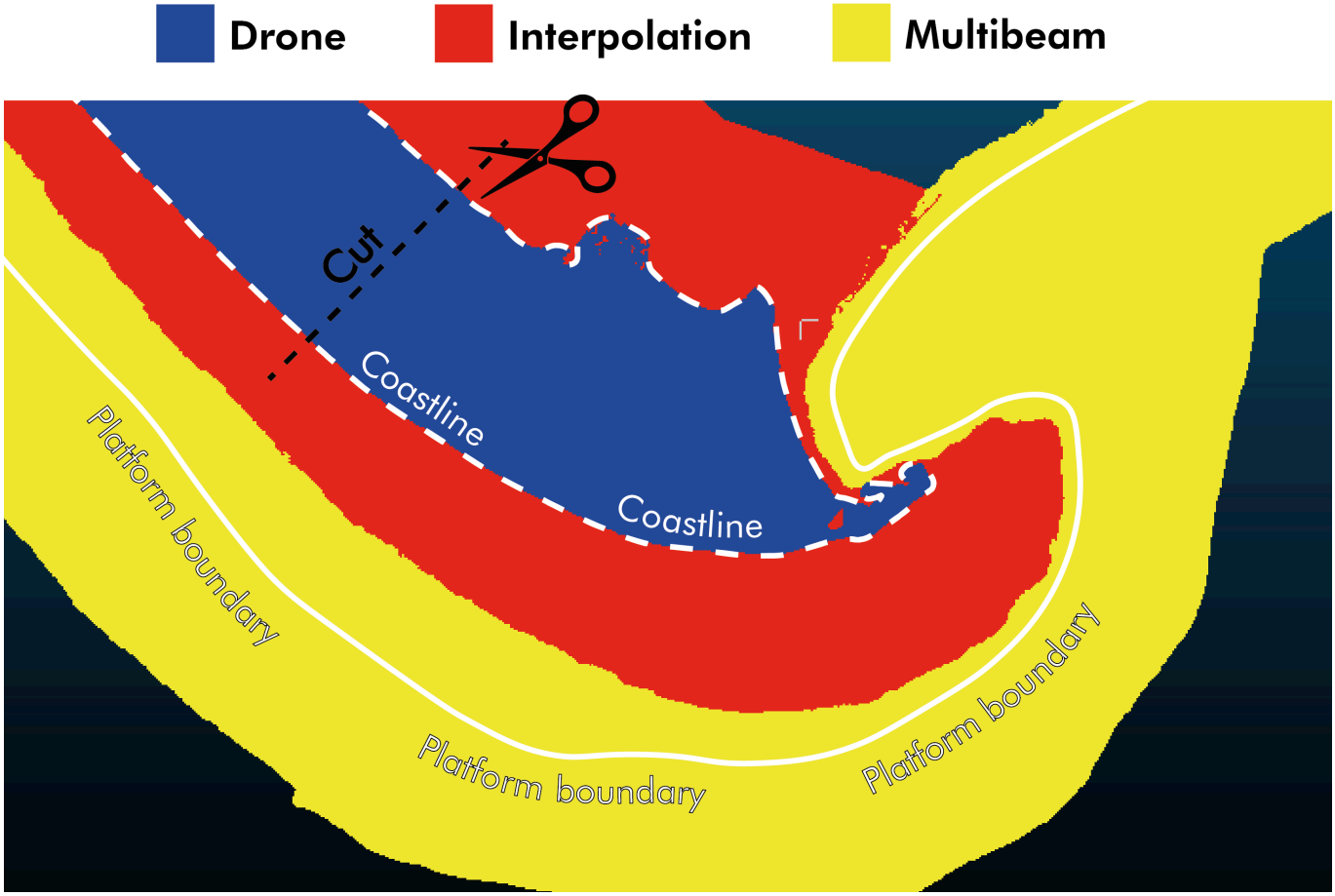

Figure 1. Sources for the complete pointcloud, example with the pointcloud from September 2020

Finally, two consecutive pointclouds were also subtracted in CloudCompare. To get the morphological changes over a period, the difference between two measured pointclouds was taken. By subtracting the pointcloud with measurements from the end of a period by the pointcloud with measurements at the start of a period, this difference can be achieved. In the resulting pointcloud positive points indicating a raise of the bed, meaning sedimentation, and negative points representing a lowering of the bed, meaning erosion (Figure 2). The dotted contour line is the storm set-up water level (0,3 m NAP), the dashed line is the regular coastline (-0,3 m NAP) and the solid line is the platform boundary (-1.2 m NAP for calculations, -2.7 m NAP for the shown contours).

The tool in CloudCompare that is used for subtracting these two pointclouds is called the Multiscale Model to Model Cloud Comparison (M3C2 Distance) tool (Lague et al., 2013). This algorithm is specially designed for calculating the orthogonal distance between pointclouds to show erosion and sedimentation, without the need to turn the pointclouds into a mesh. This tool is one of the most accurate ways to process the pointclouds and certainly more accurate than subtracting the pointclouds manually in python. Therefore, the accuracy of the pointclouds that is sacrificed by this process stays very low.

Calculating volumes with grid interpolation

Pointclouds with elevation changes have been obtained by using CloudCompare. However, for the morphological analysis mostly sedimentary volumes were used. These volumes are obtained by interpolating the pointclouds with elevation changes with linear interpolation. This results in a mesh with blocks with the same dimensions as the grid over which is was interpolated. Each block again represents an elevation change for that block. By multiplying this elevation change by the area of the block the erosion volumes and sedimentation volumes can be calculated (Figure 3).

The middle of each block is taken as the location of that particular volume change and the angle relative to the centre point is calculated from there. Now a dataset is obtained, complete with volume changes and the angle of this location to the centre point. Volumes with the same rounded up angle can be added and after that the morphological analysis as presented in the paper can be started.

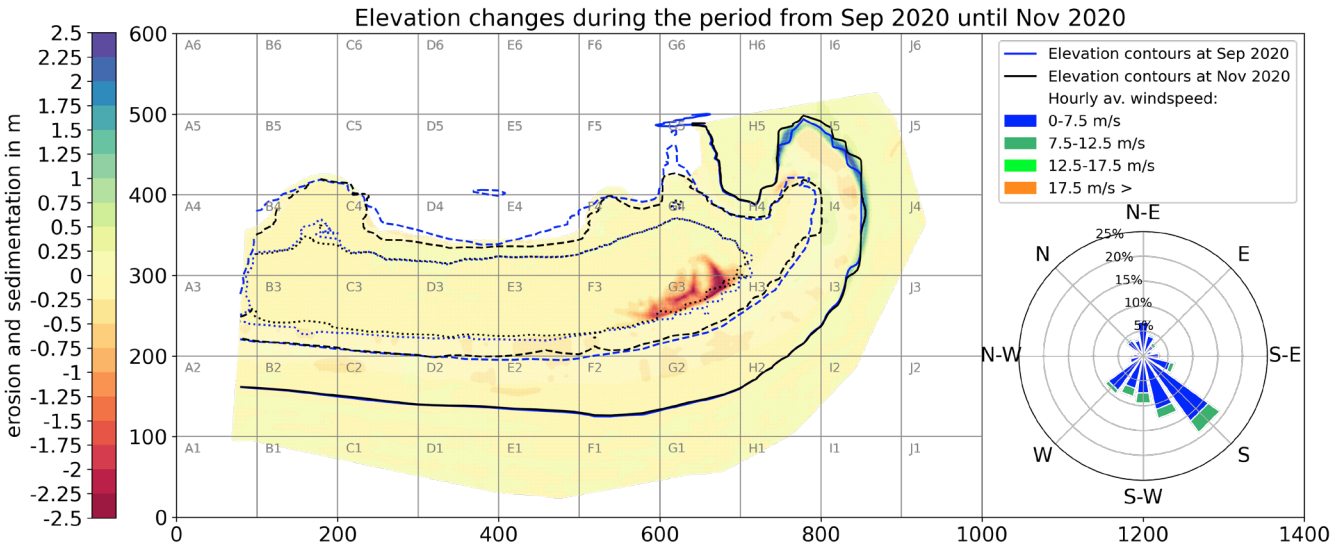

Figure 2. Example of a pointcloud that is obtained by subtracting the start pointcloud (with measured data) with the end pointcloud (with measured data). Negative elevation change is indicated in red and positive elevation change is indicated in blue.

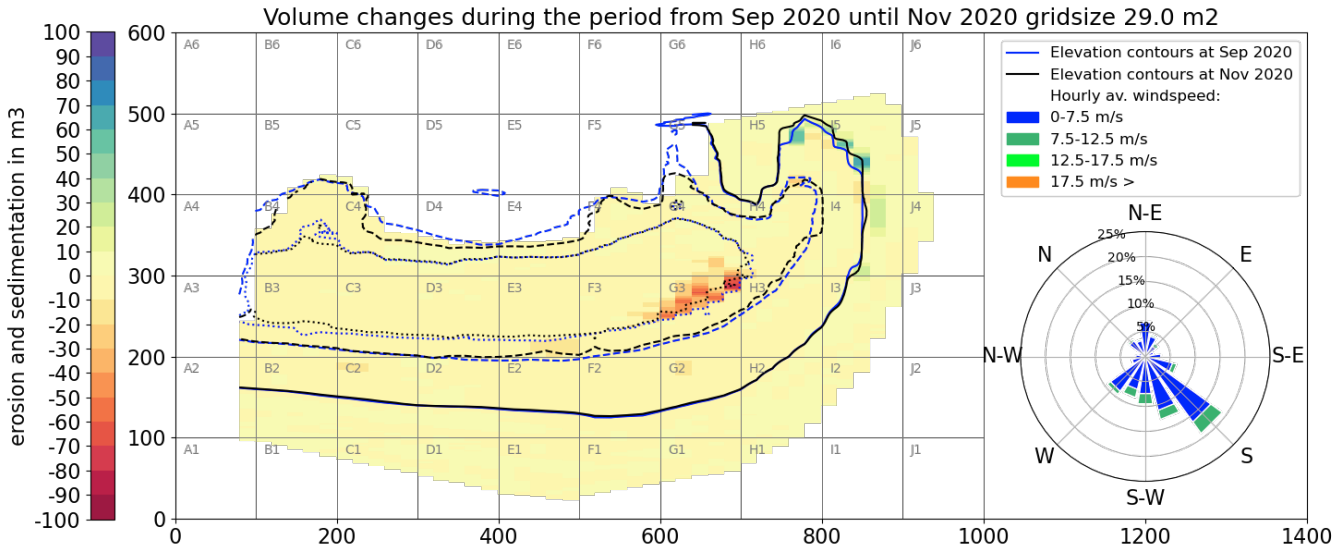

Figure 3. Example the mesh with volume changes that is obtained by the interpolation of the elevation change point-cloud (Figure 2). Erosion is indicated in red and sedimentation is indicated in blue.

The southern spit is much larger than the northern spit and therefore different grid sizes are used. For the southern spit a grid size of squares of 29 m^2 each (Figure 3) is used and for the northern spit a grid with squares of 4 m^2 is used. Larger grids result in larger inaccuracies but also shorter computation times. For a smaller spit like the northern spit, using a large grid results easily in errors. Because adjacent degrees relative to the centre point are very close to each other when the area of interest is small. It is possible for too much blocks to get attributed to one degree instead of getting distributed over multiple degrees because the location of the centre of that block is unfavourable. Therefore, the total sedimentary volumes do not change but the distribution of the volumes over adjacent blocks can get distorted at some places (Figure 4). This error is mitigated by fitting the distribution of sediment along the spit with the red line (Figure 12 of the paper). But in order for the results to be neater, also a smaller grid size was used for the northern spit as the computation time of the scripts stayed within limits. The data that resulted from the processing of the pointclouds in CloudCompare and python, allowed for the analysis of the spit morphology that is presented in the paper.

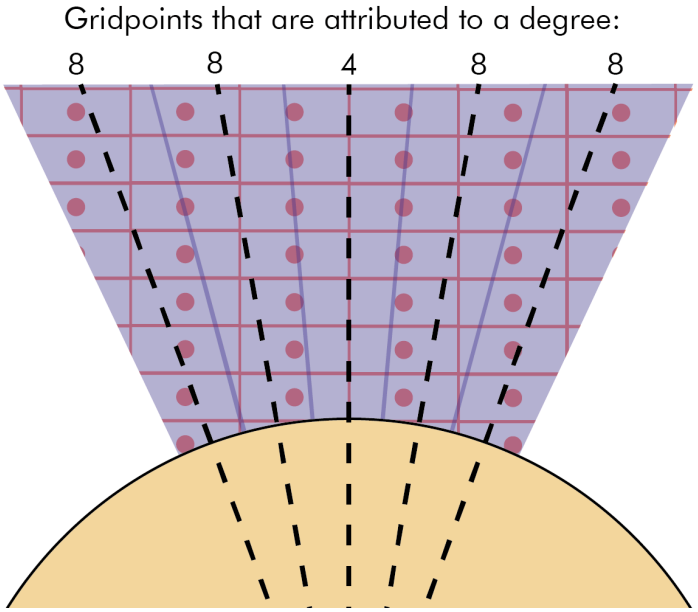

Figure 4. Error that can occur because to many or to little grid points get attributed to a certain degree due to a to large grid size. The dashed line is a singe degree, and the blue triangle symbolises everything that would get attributed to that certain degree. The grid is indicated by the purple squares with the middle indicated by a point.

Bibliography

Lague, D., Brodu, N., & Leroux, J. (2013). Accurate 3D comparison of complex topography with terrestrial laser scanner: Application to the Rangitikei canyon (N-Z). *ISPRS Journal of Photogrammetry and Remote Sensing*, *82*, 10–26. https://doi.org/10.1016/j.isprsjprs.2013.04.009

Appendix

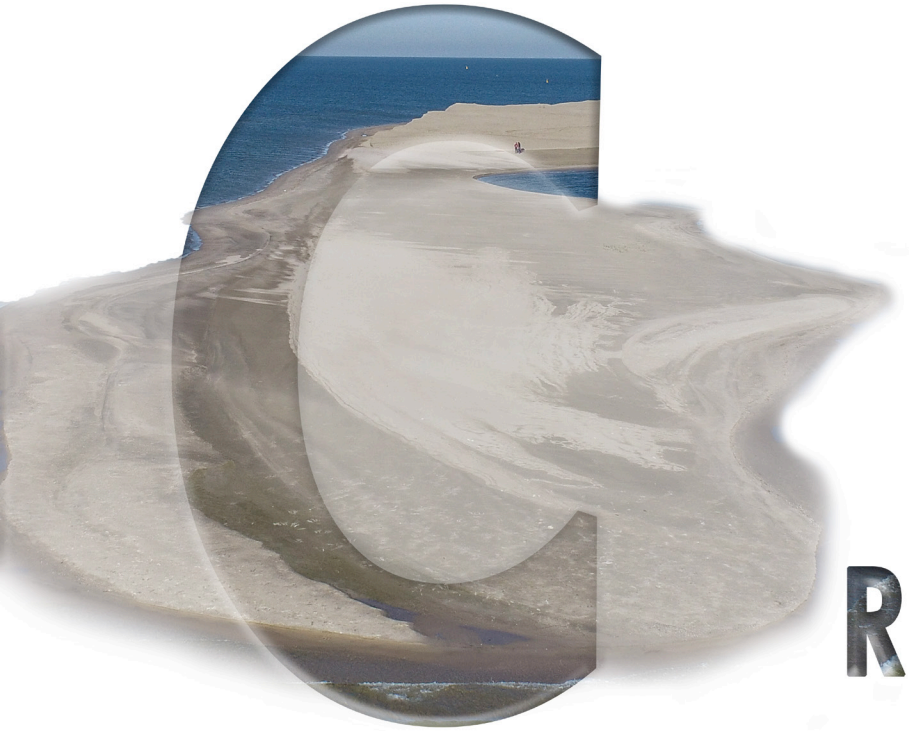

C Results

Morphodynamics during different wind conditions

Table of contents appendix C

With the pointclouds and volume calculations, explained in appendix B, morphodynamic observations and calculations can be made. This appendix is an addition to the observations and calculations from the 'spit growth quantification' section in the paper. The developments of the southern spit was observed in both a qualitative and quantitative fashion in order to verify if calculations made sense. The research of the northern spit went through a less thorough process. This is because it was of interest to see if the same method of quantifying spit relations (as has been done for the southern spit) could be applied to a different type of spit, the northern spit. So, the qualitative observations and research that was done for the southern spit, was not executed for the northern spit in order to test the quantifying method. The morphodynamic qualitative observations that are discussed in this appendix are therefore mainly about the southern spit. In the paper mainly quantitative observations are discussed, which are done to the same extent for both spits (*Results: spit growth quantification*). To eventually link the morphodynamic developments to the hydrodynamic conditions, first the morphological developments during different wind directions need to be observed.

Considering the southern spit: in general, three observations can be done when qualitatively observing the morphological developments in the pointclouds:

1. Clear scarp erosion at the proximal end of the spit, at set-up level.
2. Migration of the spit towards the NE-E direction.
3. More sedimentation on the sub-platform level, thus expansion of the submerged spit-platform, during high energy periods and more sedimentation on the platform level, thus expansion of the emerged spit, during low energy periods (see *Method* in the paper for definitions).

For the northern spit the same kind of observations can be done although these observations are done after quantification. This is because the morphology is not investigated before quantification as was the case for the southern spit. For the northern spit, the spit grows towards the NE.

1. Scarp erosion

In almost every period it was observed that severe erosion occurred at the proximal end of the spit, where the beach starts to curve away from the beach. This erosion occurred above the normal waterline, around the storm waterline (dotted lines Figure 1). This waterline is higher because of storm set-up. This means that this erosion has been caused during storms as that is the only time water comes that high. At this location the angle of incidence of incoming waves starts to increase. This increases the longshore current and stirs-up the sediment. Material from that location is then transported towards the distal end. At the location of this erosion high elevations occur and therefore a large scarp forms. Erosion of this scarp due to high currents and possible collapse, supplies the distal end with large quantities of material necessary for spit growth (Figure 1, Figure 2).

Quantification

If the set-up would be important for erosion and if the scarp erosion would be the main source of sediment for the spit, it should be observable that most of the erosion occurs during the most set-up. And most set-up occurs when the wind speeds are high and the wind direction is from the SW (225 degrees) because then the distance for set-up is the largest. The erosion at the southern head is plotted against the 95-percentile wind velocity and accompanying mean direction during a period. Clearly the erosion is strongly correlated with the storm wind velocity, probably because the distance for set-up does not vary a lot between different degrees (Figure 3). Two outliers can be defined:

- Period Aug 2019 – Oct 2019: there is a lot of erosion along the beach right after a nourishment has been done. The nourishment at the location of the scarp protrudes from the beach and therefore contracts the longshore flow significantly. This amplifies the eroding longshore currents.
- Period Sep 2020 – Nov 2020: Here a lot of erosion of the scarp has taken place but it is likely

that this is caused by the collapsing of the slope instead of a lot of hydrodynamic forcing as wind conditions were relatively calm during this period.

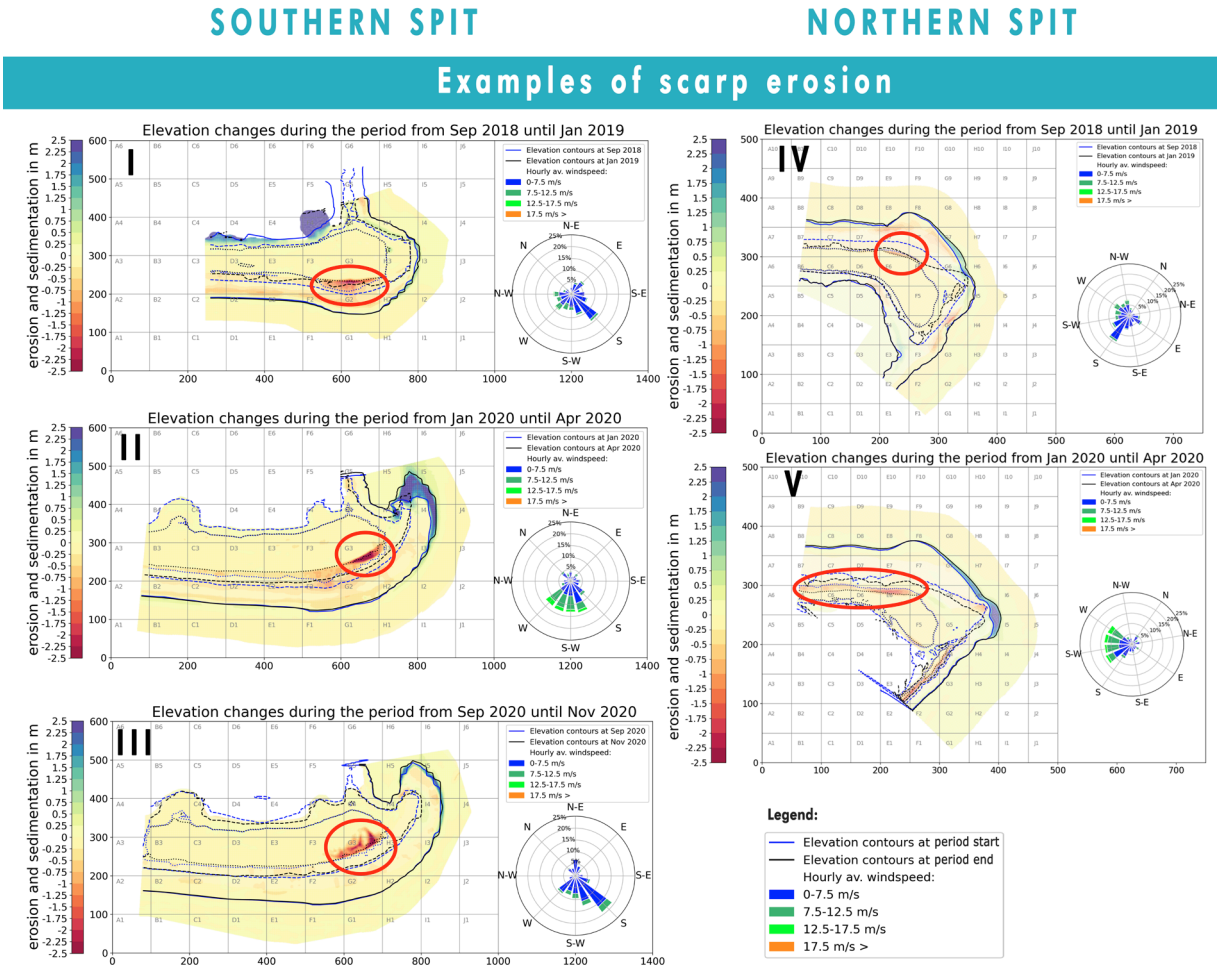

Figure 1. Pointclouds of several of the morphological periods that had significant scarp erosion (red circle). With I, II, II at the southern spit and IV and V at the northern spit.

Figure 2. Photographs and videos of the scarps on the spits in March to illustrate the location and size of the scarps. The photos and videos are made by Anne Ton & Niels van Kouwen, the orthophotos are made by Boskalis Nederland. The photo with the asterisk is made in January 2022 but illustrates the collapsing scarp well.

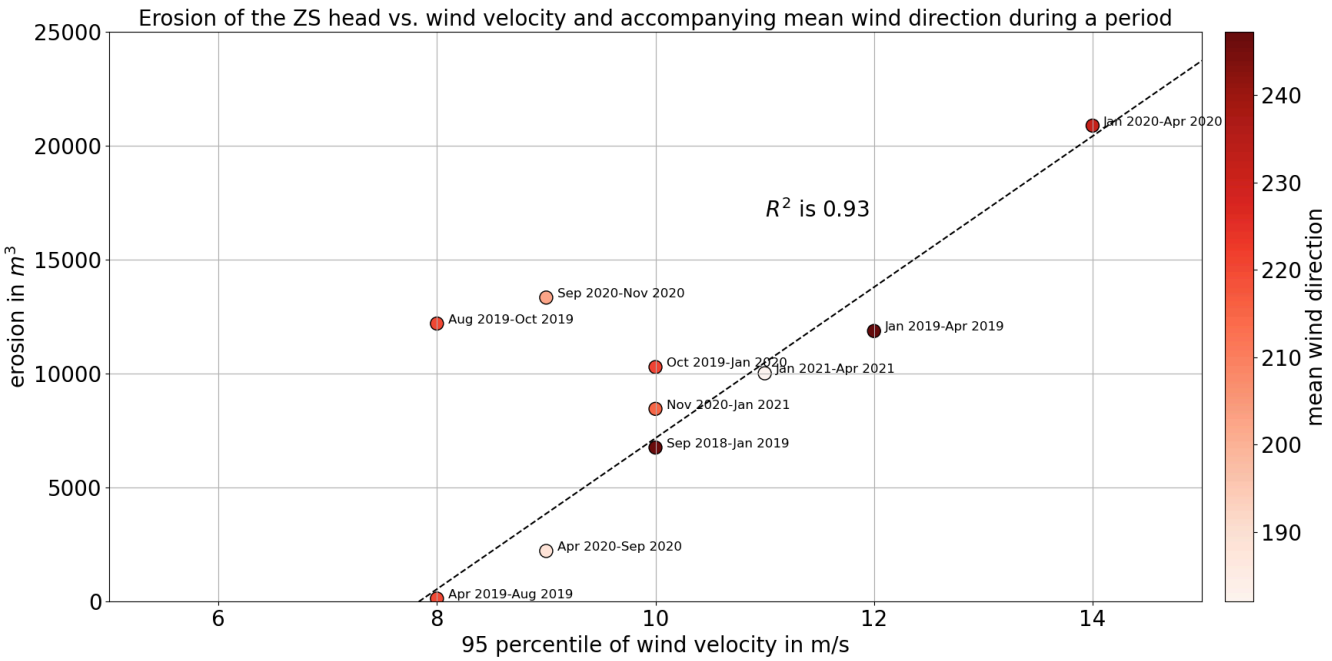

Figure 3. Erosion at the southern head vs. the storm wind velocity and the mean wind direction in degrees. With the correlation between erosion and velocity indicated by the R^2 parameter of the fit, excluding the outliers.

2. Migration of the southern spit towards the NE-E direction

When looking at the waterline it looks like the spit bends more and more to the NE. At least the parts above the water (Figure 5). This is logical if we consider Ashton et al., (2016) who show that as the waves refract and move along the curve, the angle of incidence increases, increasing the longshore current parallel to the shore. When the angle of incidence becomes higher than 45 degrees (at the fulcrum point) the longshore current starts to decrease, and sedimentation starts to occur if the energy becomes low enough. After the fulcrum point the flow direction is likely directed towards the NE and E resulting in sedimentation in those regions (Figure 4). However, in later periods the direction of the spit tip is more directed towards the E instead of the NE. This is possibly caused by the NE and E winds that occur during these periods.

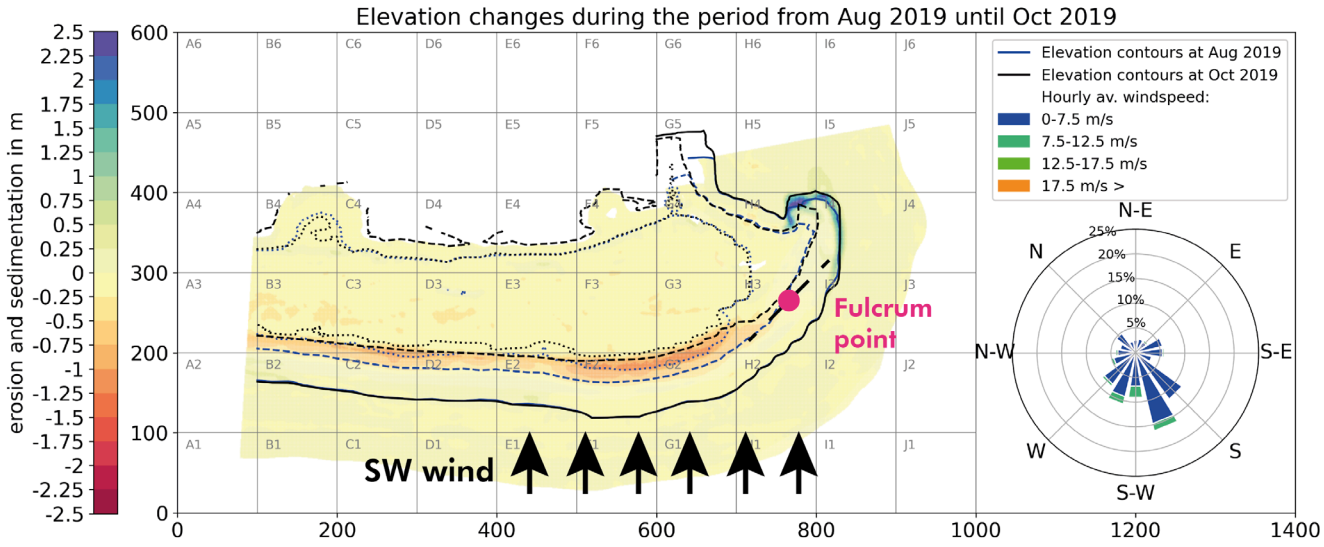

Figure 4. Sedimentation caused by low angle waves only occurs after the angle of incidence surpassed the 45 degrees (fulcrum point).

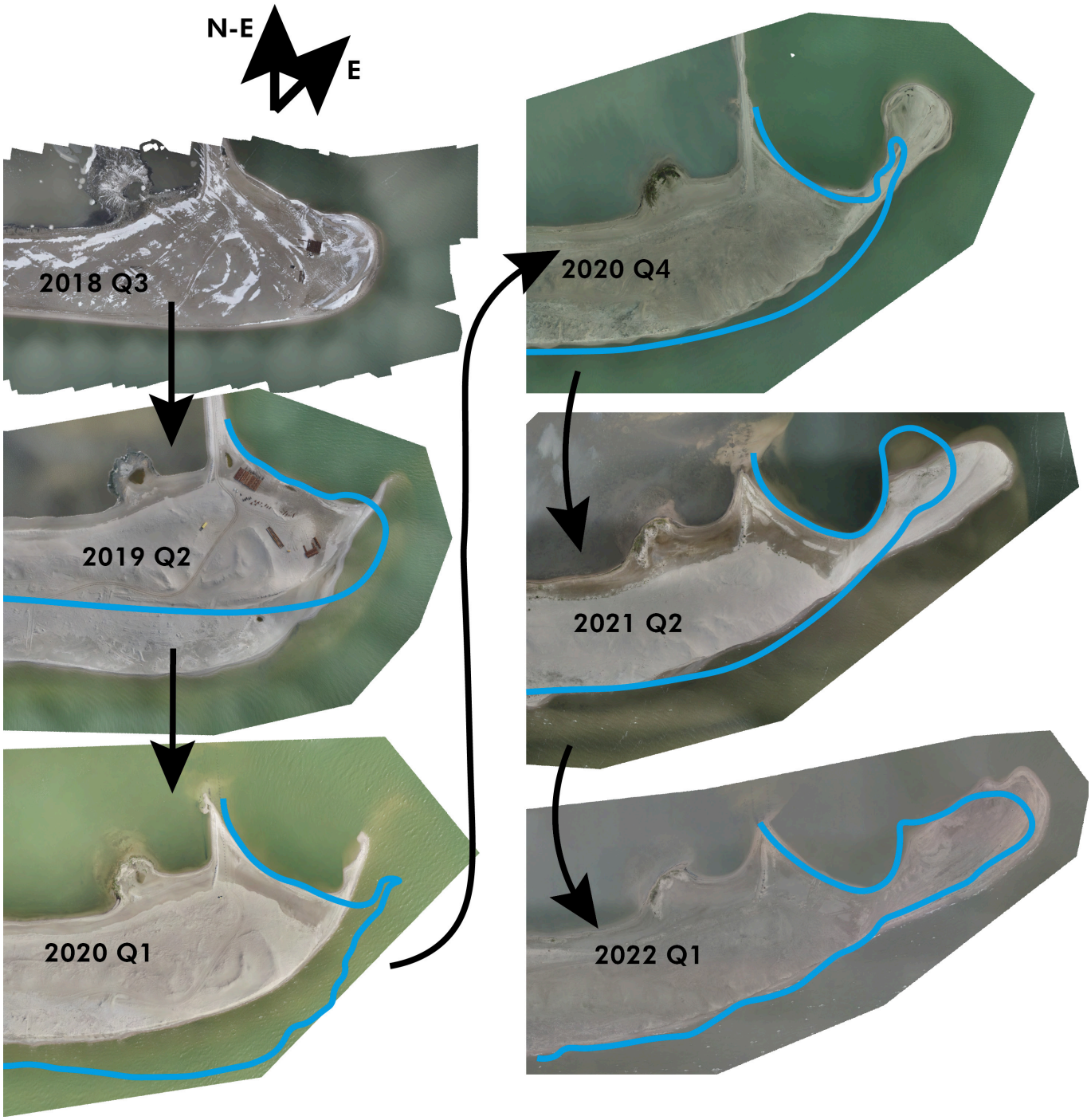

Figure 5. Southern spit tip migration over time. Orthophotos taken by Boskalis Nederland.

Quantification of the southern spit migration

As discussed in the paper, morphodynamic analysis is done by using a polar coordinate system for the x,y plane and elevation levels for the z coordinates.

This results in the graphs in Figure 7. The graphs should be read as follows:

a: Each bar in the bar graph indicates the amount of sedimentation that occurs on that particular degree relative to the centre point. The brown part is the amount of sedimentation above the waterline (-0,3 m NAP). The seagreen part is the amount of sedimentation below the waterline and above the platform boundary (-1,2 m NAP) and the blue part is the share of sedimentation below this boundary. The grey vertical lines indicate the centre of mass of a single, distinguishable deposit (group of degrees of which the sedimentation is larger than average). These centres of deposits are again visualised in graph *b*.

b: These maps show the morphological change of the spit during a period. Here red indicates erosion and blue indicates sedimentation. The centre point is indicated with a red dot with the boundary of the observed area indicated by the red dashed line (45° – 225°). The blue lines indicate the boundaries of the elevation levels at the start of the morphological period and the black lines are the boundaries at the end of the morphological period. The dotted line is the waterline during storm set-up (+0,3 m NAP), the dashed line is the regular coastline (-0,3 m NAP) and the solid line is the boundary of the platform (indicated by -2,7 m NAP on this map, -1,2 m NAP is used for calculations) (Figure 6).

c: This windrose gives the wind conditions during the morphological period that is considered. The bins are based on the different wind velocities in the hydraulic scenarios that are later modelled.

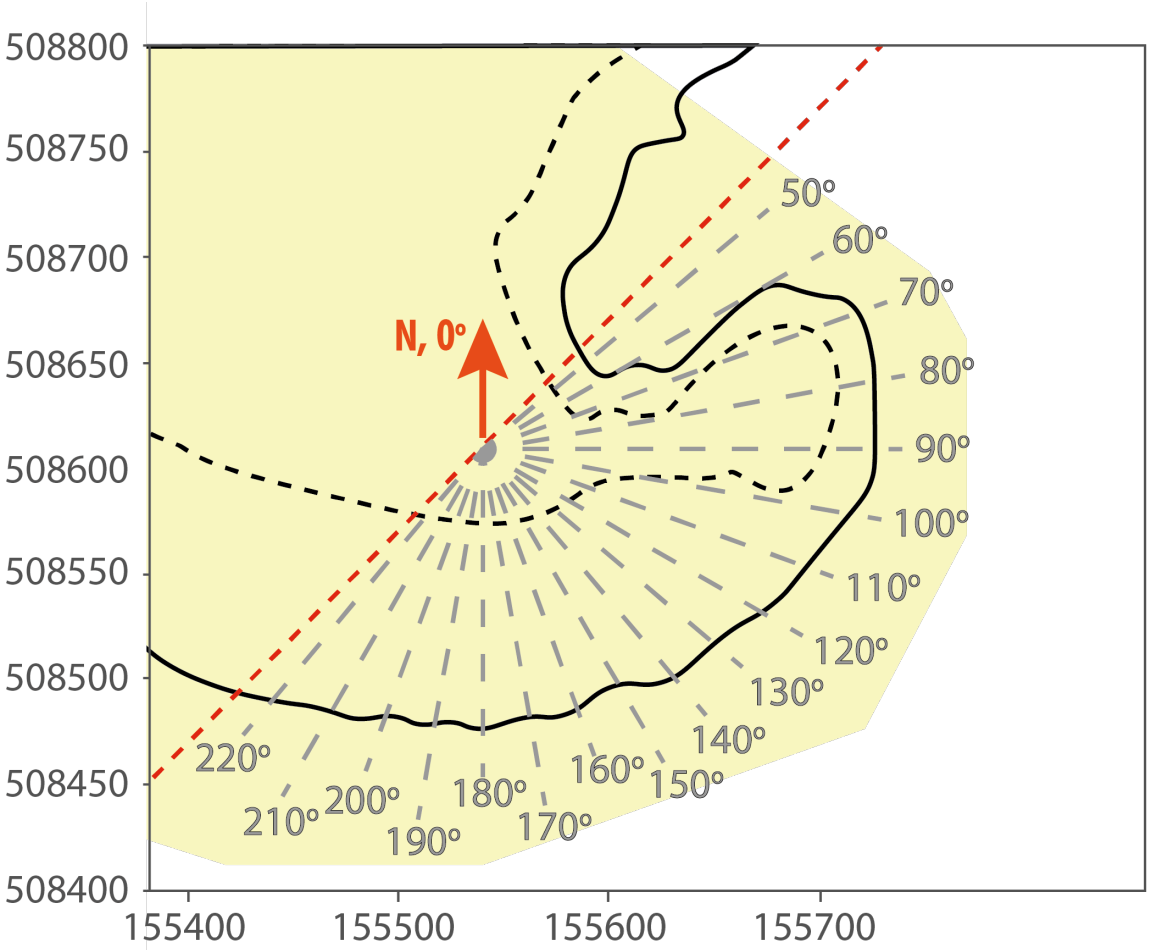

Figure 6. Orientation of the polar coordinate system around the southern spit.

Sedimentation at the southern spit, relative to the centre point (red dot) between Sep 2018 and Jan 2019

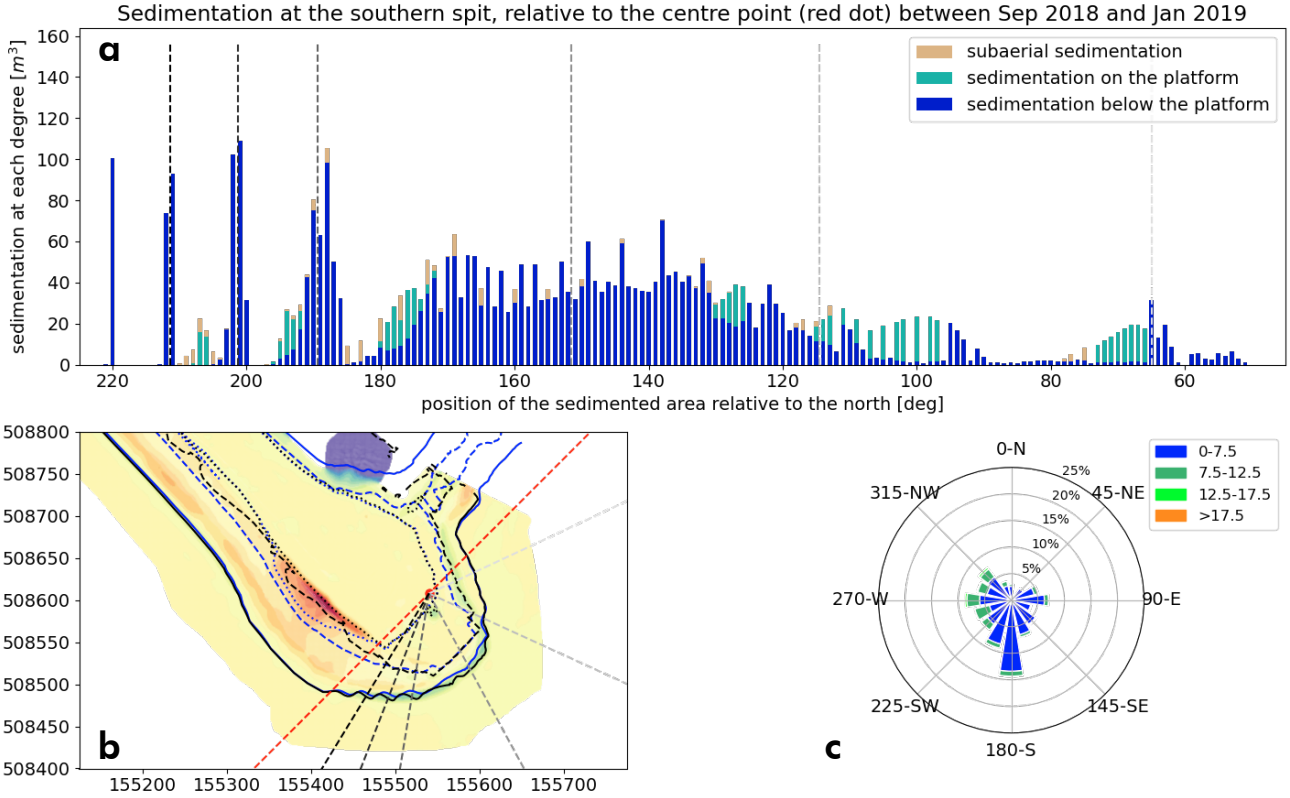

Sedimentation at the southern spit, relative to the centre point (red dot) between Jan 2019 and May 2019

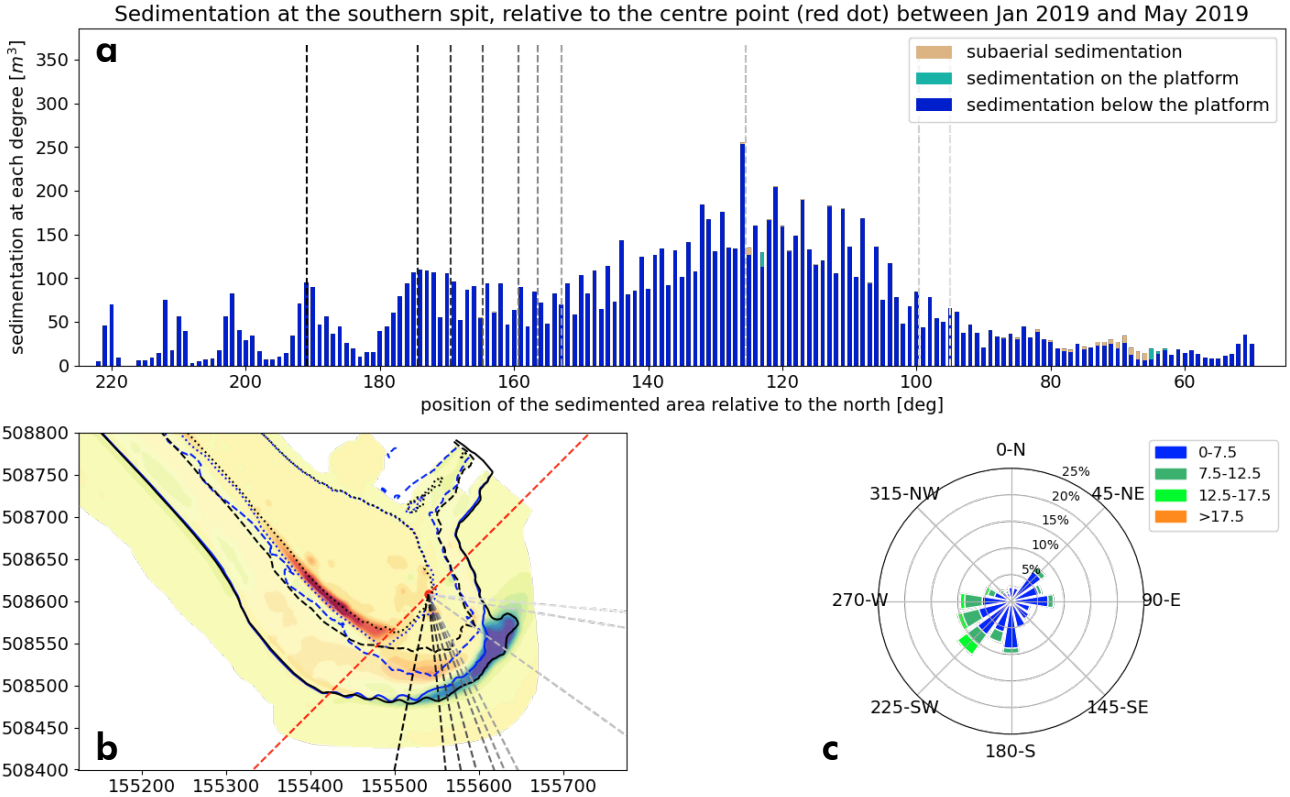

Sedimentation at the southern spit, relative to the centre point (red dot) between May 2019 and Aug 2019

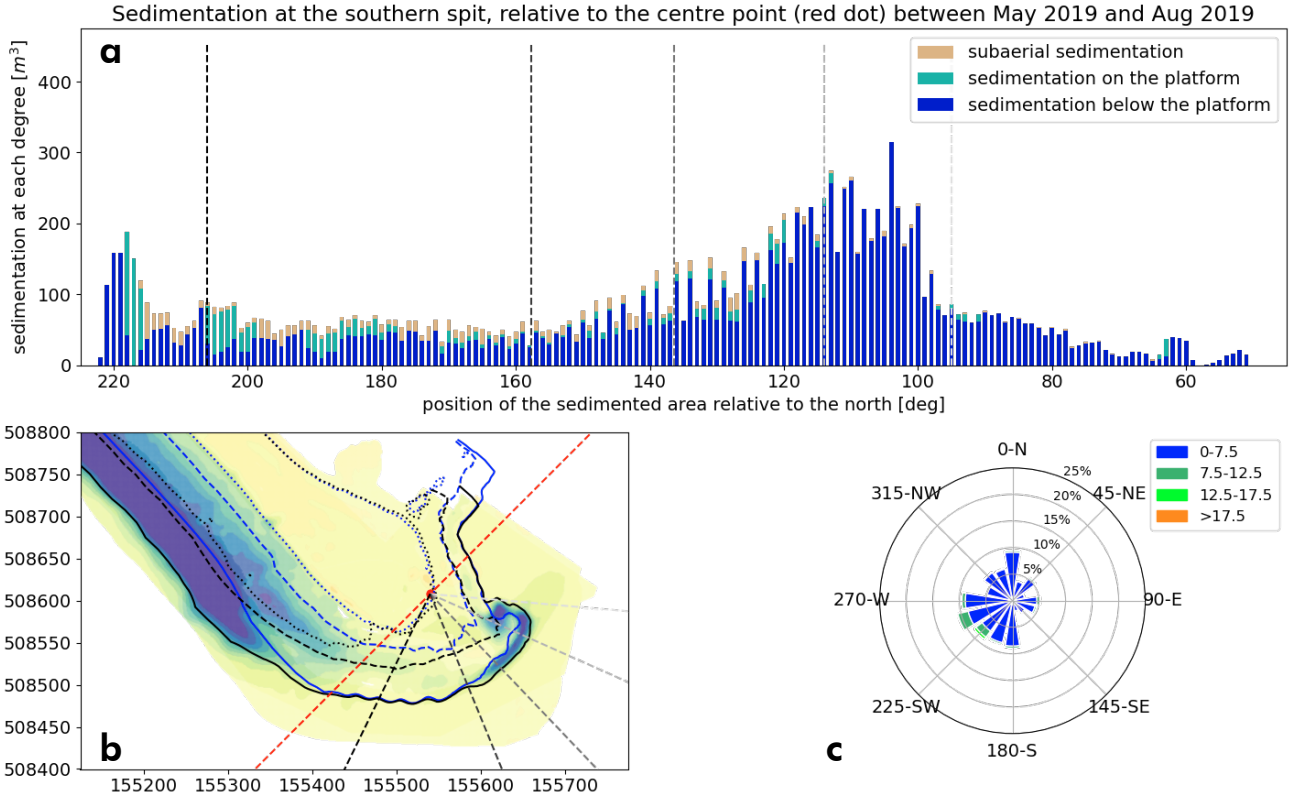

Sedimentation at the southern spit, relative to the centre point (red dot) between Aug 2019 and Oct 2019

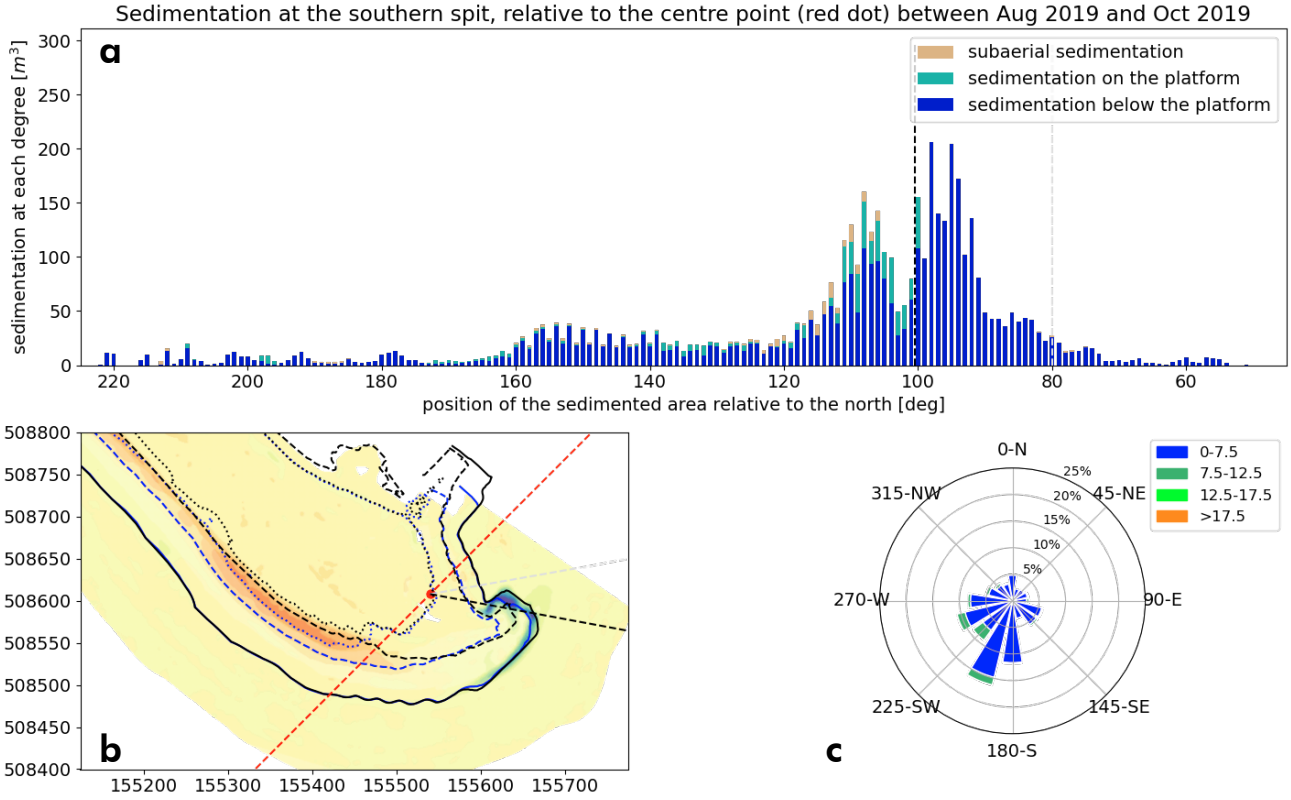

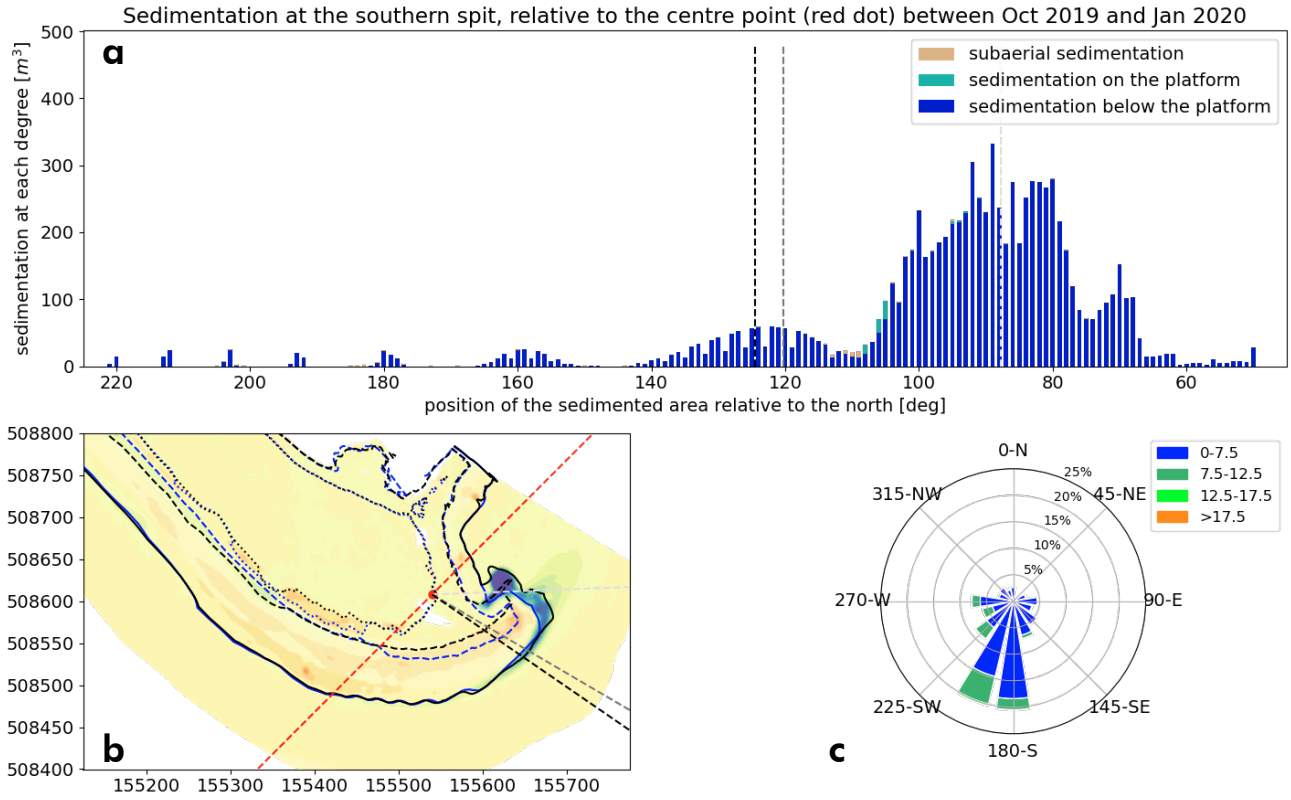
Sedimentation at the southern spit, relative to the centre point (red dot) between Oct 2019 and Jan 2020
a
subaerial sedimentation
sedimentation on the platform
sedimentation below the platform
sedimentation at each degree [m^3]
position of the sedimented area relative to the north [deg]
b
c
0-N
45-NE
90-E
145-SE
180-S
225-SW
270-W
315-NW
0-7.5
7.5-12.5
12.5-17.5
>17.5

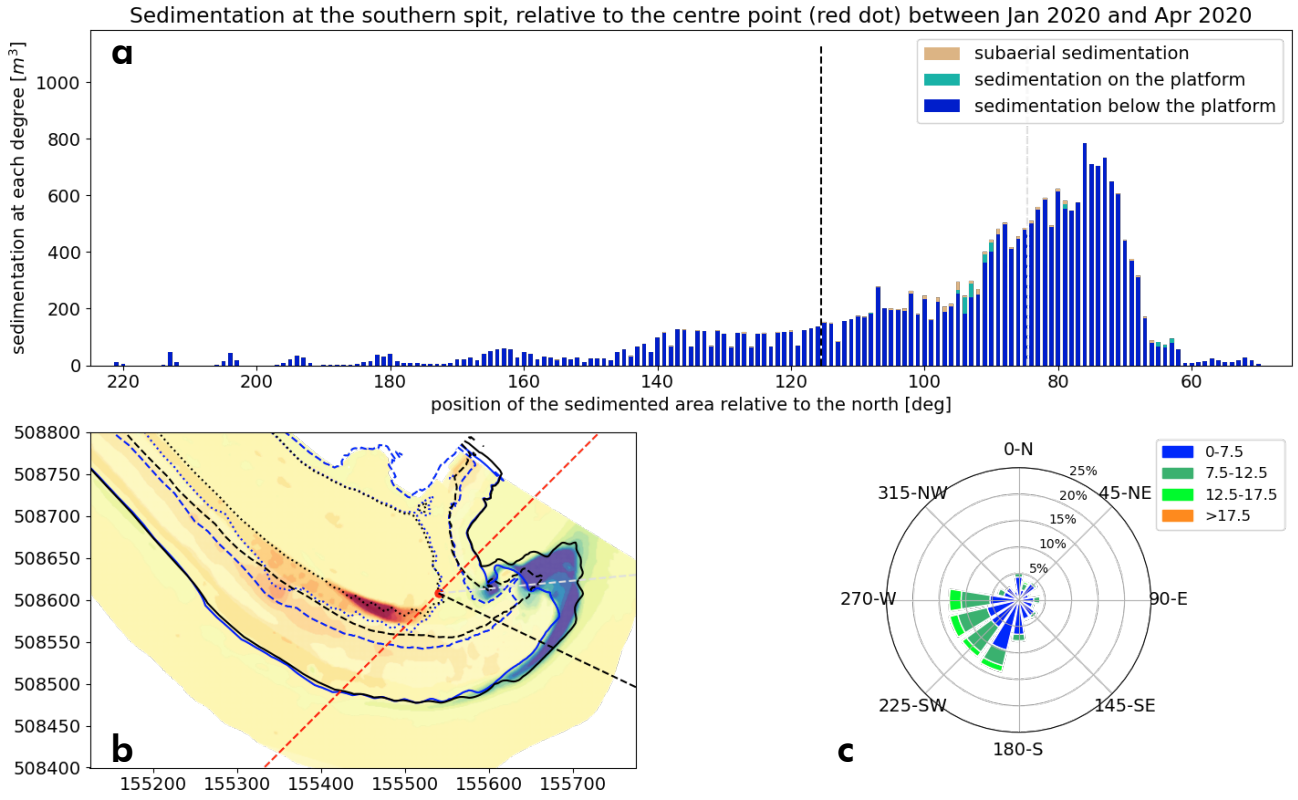
Sedimentation at the southern spit, relative to the centre point (red dot) between Jan 2020 and Apr 2020
a
subaerial sedimentation
sedimentation on the platform
sedimentation below the platform
sedimentation at each degree [m^3]
position of the sedimented area relative to the north [deg]
b
c
0-N
45-NE
90-E
145-SE
180-S
225-SW
270-W
315-NW
0-7.5
7.5-12.5
12.5-17.5
>17.5

Sedimentation at the southern spit, relative to the centre point (red dot) between Apr 2020 and Sep 2020

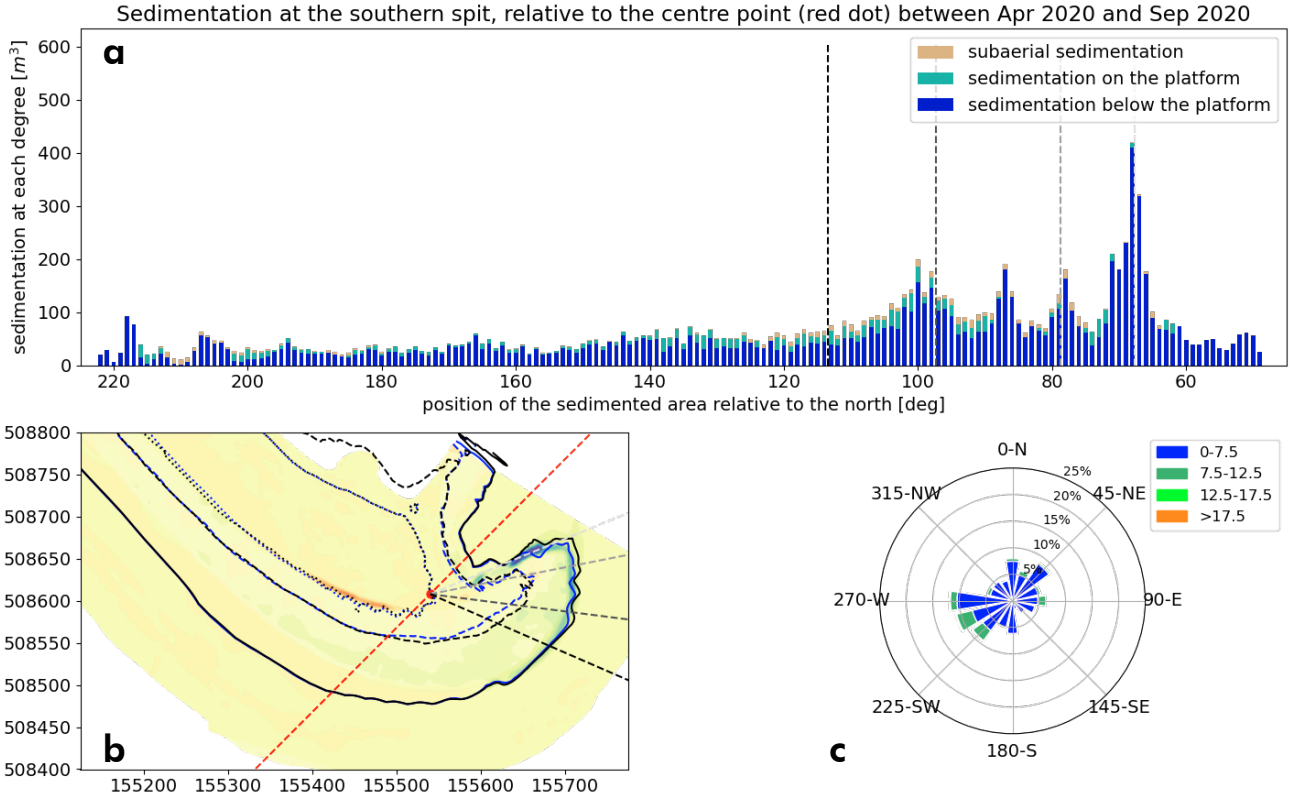

Sedimentation at the southern spit, relative to the centre point (red dot) between Sep 2020 and Nov 2020

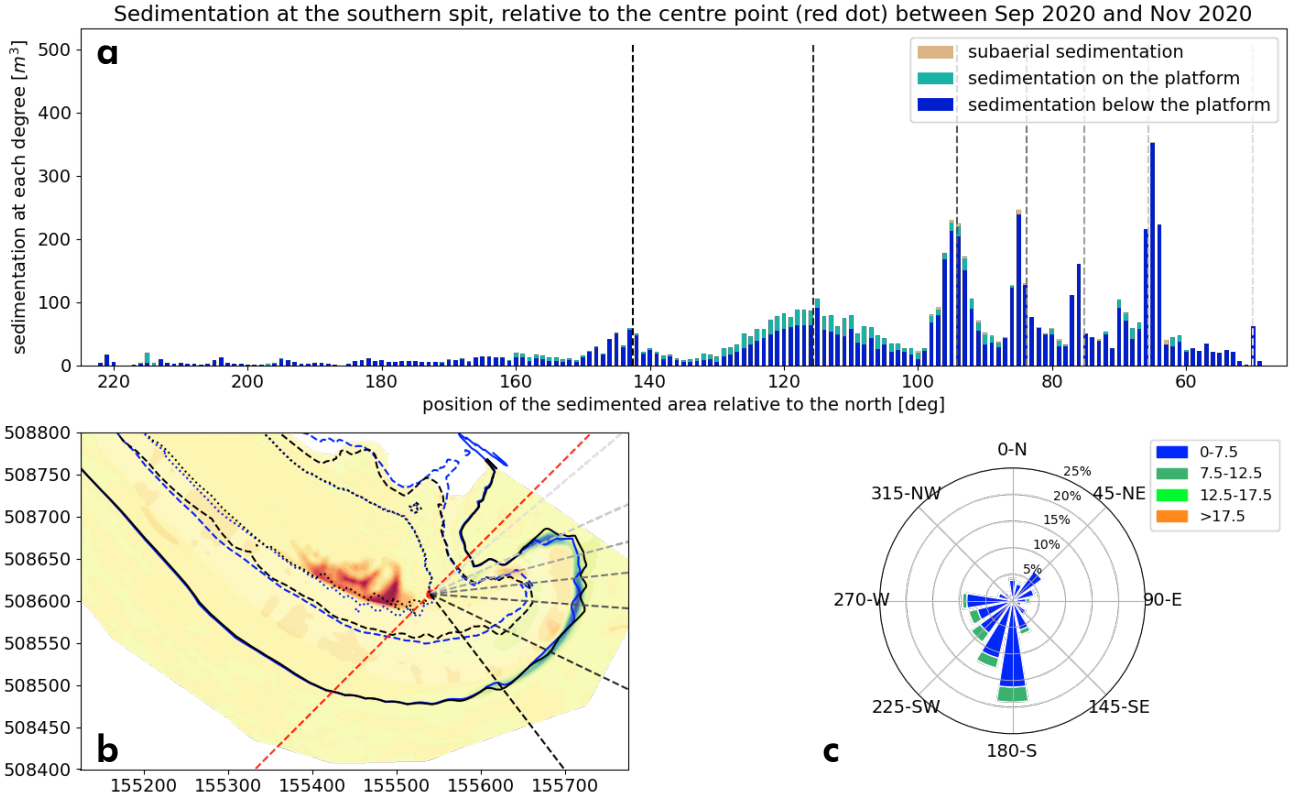

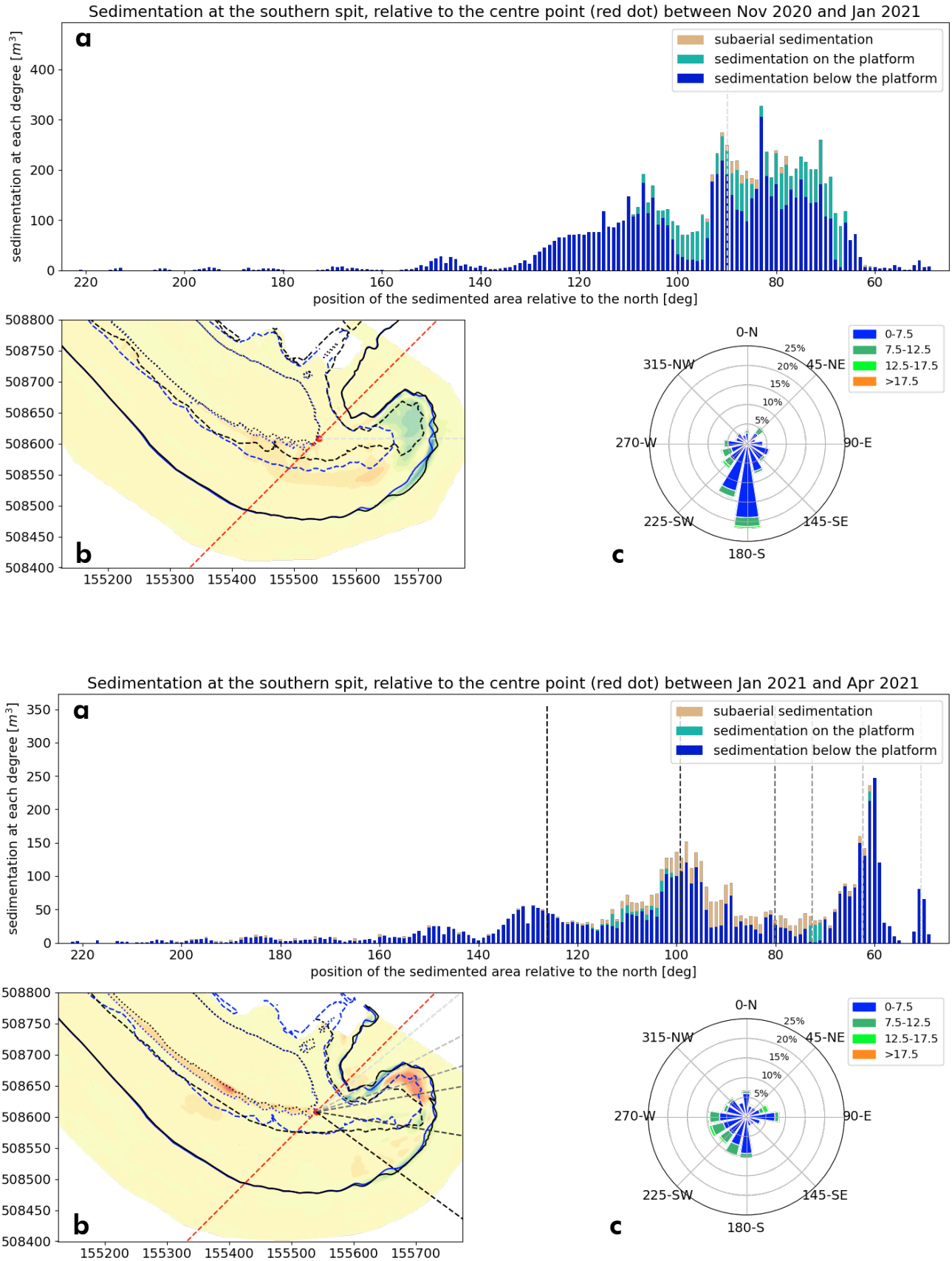

Figure 7. Figures with (a) sedimentation bar-graphs, (b) erosion/sedimentation maps and (c) windroses for each period for the southern spit.

General observations that can be made from these graphs are as follows:

- Periods with significant W and NW winds have sediment deposits at higher degrees (higher than 140°).
- Periods with almost only prevailing S winds have very little sedimentation on the platform level.
- Periods with winds from the N, NE or E also seem to have sedimentation at very low degrees (around 60°). Although the volumes seem to be relatively limited.
- Most sedimentation occurs between 110° and 70° for almost all periods, this holds for both the platform level and sub-platform level. This could mean the main development direction is between the ENE and the ESE relative to the centre point.
- The sedimentation volumes are also more when wind velocities are faster.
- It seems that less sedimentation on the platform occurs when wind velocities are faster.
- The growth rate in length in the most prominent propagation direction (110° and 70°) is on average around 40 m/year.

During qualitative analysis it looked like the southern spit first migrated towards the NE (very low degrees 45°-60°) and later moved more towards the E (around 90°). But when looking at the sedimentation instead of the location of the spit tip, it can be observed that the migration of the (growth direction of the) southern spit is relatively limited. The growth direction of the spit stayed between the 70° and the 110° degrees (Figure 8) and was therefore relatively constant over the whole measured period. Although there was often more growth of the emerged part in the 70° direction than the submerged part, where the bulk of the sedimentation occurred. This is likely caused by the mechanism that is described before. The emerged part is above the depth-of-closure, which means that everything higher than the platform boundary (-1,2 m NAP) is affected by incoming waves. Therefore the change in angle of incidence of the waves plays a significant role in the growth direction of the emerged spit (Figure 4) (Ashton et al., 2016; Ton et al., 2021; see *Method* in the paper for the definition of 'emerged spit' and 'submerged spit-platform'). Because of this extra energy near the spit tip that needs to dissipate it might orientate the emerged spit tip further towards the NE. Also, the bending of the spit towards the E seems more severe than it actually is. A lot of erosion occurs on the proximal end and the spit becomes larger in length. Because of this the curvature of the spit becomes more gradual, which makes it look like the spit is bending, while the growth direction practically stays the same.

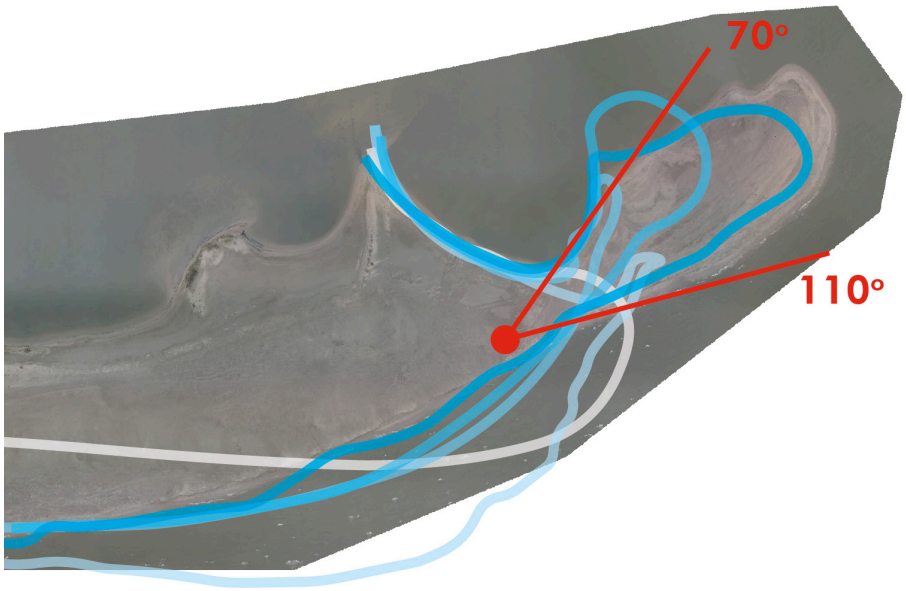

Figure 8. Growth direction of the spit compared to the change of the emerged part of the spit. The coastlines of previous moments are included with a more blue contour it this contour occurred more recent (the same periods are used as in Figure 5).

Quantification of the northern spit migration

For the northern spit the same graphs are made and should be read the same as for the southern spit (Figure 10).

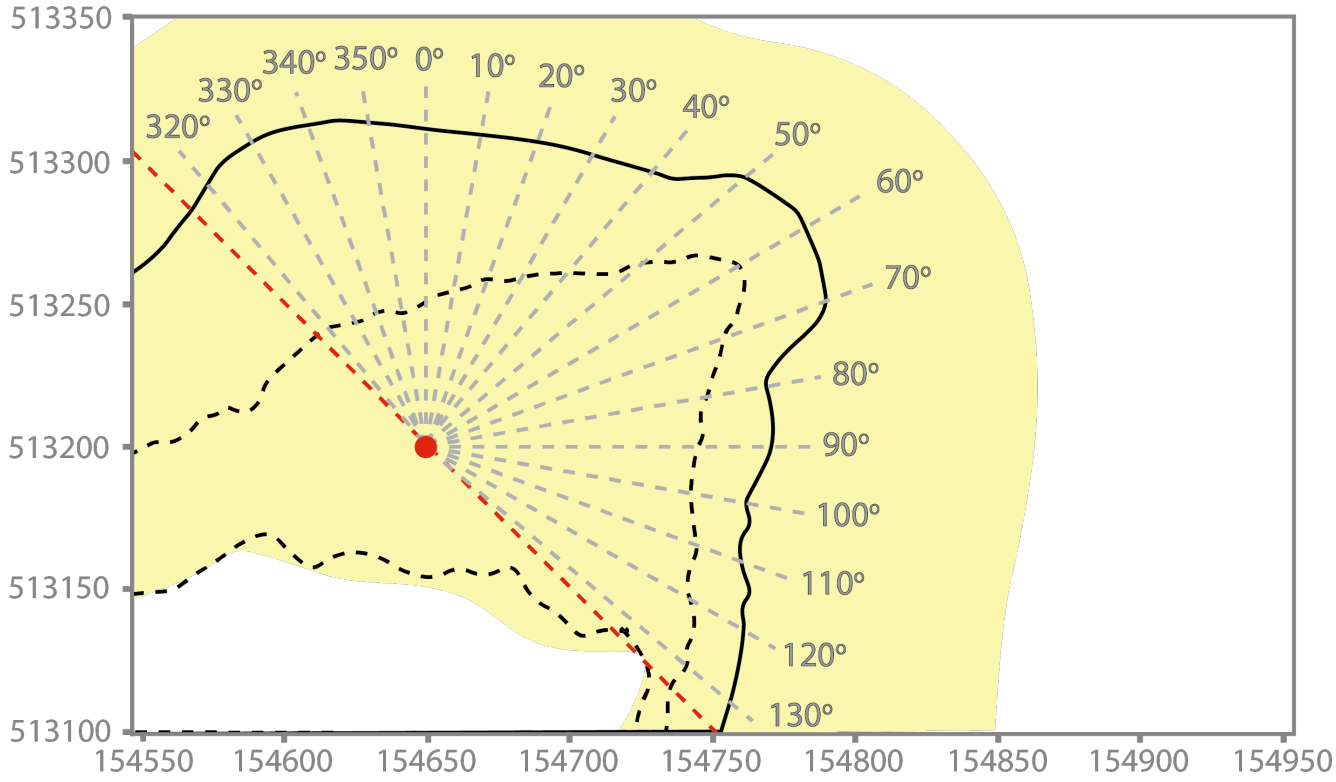

Figure 9. Orientation of the polar coordinate system around the northern spit.

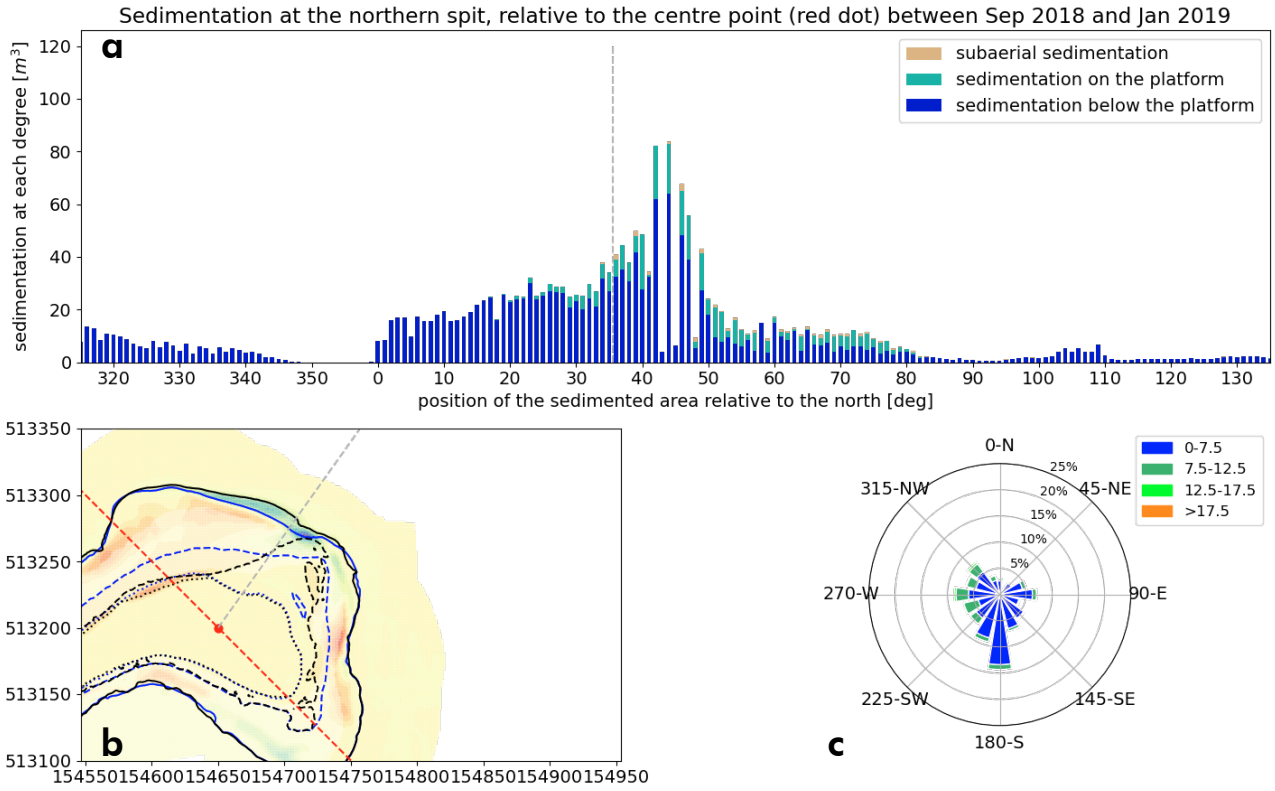

Sedimentation at the northern spit, relative to the centre point (red dot) between Jan 2019 and May 2019

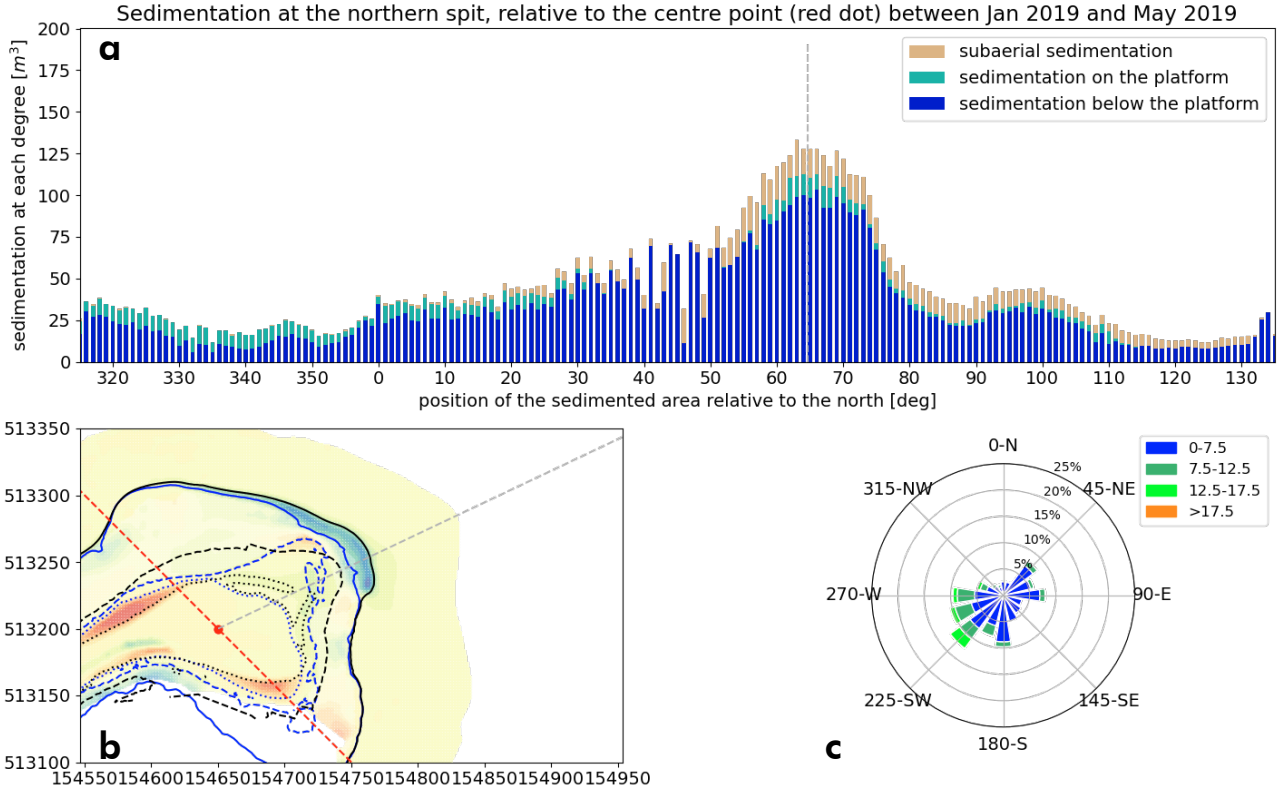

Sedimentation at the northern spit, relative to the centre point (red dot) between May 2019 and Aug 2019

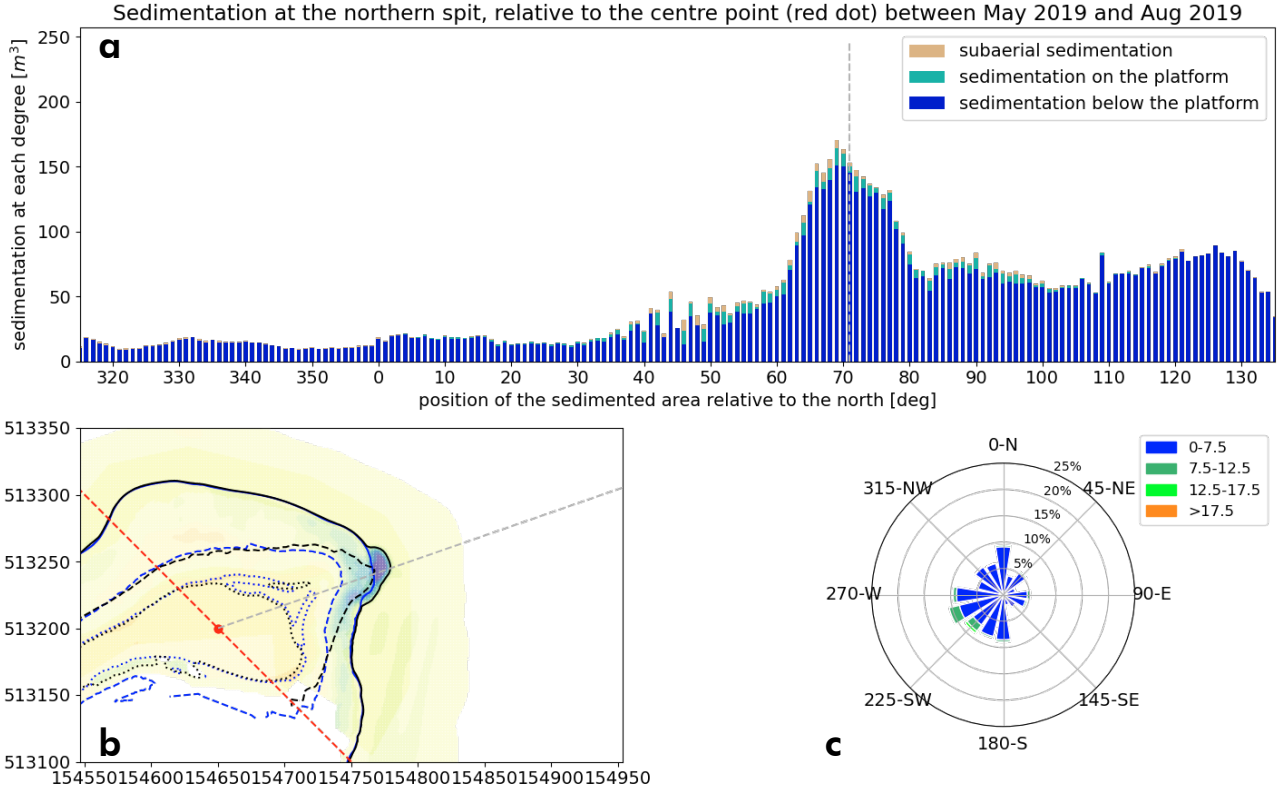

Sedimentation at the northern spit, relative to the centre point (red dot) between Aug 2019 and Oct 2019

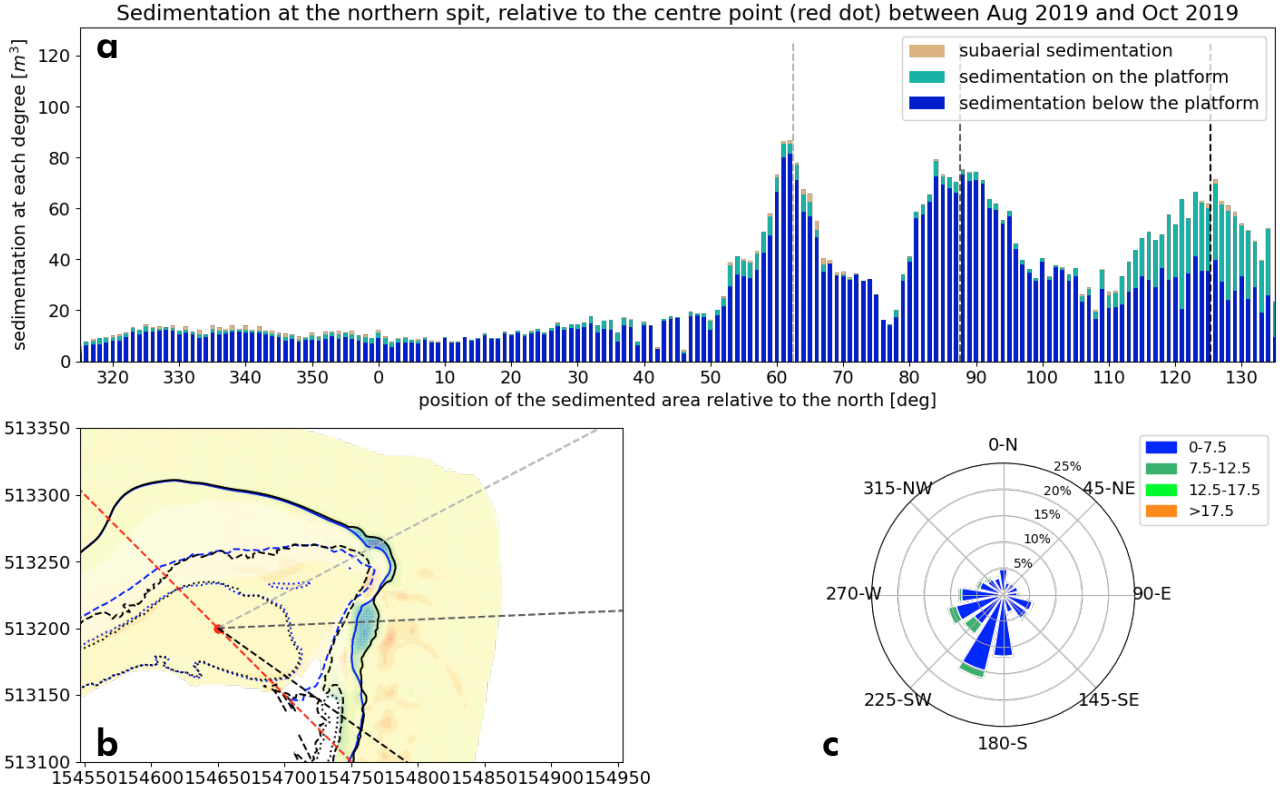

Sedimentation at the northern spit, relative to the centre point (red dot) between Oct 2019 and Jan 2020

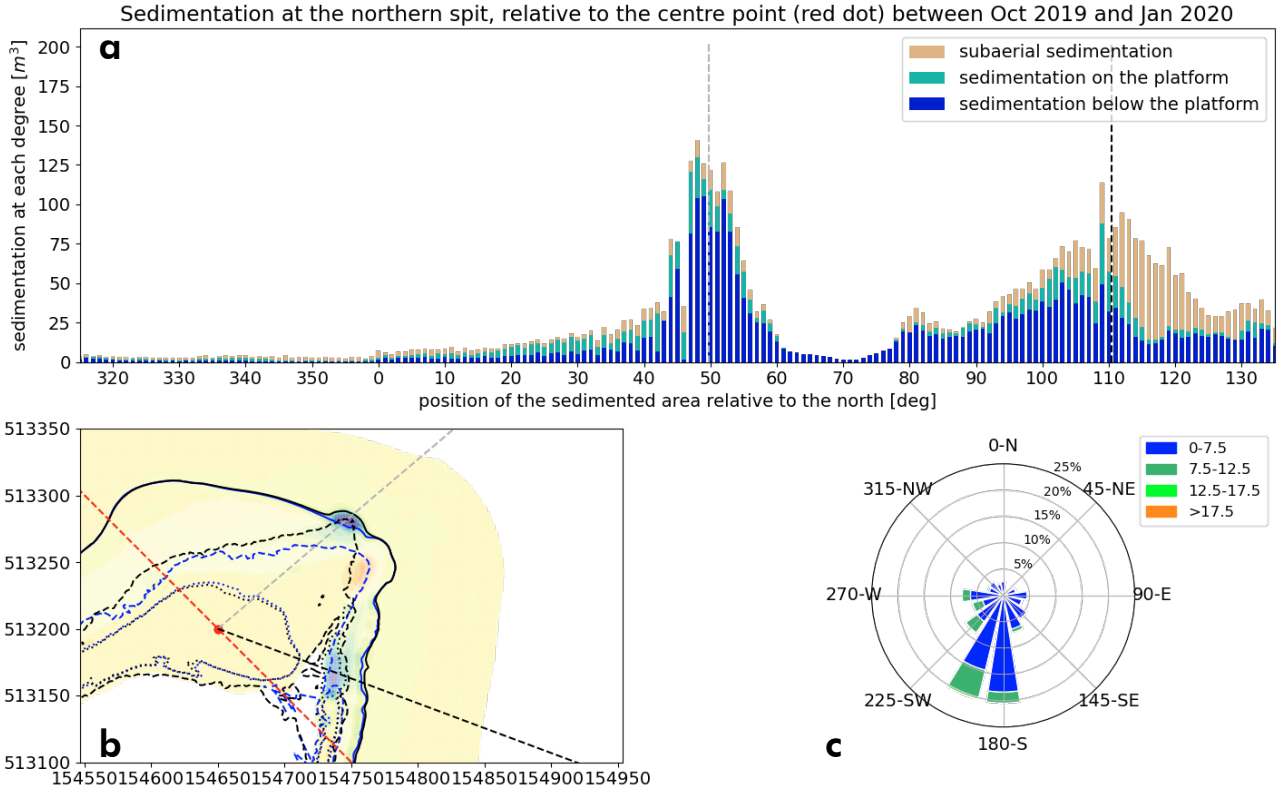

Sedimentation at the northern spit, relative to the centre point (red dot) between Jan 2020 and Apr 2020

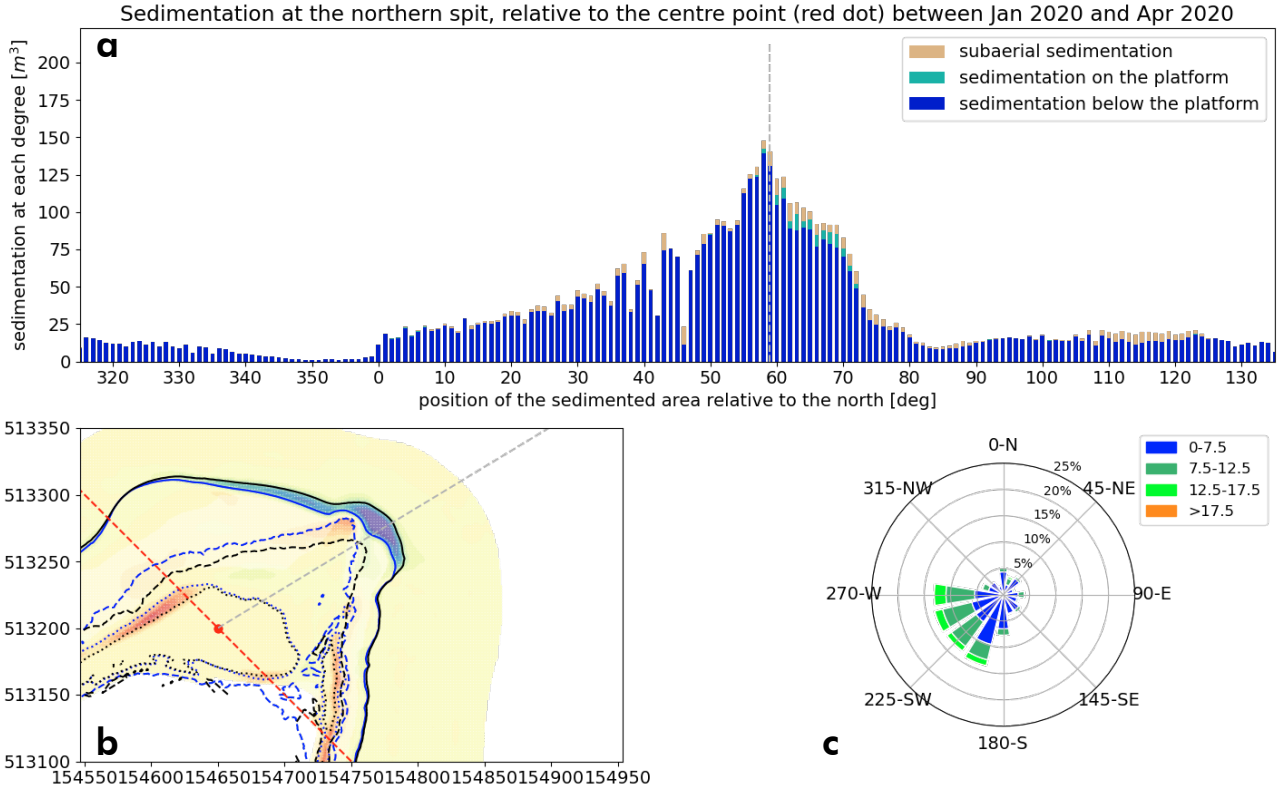

Sedimentation at the northern spit, relative to the centre point (red dot) between Apr 2020 and Sep 2020

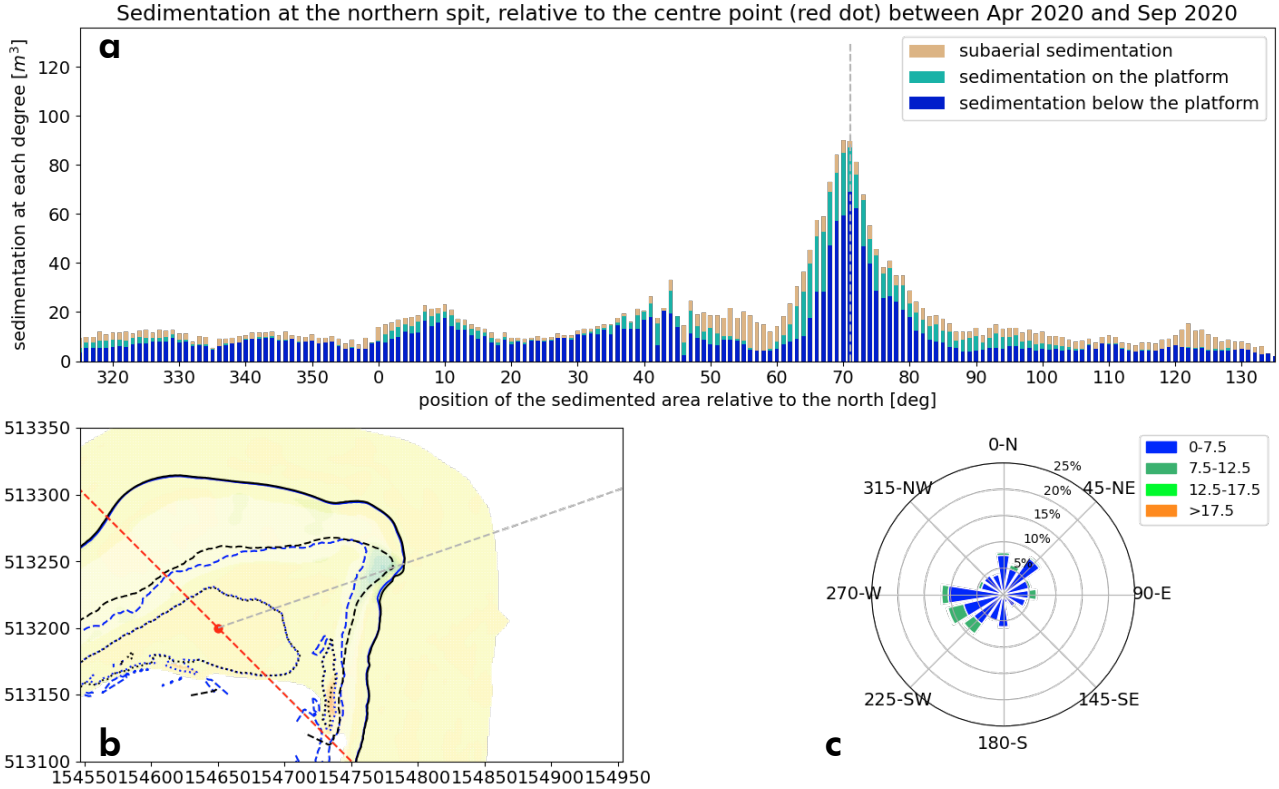

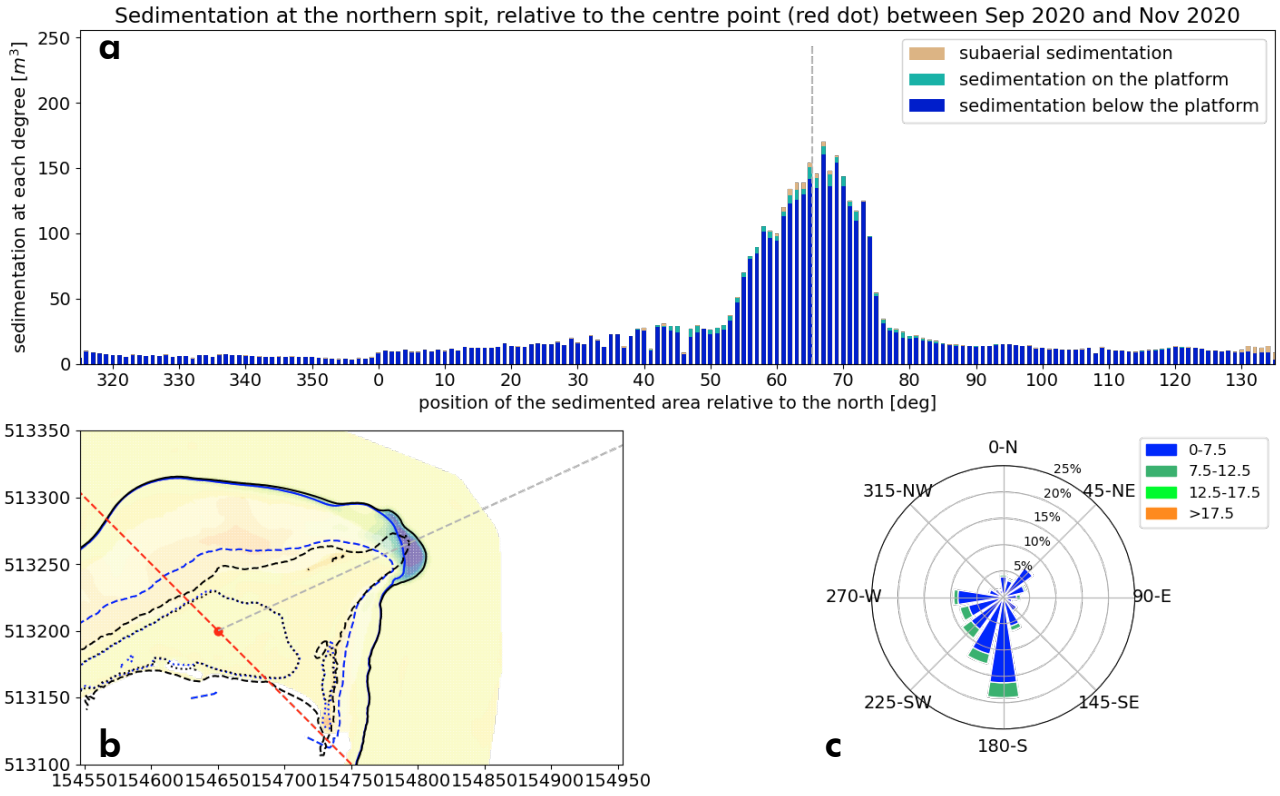

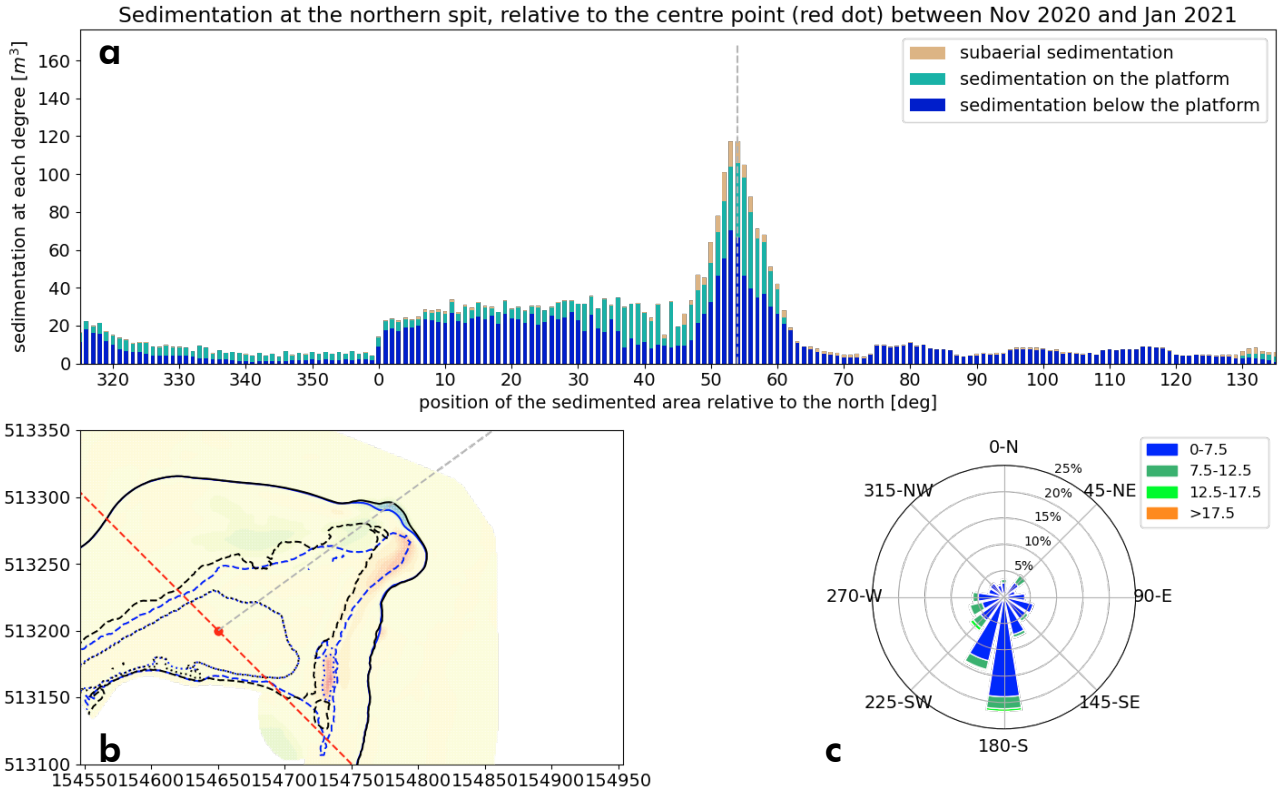

Figure 10. Figures with (a) sedimentation bar-graphs, (b) erosion/sedimentation maps and (c) windroses for each period for the northern spit.

General observations that can be made from these graphs are as follows:

- Periods with significant W winds have more deposits towards the higher degrees (70° degrees).
- Periods with almost only prevailing S winds orientate sedimentation more towards lower degrees (around 50° degrees).
- Periods with very high SW winds result in a broad field of sedimentation between 0° and 60°. It looks like currents coming from the south in these conditions are faster than the simultaneous occurring currents from the east. These southern currents move the sediment around the tip to fan it out on the other side.
- Most sedimentation occurs between 45° and 70° for almost all periods, this holds for both the platform level and sub-platform level. This means that the main development direction is to the NE.
- The sedimentation volumes are also more when wind velocities are faster.
- It seems that less sedimentation on the platform level occurs when wind velocities are faster.
- The growth rate in length in the most prominent propagation direction (45° and 70°) is on average around 20 m/year.

3. Expansion of the spit-platform during high energy periods and expansion of the emerged spit during low energy periods

When there are a lot of storm events, a lot of changes under water can be seen, but from above the waterline this spit looks often almost the same. Most of the sedimentation, in shear volumes, is done in these periods. However, sometimes it seems that the spit has grown significantly while looking at the emerged part. However, at closer inspection there has not been that much sedimentation in volumes, but a significant portion of sedimentation has occurred platform level in these cases.

It seems that during high energy events the flow velocities do not decrease enough on the platform level to allow sedimentation there. Only when flow surpasses the platform boundary, then there is room for the energy of the flow to dissipate enough for sedimentation. When flow velocities are lower, less energy has to dissipate to result in sedimentation on the platform level and allow for the emerged spit to grow (Figure 11).

Quantification

In the sedimentation graphs of the previous section, it could be seen that during periods with a lot of high energy events, significantly less sedimentation on the platform level was present. This means that the sedimentation location in the spit height profile is dependent on the wind velocity. But it is also dependent on the amount of room that is available for dissipation. The dissipation space that is applicable for sedimentation on the platform level could be expressed as the size of the spit-platform. Sedimentation above the waterline can only occur when there is a set-up (or possibly by aeolian transport) that is probably why the sedimentation volumes above the waterline are so low. Under set-up conditions wind velocities are higher and sedimentation is less likely for sediment particles with average grain size (Figure 12).

Part of the quantification has been done with the sedimentation/orientation graphs (Figure 7, Figure 10) but the precise relation between flow velocity (of which it is known from hydrodynamic analysis that it is mostly dependent on wind velocity) and the platform area will be further treated in Appendix F.

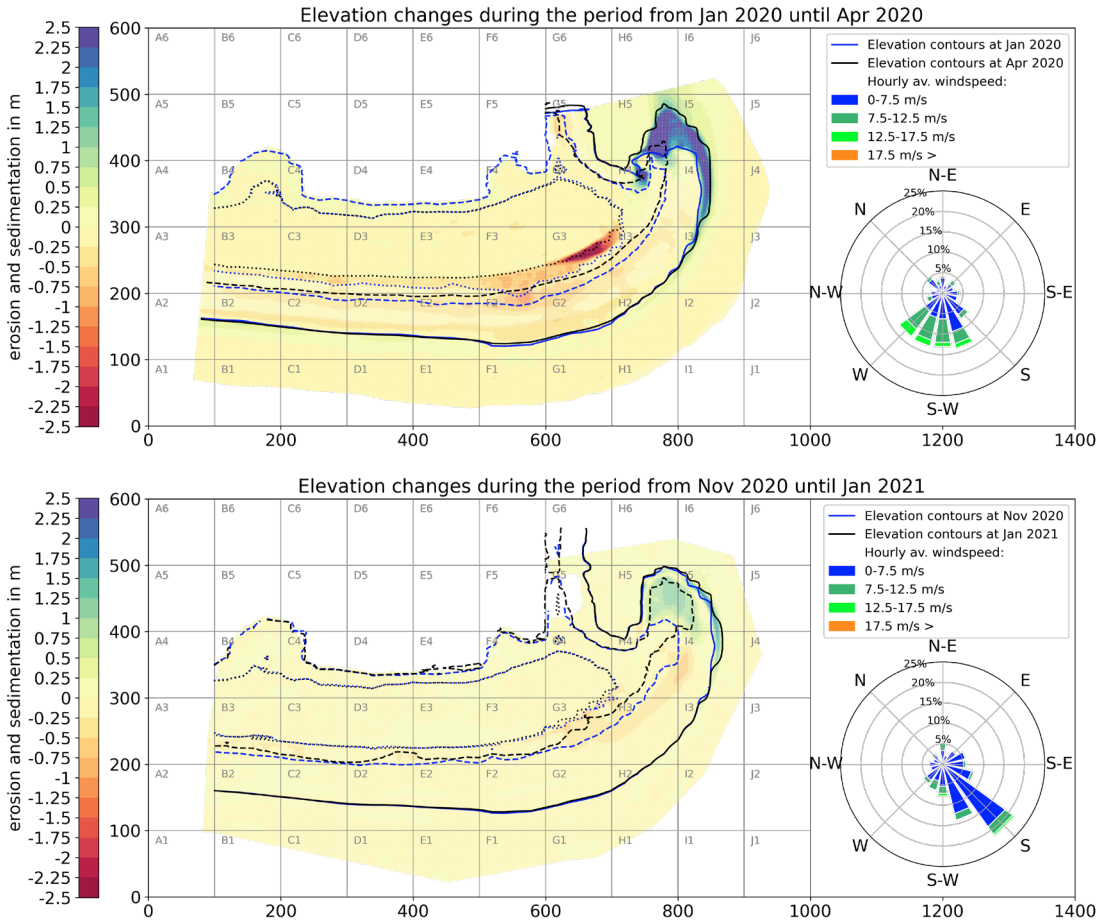

Figure 11. Difference in growth during a high energy period (above) and a low energy period (below).

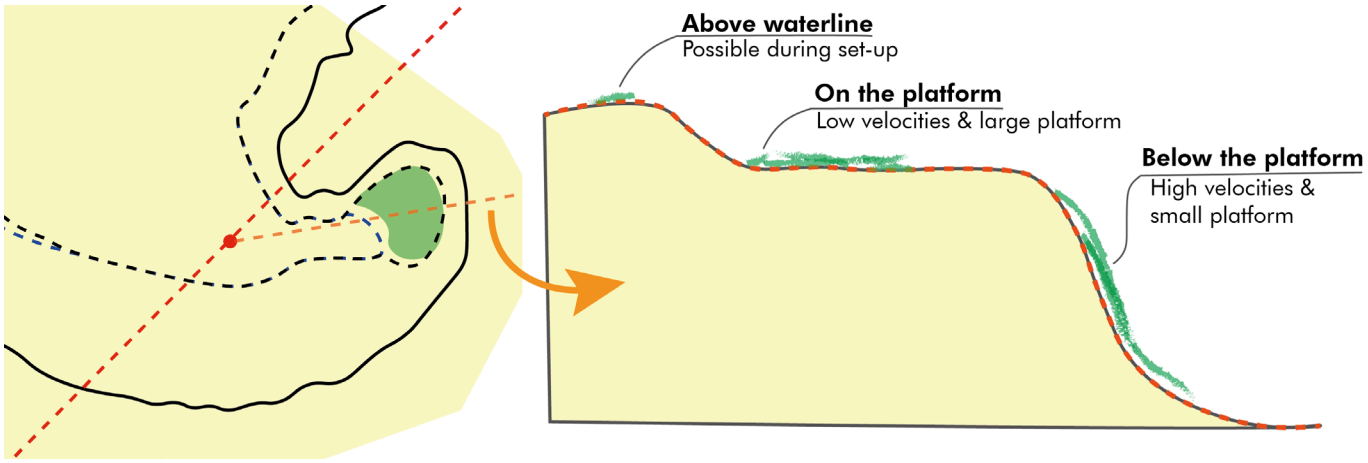

Figure 12. Sedimentation on the cross-section of the spit

Bibliography

Ashton, A. D., Nienhuis, J., & Ells, K. (2016). On a neck, on a spit: Controls on the shape of free spits. *Earth Surface Dynamics*, *4*(1), 193–210. https://doi.org/10.5194/esurf-4-193-2016

Ton, A. M., Vuik, V., & Aarninkhof, S. G. J. (2021). Sandy beaches in low-energy, non-tidal environments: Linking morphological development to hydrodynamic forcing. *Geomorphology*, *374*. https://doi.org/10.1016/j.geomorph.2020.107522

Appendix

Results

Flow directions and velocities around the spit caused by wind

Table of contents appendix D

In the previous appendix morphodynamic developments were explained by looking at different wind regimes. In fact, different wind conditions create different hydrodynamic processes and currents in the lake Markermeer which in turn result in morphodynamic changes. To get more insight in the root of the spit developments, hydrodynamics based on different wind regimes, will be analysed in this appendix. This will make it eventually possible to link the hydrodynamics and morphodynamics.

Ton et al. (2022) developed a 2DH hydrodynamic model in Delft 3D of the lake Markermeer. This model is used to observe currents around both the spits. The topography used in this model is of January 2021. In total there are 32 scenarios of combinations of wind directions and velocities to be modelled (Table 1). The wind data is obtained from the KNMI, station Berkhout (249).

Wind dir	Wind vel	Wind dir	Wind vel	Wind dir	Wind vel	Wind dir	Wind vel
N	5 m/s	N	10 m/s	N	15 m/s	N	20 m/s
NE	5 m/s	NE	10 m/s	NE	15 m/s	NE	20 m/s
E	5 m/s	E	10 m/s	E	15 m/s	E	20 m/s
SE	5 m/s	SE	10 m/s	SE	15 m/s	SE	20 m/s
S	5 m/s	S	10 m/s	S	15 m/s	S	20 m/s
SW	5 m/s	SW	10 m/s	SW	15 m/s	SW	20 m/s
W	5 m/s	W	10 m/s	W	15 m/s	W	20 m/s
NW	5 m/s	NW	10 m/s	NW	15 m/s	NW	20 m/s

Table 1. 32 scenarios consisting of different combinations of wind directions and wind velocities.

First the southern spit will be discussed and later the northern spit. The hydrodynamics from the Delft 3D model results in the graphs that can be seen at the start of each chapter. Each graph gives the behaviour of the currents around the spits for one scenario. These graphs should be read as follows:

a: Each point in the graph gives the current direction at a certain location relative to the centre point. The weighted average of the current directions on a single degree is taken from the waterline (the squares in the grid that have a velocity of 0 m/s, see graph b) up to a little over the platform boundary, weighted with the velocity. This is because current directions with higher velocities likely have more morphological impact. The current direction is the direction that the flow is going to and not where the flow has originated from. The flow velocity is the mean velocity on a single degree and indicated with a colour. The current directions can be fitted with the grey line so that there is one function for the current directions around the spit for one scenario. The same can be done for the flow velocities.

b: This map shows the current directions around the spit visually with the white arrows. The topography is indicated in grey (coastline in solid lines and the platform boundary in dashed lines). The straight grey dashed lines indicate the area over which the current directions and velocities are considered. The flow velocities around the spit are indicated by the colours.

c: This windrose gives the wind conditions for the scenario that is modelled. The windrose points to the wind direction that is modelled, and the wind velocities are indicated by the colour. Blue means 5 m/s, dark green means 10 m/s, lime green means 15 m/s and orange means 20 m/s.

Southern spit

The graphs of the southern spit look as follows:

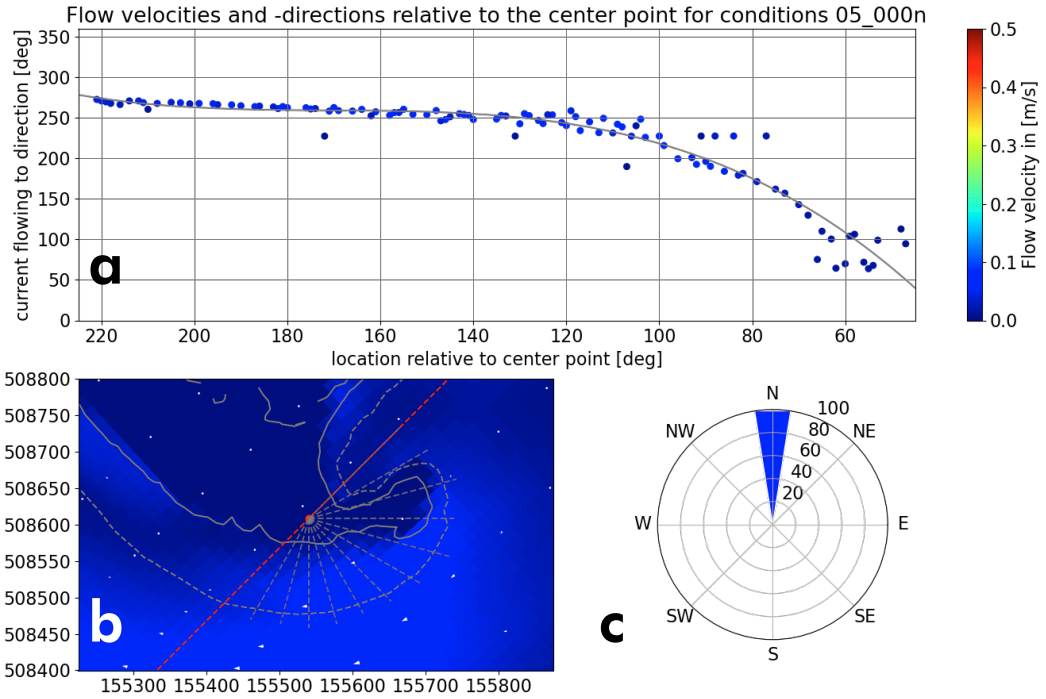

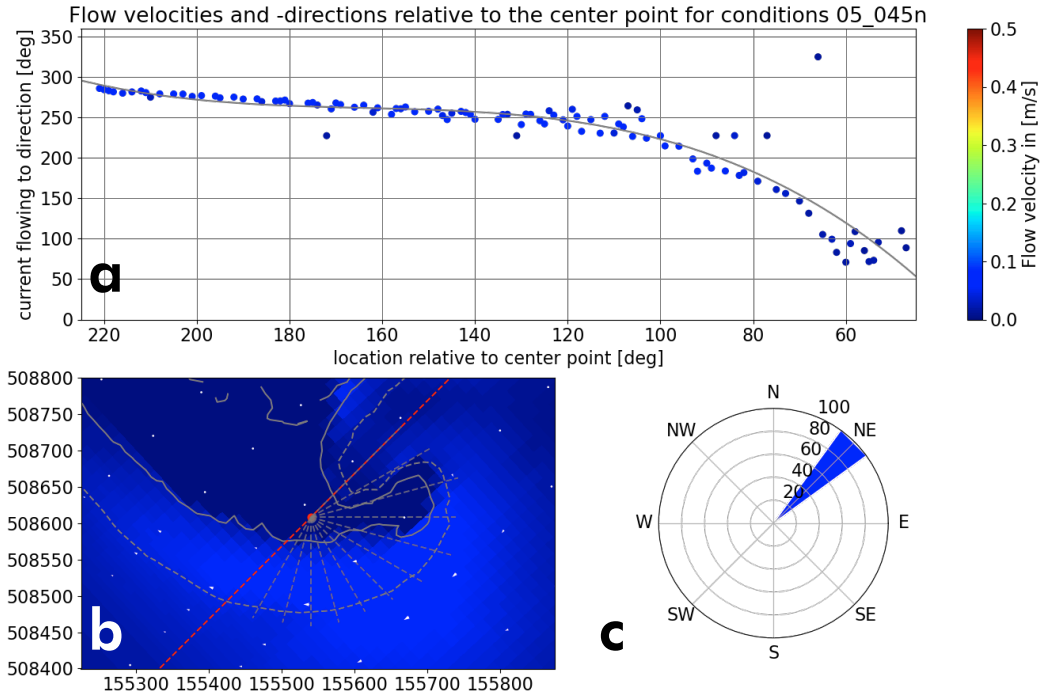

Legend

a:
- Current direction at a degree [deg]
- Current velocity at a degree [m/s]
- Fitted current directions around spit [deg]

b:
- Current velocity [m/s]
- Current direction [deg]
- Waterline
- Platform boundary
- Range of considered data around centre point
- Centre point

c: wind velocities:
- 5 m/s
- 10 m/s
- 15 m/s
- 20 m/s

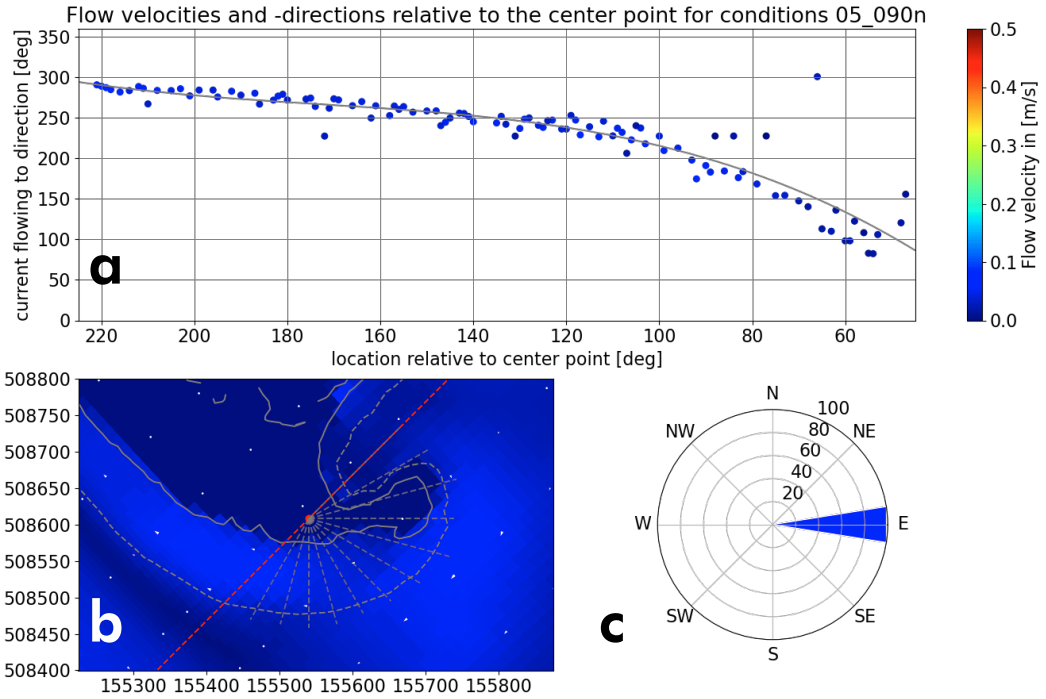

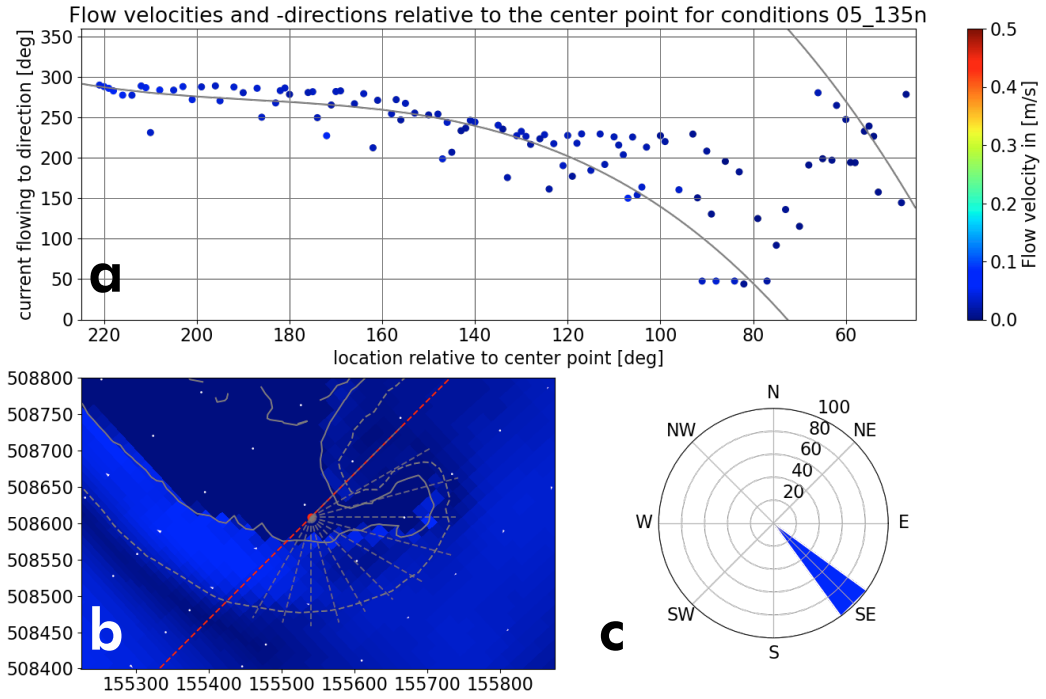

Legend

a: Current direction at a degree [deg]

Current velocity at a degree [m/s]

Fitted current directions around spit [deg]

b: Current velocity [m/s]

Current direction [deg]

Waterline

Platform boundary

Range of considered data around centre point

Centre point

c: wind velocities:

5 m/s

10 m/s

15 m/s

20 m/s

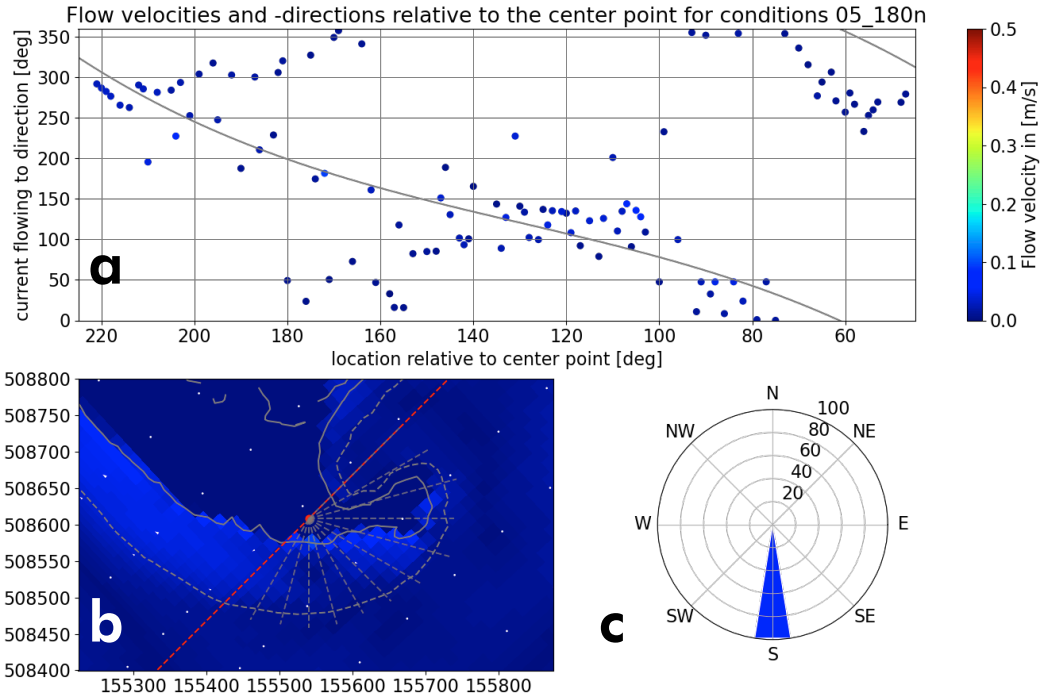

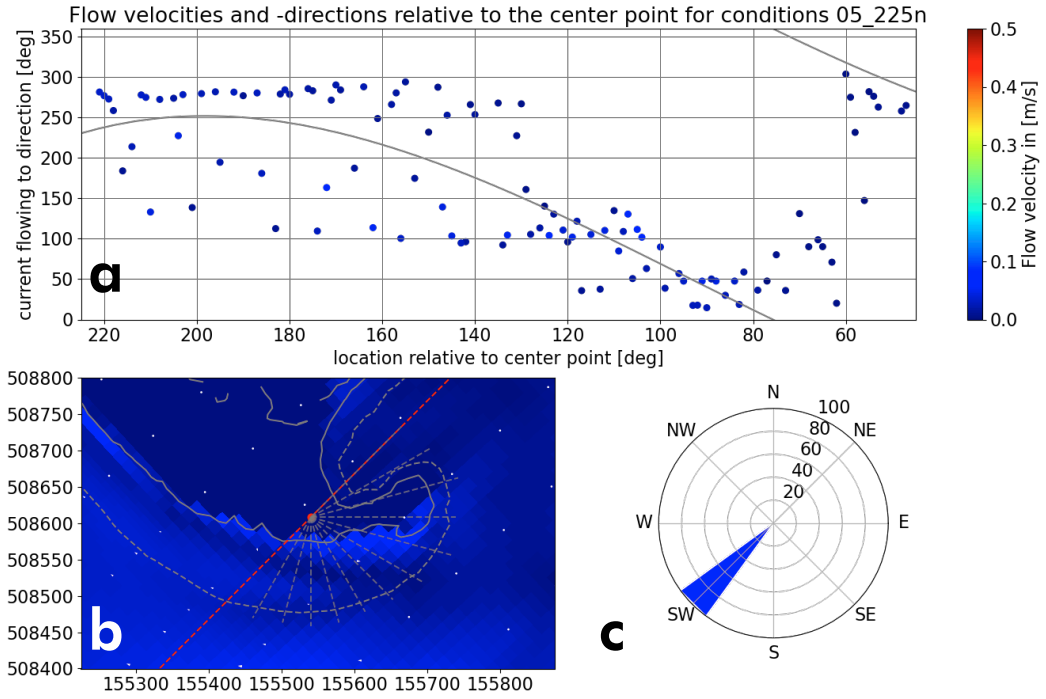

Legend

a:
- Current direction at a degree [deg]
- Current velocity at a degree [m/s]
- Fitted current directions around spit [deg]

b:
- Current velocity [m/s]
- Current direction [deg]
- Waterline
- Platform boundary
- Range of considered data around centre point
- Centre point

c: wind velocities:
- 5 m/s
- 10 m/s
- 15 m/s
- 20 m/s

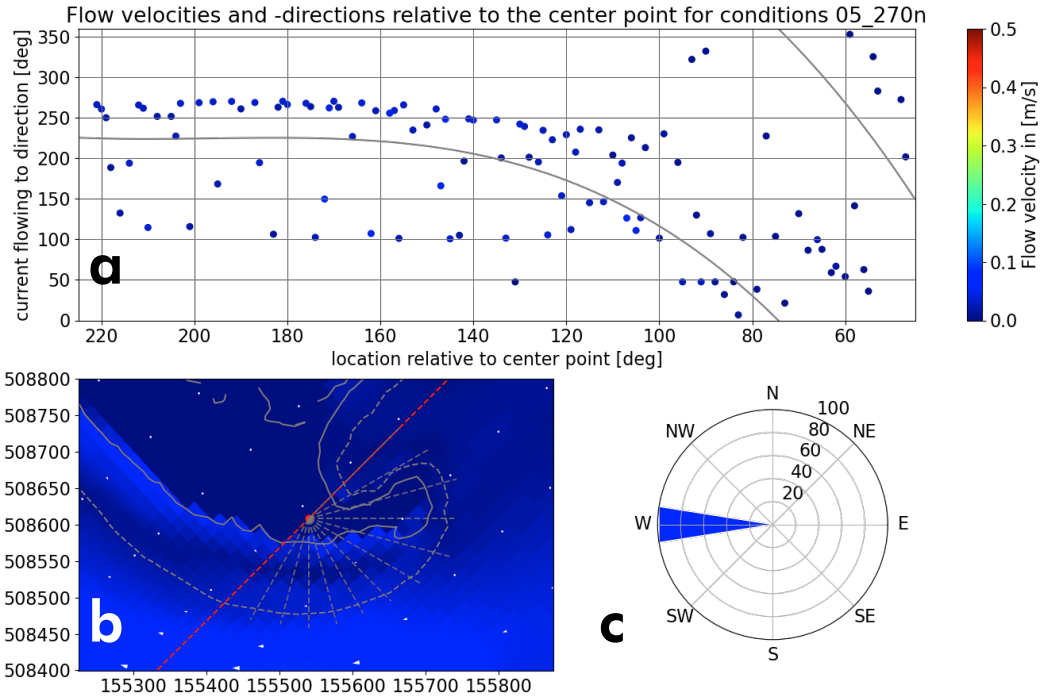

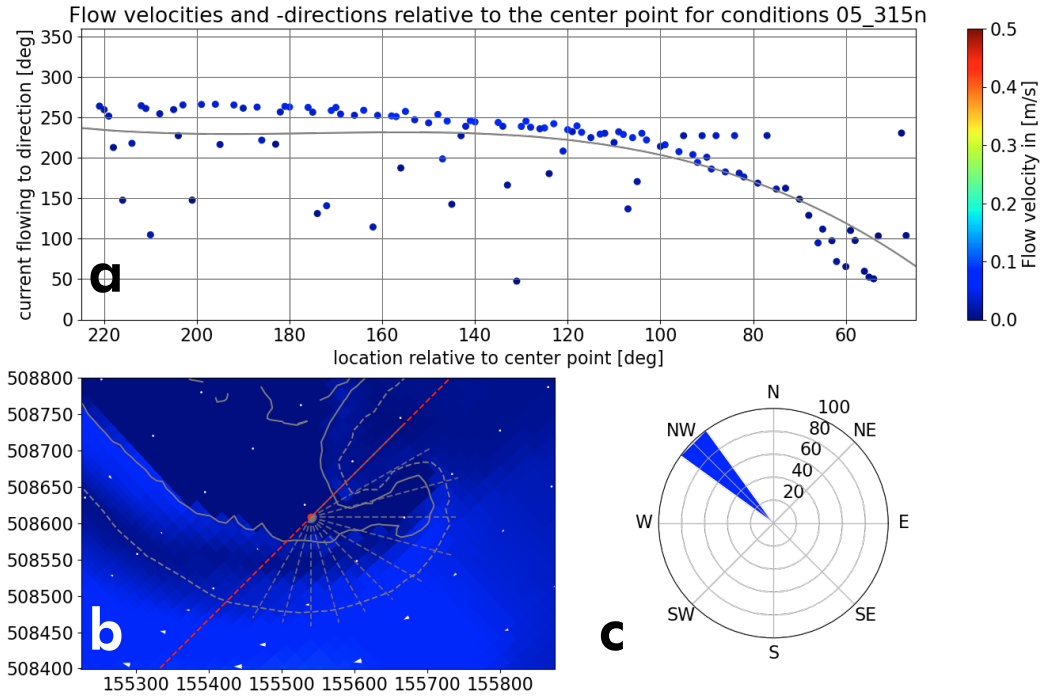

Legend

a: Current direction at a degree [deg]

Current velocity at a degree [m/s]

Fitted current directions around spit [deg]

b: Current velocity [m/s]

Current direction [deg]

Waterline

Platform boundary

Range of considered data around centre point

Centre point

c: wind velocities:

5 m/s

10 m/s

15 m/s

20 m/s

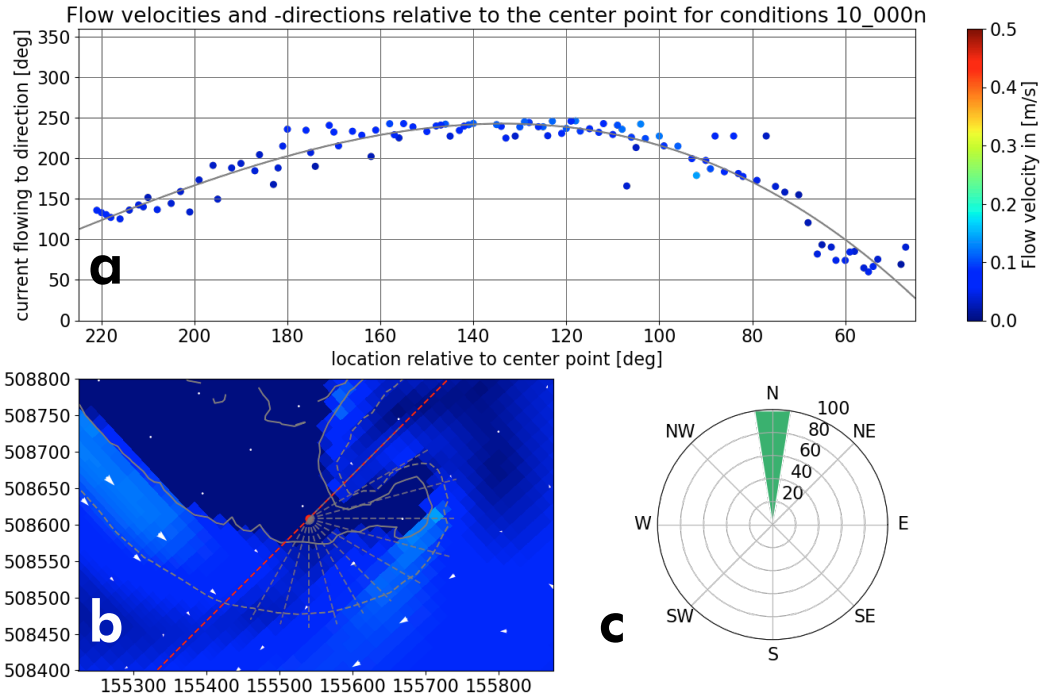

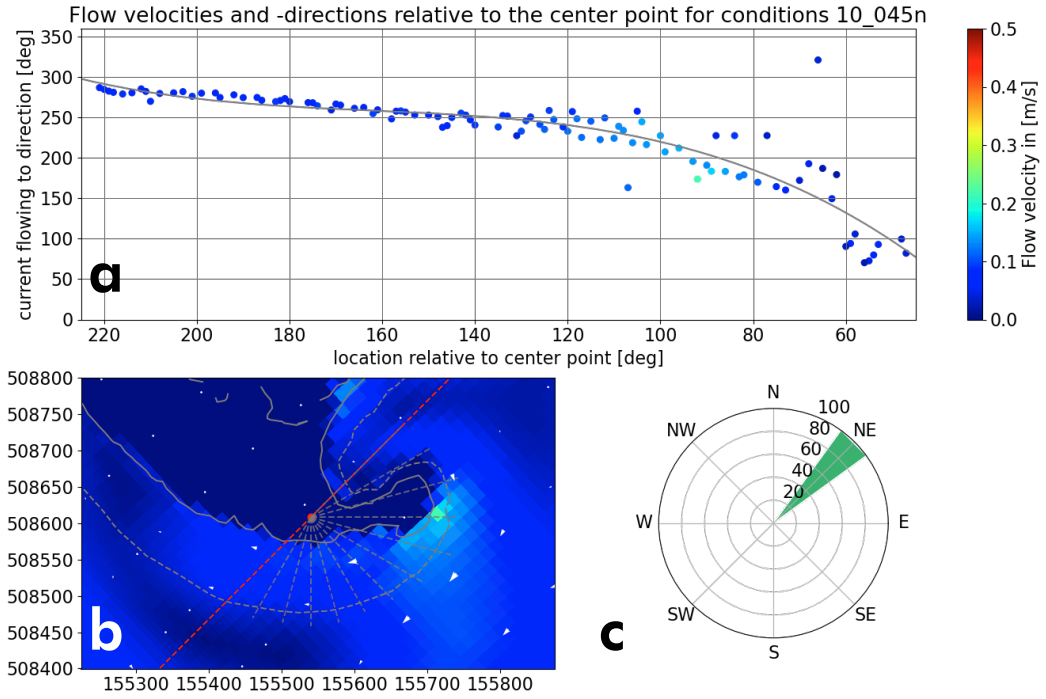

Legend

a:
- Current direction at a degree [deg]
- Current velocity at a degree [m/s]
- Fitted current directions around spit [deg]

b:
- Current velocity [m/s]
- Current direction [deg]
- Waterline
- Platform boundary
- Range of considered data around centre point
- Centre point

c: wind velocities:
- 5 m/s
- 10 m/s
- 15 m/s
- 20 m/s

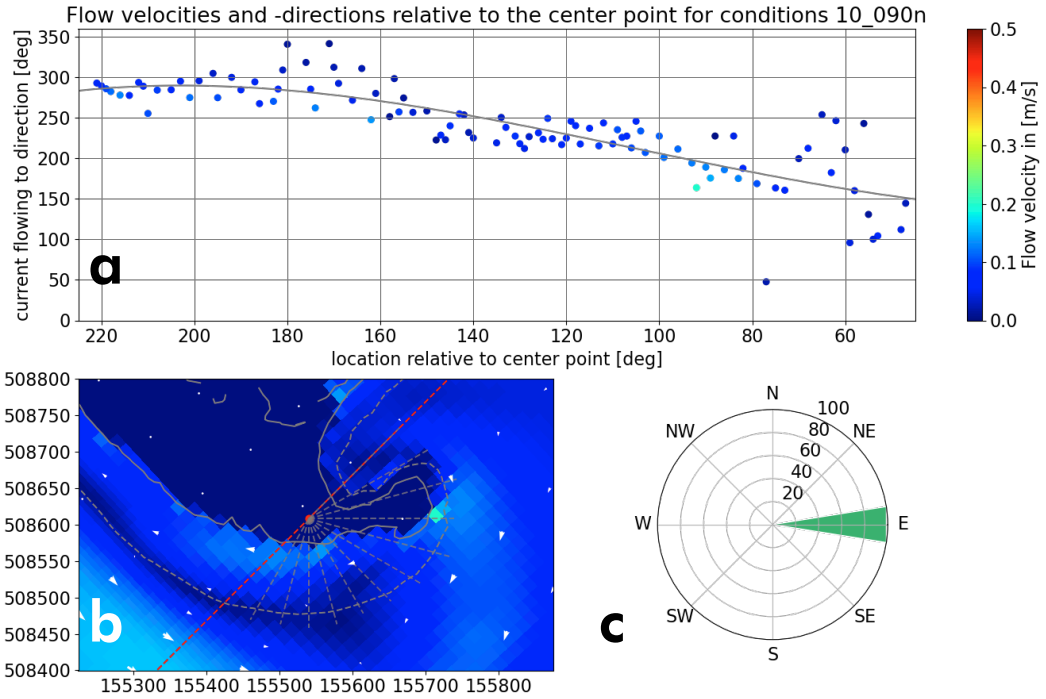

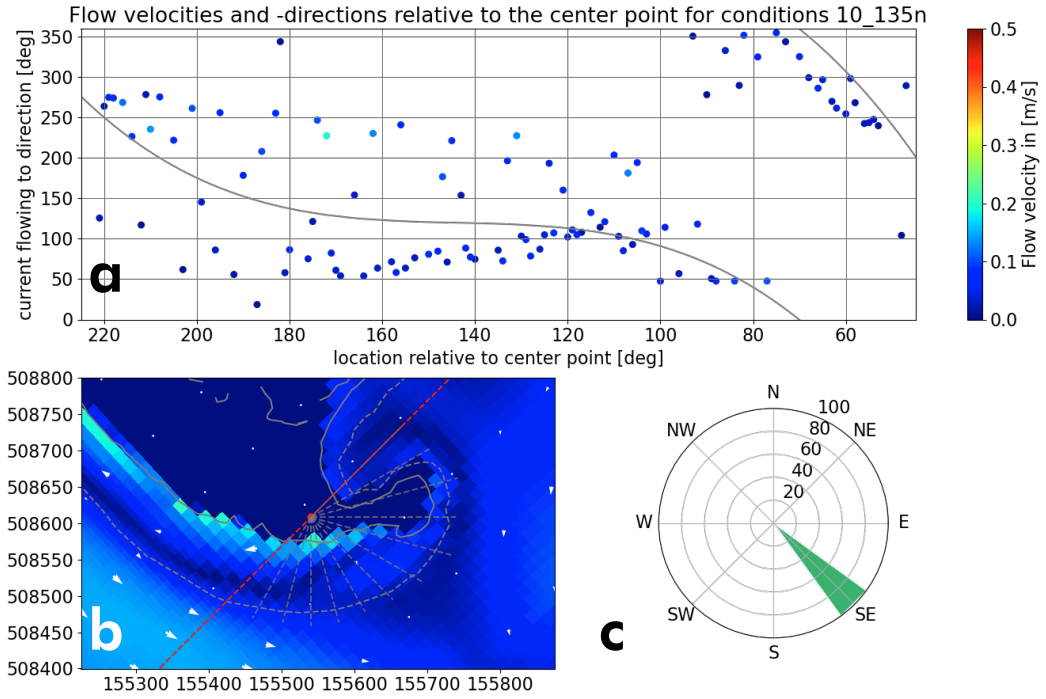

Legend

a:
- Current direction at a degree [deg]
- Current velocity at a degree [m/s]
- Fitted current directions around spit [deg]

b:
- Current velocity [m/s]
- Current direction [deg]
- Waterline
- Platform boundary
- Range of considered data around centre point
- Centre point

c: wind velocities:
- 5 m/s
- 10 m/s
- 15 m/s
- 20 m/s

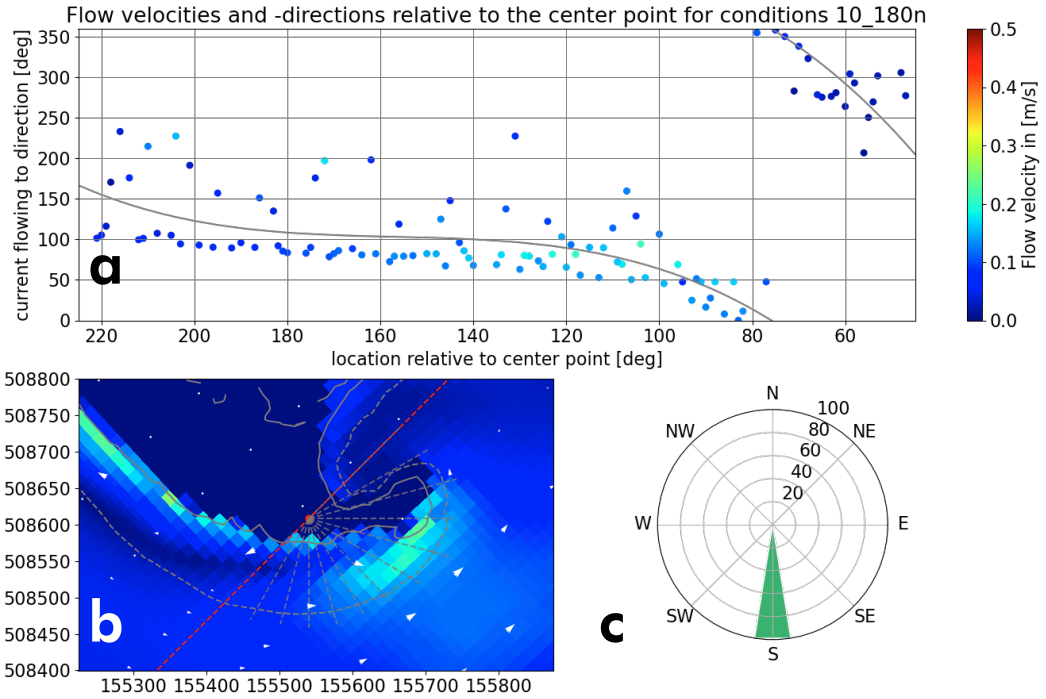

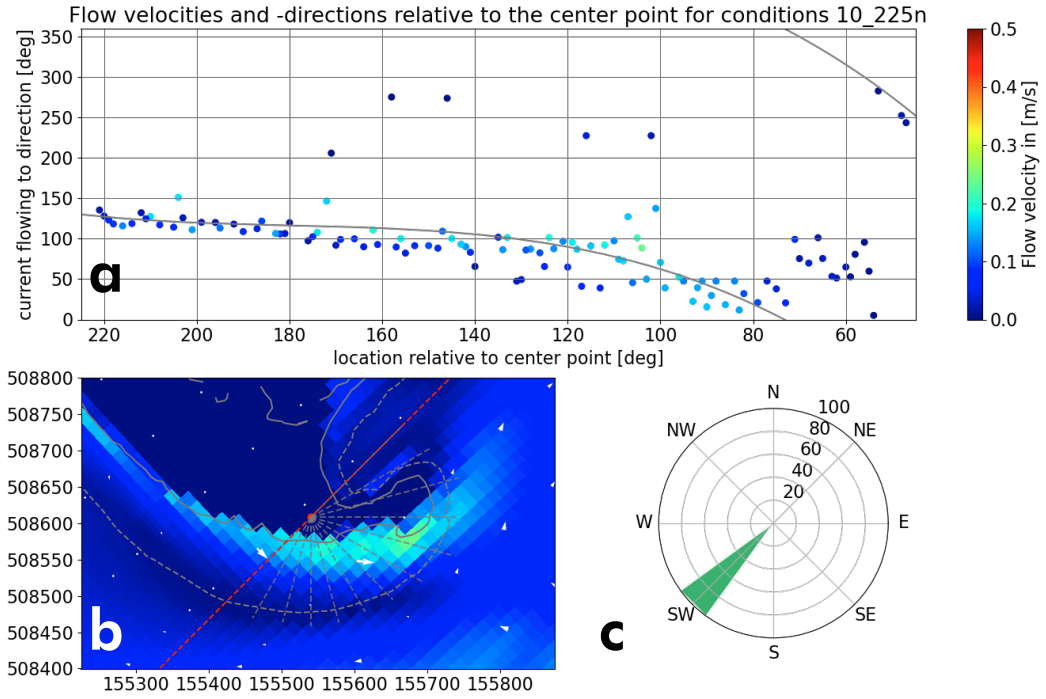

Legend

a: Current direction at a degree [deg]

Current velocity at a degree [m/s]

Fitted current directions around spit [deg]

b: Current velocity [m/s]

Current direction [deg]

Waterline

Platform boundary

Range of considered data around centre point

Centre point

c: wind velocities:

5 m/s

10 m/s

15 m/s

20 m/s

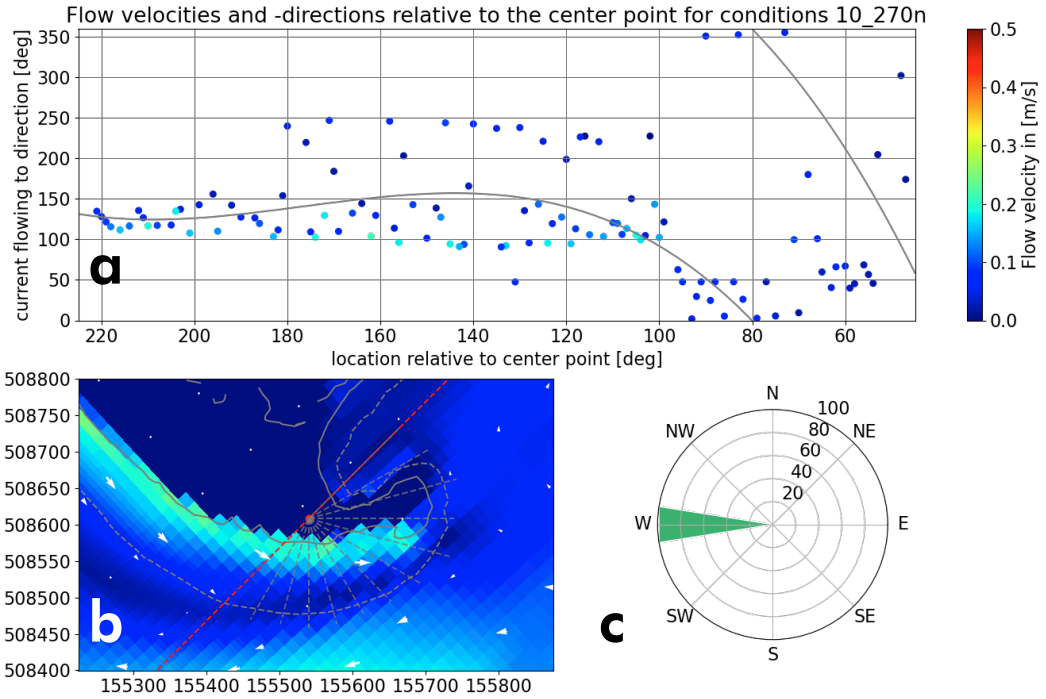

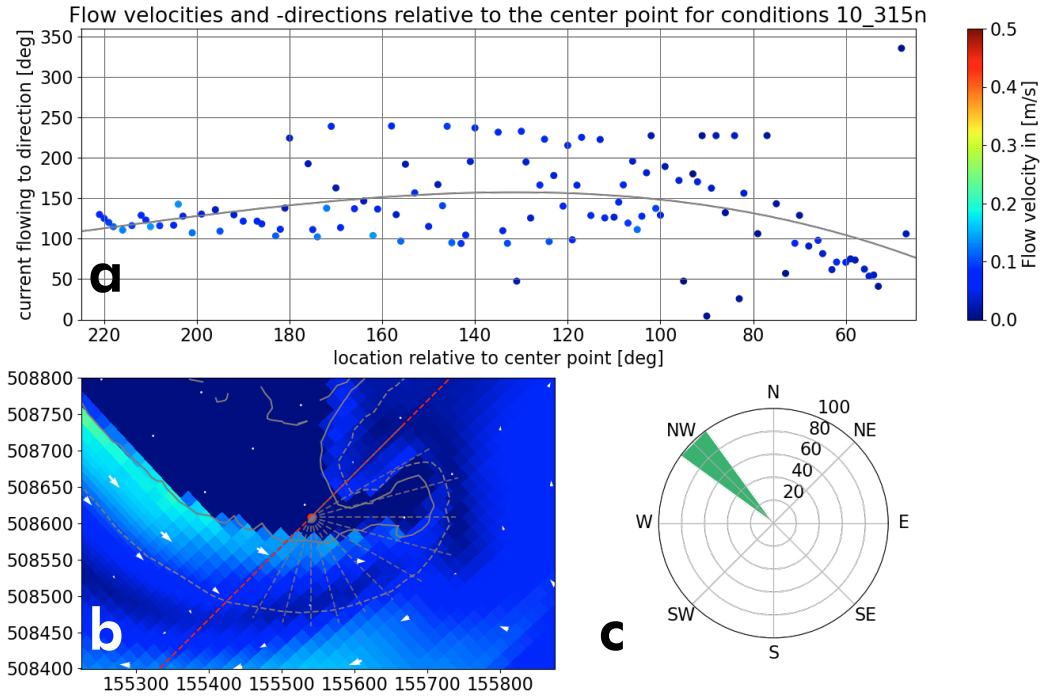

Legend

a:
- Current direction at a degree [deg]
- Current velocity at a degree [m/s]
- Fitted current directions around spit [deg]

b:
- Current velocity [m/s]
- Current direction [deg]
- Waterline
- Platform boundary
- Range of considered data around centre point
- Centre point

c: wind velocities:
- 5 m/s
- 10 m/s
- 15 m/s
- 20 m/s

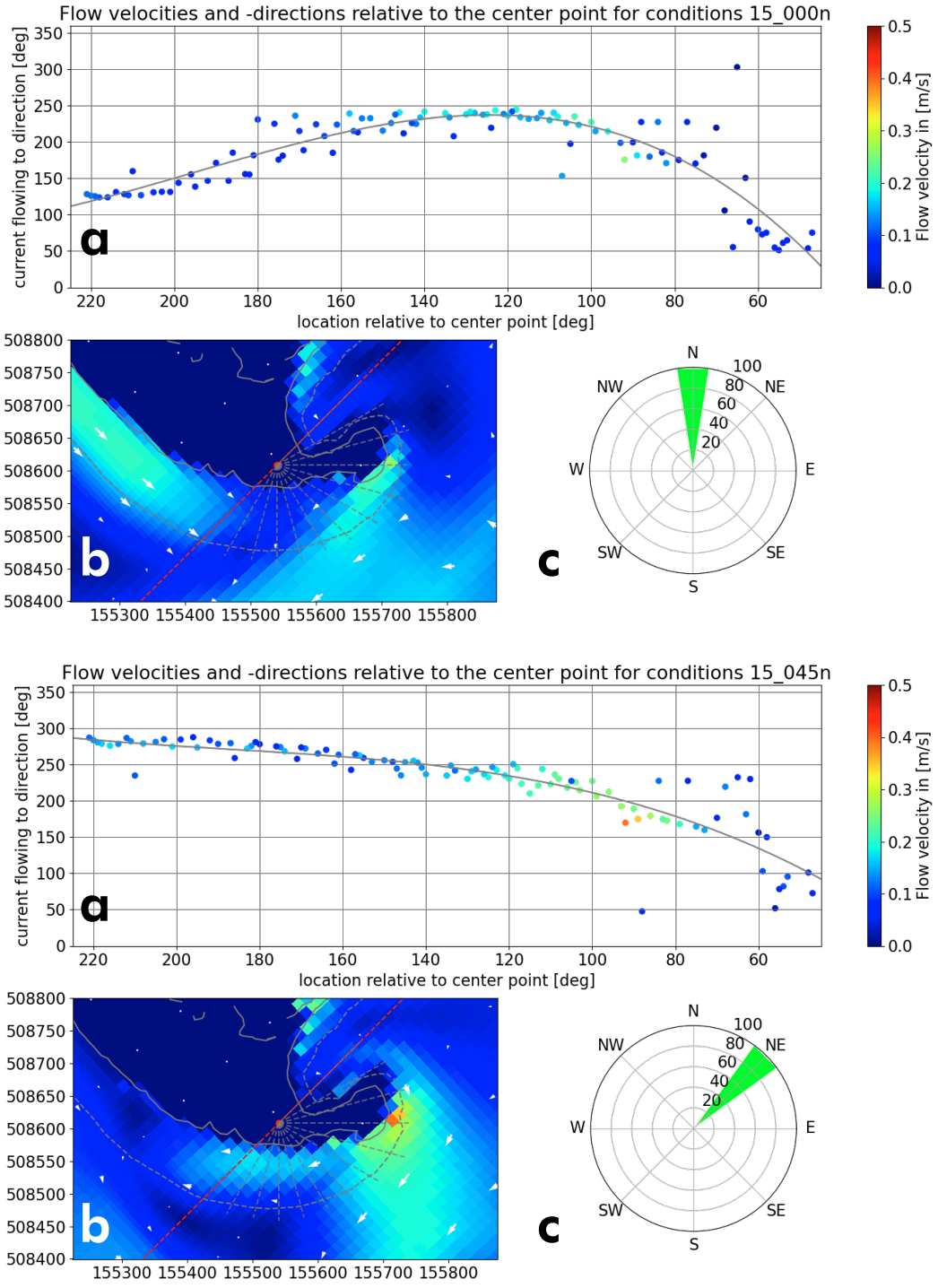

Legend

a:
- Current direction at a degree [deg]
- Current velocity at a degree [m/s]
- Fitted current directions around spit [deg]

b:
- Current velocity [m/s]
- Current direction [deg]
- Waterline
- Platform boundary
- Range of considered data around centre point
- Centre point

c: wind velocities:
- 5 m/s
- 10 m/s
- 15 m/s
- 20 m/s

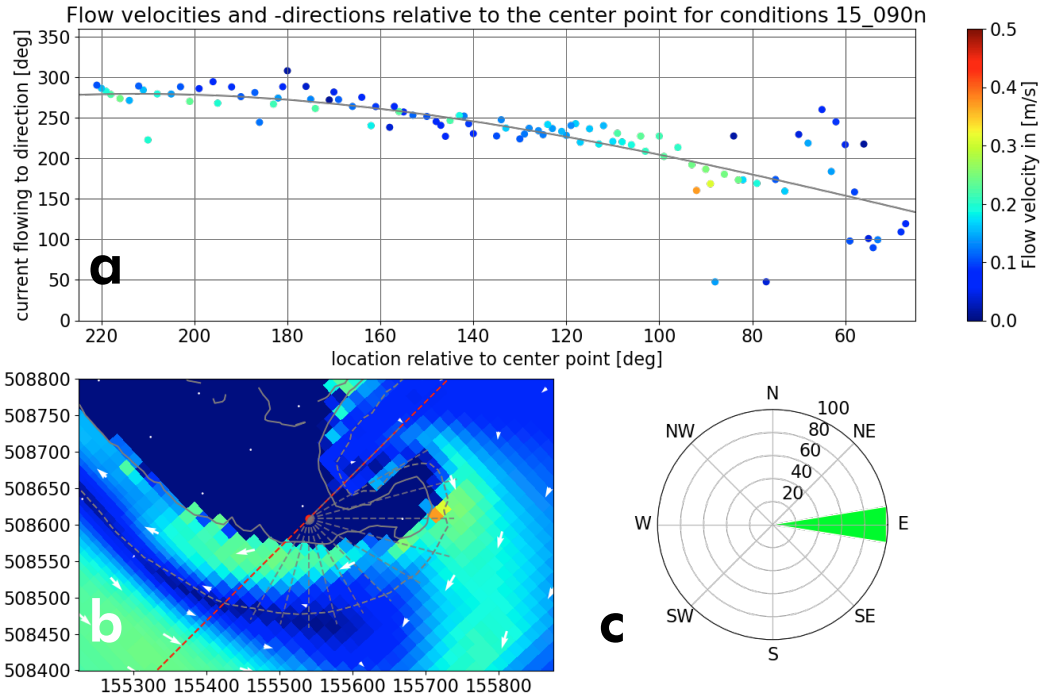

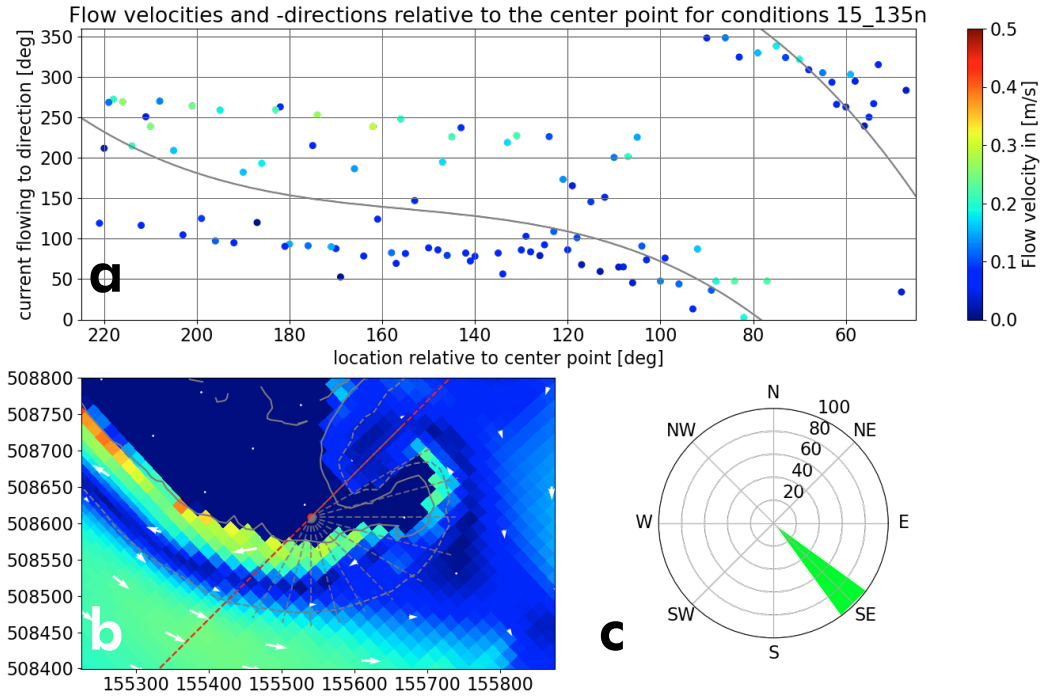

Legend

a:
- Current direction at a degree [deg]
- Current velocity at a degree [m/s]
- Fitted current directions around spit [deg]

b:
- Current velocity [m/s]
- Current direction [deg]
- Waterline
- Platform boundary
- Range of considered data around centre point
- Centre point

c: wind velocities:
- 5 m/s
- 10 m/s
- 15 m/s
- 20 m/s

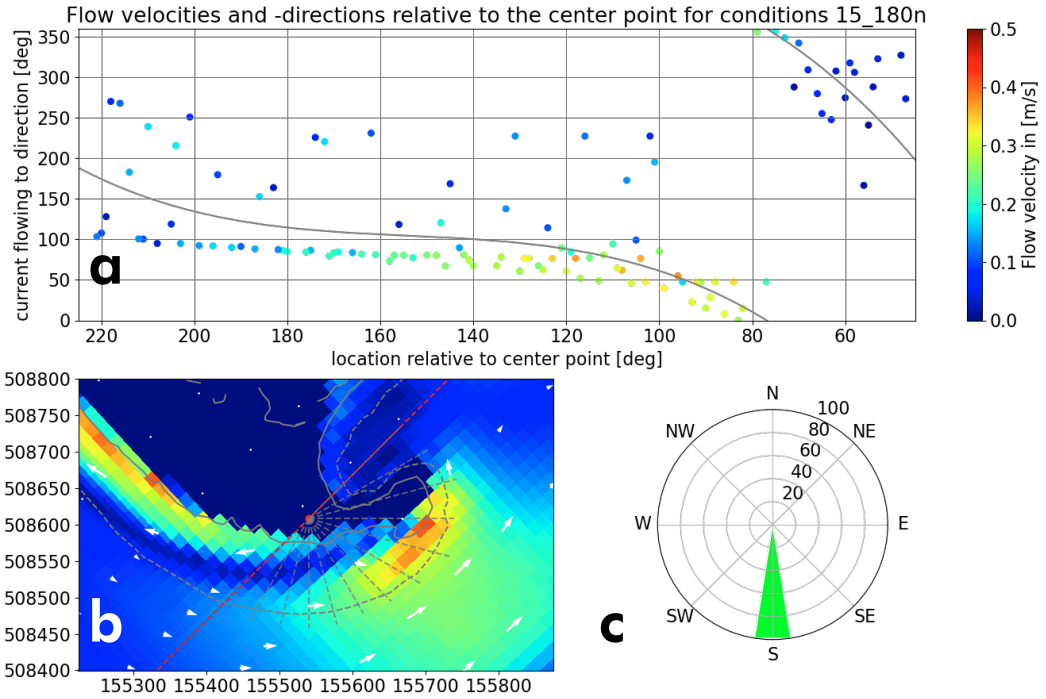

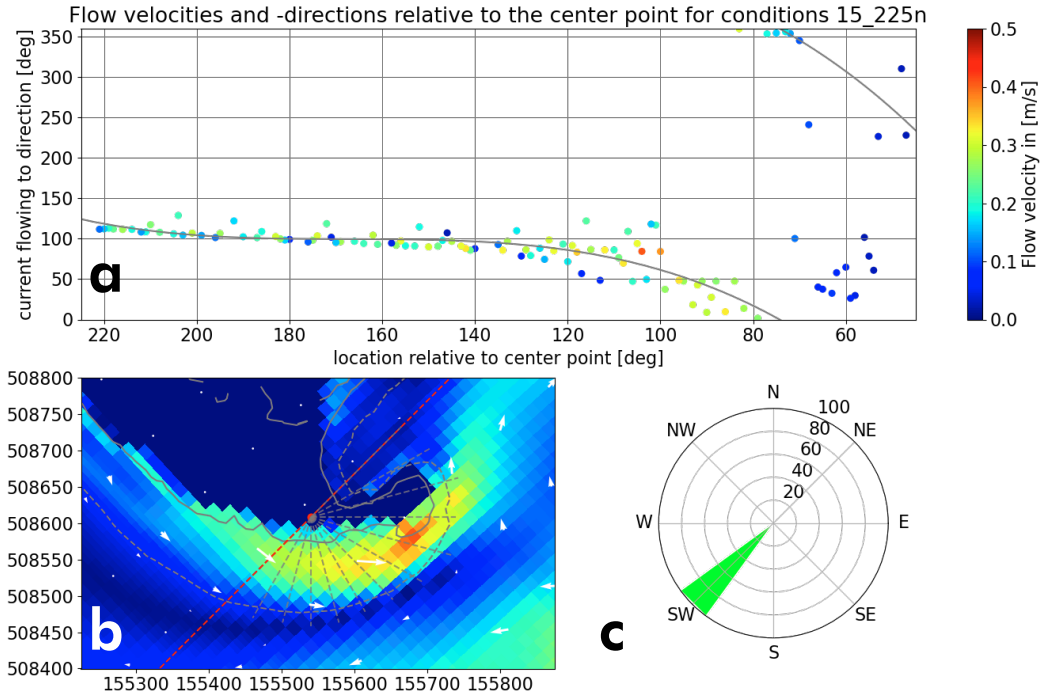

Legend

a:
- Current direction at a degree [deg]
- Current velocity at a degree [m/s]
- Fitted current directions around spit [deg]

b:
- Current velocity [m/s]
- Current direction [deg]
- Waterline
- Platform boundary
- Range of considered data around centre point
- Centre point

c: wind velocities:
- 5 m/s
- 10 m/s
- 15 m/s
- 20 m/s

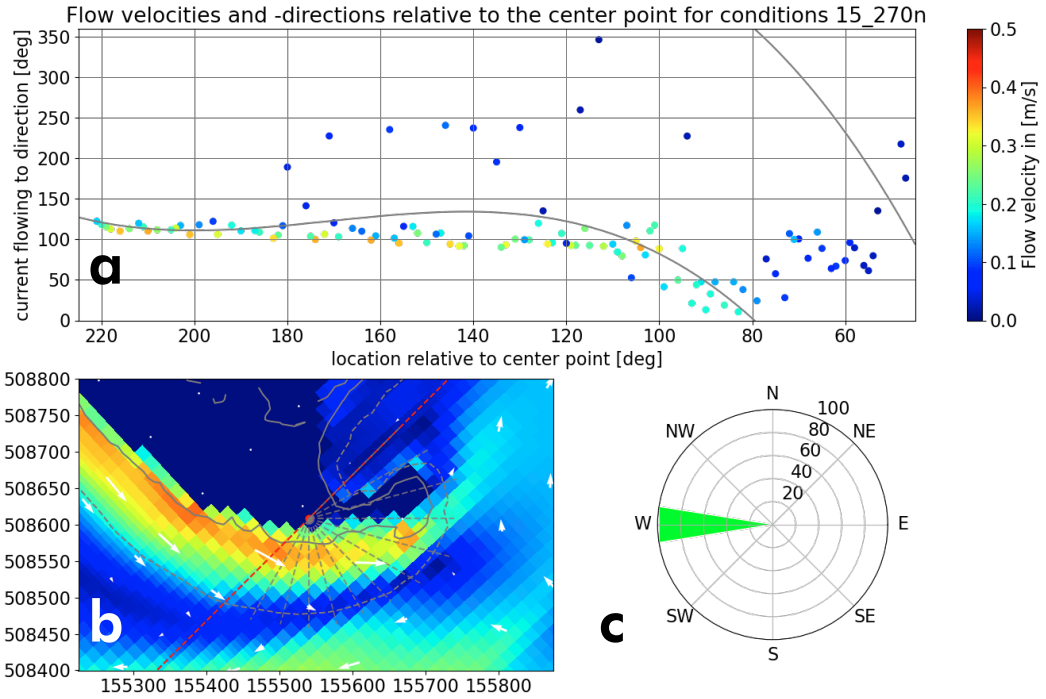

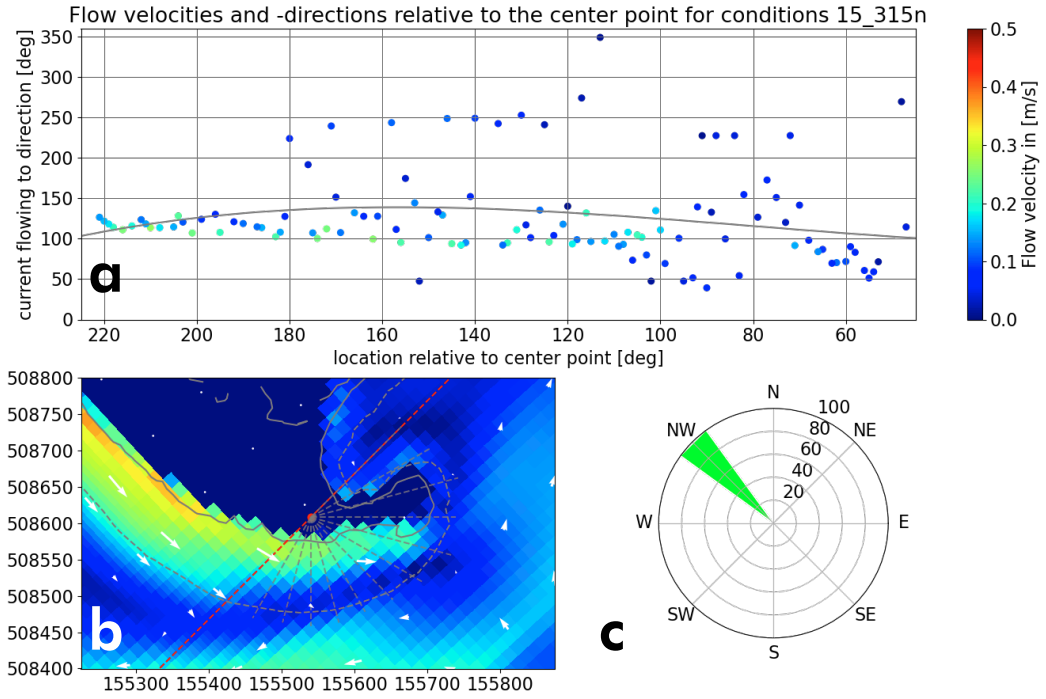

Legend

a:
- Current direction at a degree [deg]
- Current velocity at a degree [m/s]
- Fitted current directions around spit [deg]

b:
- Current velocity [m/s]
- Current direction [deg]
- Waterline
- Platform boundary
- Range of considered data around centre point
- Centre point

c: wind velocities:
- 5 m/s
- 10 m/s
- 15 m/s
- 20 m/s

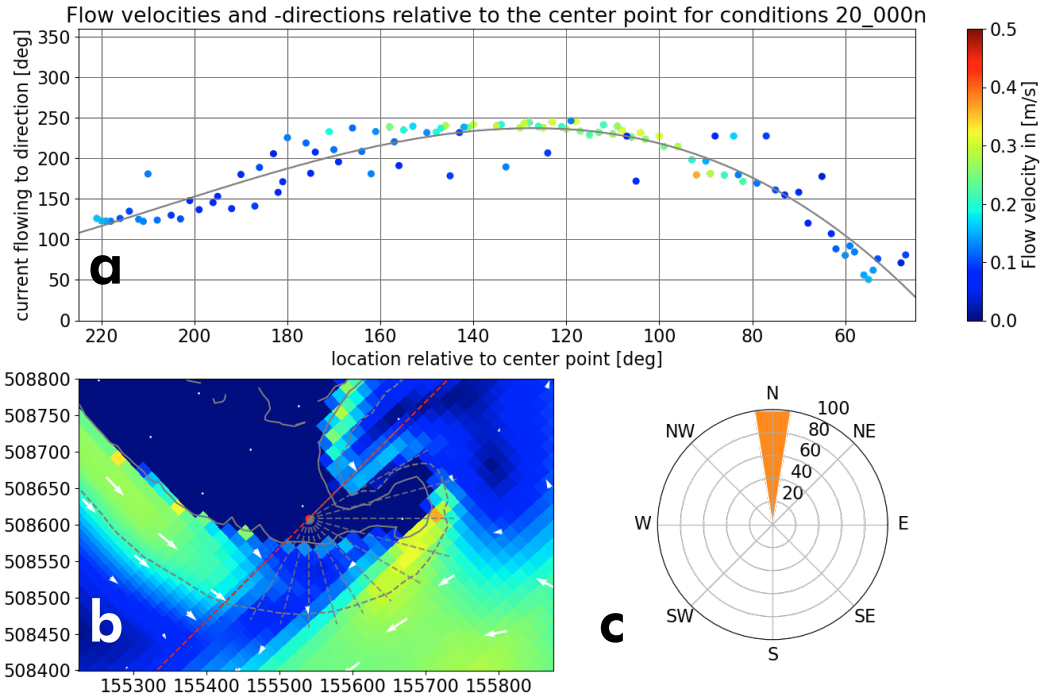

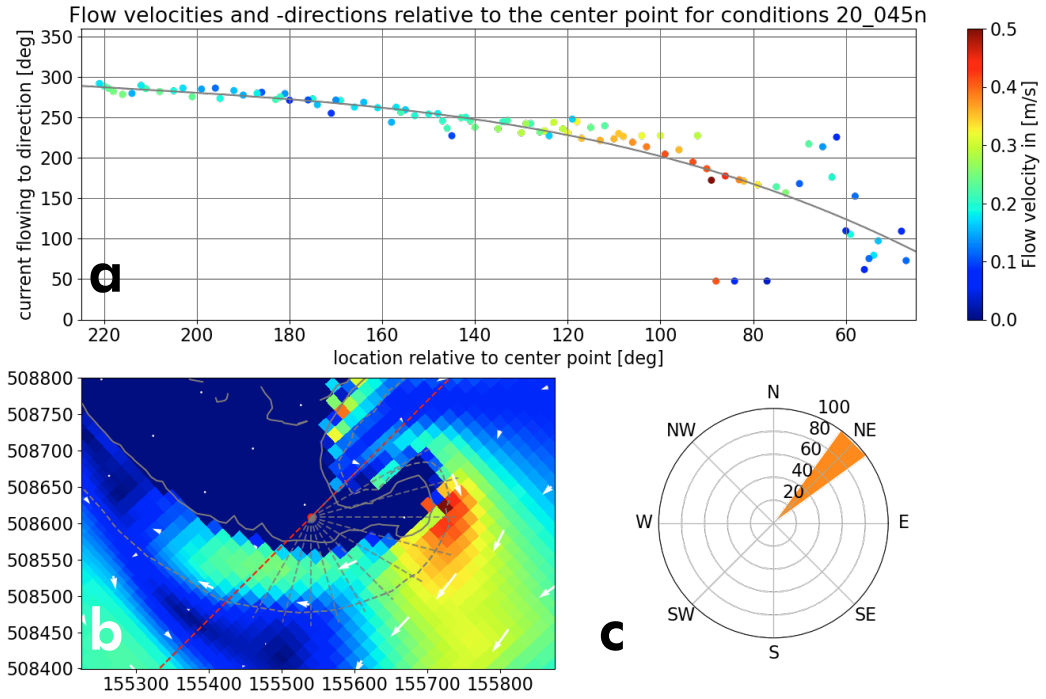

Legend

a: Current direction at a degree [deg]

Current velocity at a degree [m/s]

Fitted current directions around spit [deg]

b: Current velocity [m/s]

Current direction [deg]

Waterline

Platform boundary

Range of considered data around centre point

Centre point

c: wind velocities:

5 m/s

10 m/s

15 m/s

20 m/s

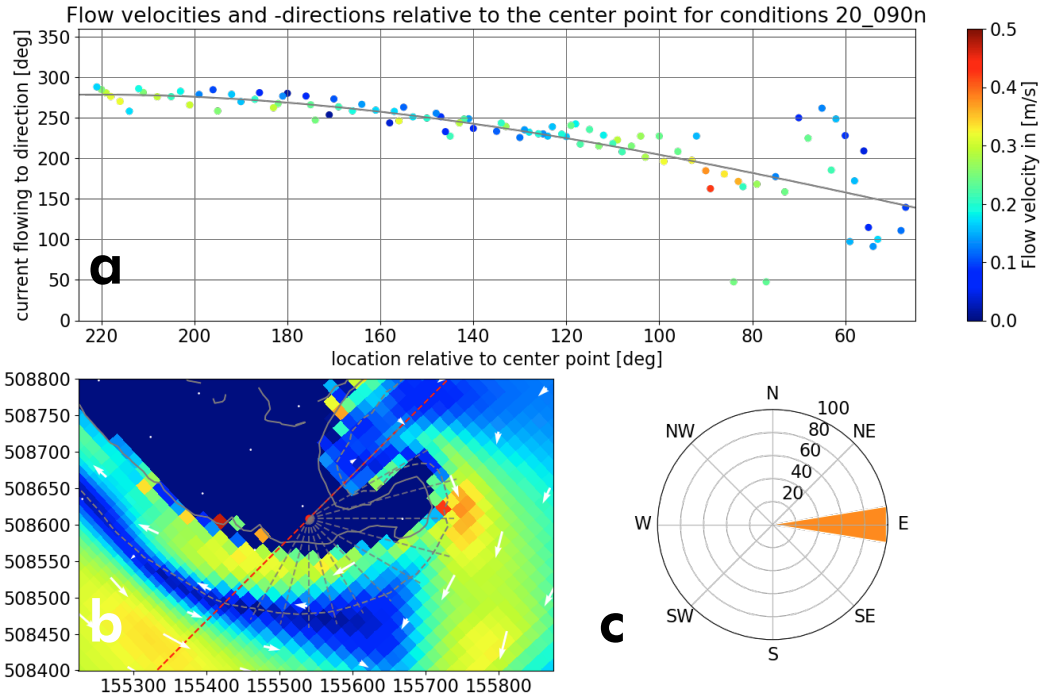

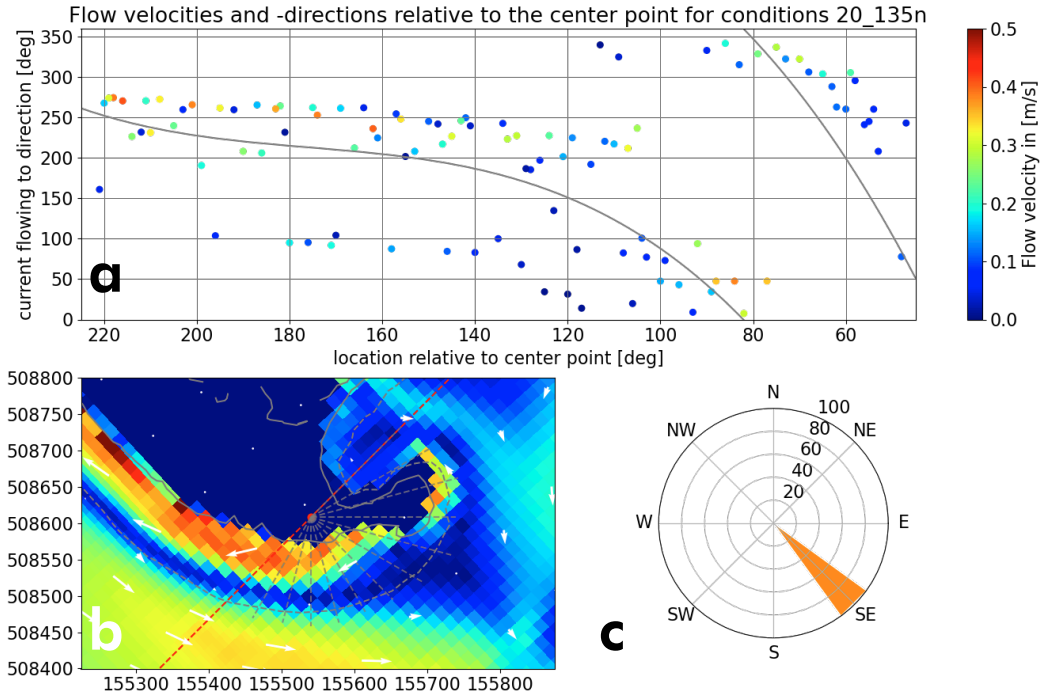

Legend

a:
- Current direction at a degree [deg]
- Current velocity at a degree [m/s]
- Fitted current directions around spit [deg]

b:
- Current velocity [m/s]
- Current direction [deg]
- Waterline
- Platform boundary
- Range of considered data around centre point
- Centre point

c: wind velocities:
- 5 m/s
- 10 m/s
- 15 m/s
- 20 m/s

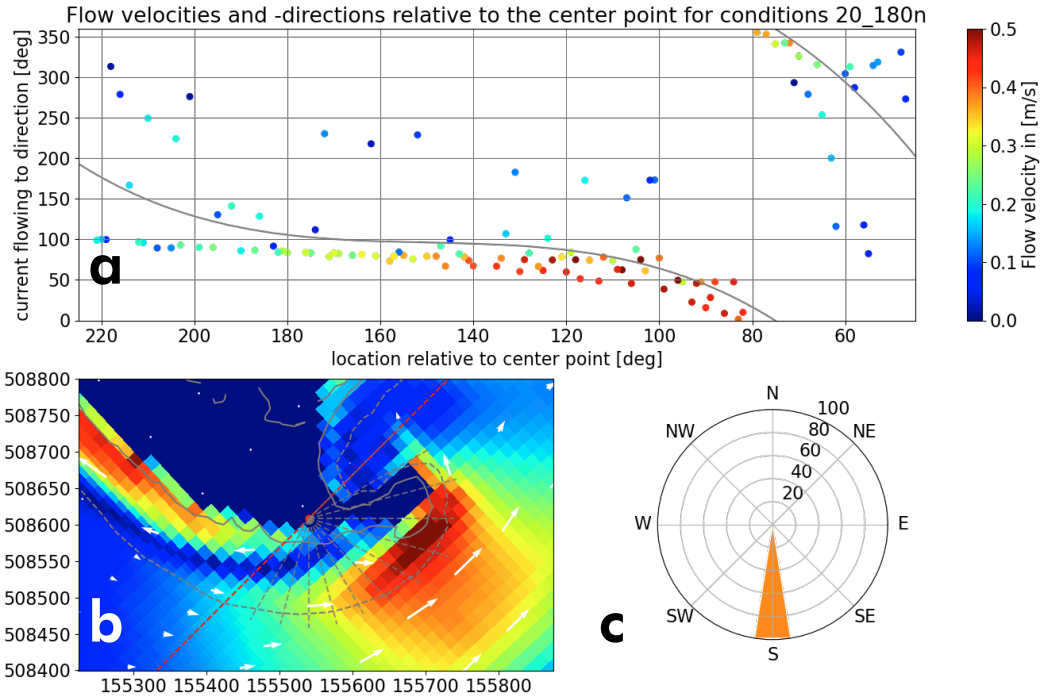

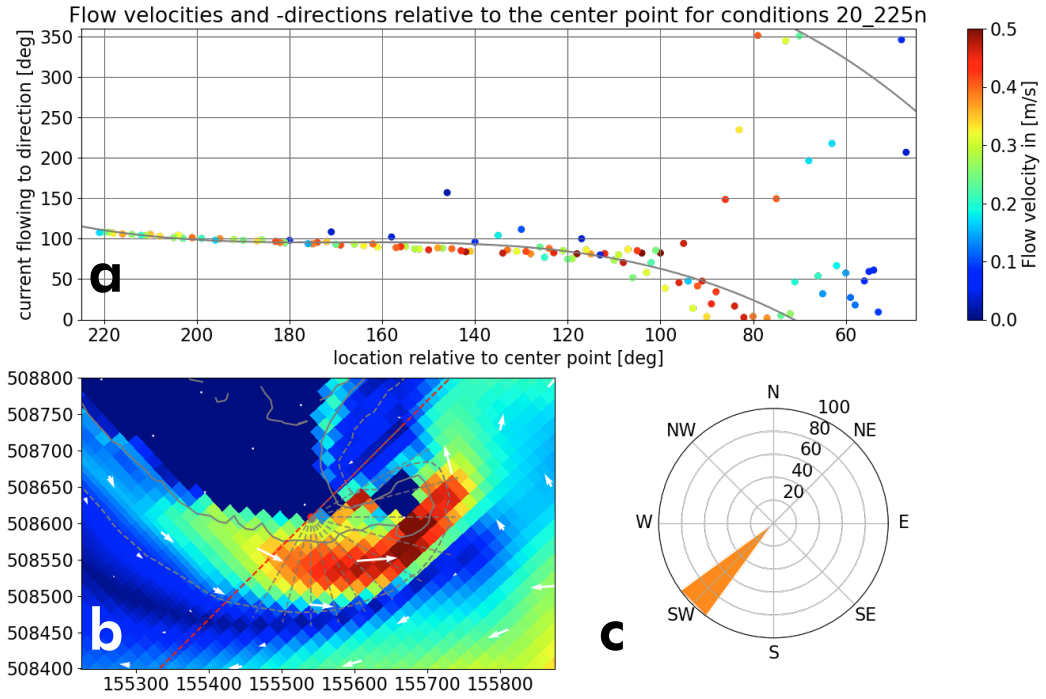

Legend

a: Current direction at a degree [deg]

Current velocity at a degree [m/s]

Fitted current directions around spit [deg]

b: Current velocity [m/s]

Current direction [deg]

Waterline

Platform boundary

Range of considered data around centre point

Centre point

c: wind velocities:

5 m/s

10 m/s

15 m/s

20 m/s

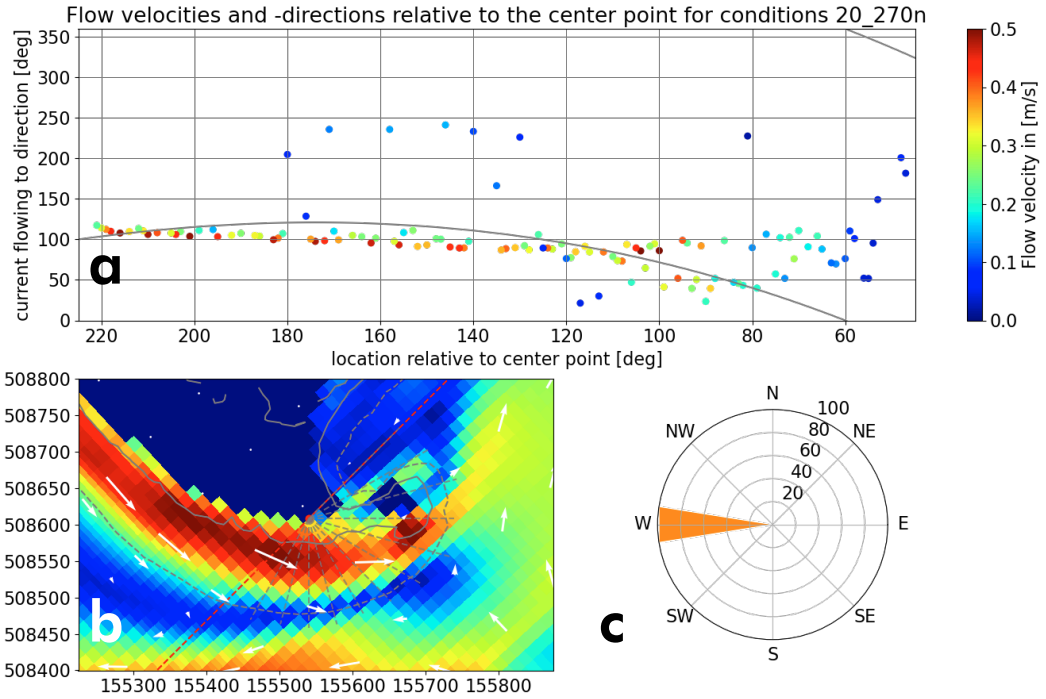

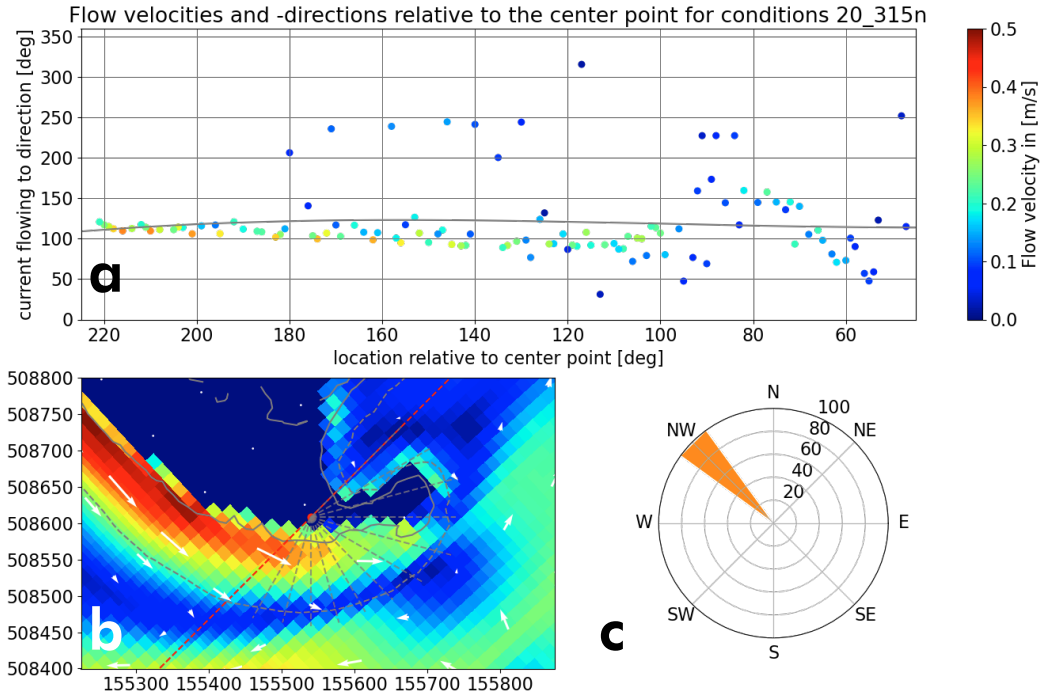

Legend

a:
- Current direction at a degree [deg]
- Current velocity at a degree [m/s]
- Fitted current directions around spit [deg]

b:
- Current velocity [m/s]
- Current direction [deg]
- Waterline
- Platform boundary
- Range of considered data around centre point
- Centre point

c: wind velocities:
- 5 m/s
- 10 m/s
- 15 m/s
- 20 m/s

From the maps (b) several observations can be done. In general, the following observations, and accompanying morphodynamic hypotheses, can be made:

1. At winds of 5 m/s the flow is very slow, especially looking at the velocities at higher wind speeds. The flow likely has too little energy to really cause significant morphodynamic changes.
2. Near the Southern spit and Zuidstrand two circulation cells can be found that affect the flows along the beach and spit. These circulation cells are influenced by the sand mining pits near the beach. For the Southern spit, not only lake circulations on the Markermeer scale are important but also lake circulations on a more local scale. It was assumed that lake circulations would result in currents at the spit, flowing parallel to the Zuidstrand. But the sand extraction pit, south of the spit, causes a flow near the distal end, that is almost perpendicular to the Zuidstrand.

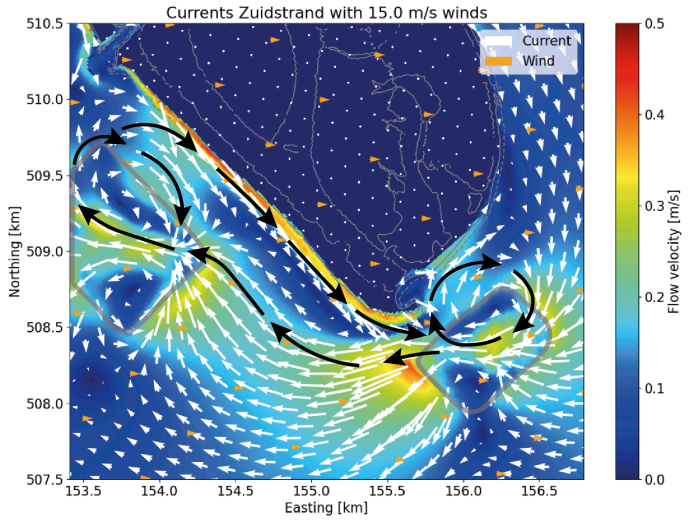

Figure 1. Example of local lake circulation at W wind (schematic currents: black, sand mining pits: grey)

3. Currents near the coast are often in the opposite direction of offshore currents. This means that on or close to the platform there is often an area where currents are very low. This may cause sedimentation and therefore temporary changes in bathymetry. For example, sand banks on the platform. This mechanism can create a sediment storage on the platform that can be transported during other wind regimes. However, although there are sometimes sandbanks on the platform, the locations where circulation currents compensate each other and flow velocities are zero, is not on the platform but further offshore. Therefore, this is likely not the mechanism that creates these sandbanks. With the exception of some temporary cases around the spit where the sedimentation of a sandbank coincides with the dip in flow velocities during S winds (Appendix H).
4. At N, NE, and E winds there is a current from the tip of the Southern spit to the beach instead of the other way around. This may cause migration of the distal end to the southwest.
5. At S and SE winds waves hit the spit on the curve creating currents in the direction of the distal end, making flow velocities high there. But these winds also create currents in the direction of the Zuidstrand. These currents likely do not carry that much sediment as they originate on the spit and therefore not much sedimentation can be expected during S winds.
6. At SW winds the flow velocities near the distal end decrease very slowly. Near the distal end velocities are still quite high and sedimentation on the platform can therefore only be expected during calmer SW winds. During these wind conditions there is little interaction with the Zuidstrand in terms of longshore currents. Erosion and sedimentation are local as longshore currents at SW winds only start to pick up around the proximal end of the spit.
7. At W and NW winds, there is more longshore current along the Zuidstrand, and this current

decreases earlier along the spit curve (than at SW winds). Therefore, more sedimentation closer to the proximal end can be expected. Also, more sedimentation at the platform can be expected.

8. Smaller wind velocities create smaller flow velocities and therefore sedimentation on the platform is more likely.
9. Near the Zuidstrand, lake circulation currents and wave driven longshore currents are hard to distinguish. It seems that lake circulations and longshore currents are often from the same direction around the southern spit.
10. Higher wind velocities, create more set-up and therefore lake circulation becomes more important. This could mean that currents would curve less around the spit.
11. At winds of 20m/s, flow velocities on the platform are very high and it is unlikely that any sedimentation occurs on the platform.

Current directions

When plotting the trends for the current directions of each scenario it becomes clear that the current directions are very similar for wind speeds 10 m/s, 15 m/s and 20 m/s. Wind speeds of 5 m/s do often have a different current pattern. At these smaller winds, set-up is very low and therefore lake circulations are almost absent. When winds start to pick-up and lake circulations increase, current patterns clearly change. However, once the lake circulations start to play a role it seems that there is almost no difference between situations with limited set-up (10 m/s winds) and large set-ups (20 m/s winds). An exception seems to be the W direction where, at very high winds, the flow does not bend as much around the spit as for lower wind velocities. For the winds from the W direction with lower velocities there seems to be the most refraction around the spit, possibly because velocities have decreased more at these lower degrees than at for example SW winds. It is therefore easier for the waves to redirect the current (Figure 2).

Also, for wind directions SE, S, SW and W a very clear direction change can be seen starting around 100° N relative to the centre point. This means that the flow bends around the distal end. An influence of the small circulation cell at the nearest sand mining pit is likely to play a role in this direction change, as currents with a more north(eastern) direction join the currents coming from the Zuidstrand at this location (Figure 1).

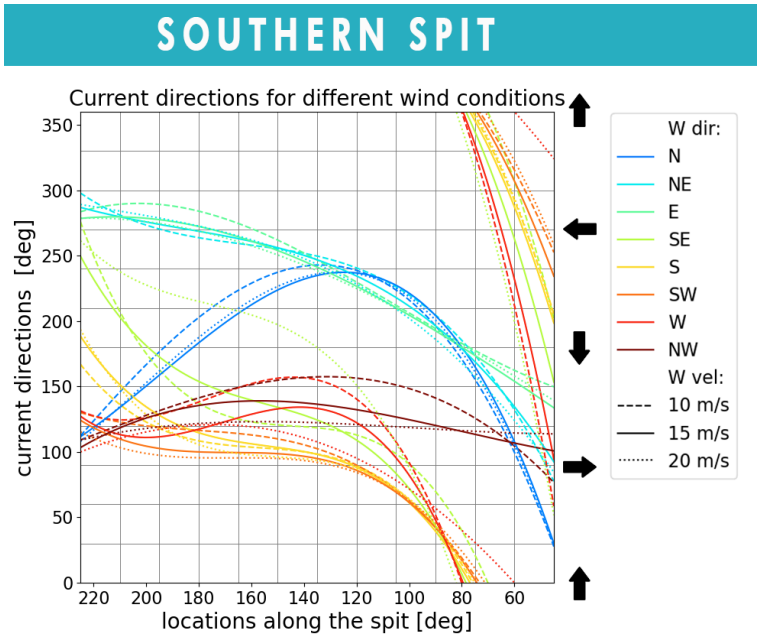

Figure 2. Current directions during different wind conditions (dashed: 10 m/s, solid: 15 m/s, dotted: 20 m/s). Each line is the gives the current directions around the southern spit for one wind condition (combination of wind velocities and directions). The arrows indicate where the current is flowing towards at that specific y-axis value.

In Figure 2, based on current directions, the currents can be divided in three groups. Each group has roughly the same current direction pattern along the spit:

SE, S, SW and W: These wind regimes result in mostly the same currents along the spit. Especially along the location where most sedimentation occurs (110° N – 70° N). The most difference can be seen at higher degrees where S and SE currents are directed away from the distal end and SW and W currents are directed towards the distal end. Also, W currents seem to be directed a bit more towards the south around 160° N than the other currents. It might be possible that sediment is transported over the platform boundary at higher degrees relative to the centre point although the difference is likely not large enough to very significant. In this group a clear flow around the distal end of the spit can be seen. This change in direction might be caused by refraction and/or local lake circulation caused by the sand mining pit.

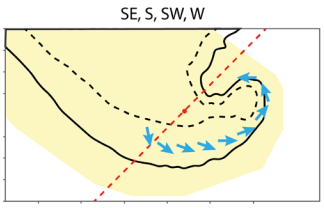

N, NE and E: The N wind direction differs from the rest at higher degrees but around the distal end, the current directions are very similar. These currents occur when the southern spit is mostly sheltered by waves and thus lake circulation will be important for this group.

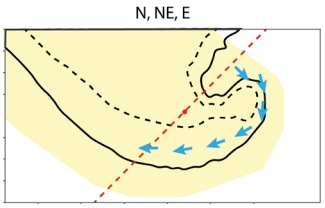

NW: This flow does not change direction as much as the other groups. Sedimentation during NW winds will therefore occur when flow velocities have dissipated or (more likely in high energy cases) when the current flows over the platform boundary. Because the waves during this regime are already high angle waves, the transportation energy of the waves dissipates very fast along the coastline. Thus, refraction has a smaller role. However, it looks like the lake circulation cell of the sand mining pit redirects the current slightly.

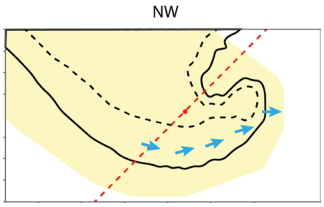

Flow velocity

With the same method as for the current directions, a fit can be made of the flow velocities along the spit for each wind scenario (Figure 3).

What again is clear for each wind regime, is that the flow velocities follow the same pattern for different wind speeds. So, when currents increase at a certain location at 10 m/s winds, currents also increase at the same location at 20 m/s winds. Naturally the faster the wind speeds, the higher the flow velocities. Current directions seemed relatively independent of wind speeds. However, the other way around, current velocities are dependent on both wind directions and wind velocities. The development of flow velocities around the spit, for each wind direction can be qualitatively expresses as has been done in Figure 4.

Flow velocities during N, NE, E and SE winds are relatively limited, especially at the northern side of the distal end. This means that it is unlikely that these currents transport a lot of sediment. The flow velocities during S winds start to pick up in the middle of the spit and stay high until the currents reach the other side. Transport of material from the middle of the southern side to the northern side of the distal end seems therefore likely. Flow velocities during SW and W winds are high when entering the spit area from the Zuidstrand and stay high until the currents arrive far onto the northern side of the distal end. Flow velocities during NW winds are also fast when entering the spit area but decrease quickly.

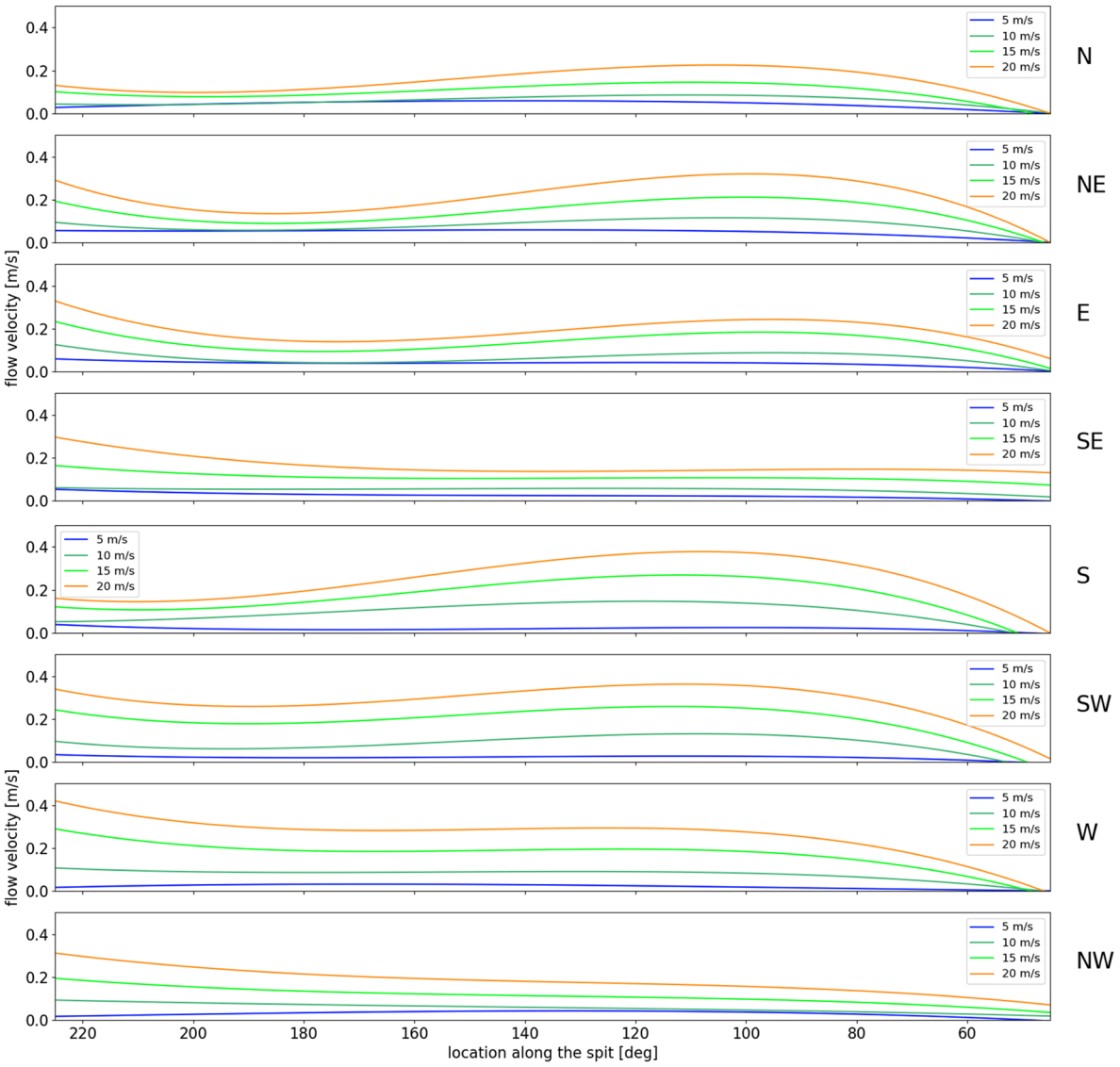

Figure 3. Fitted possible flow velocities along the spit with the flow velocities on the left side, colour indicating the wind velocity and on the right side the wind directions.

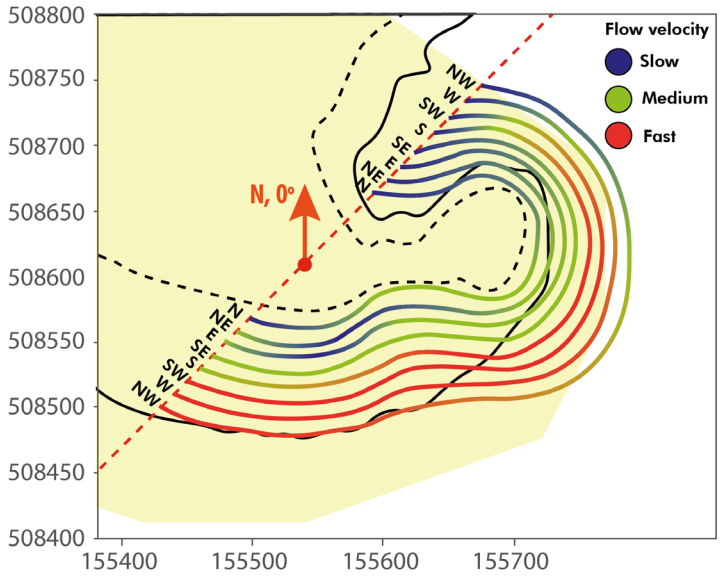

Figure 4. Schematic change in flow velocity around the southern spit for different wind directions

Northern spit

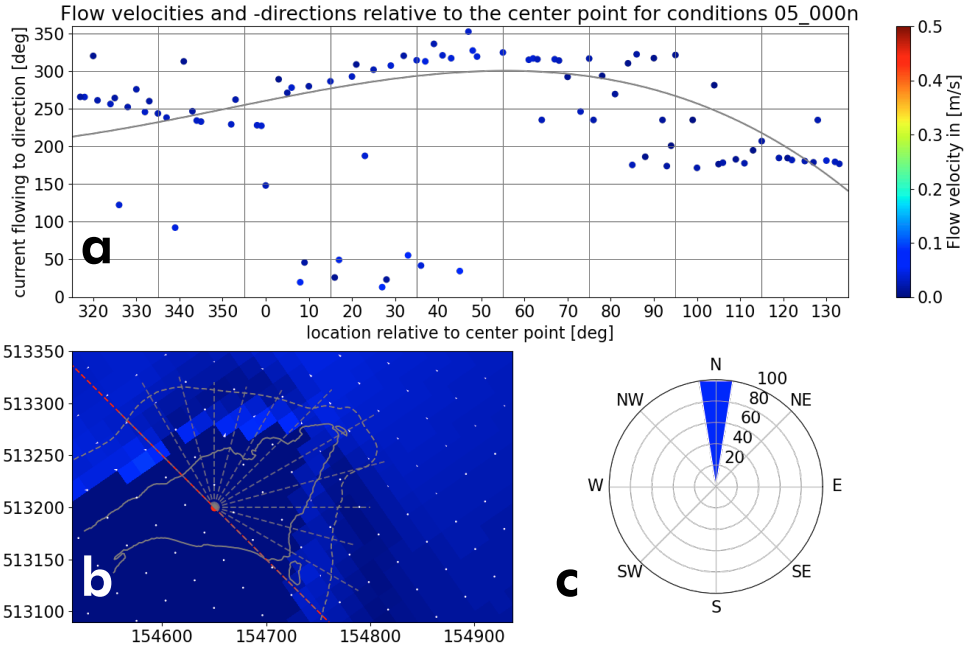

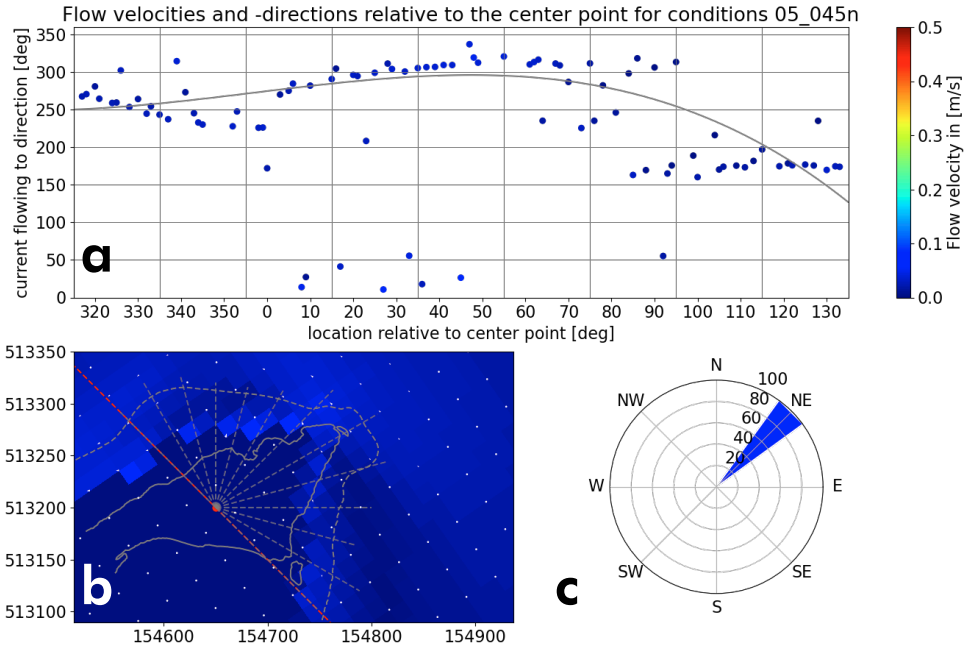

Legend

a:
- Current direction at a degree [deg]
- Current velocity at a degree [m/s]
- Fitted current directions around spit [deg]

b:
- Current velocity [m/s]
- Current direction [deg]
- Waterline
- Platform boundary
- Range of considered data around centre point
- Centre point

c: wind velocities:
- 5 m/s
- 10 m/s
- 15 m/s
- 20 m/s

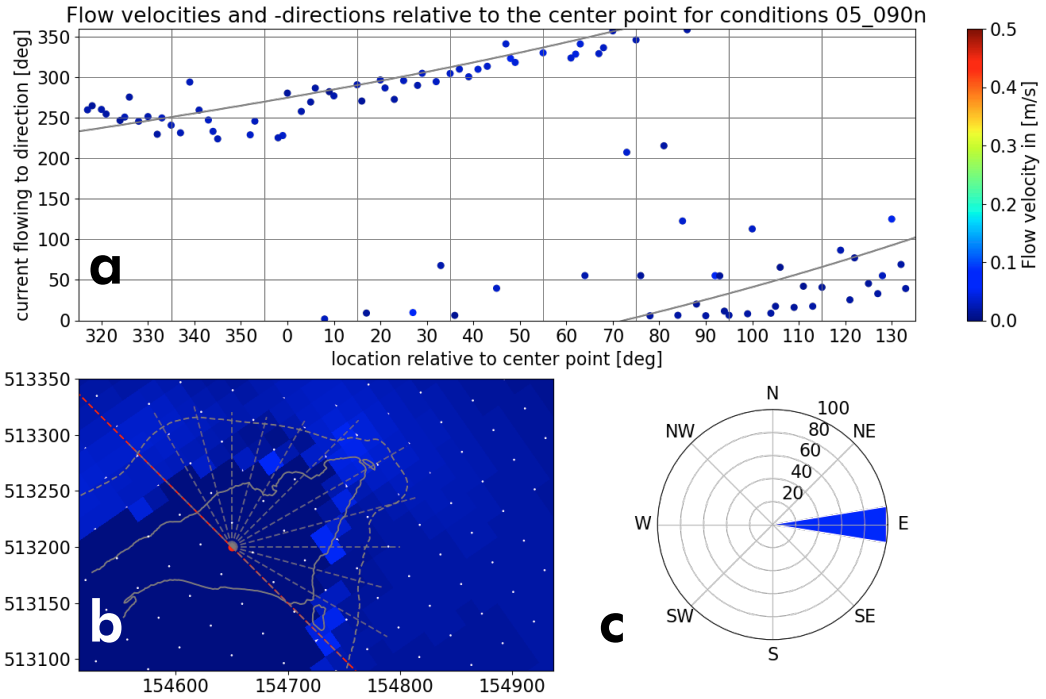

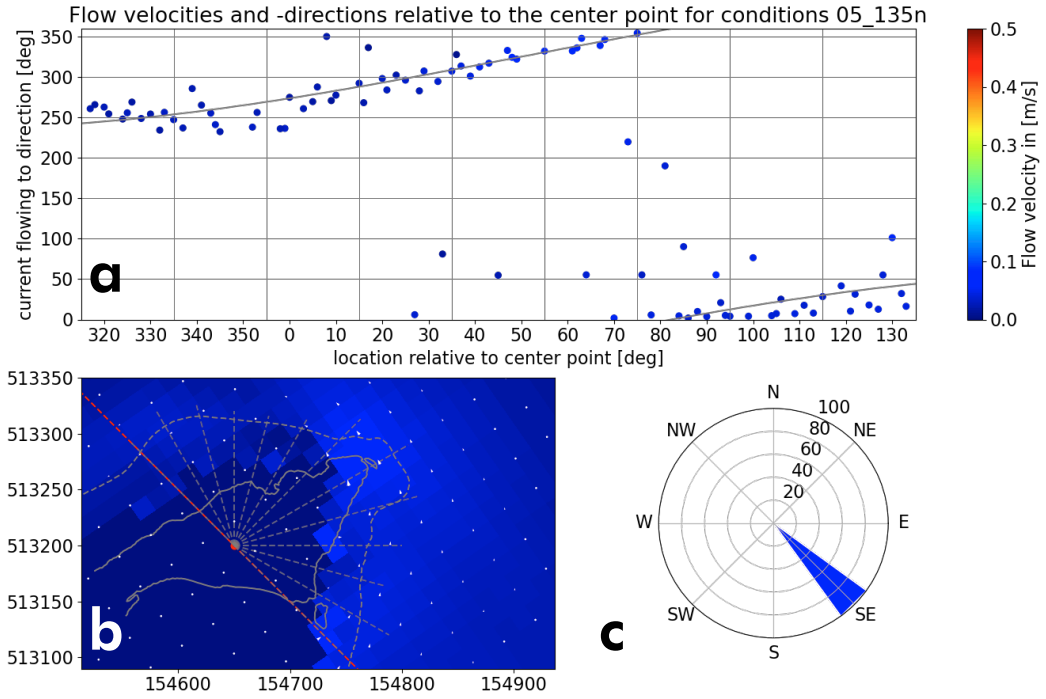

Legend

a:
- Current direction at a degree [deg]
- Current velocity at a degree [m/s]
- Fitted current directions around spit [deg]

b:
- Current velocity [m/s]
- Current direction [deg]
- Waterline
- Platform boundary
- Range of considered data around centre point
- Centre point

c: wind velocities:
- 5 m/s
- 10 m/s
- 15 m/s
- 20 m/s

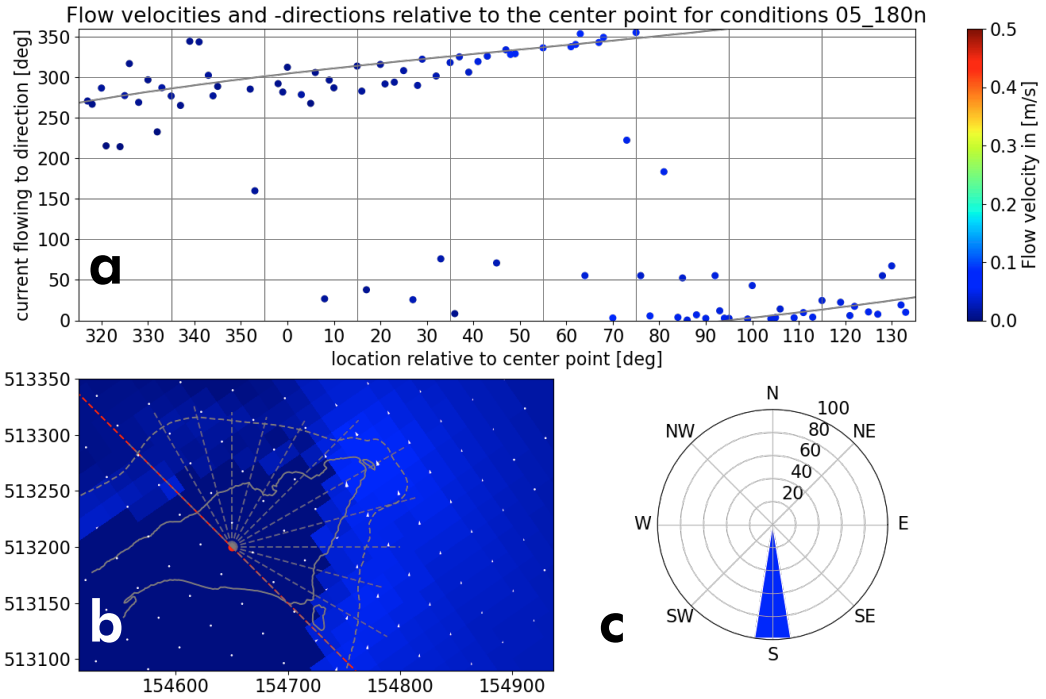

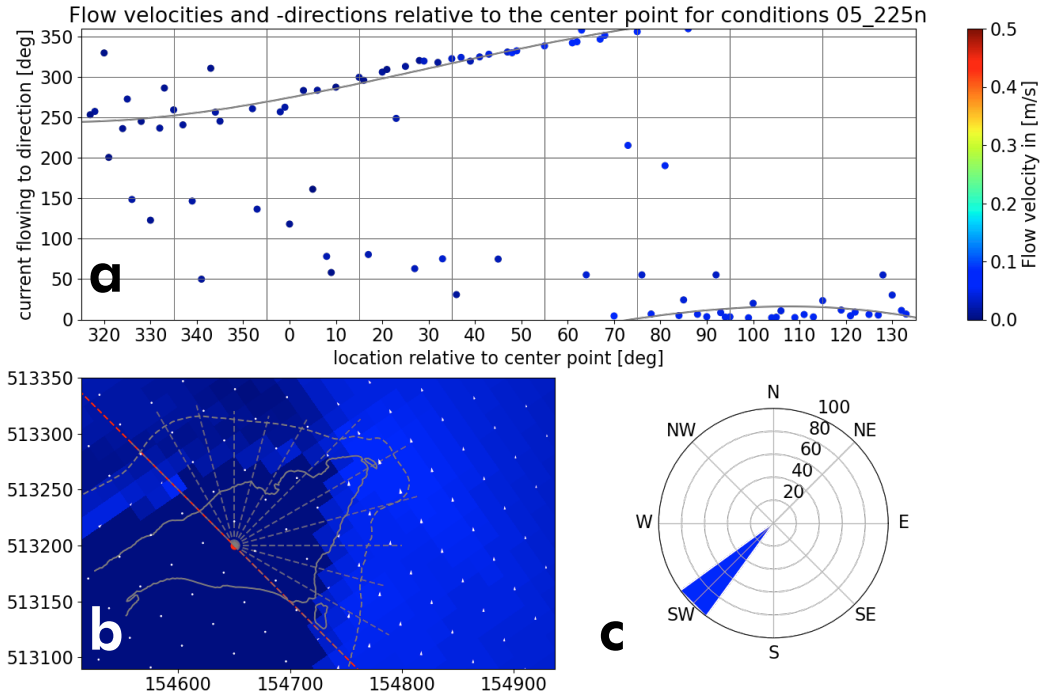

Legend

a:
- Current direction at a degree [deg]
- Current velocity at a degree [m/s]
- Fitted current directions around spit [deg]

b:
- Current velocity [m/s]
- Current direction [deg]
- Waterline
- Platform boundary
- Range of considered data around centre point
- Centre point

c: wind velocities:
- 5 m/s
- 10 m/s
- 15 m/s
- 20 m/s

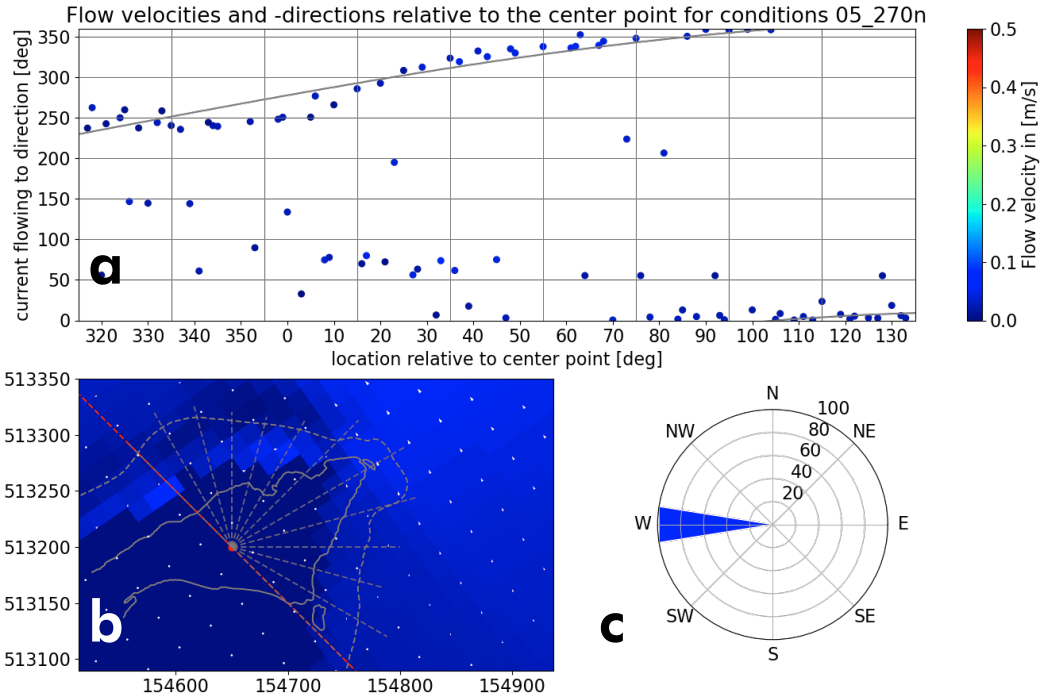

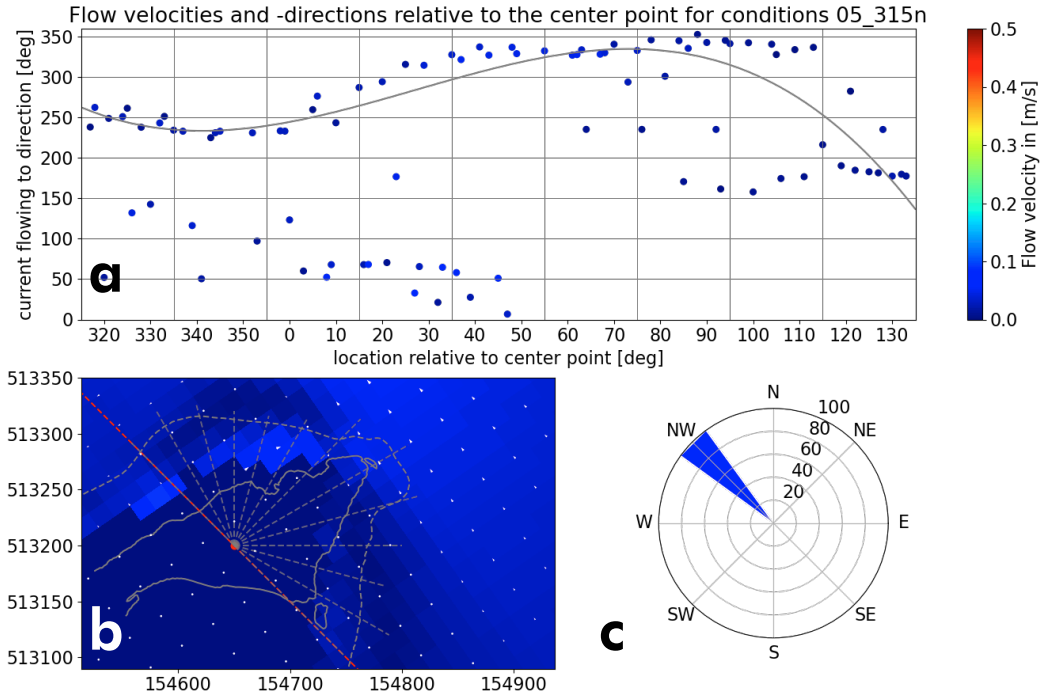

Legend

a:
- Current direction at a degree [deg]
- Current velocity at a degree [m/s]
- Fitted current directions around spit [deg]

b:
- Current velocity [m/s]
- Current direction [deg]
- Waterline
- Platform boundary
- Range of considered data around centre point
- Centre point

c: wind velocities:
- 5 m/s
- 10 m/s
- 15 m/s
- 20 m/s

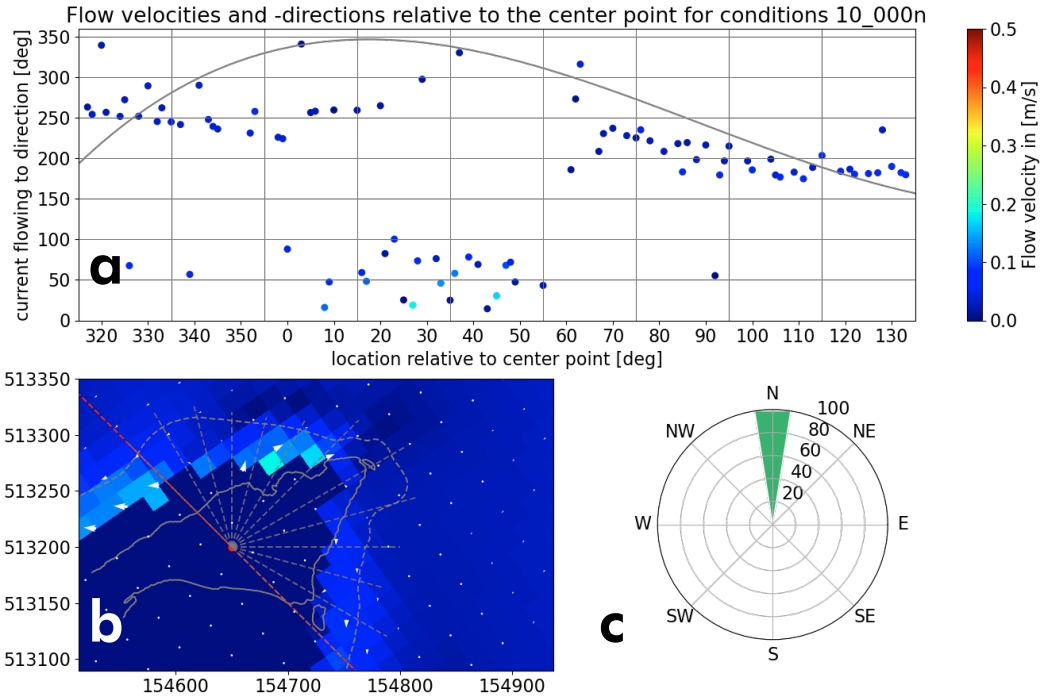

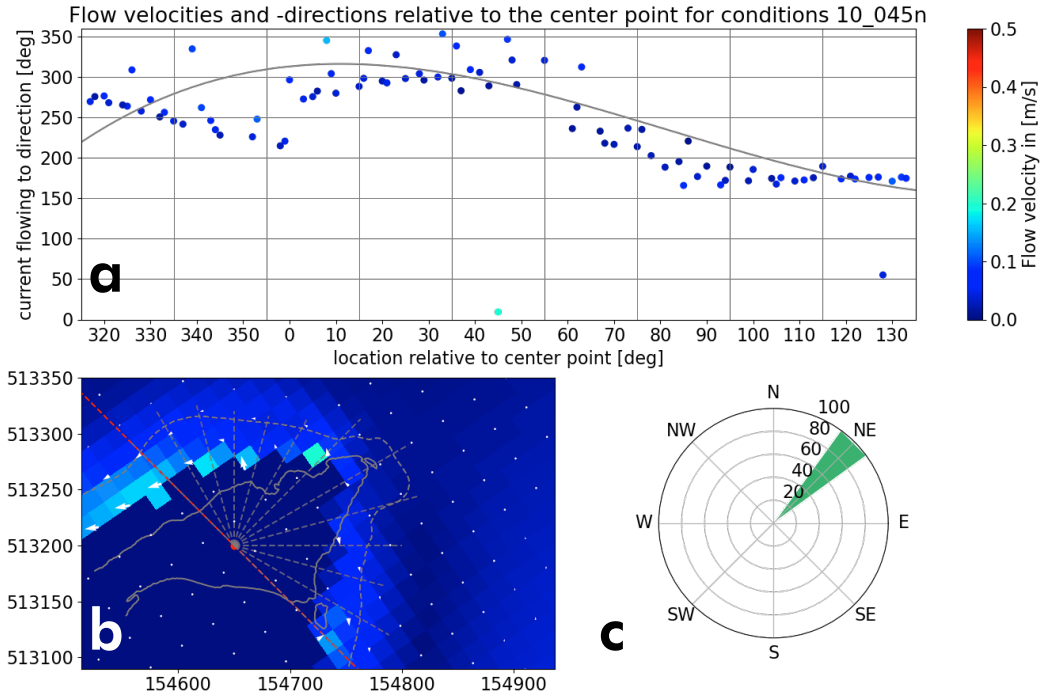

Legend

a:
- Current direction at a degree [deg]
- Current velocity at a degree [m/s]
- Fitted current directions around spit [deg]

b:
- Current velocity [m/s]
- Current direction [deg]
- Waterline
- Platform boundary
- Range of considered data around centre point
- Centre point

c: wind velocities:
- 5 m/s
- 10 m/s
- 15 m/s
- 20 m/s

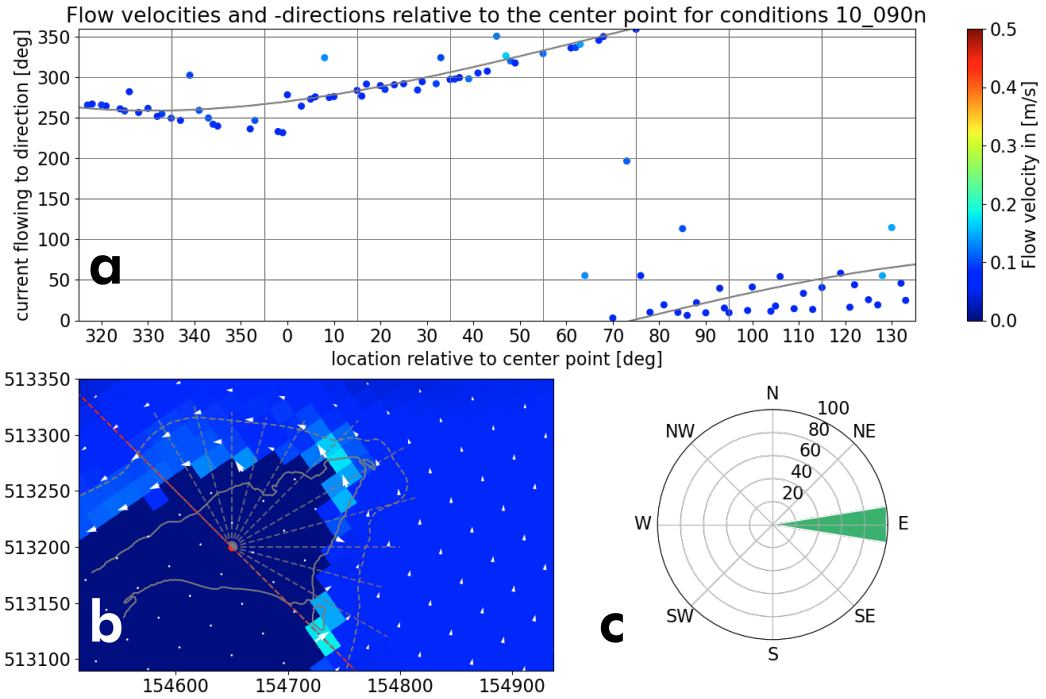

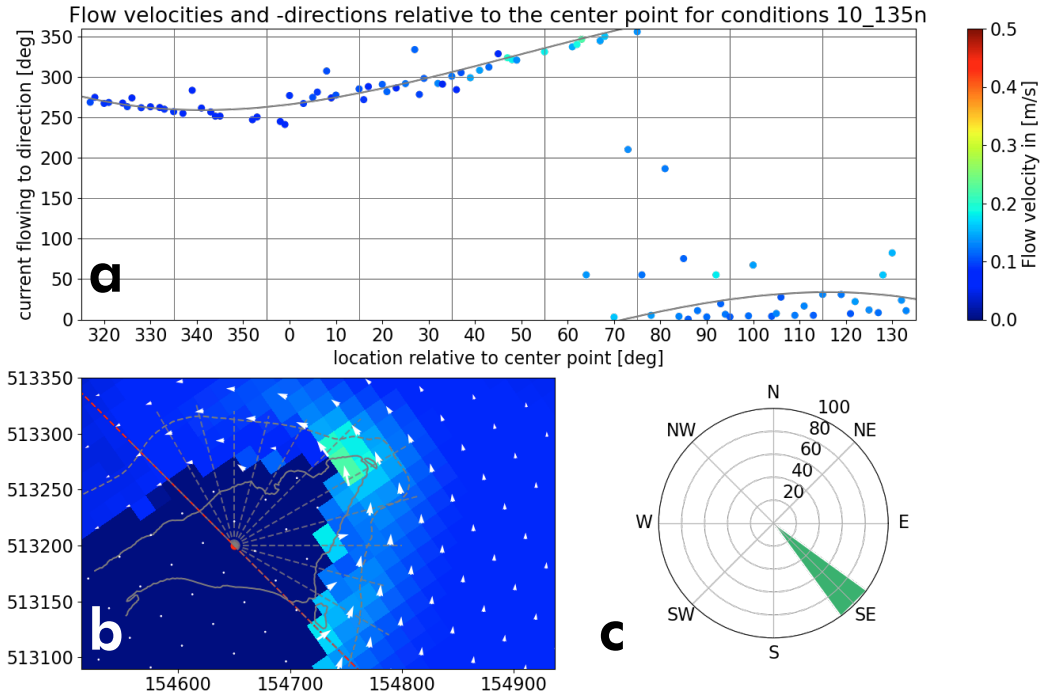

Legend

a:
- Current direction at a degree [deg]
- Current velocity at a degree [m/s]
- Fitted current directions around spit [deg]

b:
- Current velocity [m/s]
- Current direction [deg]
- Waterline
- Platform boundary
- Range of considered data around centre point
- Centre point

c: wind velocities:
- 5 m/s
- 10 m/s
- 15 m/s
- 20 m/s

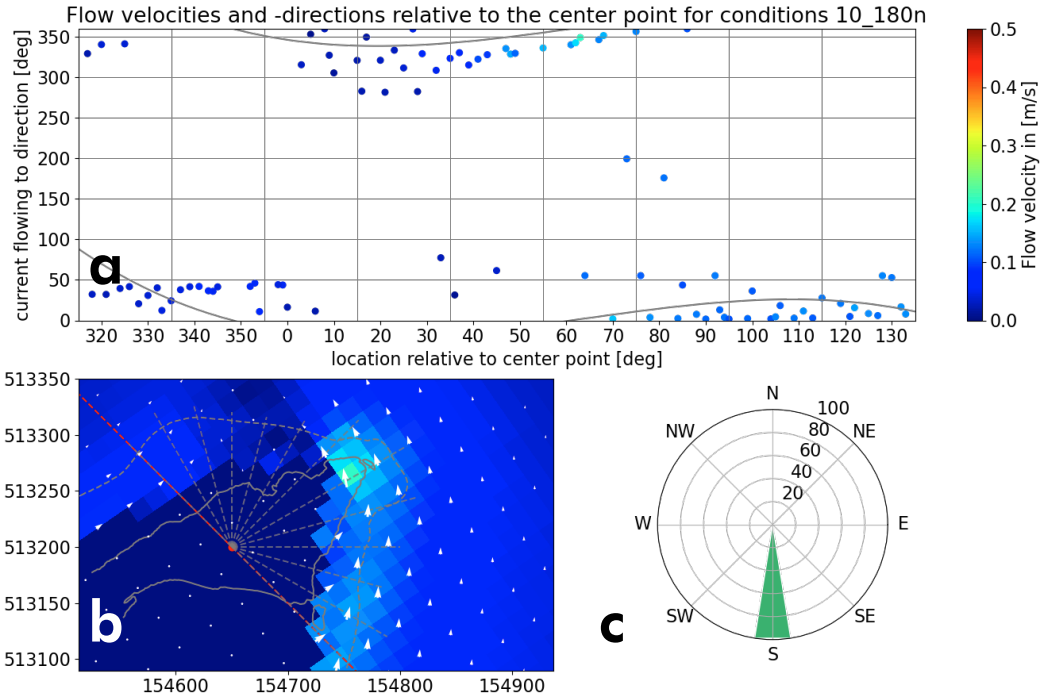

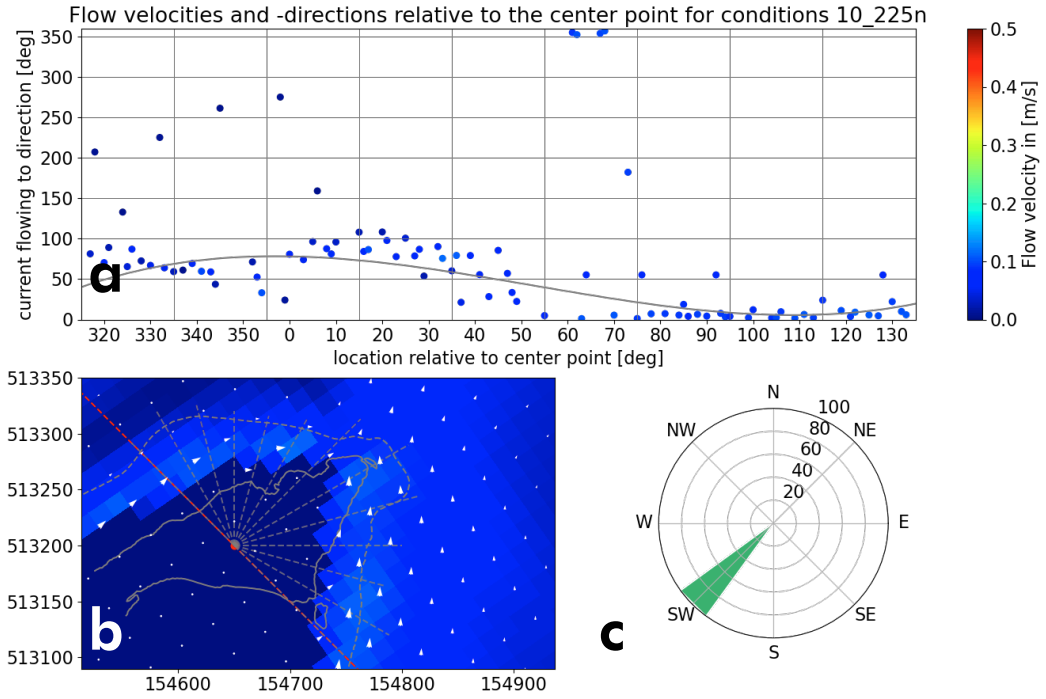

Legend

a:
- Current direction at a degree [deg]
- Current velocity at a degree [m/s]
- Fitted current directions around spit [deg]

b:
- Current velocity [m/s]
- Current direction [deg]
- Waterline
- Platform boundary
- Range of considered data around centre point
- Centre point

c: wind velocities:
- 5 m/s
- 10 m/s
- 15 m/s
- 20 m/s

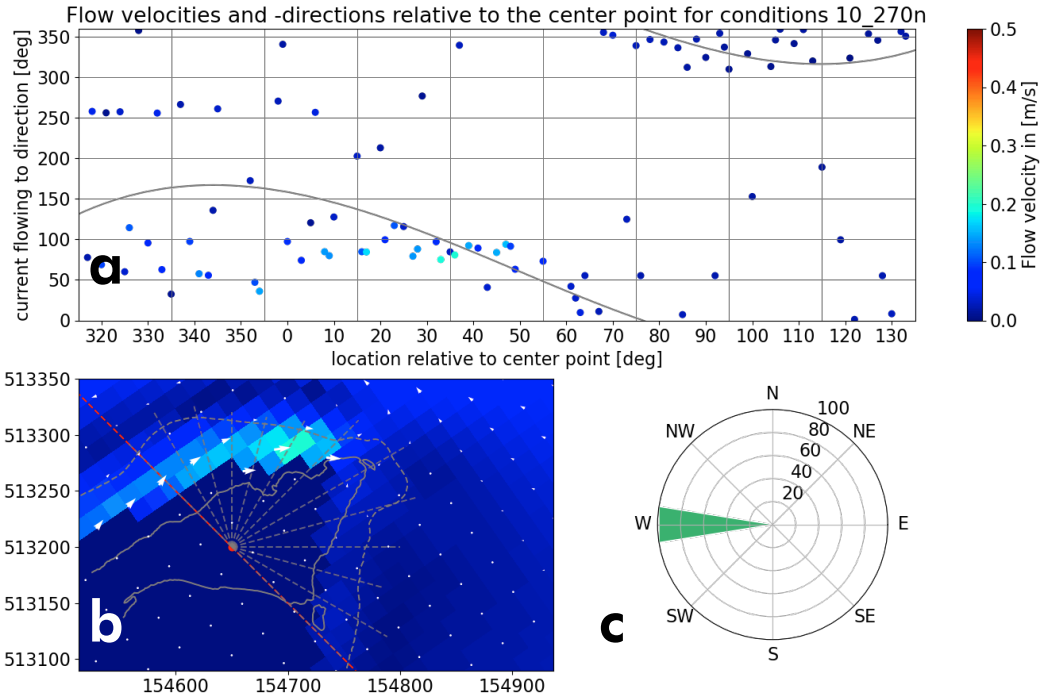

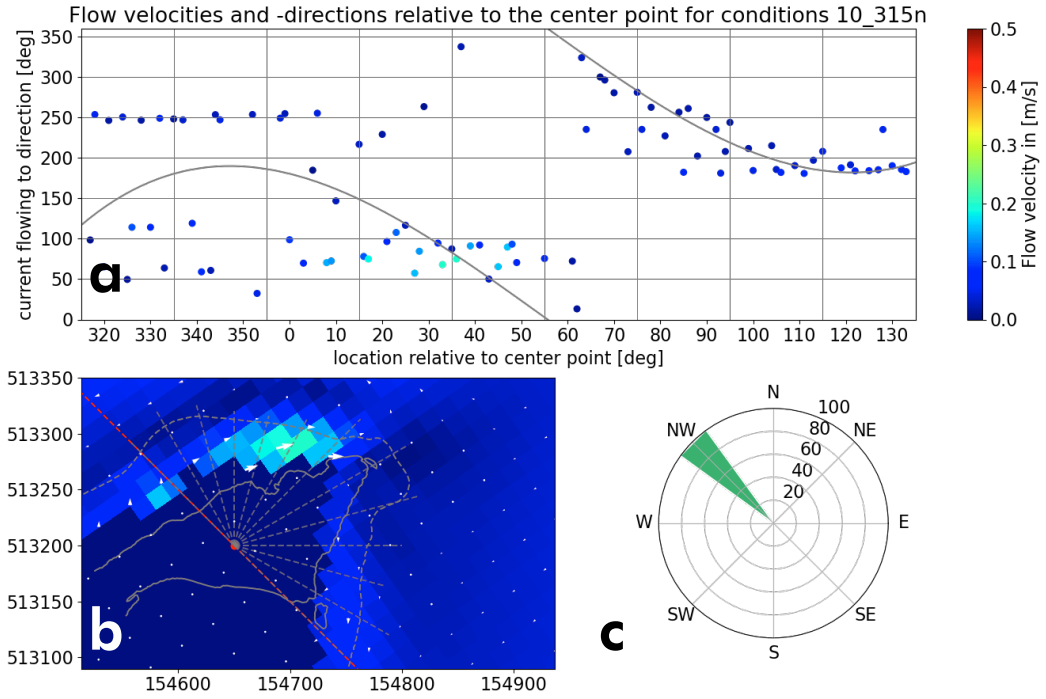

Legend

a:
- Current direction at a degree [deg]
- Current velocity at a degree [m/s]
- Fitted current directions around spit [deg]

b:
- Current velocity [m/s]
- Current direction [deg]
- Waterline
- Platform boundary
- Range of considered data around centre point
- Centre point

c: wind velocities:
- 5 m/s
- 10 m/s
- 15 m/s
- 20 m/s

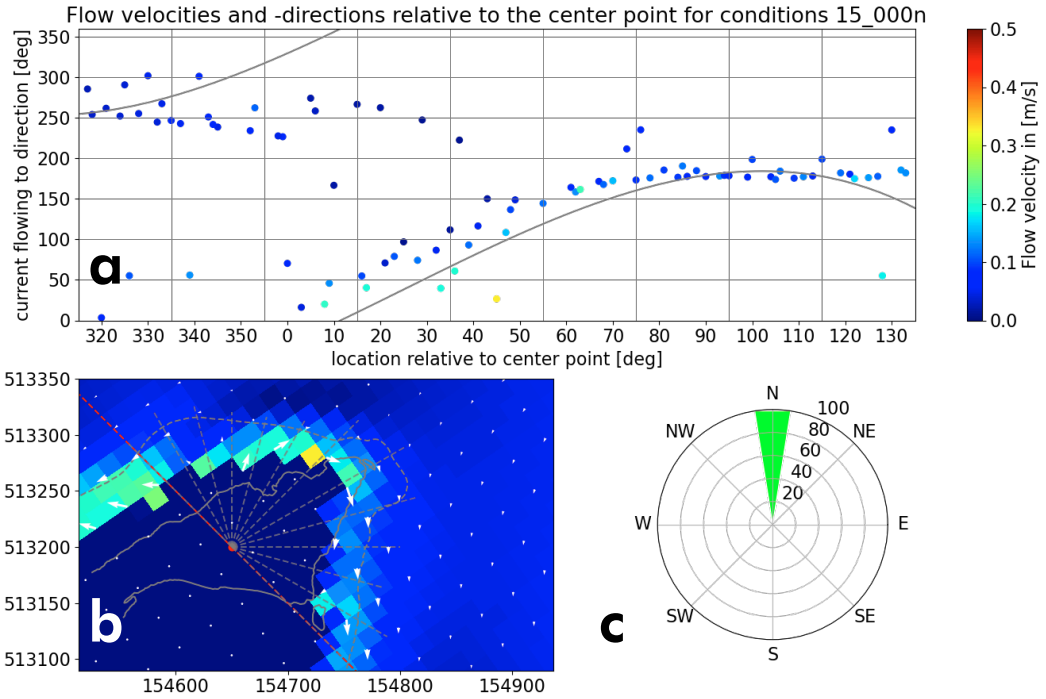

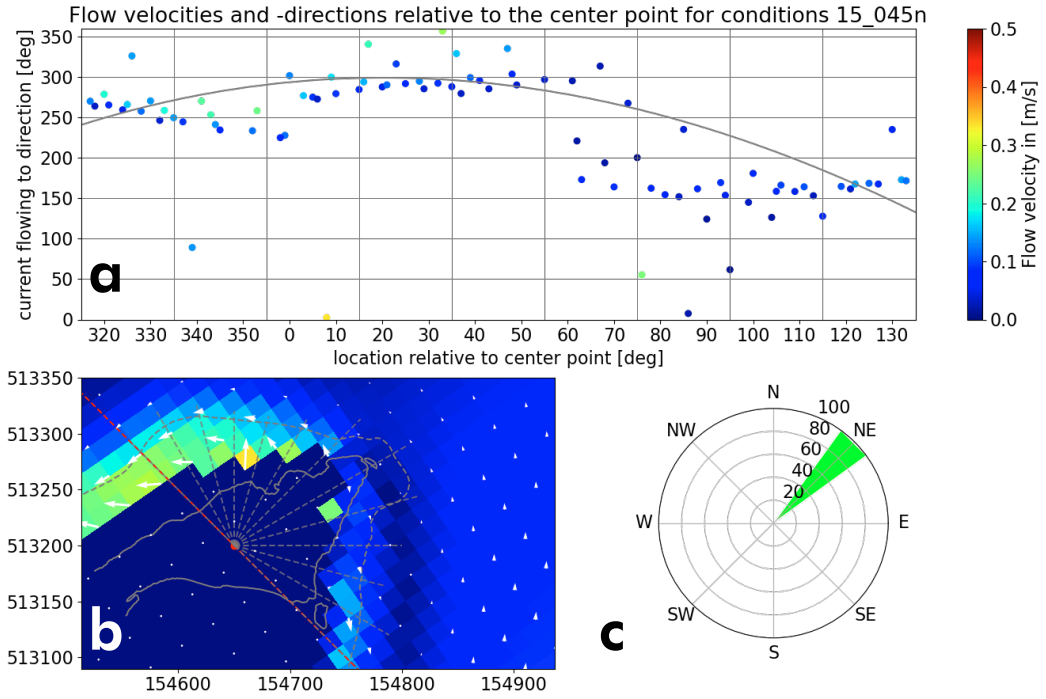

Legend

a:
- Current direction at a degree [deg]
- Current velocity at a degree [m/s]
- Fitted current directions around spit [deg]

b:
- Current velocity [m/s]
- Current direction [deg]
- Waterline
- Platform boundary
- Range of considered data around centre point
- Centre point

c: wind velocities:
- 5 m/s
- 10 m/s
- 15 m/s
- 20 m/s

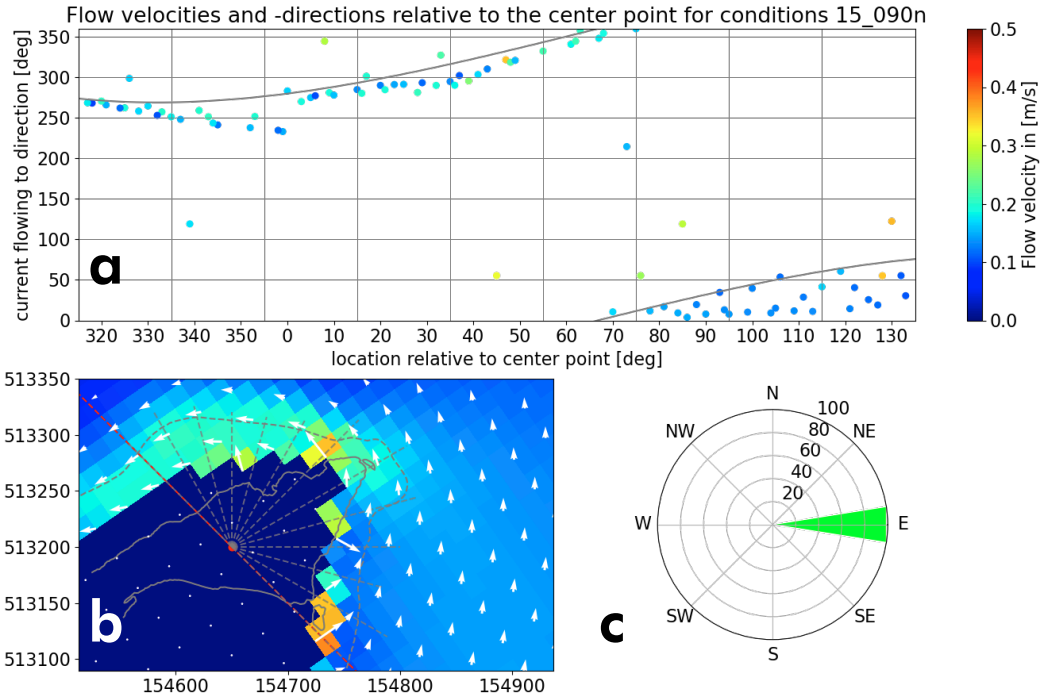

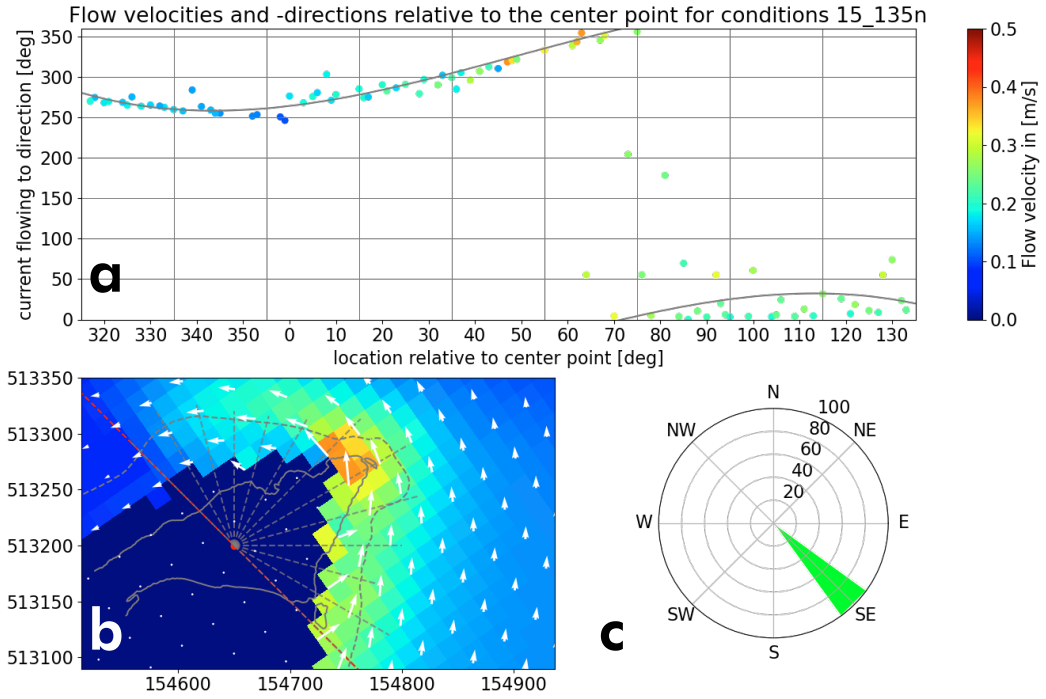

Legend

a:
- Current direction at a degree [deg]
- Current velocity at a degree [m/s]
- Fitted current directions around spit [deg]

b:
- Current velocity [m/s]
- Current direction [deg]
- Waterline
- Platform boundary
- Range of considered data around centre point
- Centre point

c: wind velocities:
- 5 m/s
- 10 m/s
- 15 m/s
- 20 m/s

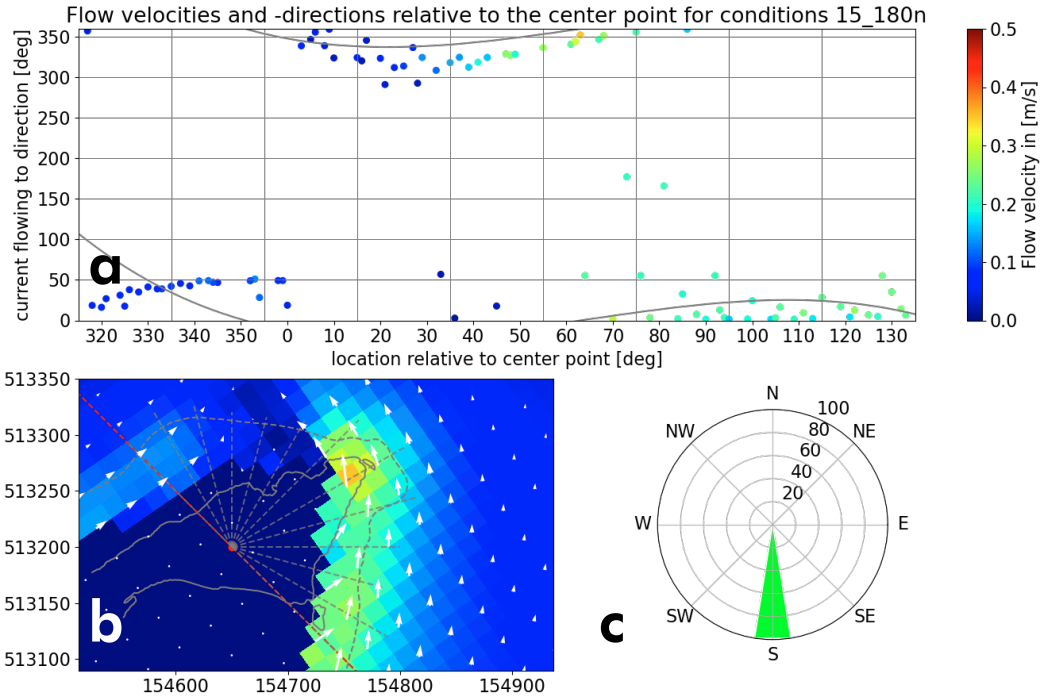

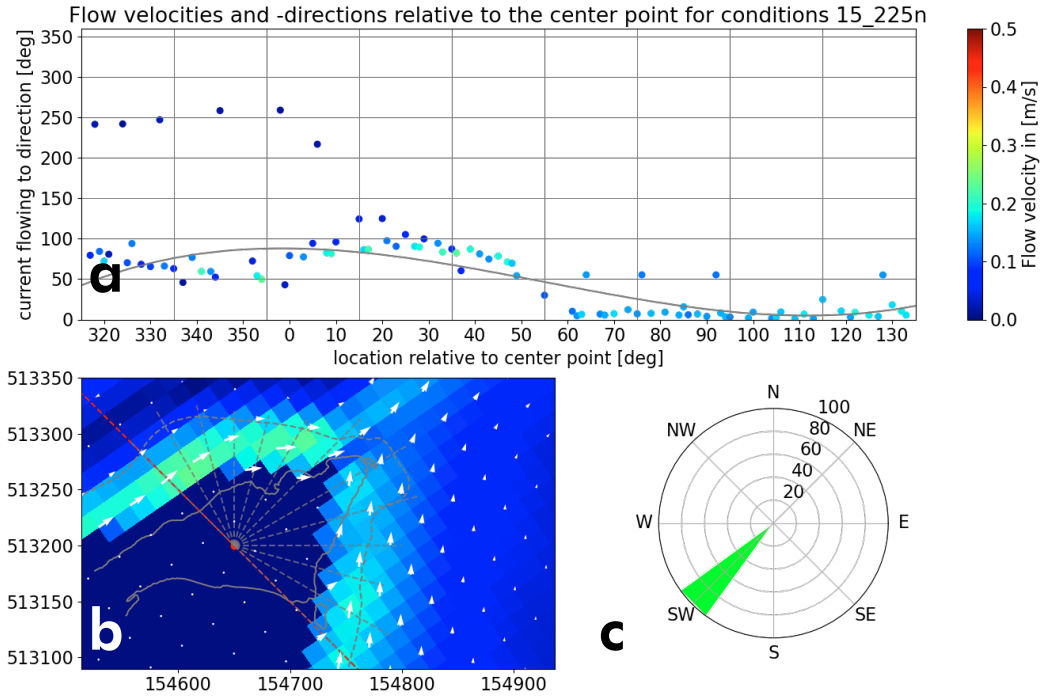

Legend

a:
- Current direction at a degree [deg]
- Current velocity at a degree [m/s]
- Fitted current directions around spit [deg]

b:
- Current velocity [m/s]
- Current direction [deg]
- Waterline
- Platform boundary
- Range of considered data around centre point
- Centre point

c: wind velocities:
- 5 m/s
- 10 m/s
- 15 m/s
- 20 m/s

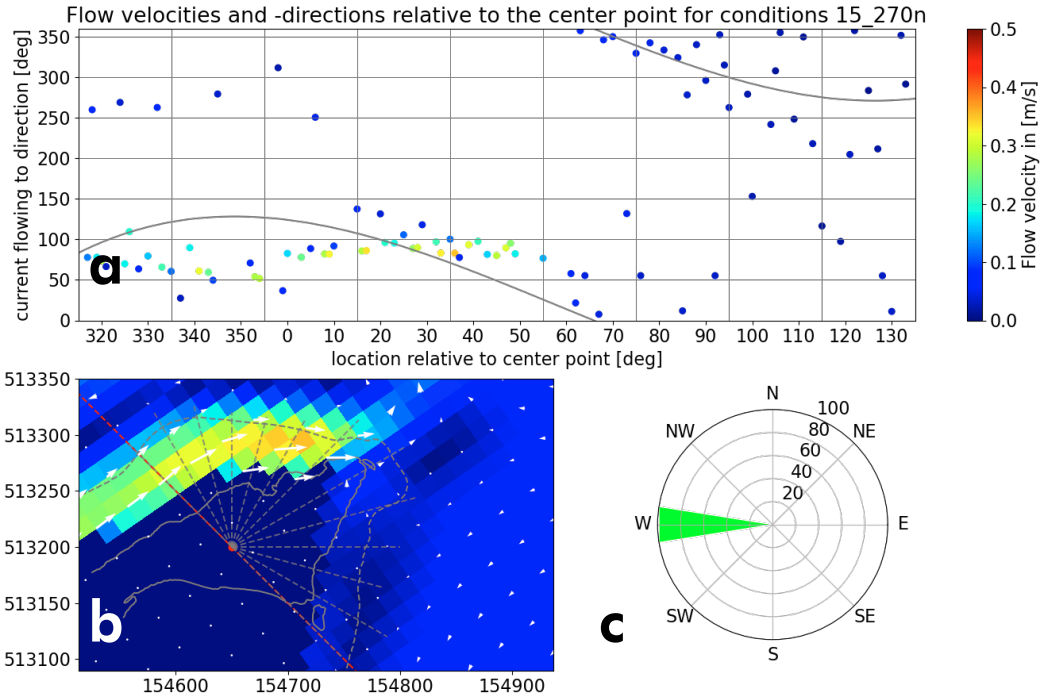

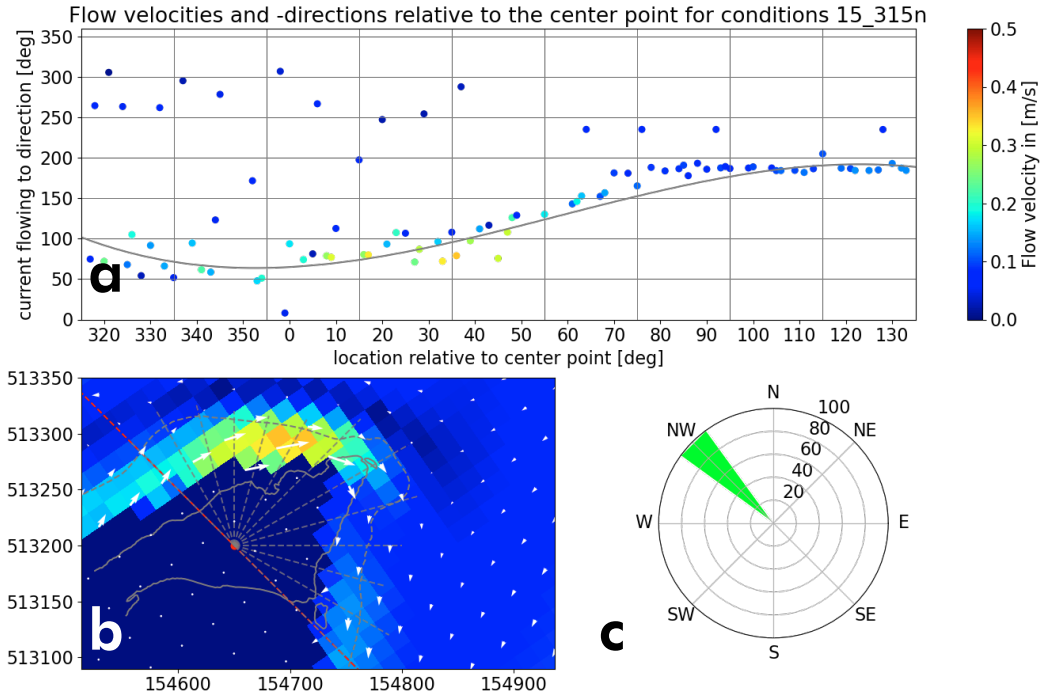

Legend

a:
- Current direction at a degree [deg]
- Current velocity at a degree [m/s]
- Fitted current directions around spit [deg]

b:
- Current velocity [m/s]
- Current direction [deg]
- Waterline
- Platform boundary
- Range of considered data around centre point
- Centre point

c: wind velocities:
- 5 m/s
- 10 m/s
- 15 m/s
- 20 m/s

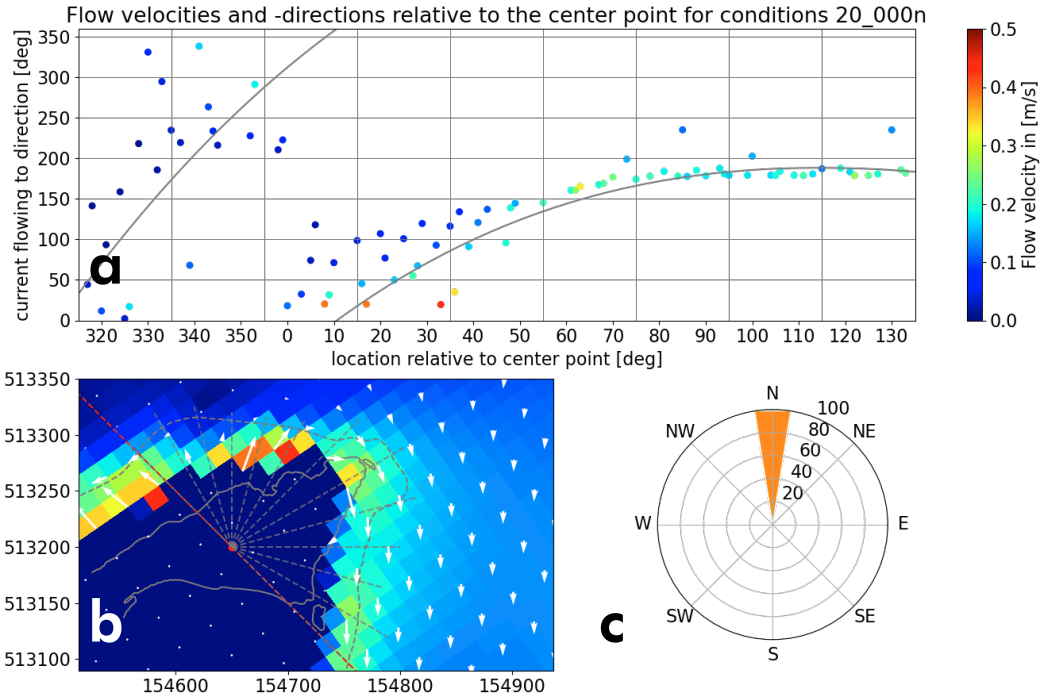

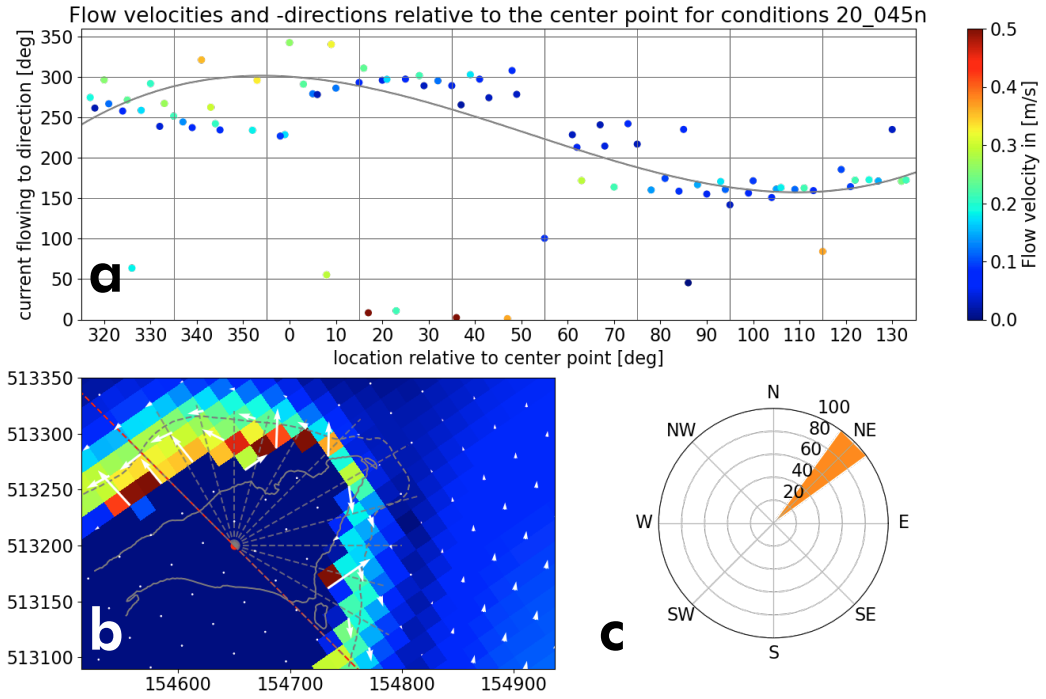

Legend

a:
- Current direction at a degree [deg]
- Current velocity at a degree [m/s]
- Fitted current directions around spit [deg]

b:
- Current velocity [m/s]
- Current direction [deg]
- Waterline
- Platform boundary
- Range of considered data around centre point
- Centre point

c: wind velocities:
- 5 m/s
- 10 m/s
- 15 m/s
- 20 m/s

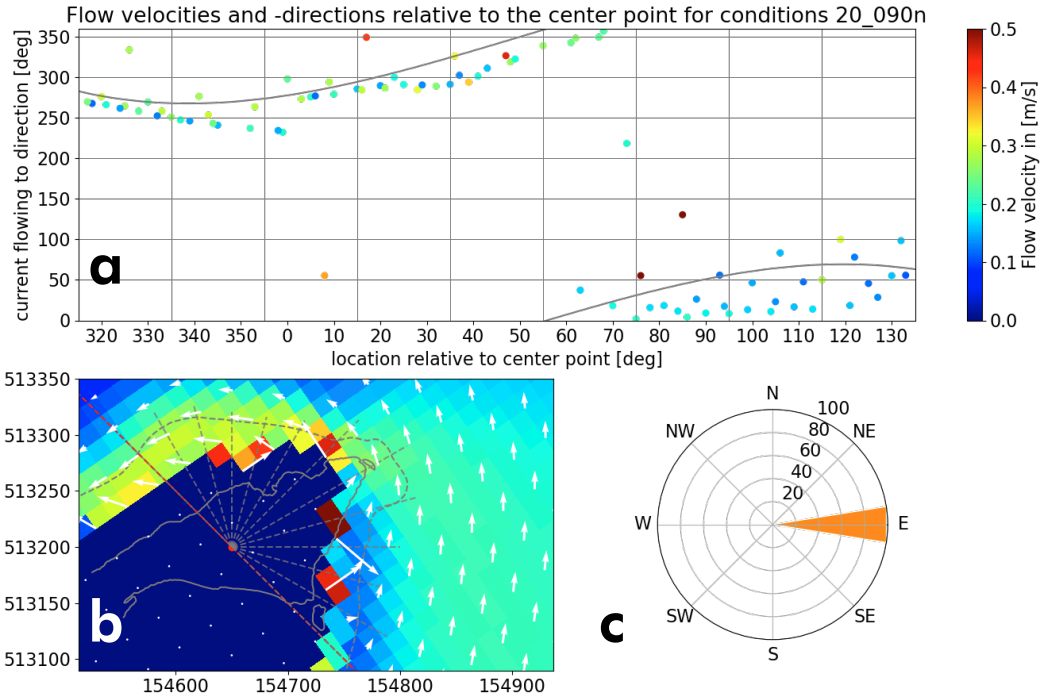

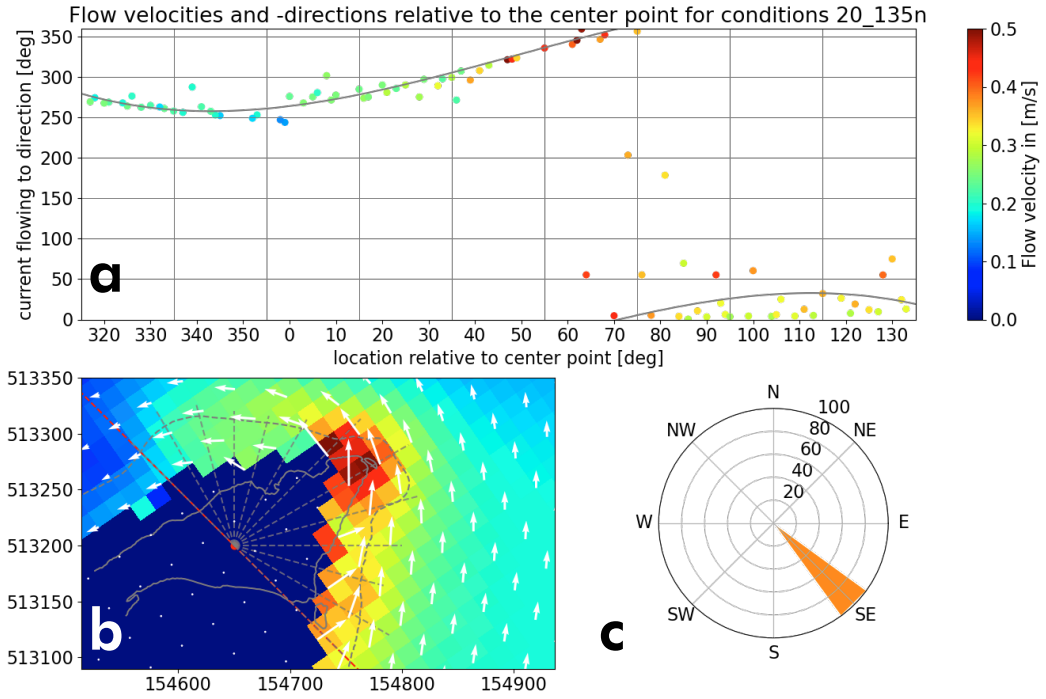

Legend

a:
- Current direction at a degree [deg]
- Current velocity at a degree [m/s]
- Fitted current directions around spit [deg]

b:
- Current velocity [m/s]
- Current direction [deg]
- Waterline
- Platform boundary
- Range of considered data around centre point
- Centre point

c: wind velocities:
- 5 m/s
- 10 m/s
- 15 m/s
- 20 m/s

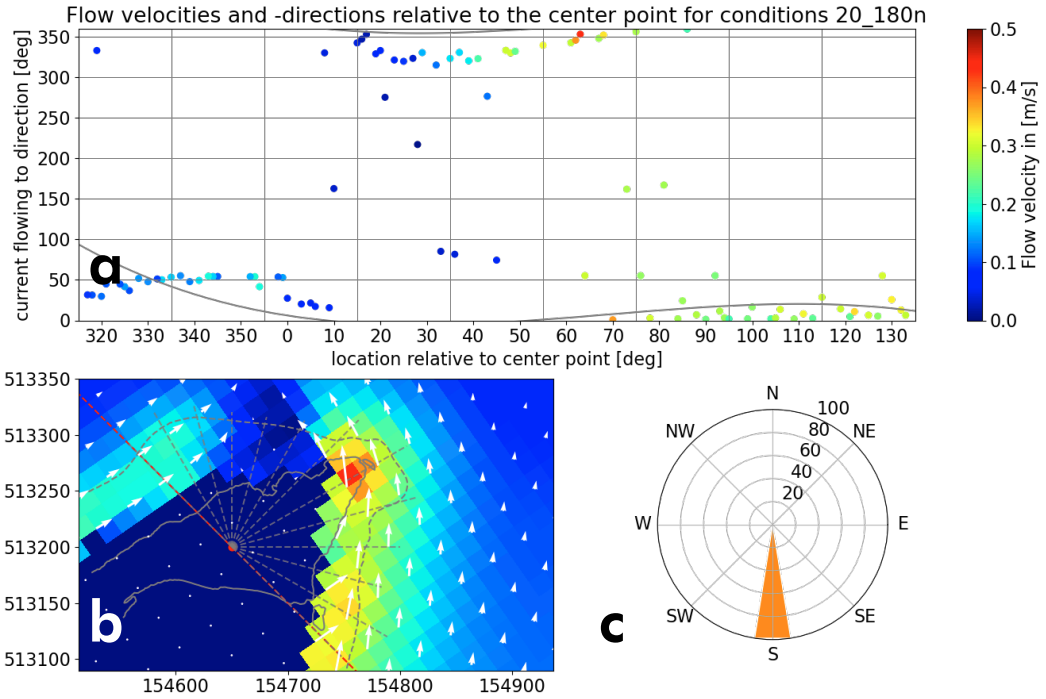

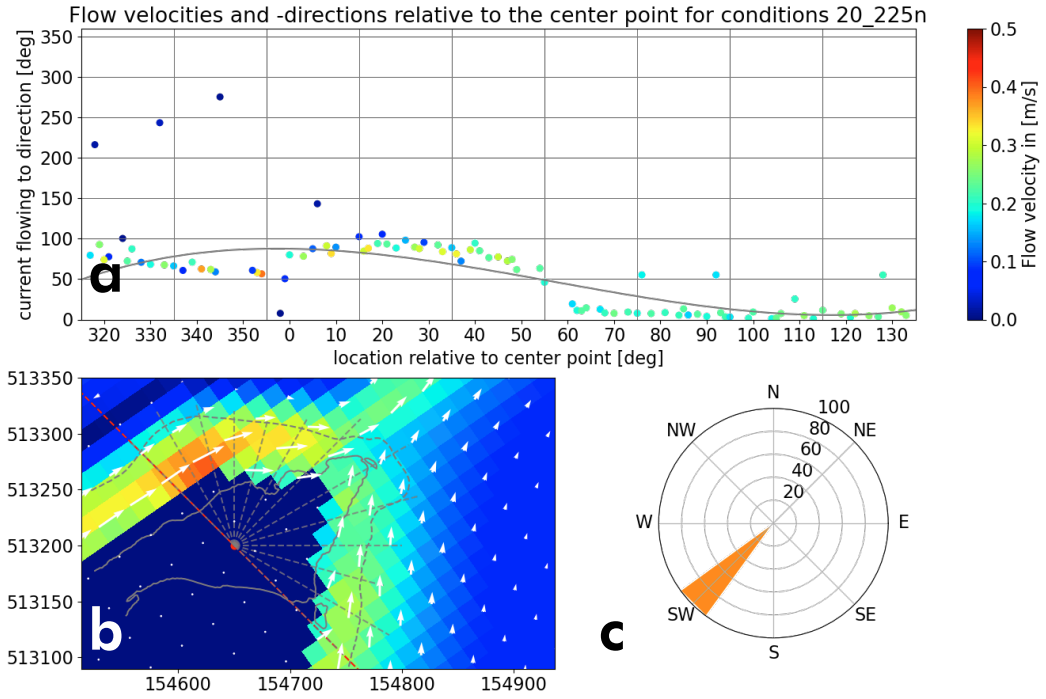

Legend

a:
- Current direction at a degree [deg]
- Current velocity at a degree [m/s]
- Fitted current directions around spit [deg]

b:
- Current velocity [m/s]
- Current direction [deg]
- Waterline
- Platform boundary
- Range of considered data around centre point
- Centre point

c: wind velocities:
- 5 m/s
- 10 m/s
- 15 m/s
- 20 m/s

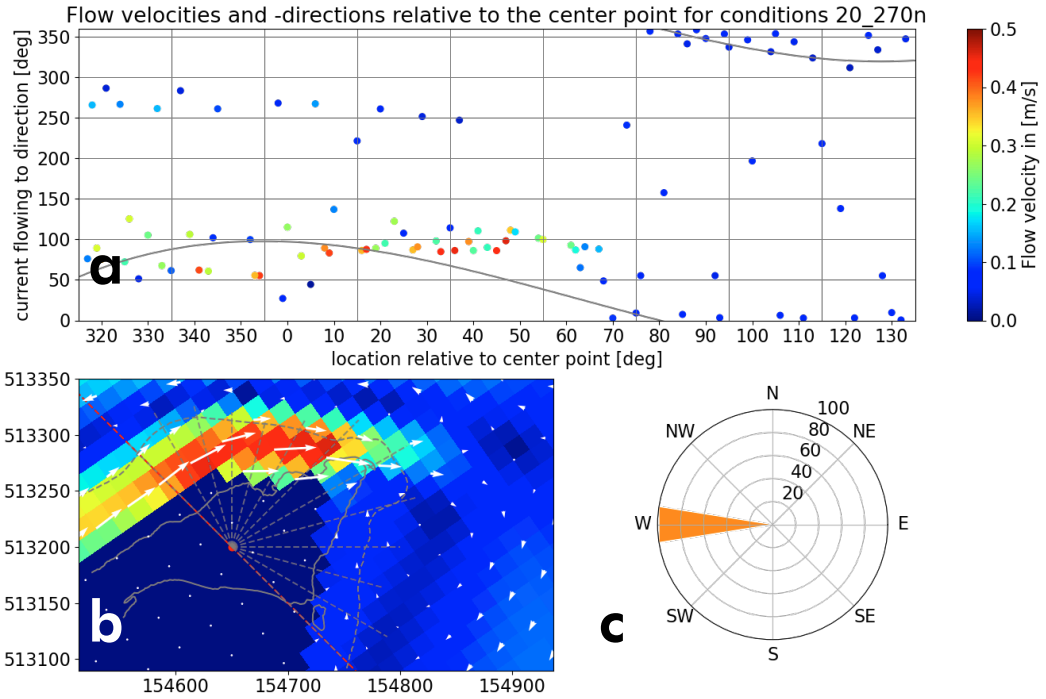

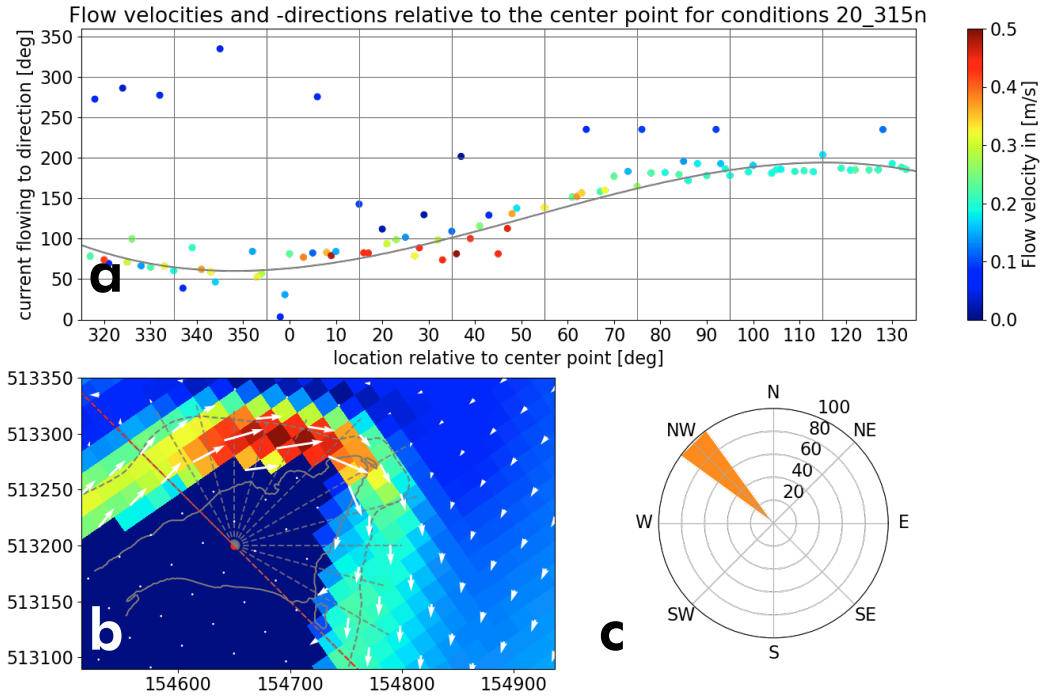

Legend

a:
- Current direction at a degree [deg]
- Current velocity at a degree [m/s]
- Fitted current directions around spit [deg]

b:
- Current velocity [m/s]
- Current direction [deg]
- Waterline
- Platform boundary
- Range of considered data around centre point
- Centre point

c: wind velocities:
- 5 m/s
- 10 m/s
- 15 m/s
- 20 m/s

From the maps (b) several observations can be done. In general, the following observations, and accompanying morphodynamic hypotheses, can be made:

1. At winds of 5 m/s the flow is very slow, especially looking at the velocities at higher wind speeds. This flow likely has too little energy to really cause significant morphodynamic changes.
2. South of the northern spit there is a large circulation cell that results in a flow coming from the south and flowing along the spit towards the north. Also, often currents come from the east originating from the Noordstrand. So, the northern spit has, because of lake circulation, currents on both side of the spit (Figure 5).

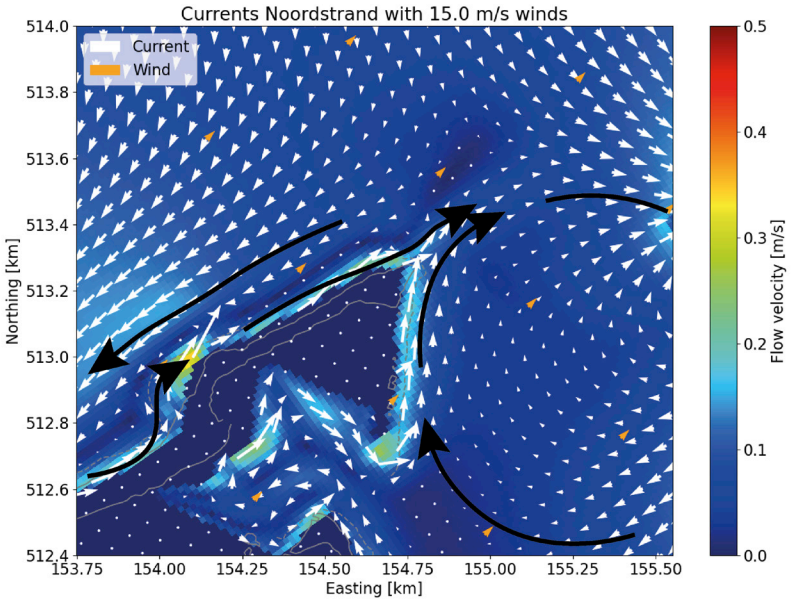

Figure 5. Example of local lake circulation at the northerns spit during SW winds (schematic currents: black)

3. Currents near the coast are often in the opposite direction of offshore currents.
4. At N and NE winds there are currents moving away from the northern spit. Therefore, these currents are unlikely to supply the spit with sediment for growth.
5. At E, SE, and S winds the current moves from the southern side of the spit towards the north, around the spit tip. This could result in migration towards the north
6. At SW winds currents approach the spit from both sides. For slower winds the current coming from the northern beach is faster but for winds around 20 m/s the lake circulation current coming from the south is faster. The combination of these currents will likely result in a simple spit.
7. At W and NW winds, there is only a longshore current coming from the Noordstrand. This current accelerates on the head and decelerates on the spit tip. These currents are important in the transportation of material from the Noordstrand.
8. Smaller wind velocities create smaller flow velocities and therefore sedimentation on the platform is more likely.
9. Higher wind velocities, create more set-up and therefore lake circulation becomes more important. This could mean that currents would curve less around the spit.
10. At winds of 20 m/s, flow velocities on the platform are very high and it is unlikely that any sedimentation occurs on the platform.

Current directions

For the northern spit the current is less similar at different wind speeds than for the southern spit but are still comparable. Especially the currents during W winds can divert their direction when wind velocities change. But other than that, the simplification that the current direction is only dependent on the wind directions holds quite well (Figure 6).

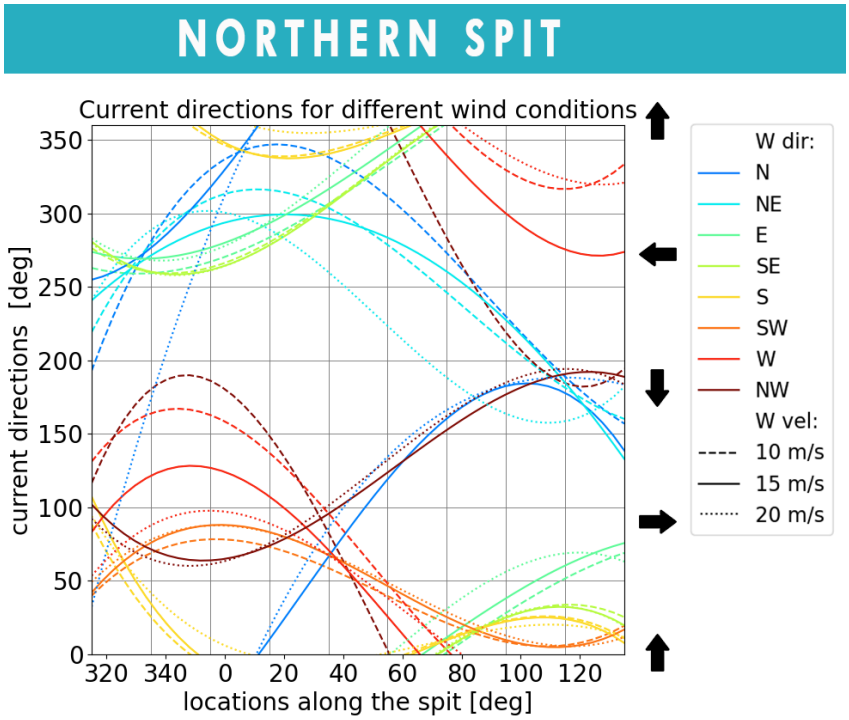

Figure 6. Current directions during different wind conditions (dashed: 10 m/s, solid: 15 m/s, dotted: 20 m/s). Each line is the gives the current directions around the southern spit for one wind condition (combination of wind velocities and directions). The arrows indicate where the current is flowing towards at that specific y-axis value.

The when considering sediment supply together with the similarity of current directions, the most clear group that can be distinguished here are the currents that occur during W, SW and S winds. During W winds the current flows from the Noordstrand to the distal end and around the tip of the spit. This current is driven by high angle waves and lake circulation along the Noordstrand. During S wind the current flows from the south side of the spit to the distal end and around the spit tip the other way around. This current is driven by a lake circulation cell to the south. The currents of the SW winds are actually a combination of the currents from the S and the W side. All currents, created by these wind directions, transport sediment to the spit tip at around 60° relative to the centre point (Figure 7).

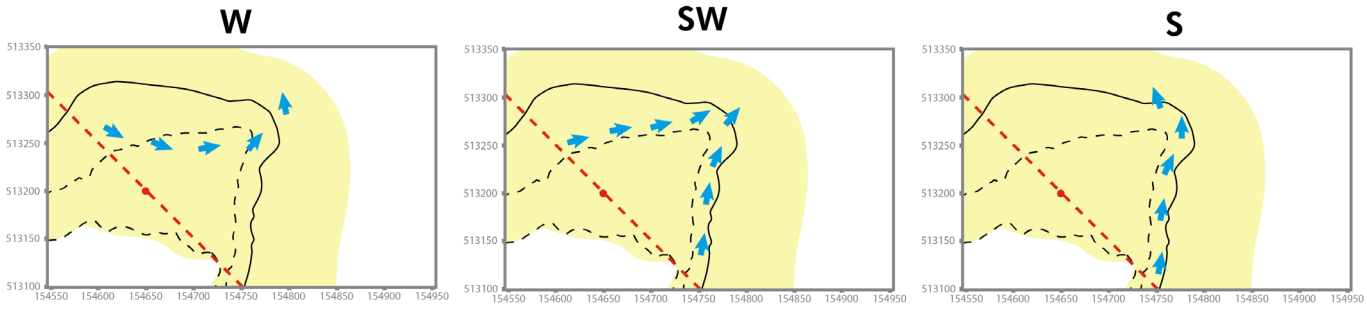

Figure 7. Visual representation of the different current that occur during S, SW and W winds.

Flow velocity

With the same method as for the current directions, a fit can be made of the flow velocities along the spit for each wind scenario (Figure 8).

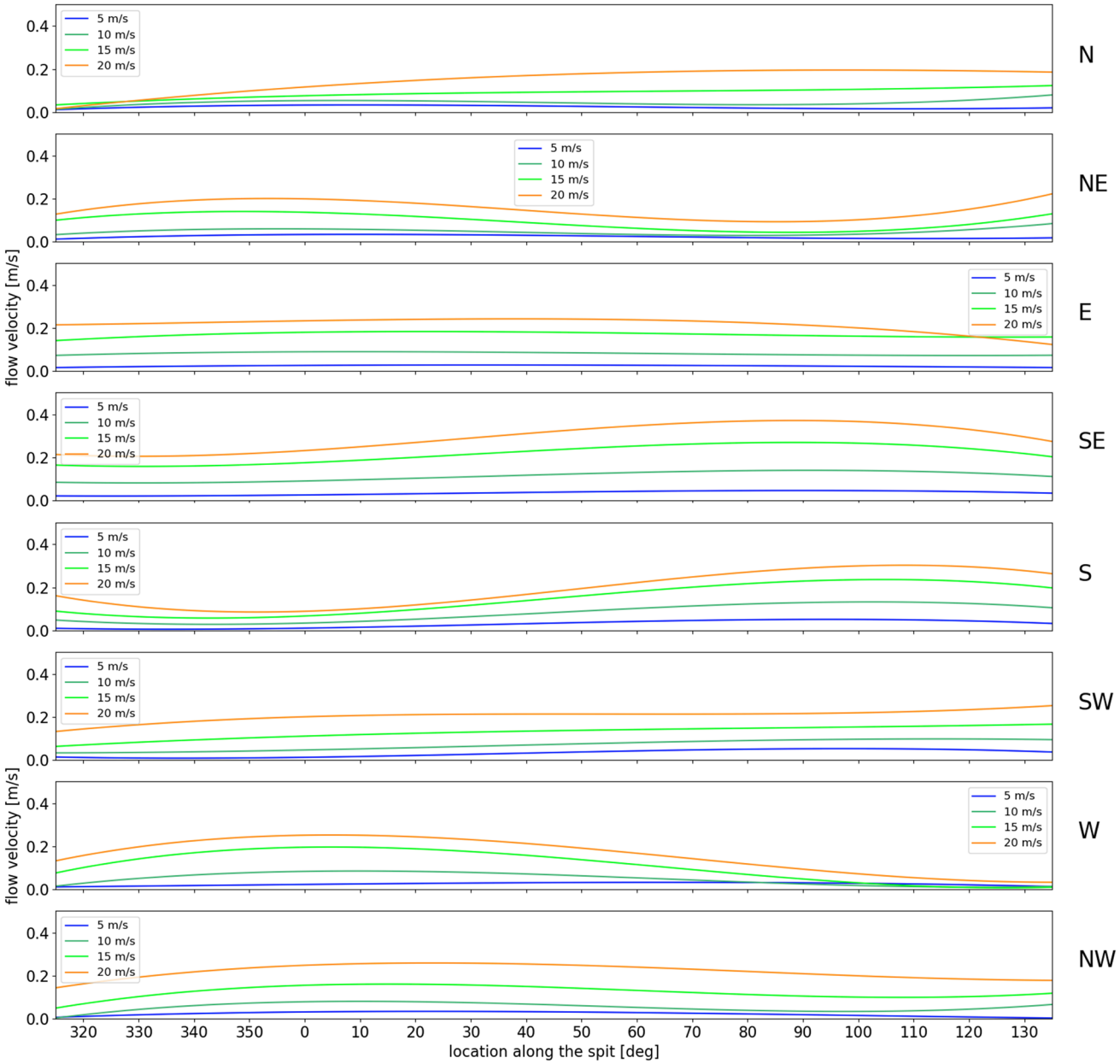

Figure 8. Fitted possible flow velocities along the spit with the flow velocities on the left side, colour indicating the wind velocity and on the right side the wind directions.

Also, for the northern spit the flow velocities follow the same pattern for different wind velocities. So, when currents increase at a certain location at 10 m/s winds, currents also increase at the same location at 20 m/s winds. Naturally the faster the wind speeds, the higher the flow velocities. The development of flow velocities around the spit, for each wind direction can be qualitatively expresses as has been done in Figure 9.

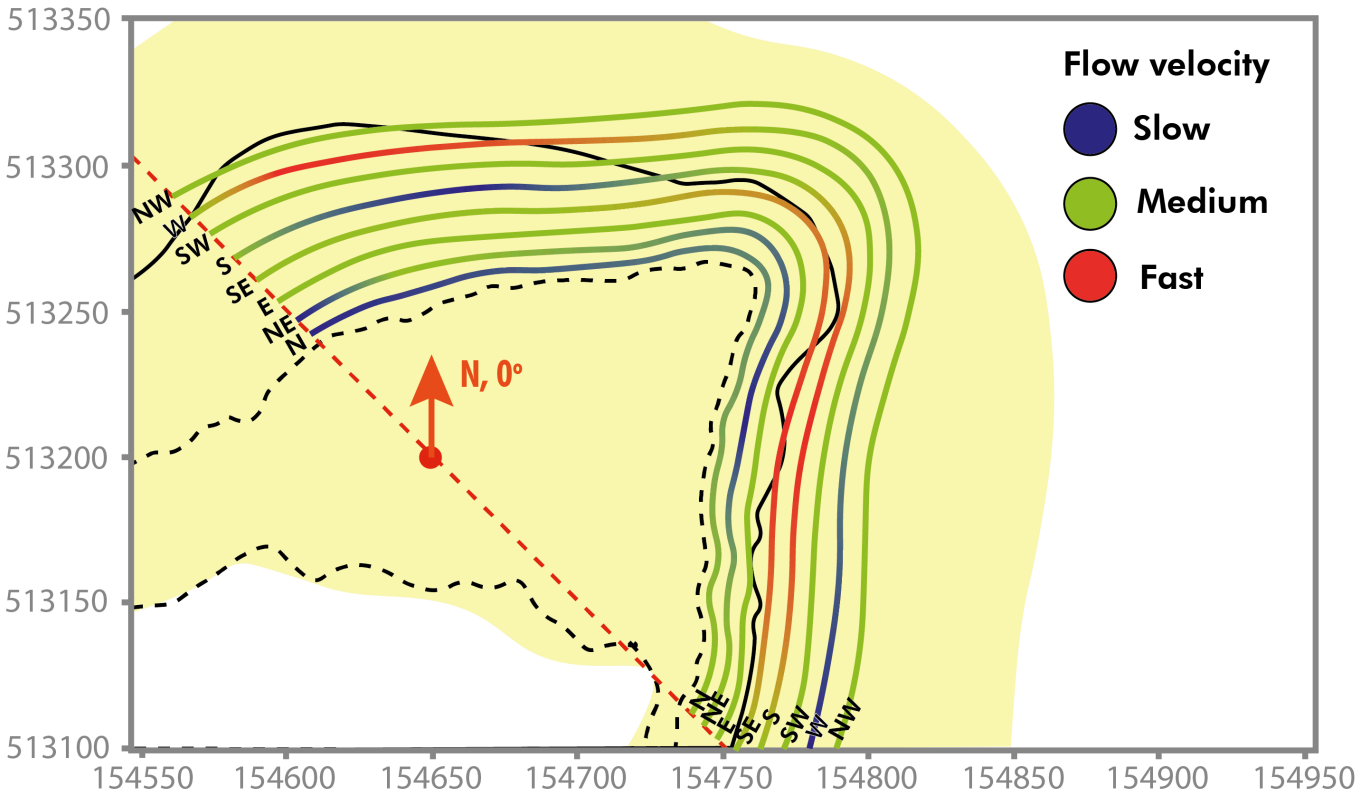

Figure 9. Schematic change in flow velocity around the northern spit for different wind directions

Flow velocities during N and NE winds are relatively limited. Although currents of wind from the NW, SW and E have different directions, the flow velocity of these currents does not change significantly around the spit. Current from winds from the S and W behave oppositely. On one side of the spit, they increase and then decrease at the other side of the spit resulting in sedimentation at that side. Flows of winds from the SE are similar to the flows during S winds, only the flow does not decrease that much at the northern side of the spit. Therefore it can be expected that at SE winds there is less sedimentation around the spit tip than during S winds (especially on the platform level).

Bibliography

Ton, A. M., Vuik, V., & Aarninkhof, S. G. J. (2022). Longshore sediment transports by large-scale lake circulations at low-energy, non-tidal beaches: a field and model study.

Appendix

E Results

Growth orientation linked to flow

Table of contents appendix E

Sedimentation current pattern

This appendix serves as a further explanation of the growth orientation section in the paper. To investigate the direction of spit growth, the elevation levels are neglected for now. For the hydrodynamics it was found that the current directions are mainly dependent on the wind direction, not the wind speeds. For every scenario of the 32 combinations between wind directions and wind speeds a fitted function has been made that describes the direction of the current around the spit. Currents transport sediment to a certain location where sedimentation takes place, at that location the spit grows. The path that this current takes is mostly dependent on the wind directions. Therefore it is likely that the location of sedimentation on the x,y-plane, relative to the centre point, is dependent on the current directions and wind directions.

With this simplification in mind, it is stated that a deposit and its location can be influenced by a number of factors:

- If a current transports the sediment to a location where dissipation can take place, a deposit is likely to form. For example, transportation over the platform boundary or transportation along the curved coastline so wave-driven transport decreases.
- Does the current flow from a location with an abundance of sediment to the sedimentation location? If there is no material to be transported likely less sediment will accrete.
- If a specific current occurs more often during a period, it is more likely that it has built a large sedimentation deposit during this period.
- If more currents flow towards a certain location it is more likely that a large sedimentation deposit builds at this location. That is a reason why for both the northern and southern spits, the location of most spit growth is also the location where the most occurring currents come together.

So, with these considerations the current patterns can be compared to the sedimentation locations. For each deposit it can be reasoned that certain significant wind conditions, thus a certain current pattern, have caused the deposit. A fast-flowing current pattern that occurs often during a period between measurements, and transports sediment towards the spit tip, is likely to have caused a deposit. Blue markers indicate the location of a deposit and the possible current directions that may have caused this deposit (Figure 1). If a deposit was found at a certain degree, say 110 degrees relative to the centre point of the northern spit, multiple markers can be plotted for this single deposit. The number of markers that are plotted for a single deposit at a degree depends on how many wind regimes occur more often than 5% of the time. If a current, caused by winds faster than 7,5 m/s, occurs more often, the marker gets bigger. Clearly, the larger markers are all situated around the same current direction patterns, indicating that there is and average current pattern that can be considered as the main driver for spit developments (Figure 1). For both spits, current patterns caused by S, SW, W (and SE smaller than 160° for the southern spit) are responsible for the bulk of sedimentation.

To bolster this reasoning, the currents caused by (SE,) S, SW and W winds, are all currents that transport sediment from the beach to the spit tip, instead of away from it. Thus, currents caused by (SE,) S, SW and W winds can be considered the only essential currents for sedimentation and can be averaged in a single line, from now on called the 'sedimentation current pattern'.

The plots in Figure 1 can be hard to read and/or process its meaning and therefore it is visually interpreted in Figure 2. The coloured circles indicate the location and size in volumes of (a group of) deposits. The arrows indicate the possible current directions at that location that occurred during the time this deposit had accreted. The red arrows indicate the currents that were incorporated in the sedimentation current pattern and the blue arrows are the current directions that where not incorporated. A large arrow means that this current direction had occurred a lot during the time this deposit had accreted, and a small arrow means that this current direction occurred barely more than 5% of the time.

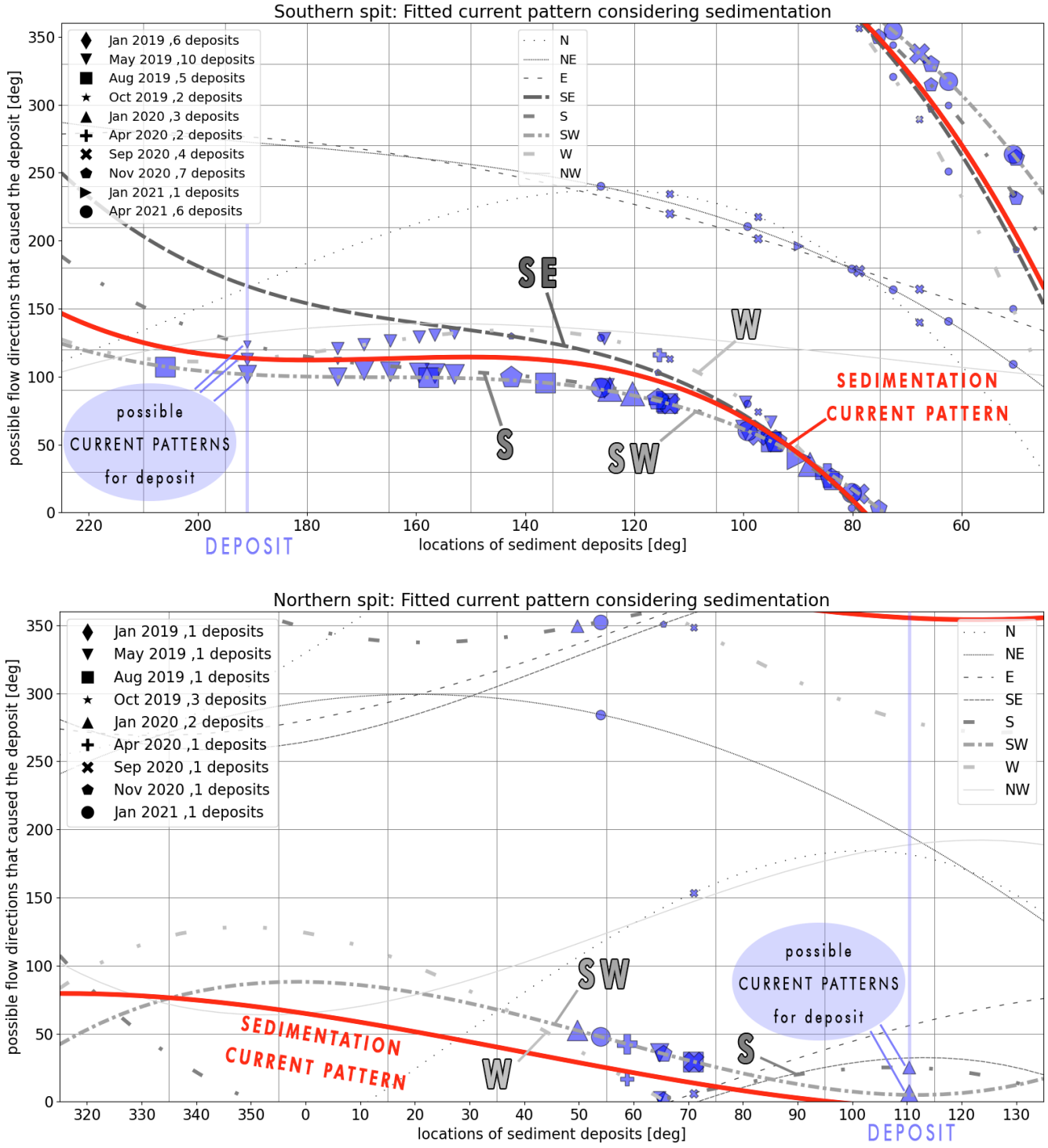

Figure 1. The sedimentation current pattern that is mainly responsible for sedimentation (red). The blue markers indicate a deposit during a morphological period. This deposit can be caused by a number of current patterns. When a current pattern occurs more than 5 percent of the time it becomes a possible current for this deposit and gets indicated by a marker. The size of the marker indicates the occurrence of the current (in this case only flows where considered, created by winds higher than 7,5 m/s) and the more likely it is that it has caused the deposit. The currents that are the most likely driver of most deposits are indicated by thick lines.

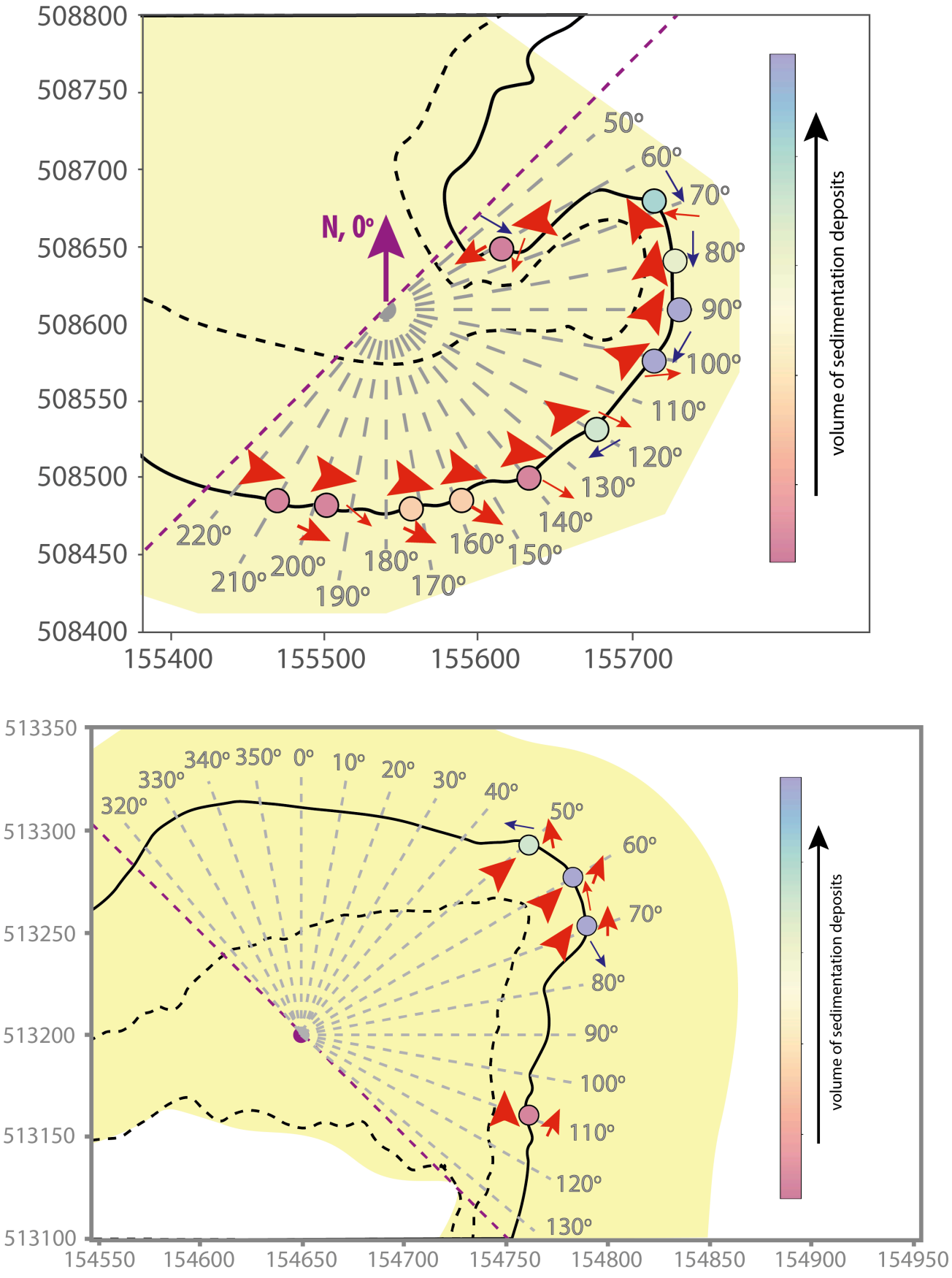

Figure 2. Visualisation of Figure 1 with the southern spit above and northern spit below. The volumes of sedimentation are schematic in this figure.

Clearly, the currents that are incorporated in the sedimentation current pattern move material from sediment rich places (like the scarps and beaches) to the locations with the most sedimentation. Also, these currents flow to places where flow dissipation can take place. They flow over the platform boundary at the locations with the largest deposits and move along the coastline around the spit tip so that waves can lose their energy. Admittedly at the southern spit, currents that are not incorporated in the sedimentation current pattern also move along the coastline but move from a location with little sediment to a location with a lot of sediment (from the northern side of the southern spit to the scarp). Lastly, the current directions that are incorporated into the sedimentation current pattern occur much more often at the location of the largest deposits. Thus, the sedimentation current pattern is a good representation of the currents that essentially induce spit growth.

Besides this, it was also observed that for the southern spit sedimentation occurred at higher degrees relative to the centre point (larger than 140°) for periods with significant W winds. Indeed, from Figure 2 it can be seen that the deposits at this location also have a current direction arrow that occurs regularly (with medium size). This arrow moves the sediment over the platform boundary at these locations, resulting in sedimentation at these degrees. This current direction is created by W winds.

This sedimentation current pattern can be combined with the distribution percentage of total sedimentation, relative to the centre point (Figure 3, I and II). Visually it becomes clear that the flows closest to the beach

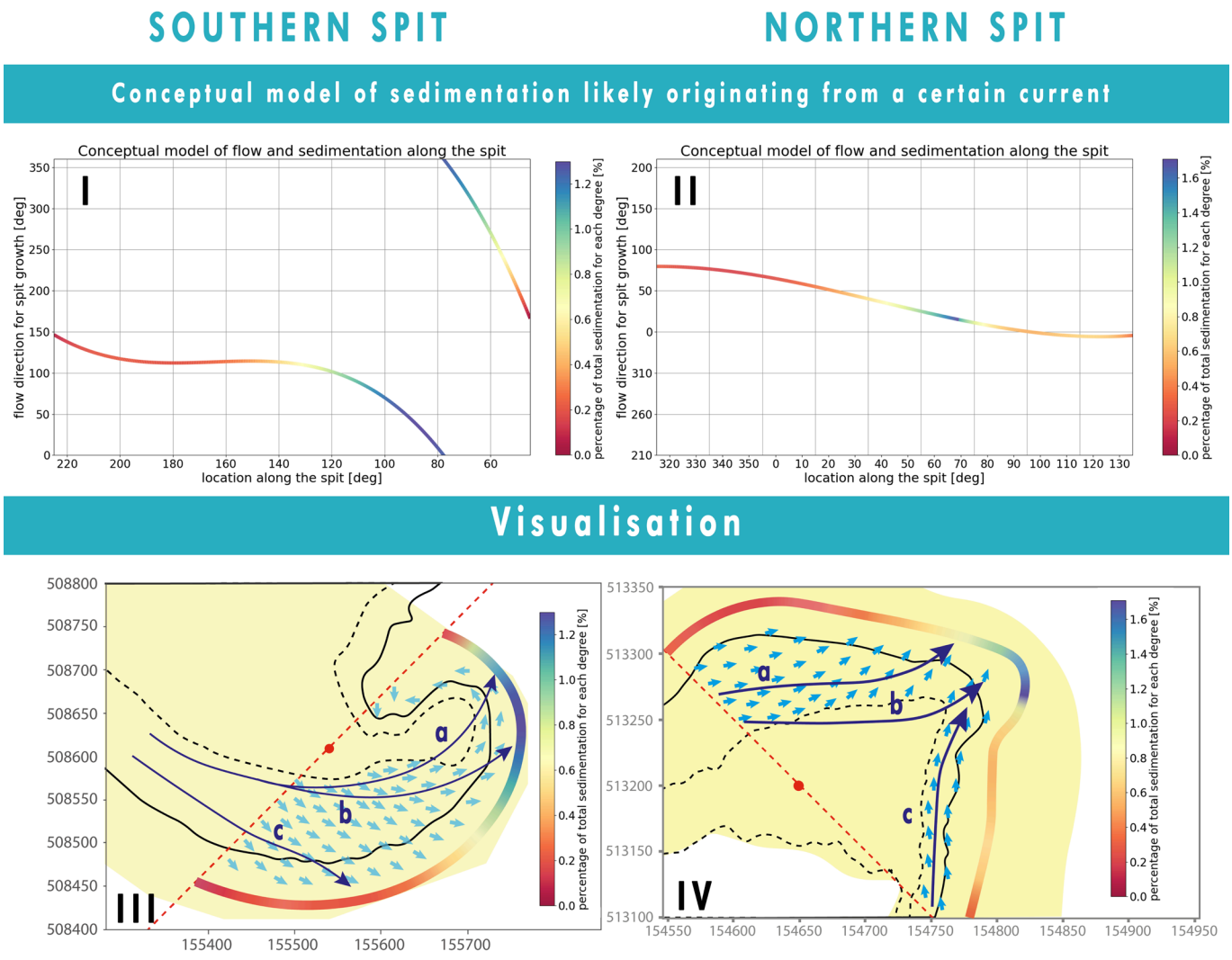

Figure 3. Representative sedimentation current pattern that is responsible for the observed spit growth directions, with distribution of sediment around the spit indicated by the colours, the sedimentation current pattern indicated with the line itself (I and II) and light blue arrows (III and IV) and the paths of sediment indicated by the dark blue arrows (III and IV).

transport the most sediment, from the beach and scarp at the proximal end. As it is those flows that eventually pass over the spit-platform boundary at the locations where most sedimentation takes place (Figure 3,III and IV). Thus, the dissipation space that arises as the flows pass over the spit-platform boundary is a very important mechanism for the growth direction of the spits. For the sedimentation on the platform level the transportation of sediment by the sedimentation current pattern along the curves of the coastline, so that waves can gradually lose their energy also is of influence, especially for the southern spit. Also, for the southern spit the current only starts to divert to the east quickly when the current originating from the beach meets the small lake circulation eddy, caused by a sand mining pit to the south of the spit. This change in direction might be an important factor in the bend that is formed on this spit (Figure 3,III).

Sediment supply to the spit

Southern spit

Previously it was concluded that the SE, S, SW and W wind directions were the important wind directions for spit development. For each of these wind directions, the sediment supply for spit growth can be determined:

- *SE and S wind regimes:* Currents during SE and S winds originate from the middle of the spit curve and then move westward to the Zuidstrand and eastward to the distal end. Spit growth during SE and S wind is supplied by material from the southern curve of the spit itself.
- *SW wind regimes:* Longshore currents during SW winds originate at the proximal end and then move towards the distal end. The scarp is located at the location where longshore currents start to accelerate. Spit growth during SW is supplied by material from the scarp and the western part of the spit itself.
- *W wind regimes:* longshore currents come from the Zuidstrand, accelerate at the distal end at the location of the scarp and then decelerate along the spit curve. Spit growth during W wind regimes is likely supplied by the material from the Zuidstrand and the scarp.

The scarp seems to be an important sediment supplier for many currents, especially because the significant erosion that occurs at that location, almost every period. This means a lot of sediment becomes available for transport towards the distal end. For SE and S wind regimes the spit curve itself is the most important sediment supplier, but the volumes available here are less abundant.

Before, it was already seen that currents approaching the spit from the offshore parts of the platform pass over the platform boundary relatively quickly but do not result in a lot of sedimentation. These currents likely do not pass the scarp and do not transport the abundance of available material over there. These currents are therefore only supplied by the Zuidstrand. With this reasoning it is likely that the supply of the Zuidstrand to the spit is limited. This is something van Santen (2016) also concluded. Therefore, it is likely that the Southern spit is mainly supplied by the scarp. The paths of transport of sediment are indicated in Figure 4.

Northern spit

For the northern spit it was concluded that the S, SW and W wind directions were the important wind directions for spit development. For each of these wind directions, the sediment supply for spit growth can be determined:

- *S wind regimes:* During S winds there is a single current originating from lake circulation to the south. This current moves along the south side of the spit and picks up sediment there. However, the sediment at that location is relatively limited and the volumes of erosion at that side are not high enough to explain the large amounts of sedimentation at the spit tip. It is more likely that most of the

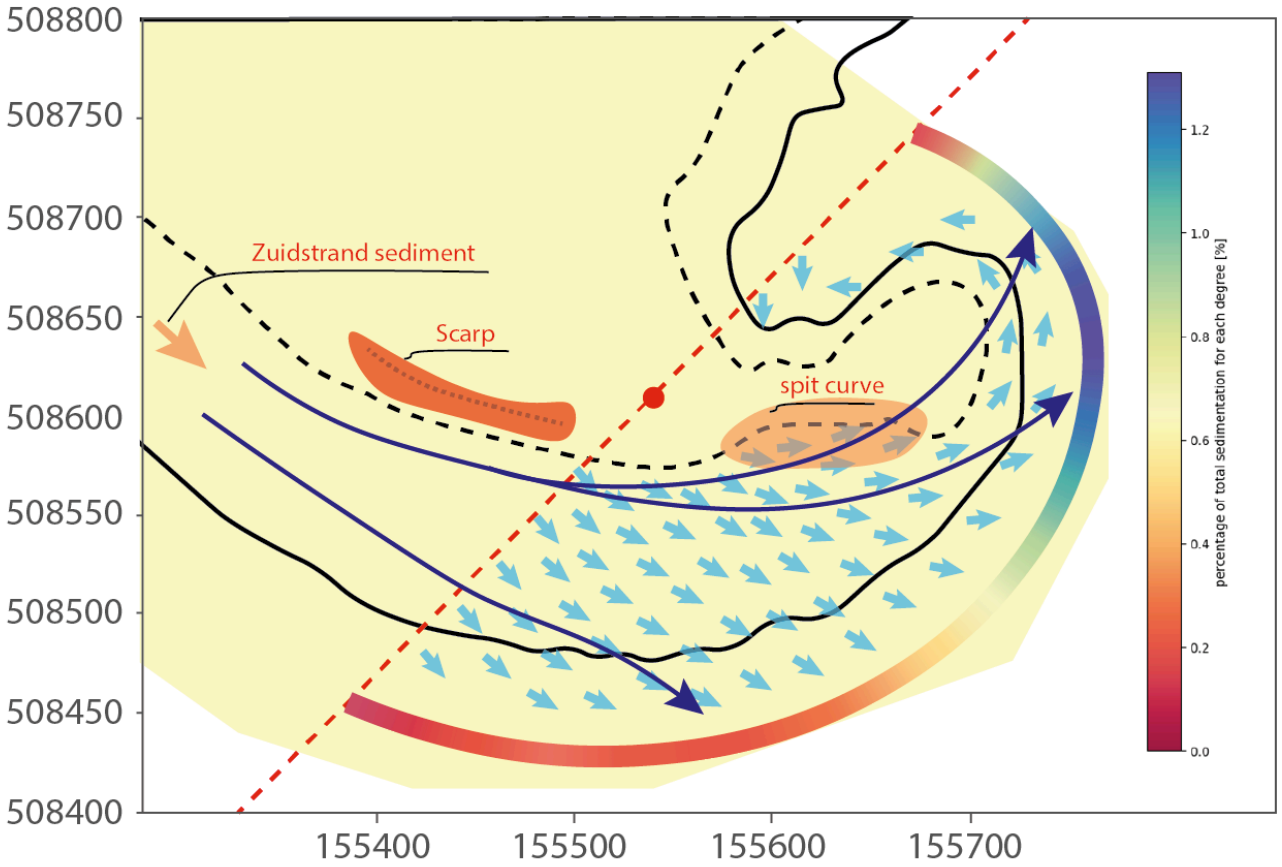

Figure 4. Sedimentation sources and paths of the southern spit. The sedimentation current pattern is indicated by the light blue arrows, the paths of the sediment are indicated by the darker blue arrows and the sediment sources are indicated in red, with denser fields indicating a higher sediment supply.

sedimentation by the currents from the S wind regime is the result of reorganization of the sediment that is deposited by SW and W winds. These currents at S winds transport the sediment from the south side of the spit tip to the north side of the spit where the currents slow down and sedimentation takes place. This in contrast to the fast currents from the SE wind regime that do not transport material around the spit tip but mostly move offshore in front of the spit tip. That is why the SE winds are not incorporated in the sedimentation current pattern.

- *W wind regimes:* A longshore current flows from the Noordstrand along the scarp to the spit tip and then moves away to the north. This current is a combination of the lake circulation current around the Noordstrand and high angle waves. In this case the Noordstrand and the scarp many supply the spit growth but erosion at the northern side of the spit can also supply the spit to some extent. An important remark for these currents is that especially during higher W winds (but also during SW winds) the flow is pushed onto the subaerial parts of the spit and flows over the land to eventually deposit material at the location where most sedimentation is observed (60° – 70° relative to the centre point).
- *SW wind regimes:* The currents during this wind regime are a combination of the currents during S and W winds. A current approaches the spit from the north because of lake circulation and waves and a lake circulation current approaches the spit from the south. All sediment sources contribute to the sediment supply but the scarp and Noordstrand likely supply the most as these sources have the most abundance in material.

Again, the scarp seems to be an important supplier of sediment, as much erosion is observed here, especially during high energy periods. But in contrast to the Zuidstrand, the Noordstrand also seems to be an important supplier of sediment, especially during periods with prevailing W and SW winds. This can be seen by the

large amount of sedimentation that often can be observed at the platform boundary at the northern side of the spit tip (0°-40° relative to the centre point). That is the location where flow paths originating from the Noordstrand that are flowing further from the coastline, move over the platform boundary. These flows are only supplied by the Noordstrand. Although another explanation may be that very fast currents during S winds transport material from the spit tip to these locations. As said before, the sources on the northern and southern side of the spit itself have less sediment and are therefore less important as a sediment source. That is why the S current is mainly important for the relocation of sediment deposited by the currents created by the SW and W winds (Figure 5).

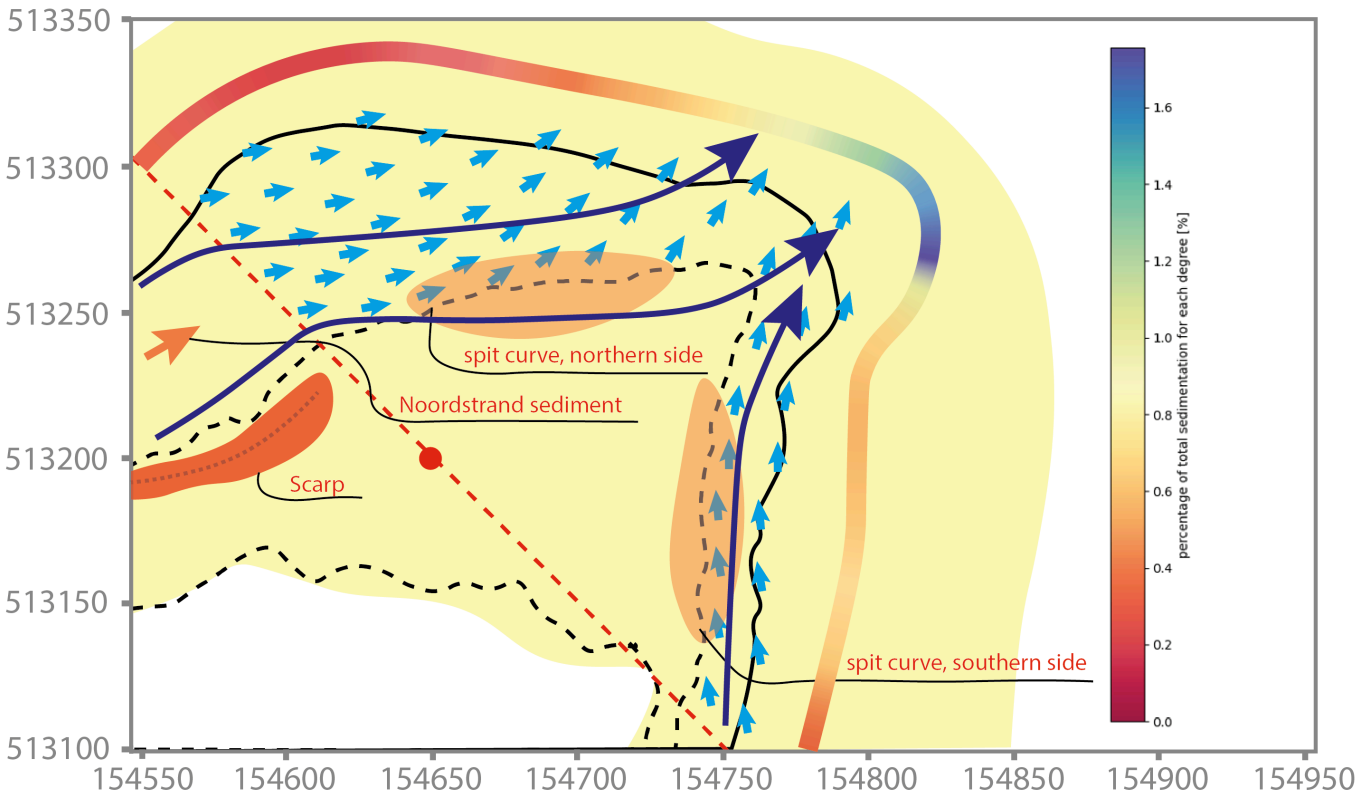

Figure 5. Sedimentation sources and paths of the northern spit. The sedimentation current pattern is indicated by the light blue arrows, the paths of the sediment are indicated by the darker blue arrows and the sediment sources are indicated in red, with denser fields indicating a higher sediment supply.

Bibliography

van Santen, R. (2016). *Marker Wadden - ontwerp en verificatie zachte randen*.

Appendix

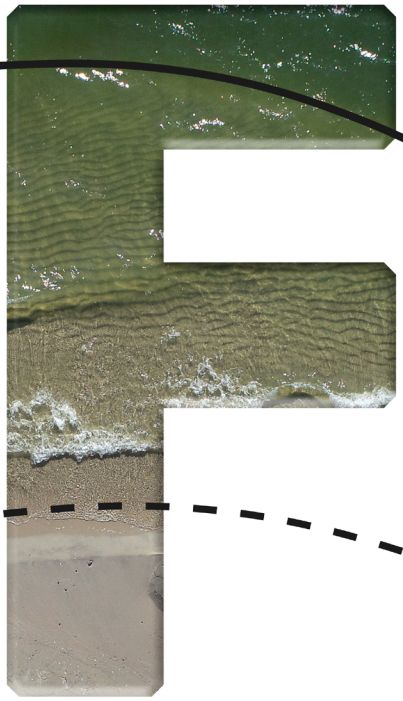

Results

Sedimentation on elevation levels

Table of contents appendix F

Transportation energy and flow dissipation

It is often assumed that the emerged part of a spit and the submerged part of the spit grow in the same amount (Kraus & Asce, 1999). However, in this research it was quickly seen that the growth of the submerged spit-platform not necessarily meant growth of the emerged spit. When sedimentation occurs on the platform level, the emerged spit eventually grows in length. When sedimentation occurs on the sub-platform level the submerged spit-platform eventually grows in length (Figure 1).

It has been observed during the morphology research that sedimentation occurs predominantly on the sub-platform level during high energy periods and significant sedimentation occurs on the platform level during lower energy periods. High winds during these high energy periods create fast flow velocities. When flow velocities are high, the transporting energy of the current is high. When these velocities are too high there is not enough dissipation on the platform level to decrease the transporting energy enough to accommodate sedimentation on top of the platform. Based on the results, the flow will then continue to transport the material until the material gets transported over the platform boundary. Here the space to dissipate is more often than not enough to accommodate sedimentation. Therefore, it seems logical that there is only sedimentation on the sub-platform level during high energy periods and only during the lower energy periods the incoming transporting energy is sufficiently low for the dissipation mechanisms on the platform level to accommodate sedimentation there. Flow velocity is a good parameter to represent the incoming transporting energy.

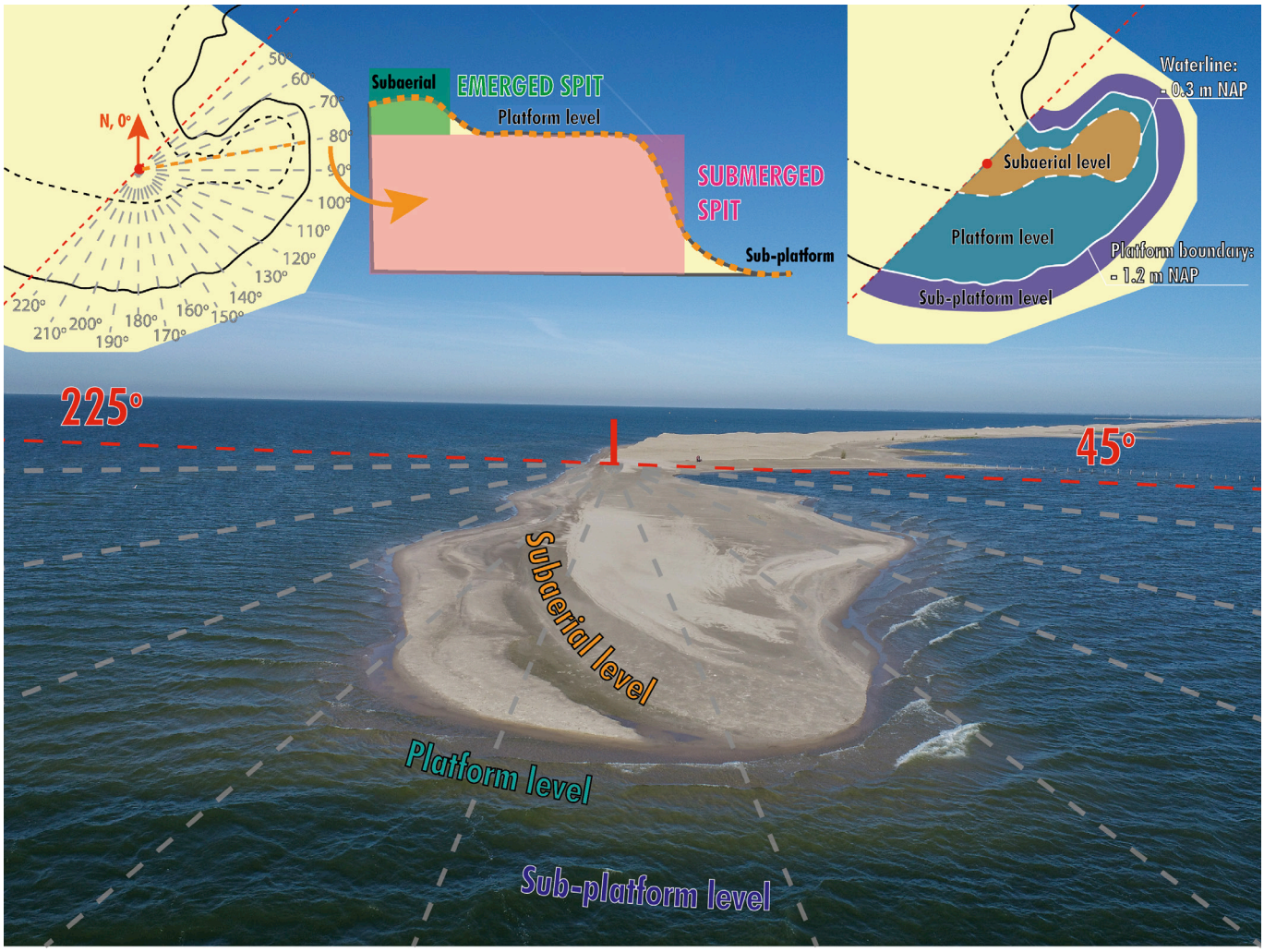

Figure 1. Example of the orientation method used for the data analysis with degrees relative to the north and levels based on bathymetry (Rijkswaterstaat, 2018; Ton et al., 2021).

Besides incoming transporting energy also flow dissipation is important for the ratio between sedimentation on the platform level and sedimentation on the sub-platform level. The most important flow dissipation mechanisms that influence flow dissipation around the spit is the mechanism of Uda (2018), and the mechanism of Ashton et al. (2016). The mechanism of Uda states that sedimentation occurs when flow velocities decrease because suddenly more room is available for the current. On the platform level more flow dissipation space becomes available when the coastline bends away because of the curvature of the spit or when the emerged spit becomes narrower. Then the width of the platform increases, and the current has more space to dissipate (Figure 2, I). Also, when the currents flow over the subaerial level during storm set-up there is a flow over the 'regular' coastline onto the platform. In this case the depth and therefore the flow dissipation space increases. Then also sedimentation on to platform level can occur (Figure 2, II). For the sub-platform level, it seems evident that when the currents flow over the platform boundary the depth increases dramatically resulting in significant flow dissipation of the transporting energy (Figure 2, III). It is often assumed that all material that enters the spit system at the proximal end accretes around the spit because of this large depth difference (Kraus & Asce, 1999).

The mechanism of Ashton states that the wave-driven longshore current decreases as the angle of incidence of the waves surpasses 45°. On top of this the refraction that occurs during this change in wave angle also causes flow dissipation of wave-driven energy (Figure 2, IV). This combined mechanism is most important on the platform level as this level is above the depth-of-closure (Ton et al., 2021). Also, this mechanism may result is extra flow dissipation on top of the platform that results in relatively more sedimentation on the platform level.

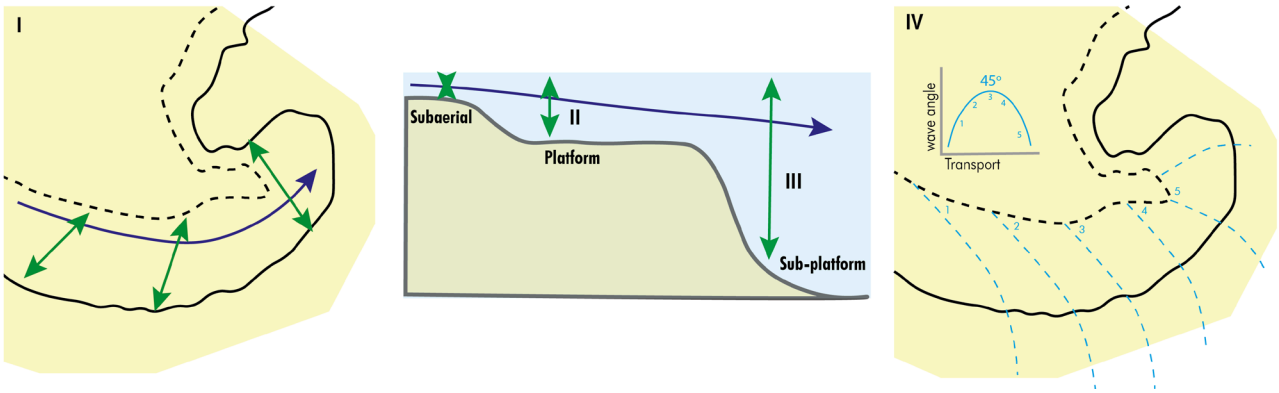

Figure 2. Dissipation mechanisms around the spit. With the flow path in dark blue, the space for the flow indicated in green and the wave crests indicated in lighter blue.

The parameter that is chosen to represent the loss of transportation energy, is the area of the platform (on the platform level) on which sedimentation takes place. A large area indicates that there is a lot of space for flow to dissipate. When the spit-platform is not large enough less energy will dissipate on the platform and most energy will dissipate below the spit-platform boundary. Also, when flow energy dissipates, particles do not drop down immediately but slowly descend while going with the flow, the platform must be large enough to 'catch' this particle. This parameter is sufficient to see if there is a relation between the dissipation of transporting energy and sedimentation on the platform energy. However, the best way to physically describe the dissipation of transporting energy is to calculate the different flow paths (current patterns) that occurred during a period with different wind conditions and then calculate the decrease in velocity along these paths. But, this is very time consuming and complex to calculate and even harder to represent in a figure. Therefore the surface area of the platform is taken instead.

To summarize, the ratio between sedimentation on the platform level, that accommodates emerged spit growth, and sedimentation on the sub-platform level, that accommodates submerged spit-platform growth, is dependent on the transporting energy that enters the area, represented by the incoming flow velocity, and the gradual loss of this energy, that is represented by the area of the spit-platform. When this ratio is high

there is a lot of sedimentation on the platform level and when this ratio is almost zero, almost all the material is deposited below the platform boundary on the sub-platform level.

The calculation of the flow velocity

As said before the flow velocity does not represent the decrease in transporting energy but the incoming transporting energy. Therefore, not an average is taken of the velocity around the spit but the velocity right before the location of the largest sedimentation. Which means this is the incoming energy at the moment that the most important significant dissipation mechanisms kick in. For the southern spit this is at 100 degrees relative to the centre point and for the northern spit this is at 60 degrees relative to the centre point (Figure 3). For the northern spit the location of 60 degrees is taken instead of 80 degrees (flow comes from both sides) because most sediment likely comes from the northern side of the spit (Appendix E).

For a period of which the sedimentation ratio is considered, the hourly wind conditions are divided into the 32 wind scenarios. For each of this hourly wind conditions the flow velocity at the desired location can be calculated using the fitted formulas derived for each scenario (Appendix D). In the paper and Appendix G it was shown there needs to be a certain amount of transporting energy before significant sedimentation takes place. Also, it has been shown that morphological developments in environments like the lake Markermeer are mainly dependent on high energy events (Ton et al., 2021; Vila-Concejo et al., 2020). Therefore, not the mean flow velocities during a measurement period were considered but the 97% quantile of the all the flow velocities that are computed for every hour during a period. This 97% quantile proved to be a threshold that still showed the ratio between low energy events and storm events but also showed flow velocities that where more representative regarding their morphological effect.

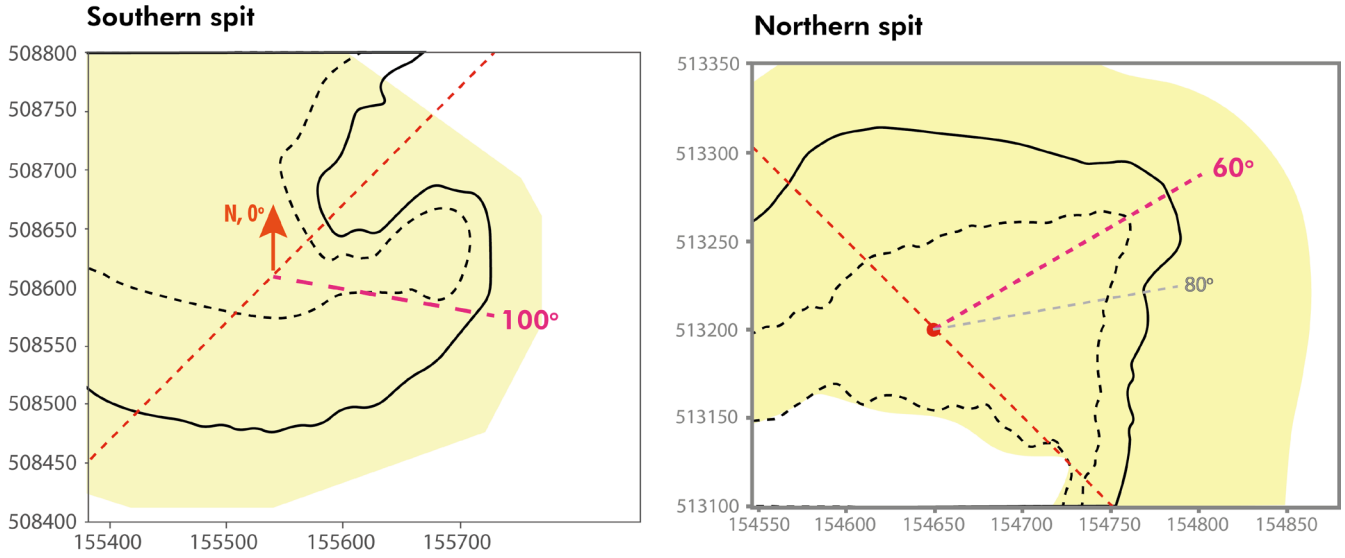

Figure 3. Location where the flow velocity is computed for each hourly wind measurement.

The calculation of the platform area

For the platform area firstly the pointcloud of the topography of the spit at the start of a period is linearly interpolated. This gives a mesh with grids with a size of 29 m^2 per square for the southern spit and 4 m^2 per square for the northern spit. For each square it can be determined if the average height of this square is

above the platform boundary (-1,2 m NAP) and below the waterline (-0,3 m NAP). In other words, it can be determined from the data in the pointcloud if the concerned square is on the platform level. If that is the case than the area of this square can be added to the other squares that are on the platform level to eventually get the size of the entire platform area.

For the northern spit the whole spit-platform is considered as currents can come from multiple directions, and sedimentation can occur everywhere on the spit-platform. Also, the northern spit has a smaller platform area so changes in the spit-platform can still be observed when the whole spit-platform is considered. For the southern spit only, a square is considered if the x-coordinate is larger than 155525 m. This is because almost all sedimentation on the platform level occurs after this boundary and because the spit-platform of the southern spit is so large that changes in the spit-platform would be harder to see if the whole platform was considered (Figure 4).

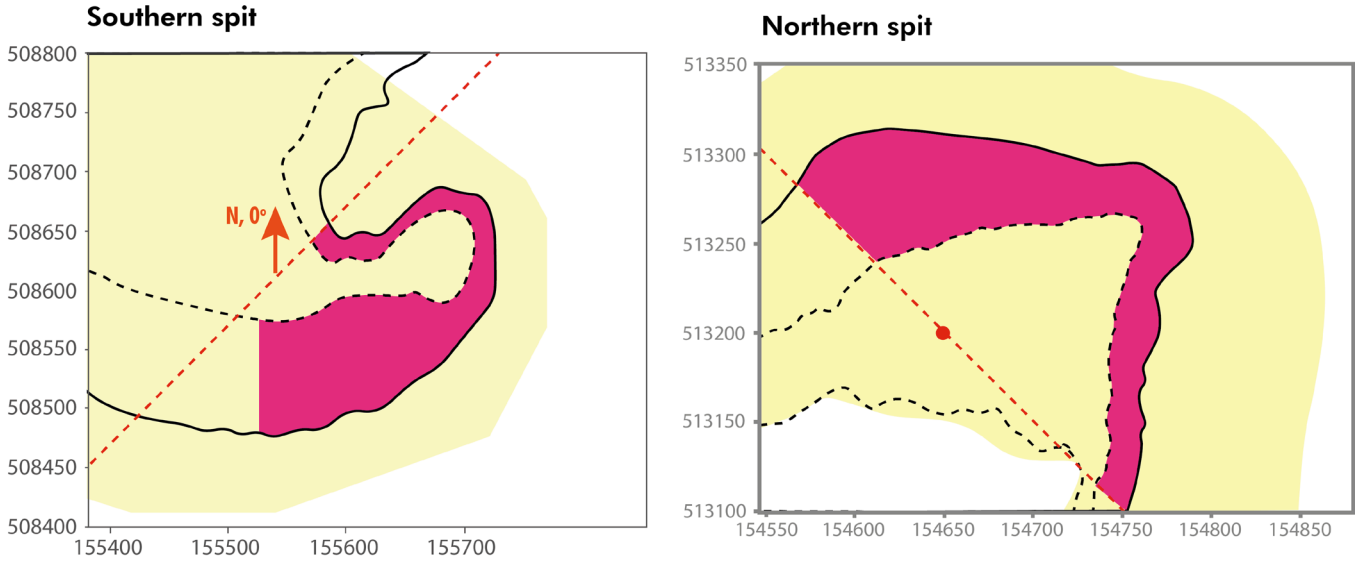

Figure 4. Schematisation of the spit-platform area that is used for each spit

Platform area and flow velocity versus sedimentation ratio

For every measured period the platform area at the start of the period can be computed. It is on this surface that sedimentation will take place if sedimentation would take place on the platform level. Also, for every measured period the 97% quantile of the incoming flow velocity can be computed, and the sedimentation ratio can be computed by dividing the sedimented volume on the platform level by the sedimented volume on the sub-platform level. These values for every period are presented in Figure 5 on the end date of each period.

Indeed, when the sedimentation ratio is low, the flow velocities are high or the platform area is small, or a combination of both. When the ratio is high often the platform area is large, but flow velocities must not be too high, otherwise the ratio becomes very low again. This happens in April 2020 for example.

Figure 5 shows that there is a relation between the spit-platform size and the flow velocity vs. the sedimentation ratio. These two parameters both have a strong influence on the division of sediment between the platform level and the sub-platform level and therefore influence on the growth of the emerged spit relative to the growth of the submerged spit-platform.

Southern spit

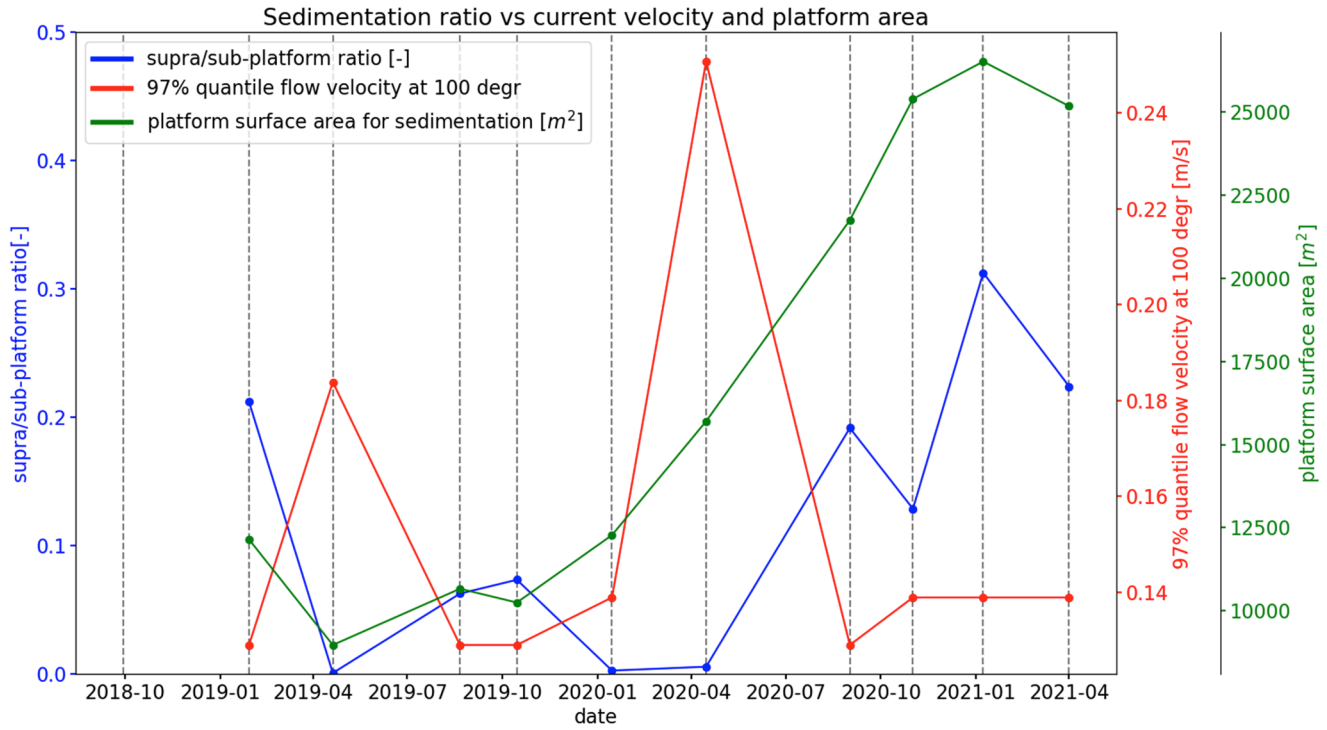

Northern spit

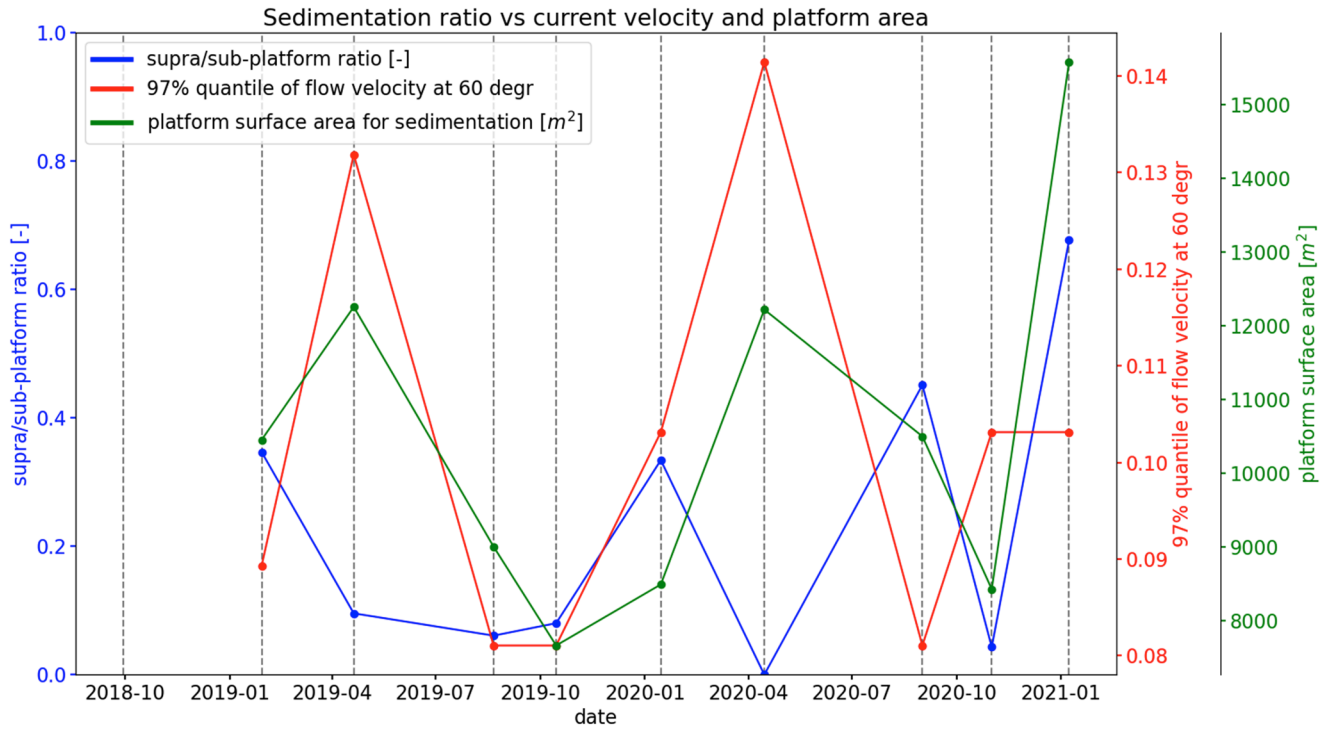

Figure 5. The sedimentation ratio (blue), platform surface area (green) and incoming flow velocity (red) over time. With the measurement moments indicated by the grey lines.

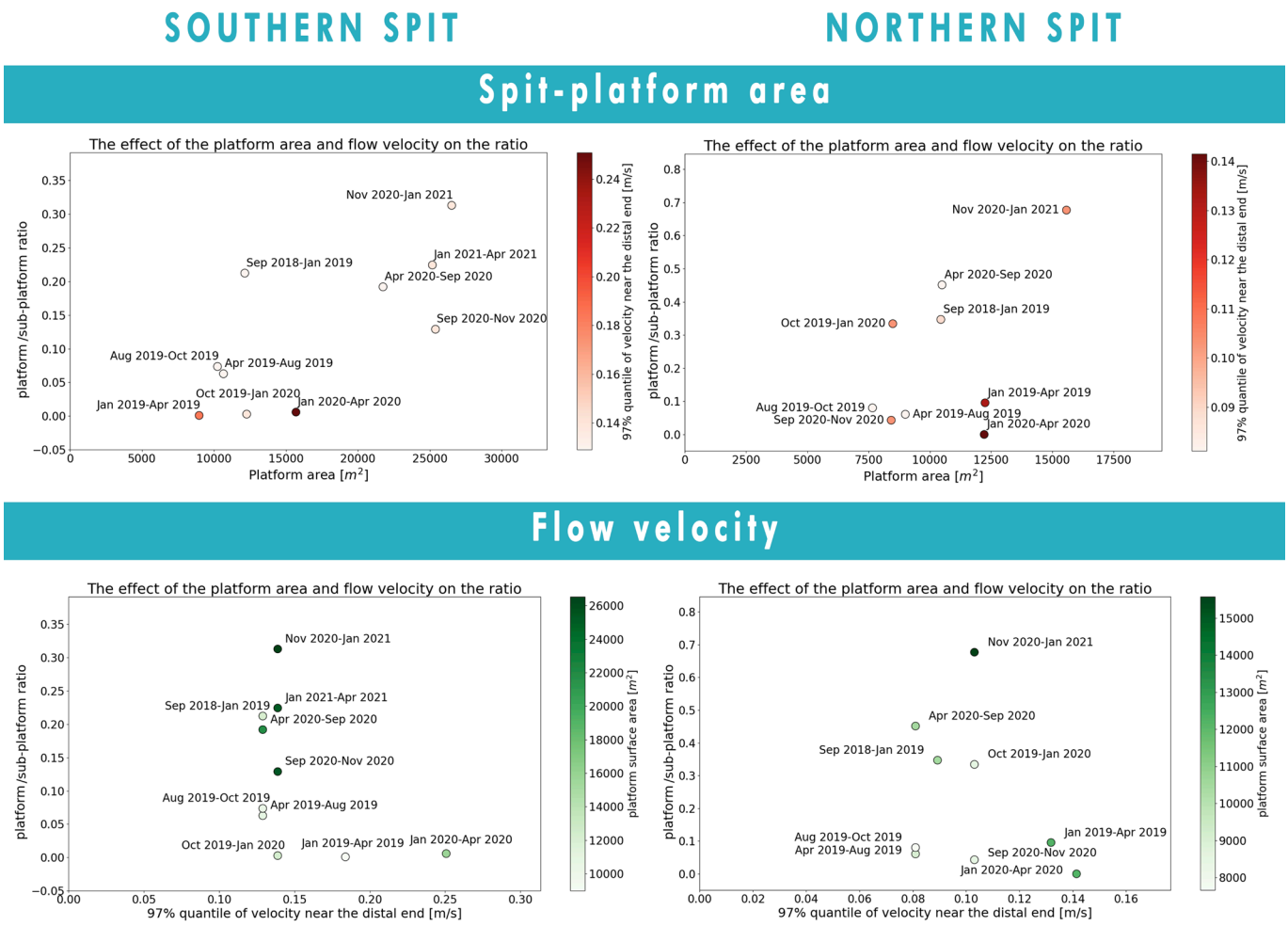

Figure 6. Individual relations of the spit-platform area and the flow velocity with the sedimentation ratio.

The relations with the spit-platform surface area show that when the surface area increases the sedimentation ratios also increase. But this increase can be hampered by large flow velocities as can be seen for the northern spit. For the flow velocities it can be seen that slightly smaller flow velocities also result in larger sedimentation ratios. But in both graphs it seems that for most cases the platform area is of the largest influence on the ratio. The highest ratios are around the largest platform areas. However, during high energy periods, when incoming flow velocities are high, the sedimentation ratio decreases dramatically. It seems that during low energy periods the sedimentation ratio is mostly dependent on the platform size and during high energy periods the sedimentation ratio is mostly dependent on the incoming flow velocity (Figure 6).

So again it is found that the spit-platform surface area and the incoming flow velocity are of importance for the sedimentation ratio. But because these two parameters are so intertwined with the sedimentation ratio it is difficult to show a mathematical relation for each individual parameter and the sedimentation ratio.

Outliers (because of erosion)

The platform area and the flow velocity are not the only parameters that influence the sedimentation on the platform level. For example, an overabundance of sediment due to scarp collapse on the proximal end may be of influence. However, one of the most important factors that is not considered is erosion on the platform

level. The depth-of-closure is around the spit-platform boundary and therefore waves can stir-up accreted sediment on top of the spit-platform and transport it again to the sub-platform level (Ton et al., 2021).

It can be the case that large amounts of sediment have accreted on the platform level during a calm period, but that one short high energy event had stirred-up a lot of material on the platform again so that currents could have transported it elsewhere. In those cases, the sedimentation ratio is much smaller than expected.

This is most likely what happened during the period of September 2020 – November 2020 at the southern spit. Here the ratio is lower than expected and it was found that there was one very high peak in flow velocities after a low energy period that may have eroded away the material on top of the platform (Figure 7). The same is likely to have happened for the period of April 2019 – August 2019 at the northern spit (Figure 8).

Also there seems to be a threshold before large scale sedimentation takes place (paper and Appendix G). Therefore, it may also be possible that during a period there are only very small velocities that do not transport sediment and very large velocities that only transport sediment to the sub-platform level. It is possible that flow velocities with just the right magnitude for platform sedimentation do not occur during a period. In that case the ratio may also be very low in a period with mostly very low energy hydrodynamics.

From now on the period between September 2020 and November 2020 for the southern spit and the period between April 2019 and August 2019 for the northern spit will be considered as outliers. Because of the influence of erosion, but also because of other parameters, it is impossible to find a clean relation between a combination of the platform area and flow velocity and the sedimentation ratio. However, using only these parameters it still is possible to approach reality.

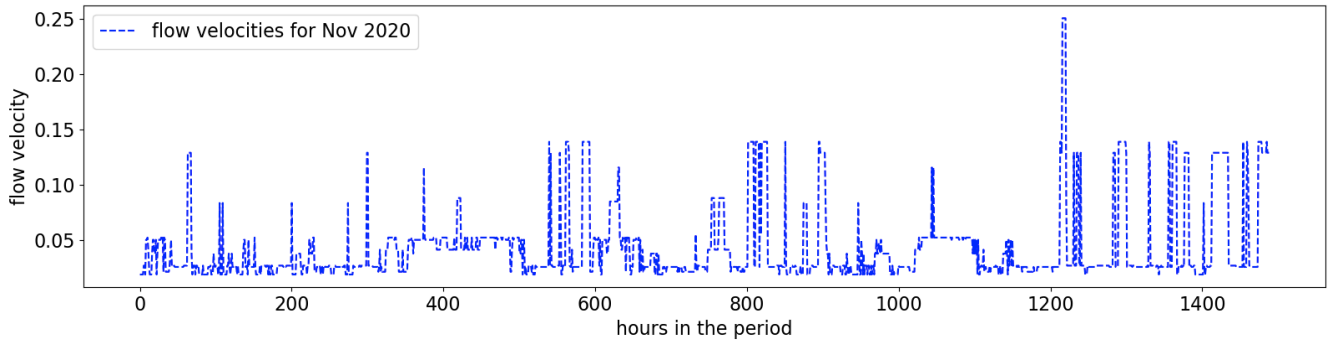

Figure 7. Flow velocities on the distal end of the southern spit between September 2020 and November 2020 in m/s.

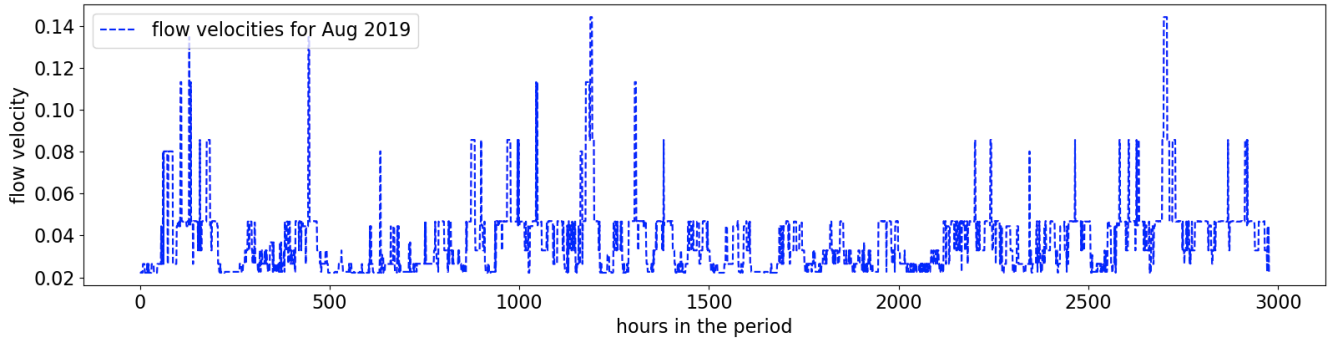

Figure 8. Flow velocities on the distal end of the northern spit between April 2019 and August 2019 in m/s.

Platform surface area and flow velocity combined

Thus, a combination of the platform surface area and the incoming flow velocity should be positively correlated with the sedimentation ratio. However, the contribution of the platform area and flow velocity is not exactly equal. To determine the best combination of both parameters the following has been done. The platform area is multiplied with the flow velocity for each period and is put on the x-axis. Then this flow velocity is given a negative exponent. This exponent is negative because small platform areas and large flow velocities have the same effect on the sedimentation ratio. This exponent can give the flow velocity more weight in the combination or can make the platform area more dominant depending on the size of the exponent. Then a large array of exponents, some high and some low, are tried to find the best combination of platform area and flow velocity. The combination that results in a linear fit on the sedimentation ratio with the highest R^2 value is the most accurate combination (Figure 9).

The platform area and flow velocity have roughly the same order of magnitude contribution when it comes to their effect on the sedimentation ratios. Also, although the flow velocities and platform areas differ between the two spits, their relation relative to the sedimentation ratio is comparable. The exponent on the flow velocity is the exponent for which the accuracy of the fit is highest and is purely a representation for the importance of the flow velocity relative to the platform area for the sedimentation ratio. For both spits this exponent shows that the higher the incoming flow velocities are, the more important this parameter becomes for the sedimentation ratio, as was also observed in Figure 6. This effect is more severe for the southern spit than for the northern spit. The first number of the best fit represents the slope of the fit which is not the same for the southern and northern spit as the parameters that are computed for both spits are case specific.

Thus, when there is a high energy period, most of the sedimentation occurs on the sub-platform level. This means that the submerged spit-platform grows in length. This has as a consequence that platform area increases which promotes sedimentation on the platform level. This results in growth of the emerged spit part, which decreases the platform area and makes it more likely for sedimentation to occur on the sub-platform level. Therefore, the growth of the emerged spit relative to the submerged spit-platform is in a negative feedback loop. Growth of one promotes the growth of the other.

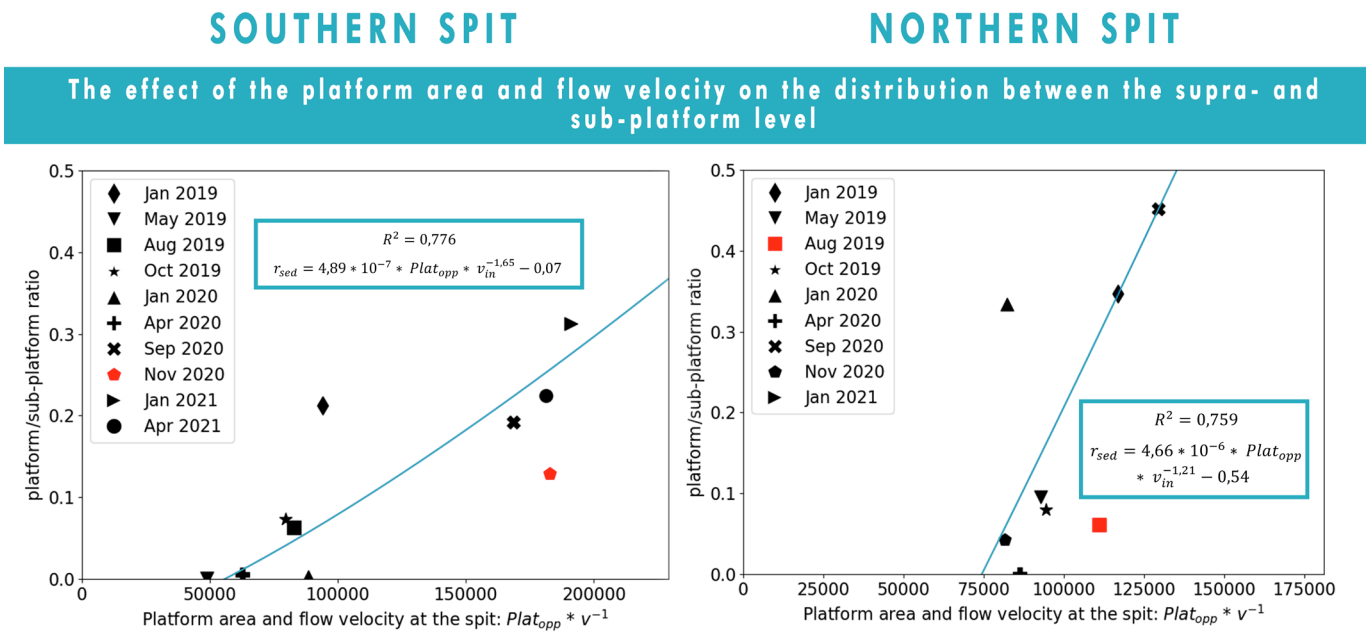

Figure 9. The relation between the sedimentation ratio and platform area and flow velocity. In red the outliers are indicated. These points where likely affected by an erosion event that eroded the sedimentation on the platform away, resulting in a relative low ratio. The height of R^2 indicates the quality of the approximation.

Bibliography

Ashton, A. D., & Murray, A. B. (2006). High-angle wave instability and emergent shoreline shapes: 2. Wave climate analysis and comparisons to nature. *Journal of Geophysical Research: Earth Surface*, *111*(4). https://doi.org/10.1029/2005JF000423

Ashton, A. D., Nienhuis, J., & Ells, K. (2016). On a neck, on a spit: Controls on the shape of free spits. *Earth Surface Dynamics*, *4*(1), 193–210. https://doi.org/10.5194/esurf-4-193-2016

Kraus, N. C., & Asce, M. (1999). *ANALYTICAL MODEL OF SPIT EVOLUTION AT INLETS*. ASCE.

Ton, A. M., Vuik, V., & Aarninkhof, S. G. J. (2021). Sandy beaches in low-energy, non-tidal environments: Linking morphological development to hydrodynamic forcing. *Geomorphology*, *374*. https://doi.org/10.1016/j.geomorph.2020.107522

Uda, T. (2018). *Spits* (pp. 1–5). https://doi.org/10.1007/978-3-319-48657-4_297-2

Vila-Concejo, A., Gallop, S. L., & Largier, J. L. (2020). Sandy beaches in estuaries and bays. In *Sandy Beach Morphodynamics* (pp. 343–362). Elsevier. https://doi.org/10.1016/b978-0-08-102927-5.00015-1

Appendix

Results

Total sedimentation & the predictive model

Table of contents appendix G

The relations found in Appendix E and F provides an approximation of the three-dimensional distribution of the sediment around the spit. This distribution can be calculated with parameters that can be derived by either using the topography at the start of a period (this can be used to calculate the platform surface area for example) or by using the wind conditions that result in hydrodynamic parameters like current directions and flow velocities.

If the total amount of sedimentation also can be calculated by using the wind conditions in a period, it can be approximated where volumes of material accrete around the spit and how large these volumes are. This would result in a new predicted topography. So, by knowing the topography of the spit at the start of the period, and the (most likely) wind conditions during a period, a new topography of the spit at the end of this period can be predicted.

To investigate the practicability and effectivity of such a predictive model, a one-year long period for the southern spit is modelled. The year of April 2021 – March 2022 is a well-balanced representation of the diversity of conditions that can occur at the Marker Wadden islands, with large storms like Eunice and Franklin but also calm summer conditions. There is also enough data of the southern spit to verify the eventual prediction.

Total sedimentation

As said before, the total amount of sedimentation is needed to do predictions. An empirical linear relation helps to estimate the total volume of sediment that will be deposited around the spit, because of certain wind conditions. This relation can be found in the same manner as has been done for the sedimentation ratio of Appendix F.

From the morphology research (paper and Appendix C) it quickly turned out that faster winds, and therefore faster flow velocities, resulted in higher volumes of sedimentation around the spit. Therefore, it is likely that the flow velocities that occur around the spit are positively correlated with the total amount of sedimentation. To bolster this find, it also turned out that faster flow velocities are strongly correlated with erosion of the scarp (Appendix C). And material from the scarp is one of the most important sources of sediment for the spits (Appendix E).

Also, in the paper and Appendix E it was deducted that only currents resulting from winds from the SE, S, SW and W transport sediment to the distal end of the spit where it is deposited. So, the more these currents occur during a period, the more material should be transported to the spit and the more sedimentation should take place. It is therefore logical to state that the percentage of occurrence of these (SE, S, SW and W) winds is positively correlated with the total volume of sedimentation around the distal end.

In the same fashion as has been done for the sedimentation ratio (Appendix F) the 97% quantile of the flow velocity at 100° relative to the centre point and the percentage of occurrence of SE, S, SW and W winds are multiplied on the x-axis. Again, these two parameters are not equal and therefore the flow velocity has a positive exponent. This results in a linear relation between the two parameters and the total volume of sedimentation. The volumes of sedimentation are calculated per day as not all periods have the same length. It is evident that more sedimentation can occur during a longer period (Figure 1). With this relation the predictive model for the southern spit can be constructed.

Clearly this relation does not pass through zero (Figure 1). This means that for very low flow velocities during a period no large-scale sedimentation will occur on the spit. Therefore, there should be a certain threshold of transporting energy for morphodynamics to take effect. This fits in well with the concept of low energy or storm-dominated environments like lake Markermeer that are dependent on high energy events for its morphodynamics (Vila-Concejo et al., 2020).

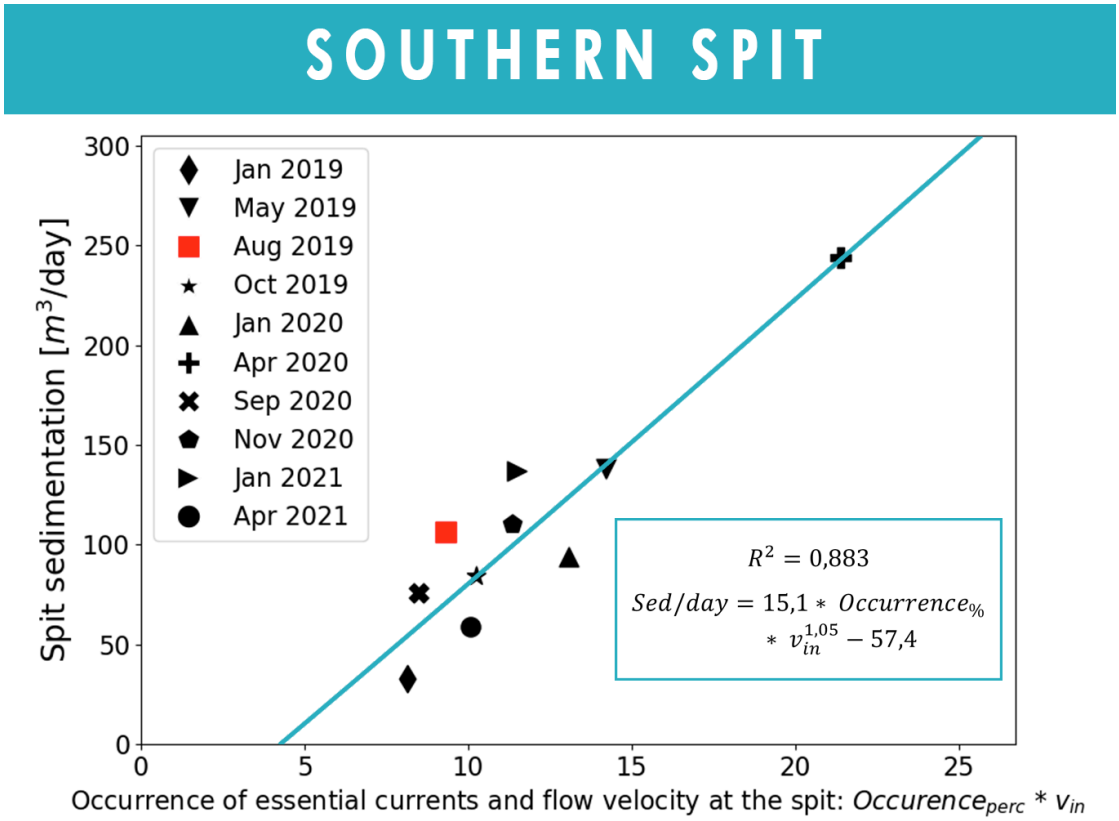

Figure 1. Expected sedimentation per day, dependent on the occurrence of wind regimes that drive sediment supplying currents, and the flow velocity. The height of R^2 indicates the quality of the approximation. The red outlier is not considered as a nourishment took place during that period.

Predictive model: using empirical parameters

With the topography at the start of the period and the wind conditions during the period as input, all empirical relations can be calculated for the predicted period.

First all desired parameters need to be computed from the topography and wind conditions to fill in the empirical relations. The platform surface area is computed with the pointcloud from the start of the period with the same method as described in Appendix F. As is the case for the 97% quantile of the flow velocity at 100° relative to the centre point (Appendix F). Lastly, the percentile of occurrence of the SE, S, SW and W winds during the period is calculated.

With these parameters the empirical relations found before can be used. First the total volume of sedimentation, cumulative around the entire spit, is calculated. This is a linear relation in the form of ax+b. With x as a combination of the percentage of occurrence of the sedimentation current pattern ($Occurence_{\%}$) and the 97% quantile of the flow velocity during the period. The fit from Figure 1 can be filled in with these parameters to extrapolate the new total sedimentation. The fit, which is based on cumulative sedimentation of previous periods, helps predicting the future total sedimentation volume. By multiplying the resulting volume/day with the number of days in the period this eventually results in equation 1 for the southern spit.

$$1) \quad Sed_{tot} = \left(15{,}1 * Occurrence_{\%} * v_{97\%,\ 100^o}^{1{,}05} - 57{,}4\right) * days$$

With equation 1 the total cumulative volume of deposited material during the period is computed. How this volume is distributed around the spit relative to the centre point. This can be determined by the general distribution of material that was fitted before (paper Figure 12 and repeated in Figure 2).

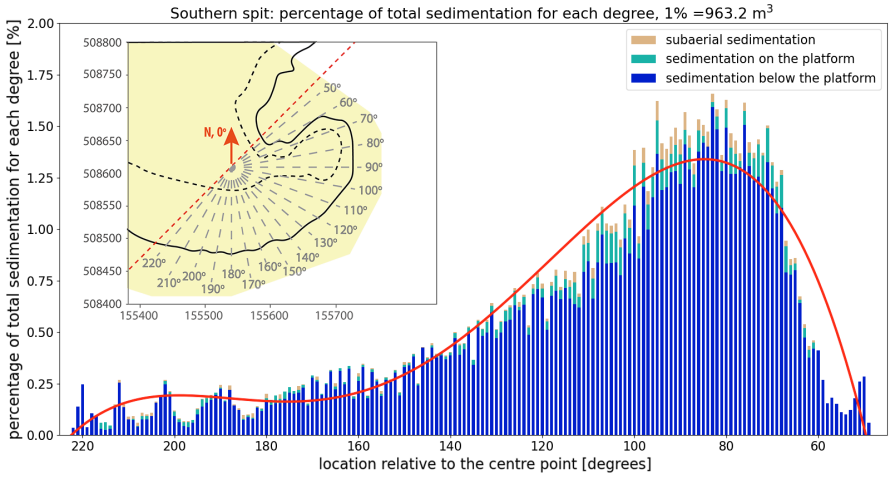

Figure 2. Distribution of sediment around the southern spit for the entire dataset. Each bar gives the percentage of the total sedimentation that occurred on that particular degree. With a fitted relation for the distribution of total sediment in red. The distribution in the elevation of sedimentation locations can be seen by the size difference between the sub-platform level (blue) and the platform level (turquoise). The red line gives a fitted distribution of sediment around the spit that will be used later to link sedimentation to hydrodynamic drivers.

The fit (red line Figure 2) that has been made from this distribution gives the expected percentage, of the total amount of sediment in that period, that has and will accrete for each degree. This fit is a function to the fourth order with as x values the 180 degrees around the spit. By multiplying this fourth order function at a certain x (degree) with the total amount of sedimentation for that period, the projected accreted for that single degree will be calculated. Thus the only input conditions for this function are therefore the degree relative to the centre point (x) and the total amount of sedimentation (equation 1) which gives equation 2. In this equation every exponent and other value than the variables, come from the fact that this is a to the fourth order, fitted function.

2) $$Sed_{at\ degree\ x} = (-3{,}43 * 10^{-8} * x^4 + 2{,}10 * 10^{-5} * x^3 - 4{,}58 * 10^{-3} * x^2 + 0{,}41 * x - 11{,}26) * \frac{1}{100} * Sed_{tot}$$

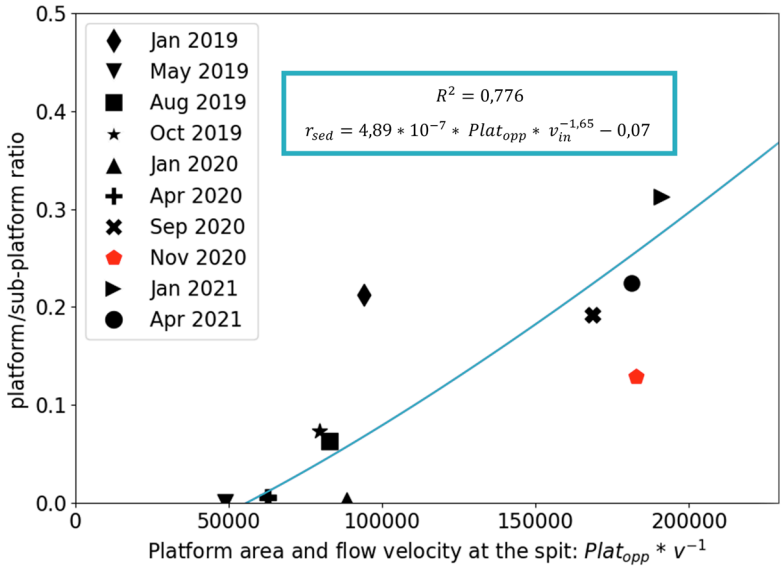

Figure 3. The relation (best fit) between the sedimentation ratio and platform area and flow velocity. The markers give the size of the platform at the start of a period divided by the flow velocity during this period. The indicated date is the date on which the measurement is taken, thus the date at the end of the considered period. In red the outlier periods are indicated. These points where likely affected by an erosion event that eroded the sedimentation on the platform, resulting in a relative low ratio. The height of R^2 indicates the quality of the approximation.

With equation 2 it is known what the volume of sedimentation has been over the period for each degree relative to the centre point. Which part of this volume has been accreted on the platform level, and therefore causes lengthwise growth of the emerged spit, and which part has accreted on the sub-platform level, and therefore cause lengthwise growth of the submerged spit-platform, can be calculated with the sedimentation ratio from Appendix F (also Figure 3). The resulting fitted ratio has been based on the correlation between the size of the spit-platform and the incoming flow velocity, and the sedimentation ratio. This fitted ratio is again in the form of ax + b with x a combination of the platform area and flow velocity. The flow velocity has a negative exponent corresponding with the best fit possible. This fitted ratio is than again used to estimate the sedimentation ratio for the values that where present in the case that we want to predict (equation 3).

$$3) \quad ratio = 4{,}89 * 10^{-7} * plat_{area} * v_{97\%,\ 100^o}^{-1{,}65} - 0{,}07$$

By multiplying this ratio with the sedimentation volumes for each degree, the volume for the growth of the emerged spit is known ($vol_{deg,\ em}$) for that degree and the volume for the lengthwise growth of the submerged spit-platform is known ($vol_{deg,\ sub}$) for that degree. The ratio is only considered for the degrees that are around the distal end and degrees on the northern side of the spit as there is generally no sedimentation at the waterline on the southern side of the spit. On the southern side mostly erosion occurs. Therefore, for the degrees lower than 100°, the sedimentation at that degree is divided over the emerged spit and submerged spit-platform. And for degrees higher than 100° all the sediment goes to the submerged spit-platform. By using the ratio on the sedimentation at every degree the shift of the waterline and the platform boundary in the offshore direction can be calculated.

Predictive model: Structure and prediction of contours

For each degree the profile can be simplified in the same manner as has been done for the whole analysis. The profile is reduced to a ''stair''-like structure with three levels and two boundaries. This can also be seen as two blocks. One block with the subaerial level on top, the platform level at the bottom and the waterline as the face, this is the emerged spit. And one block with the platform level on top, the sub-platform level on the bottom and the platform boundary as face, this is the submerged spit-platform (Figure 4).

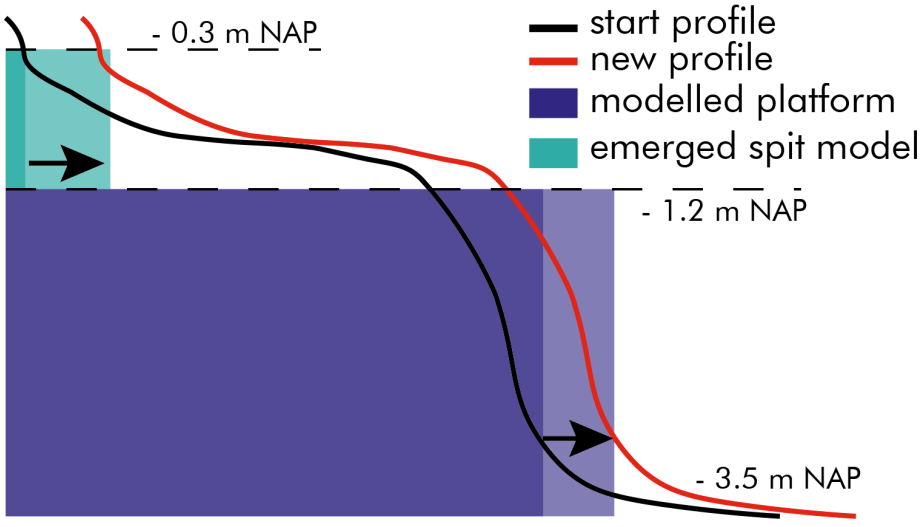

Figure 4. Schematic representation of the model. If the emerged part of the spit should grow in reality (start profile to new profile) at a certain degree relative to the centre point, the seagreen bar at that degree increases. The same holds for the submerged platform and the blue bar.

The elevation boundaries are determined by observing various locations around the spit for different pointclouds and by verifying it with profiles found by Ton et al. (2021) on the Zuidstrand. For each degree this emerged block and submerged block can be made. Also, for each degree the volumes are known that need to be added to each block to obtain the new locations of the waterline and the platform boundary at these degrees.

First the locations of the waterline and the platform boundary at the start of the period needs to be calculated by using the pointcloud of the topography at the start of the period. Then these locations need to be converted to polar coordinates. For each degree the distance of the waterline to the centre point needs to be computed. The same holds for the platform boundary. Once this is done the starting point of the face of each block is known.

The offshore shift of the block can be calculated by dividing the volume that needs to fill each block by the width and the height of the block. The width is calculated by multiplying the distance of the original waterline and platform boundary to the centre point, by the tangents of one degree. The height of each block is known because of the schematisation that is used (Figure 4). Then the shift of the waterline and platform boundary can be calculated with equations 4 and 5.

$$4)\quad \Delta dist_{waterline} = \frac{vol_{deg,\ em}}{0{,}9 * \tan(1^o) * dist_{old,\ waterline}}$$

$$5)\quad \Delta dist_{plat.boundary} = \frac{vol_{deg,\ sub}}{2{,}3 * \tan(1^o) * dist_{old,\ plat.boundary}}$$

Once these shifts in distances are added to the old distances of the waterline to the centre point and the platform boundary to the centre point, the new distances are known. These distances at each degree can then again be converted back to the Cartesian coordinate system in order to plot the predicted waterline location and predicted platform boundary location for each degree (Figure 5).

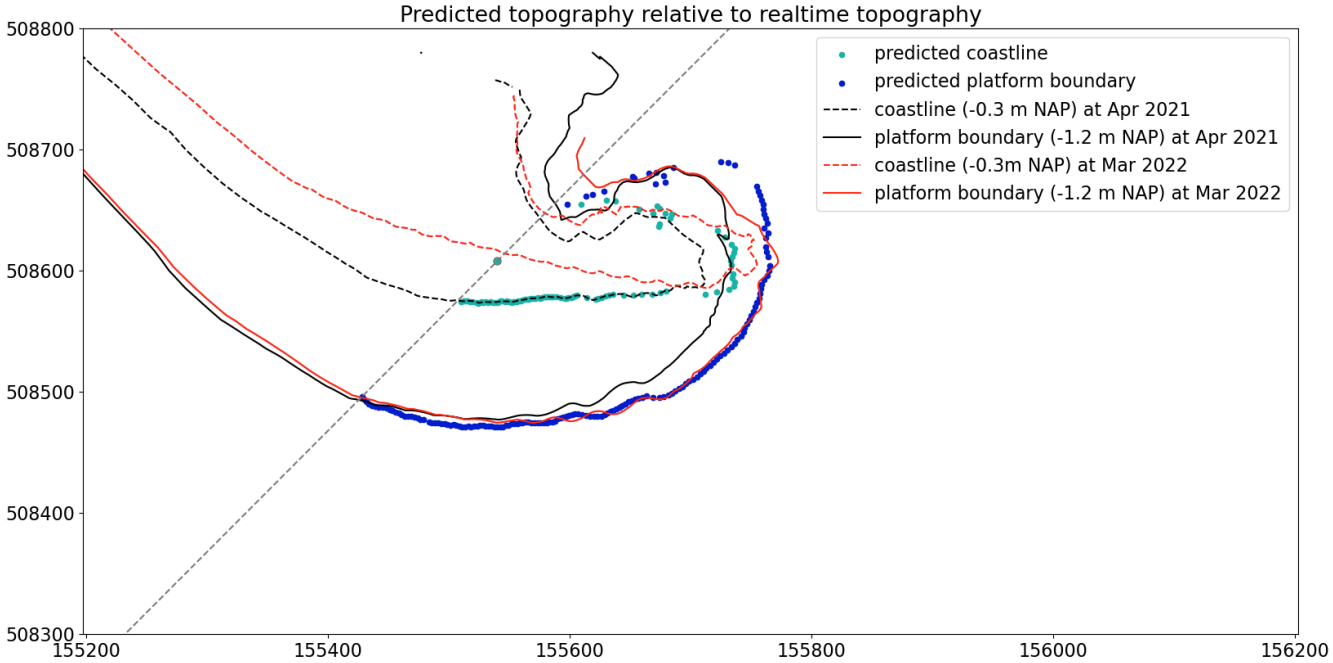

Figure 5. Predicted coastline- and spit-platform boundaries for the year Apr 2021-Mar 2022, compared to the real spit growths in that year.

Although this model is simplified and only used to illustrate the potential of the found empirical relations, the predictions are close to the reality. Especially considering the predictions for the submerged spit-platform. The predictions for the emerged part are less accurate. Mostly because of erosion which is not considered in this model. Erosion is much more of relevance for the emerged spit than for the submerged spit-platform because the emerged spit is above the depth-of-closure (Ton et al., 2021). This effect can clearly be seen on the southern side of the spit where erosion is abundant and the waterline retreats, instead of progresses. Another improvement for the prediction of the emerged spit is to not use an average sedimentation ratio as is used here, but a distribution of sedimentation ratios, for each degree around the spit. Because in this prediction the growth of the emerged spit is underestimated at the tip, where the emerged spit grows the most. And overestimated at the very northern side of the spit (around 50° relative to the centre point) because at that location there is often very little sedimentation on the platform level.

In general, this method is computationally very inexpensive but can still give satisfying predictions for the three-dimensional spit bathymetry. However, as said before this prediction is used as an experiment to see the practicability of the used method for spit analysis and the resulting empirical relations. The model is built with a lot of knowledge about the spit and its behaviour beforehand. Therefore, one should be wary to implement the same method to do predictions for another spit without carefully considering if the predictions are logical and in agreement with the trends in reality.

Bibliography

Ton, A. M., Vuik, V., & Aarninkhof, S. G. J. (2021). Sandy beaches in low-energy, non-tidal environments: Linking morphological development to hydrodynamic forcing. *Geomorphology*, *374*. https://doi.org/10.1016/j.geomorph.2020.107522

Vila-Concejo, A., Gallop, S. L., & Largier, J. L. (2020). Sandy beaches in estuaries and bays. In *Sandy Beach Morphodynamics* (pp. 343–362). Elsevier. https://doi.org/10.1016/b978-0-08-102927-5.00015-1

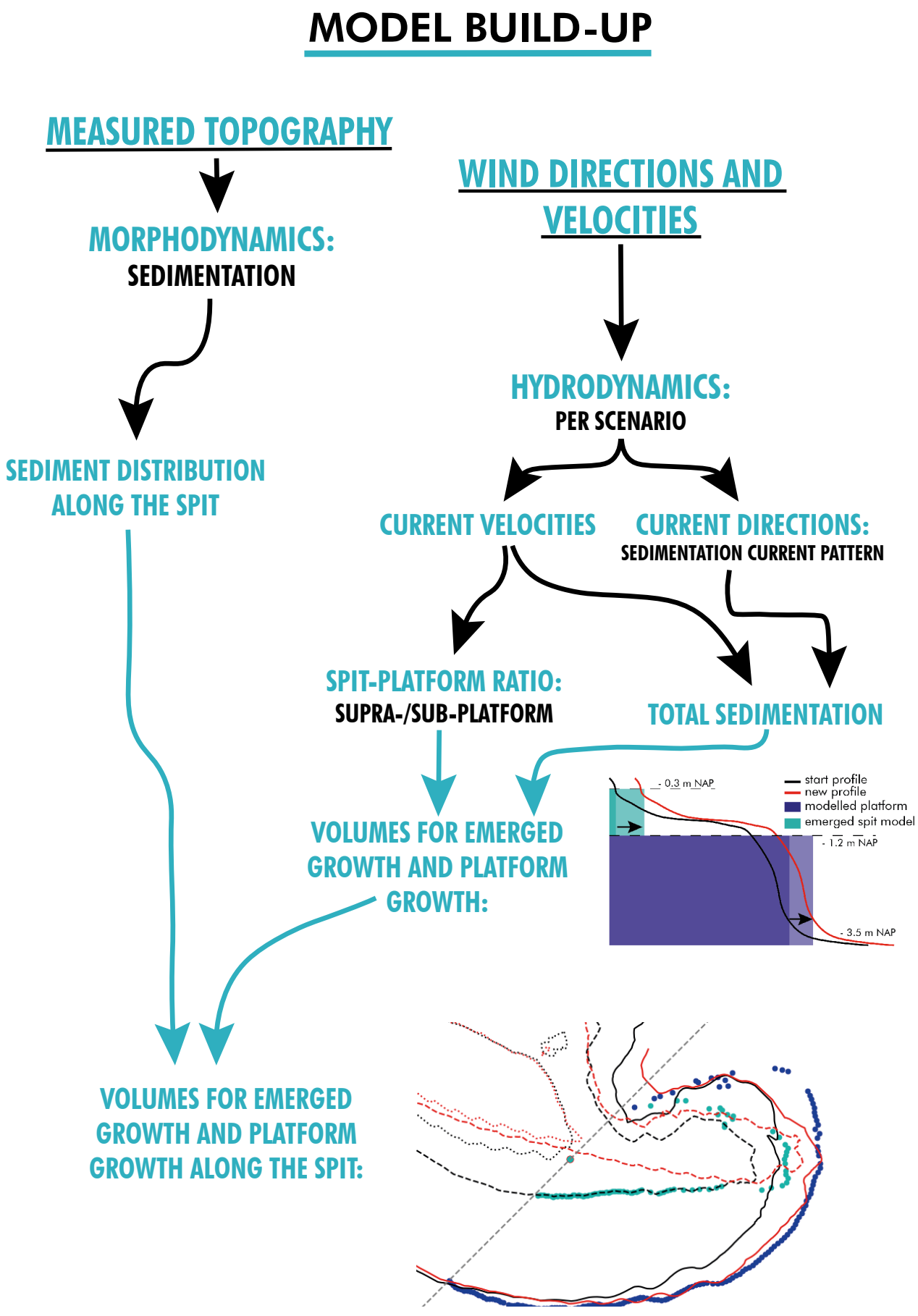

Figure 6. Flow chart of the used data and relations for the predictive model

Appendix

H

Extra Results

Sediment balance southern beach & spit

Table of contents appendix H

In the Appendices before, it was constantly assumed that practically no material got lost offshore based on the assumptions of Kraus & Asce (1999). All material that enters the spit area should accrete around the spit. Also, it was stated in Appendix E that a significant portion or even most of the material that accreted around the spit and provided the spit growth, originated from the proximal end of the spit with its large scarp. To further investigate these findings a sediment balance of the entire Zuidstrand is made to identify the most important sediment sources and sinks.

Volume maps of the Zuidstrand

The same pointcloud post-processing is done for the entire Zuidstrand system, as has been described for the spit in Appendix B. This results in a mesh that indicates the erosion or sedimentation in volumes at a square (of 29 m^2) during a period (Figure 1). In this volume map only the squares with an elevation difference of more than 10 cm are considered. This has been done because of the following reason. The area of the Zuidstrand (around 75 ha) is significantly larger than the considered area of the southern spit. The measurement error of the entire pointcloud in general can be up to 5 cm. This means that even if an average error is made of 1 cm, a mistake would be made in calculating the total changed volumes of 7500 m^3. So, by only taking into account the areas that are perceived to have significant change over the period, the area that is concerned is reduced drastically and therefore also the error for calculating volumes.

The volume maps are as seen in Figure 1. With the erosion indicated in red, accretion indicated in blue and the contour lines at the start of each period indicated in black (above the storm set-up level: dotted, waterline: dashed, platform boundary: solid). The black dashed vertical line indicates the boundary between the beach and the spit area. During some periods nourishments were added resulting in large sedimentation spots on the maps. The volumes of these nourishments are hard to verify but an approximation was done based on the principle that the net sediment balance should be around zero. These periods were:

- September 2018 – January 2019 (northern side of the Zuidstrand) → 370.000 m^3
- May 2019 – August 2019 (around the head) → 200.000 m^3
- September 2020 – November 2020 (behind the breakwater at the beginning of the Zuidstrand) →130.000 m^3

So, the total volume of sediment, nourished during the considered timeframe is around 700.000 m^3.

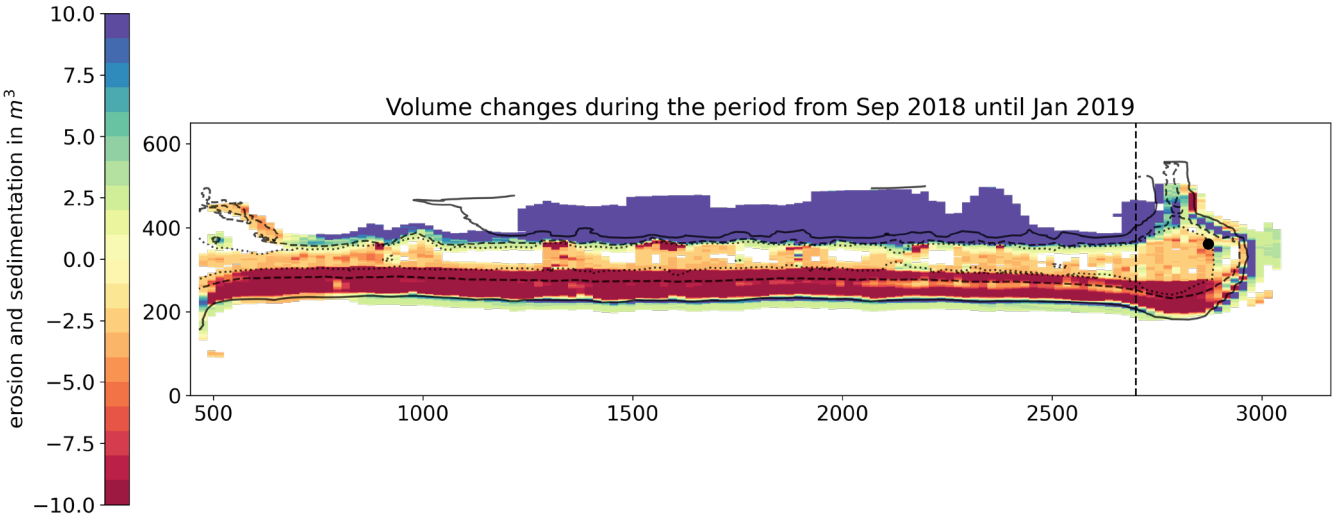

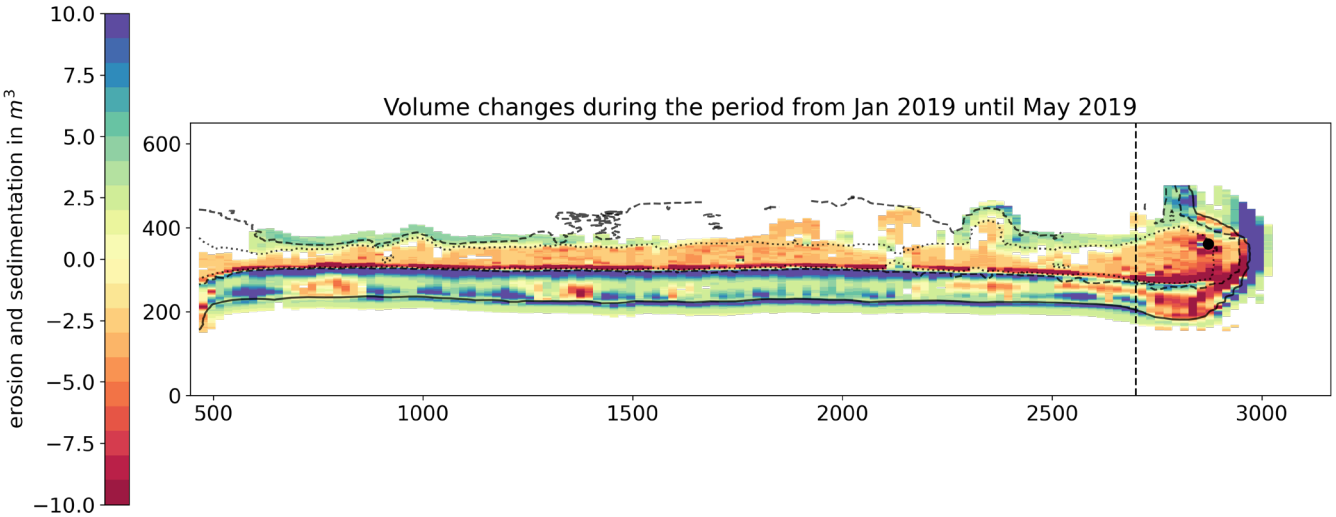
Volume changes during the period from Jan 2019 until May 2019
erosion and sedimentation in m^3
10.0
7.5
5.0
2.5
0.0
−2.5
−5.0
−7.5
−10.0
600
400
200
0
500
1000
1500
2000
2500
3000

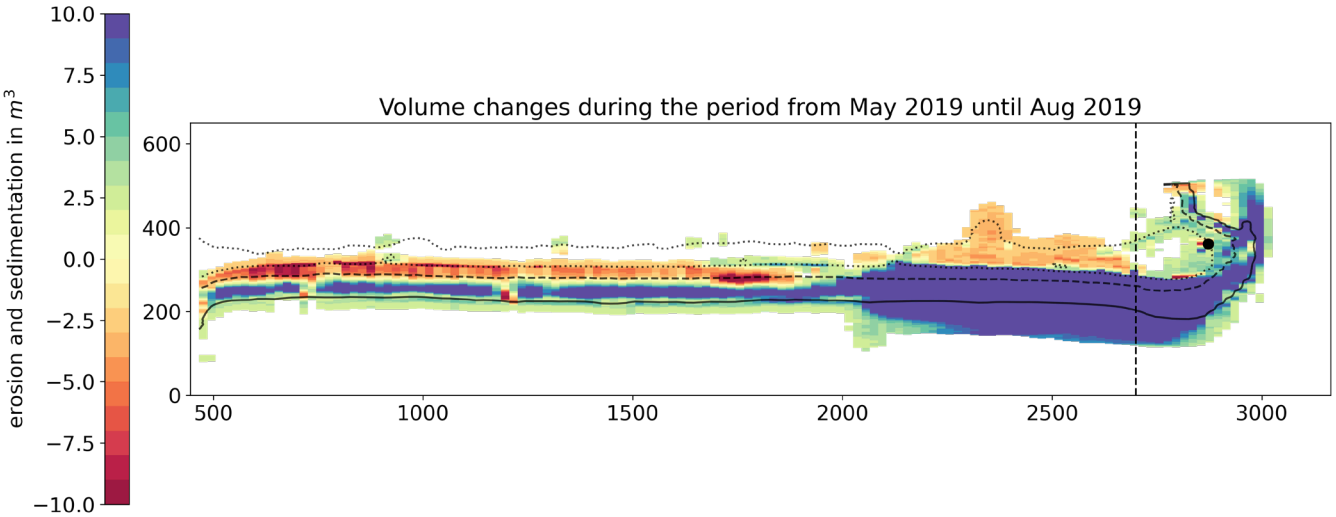
Volume changes during the period from May 2019 until Aug 2019
erosion and sedimentation in m^3
10.0
7.5
5.0
2.5
0.0
−2.5
−5.0
−7.5
−10.0
600
400
200
0
500
1000
1500
2000
2500
3000

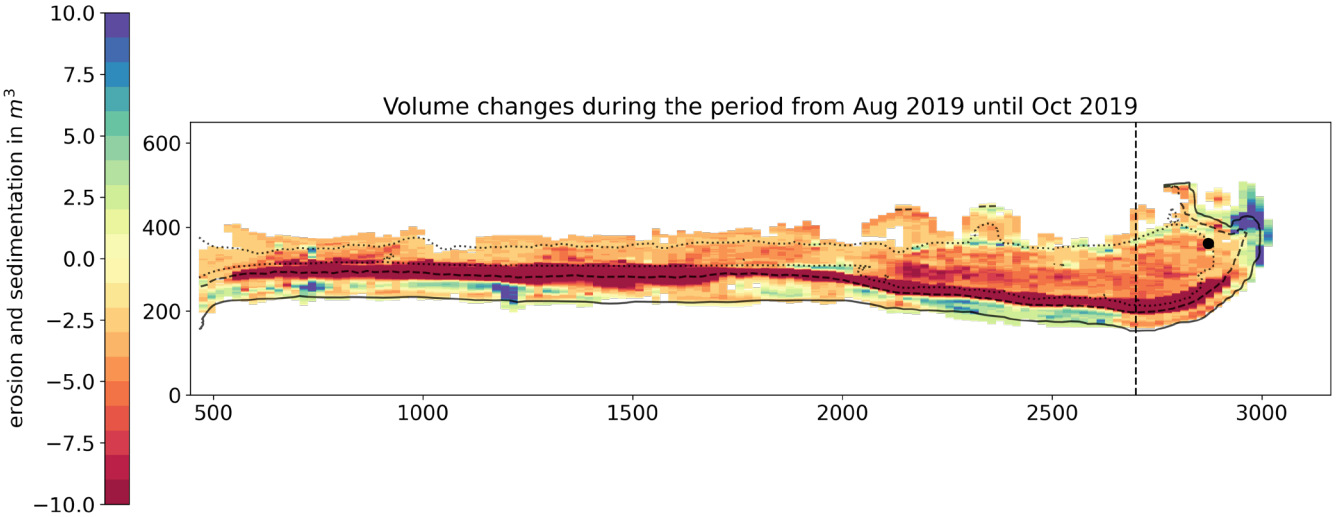
Volume changes during the period from Aug 2019 until Oct 2019
erosion and sedimentation in m^3
10.0
7.5
5.0
2.5
0.0
−2.5
−5.0
−7.5
−10.0
600
400
200
0
500
1000
1500
2000
2500
3000

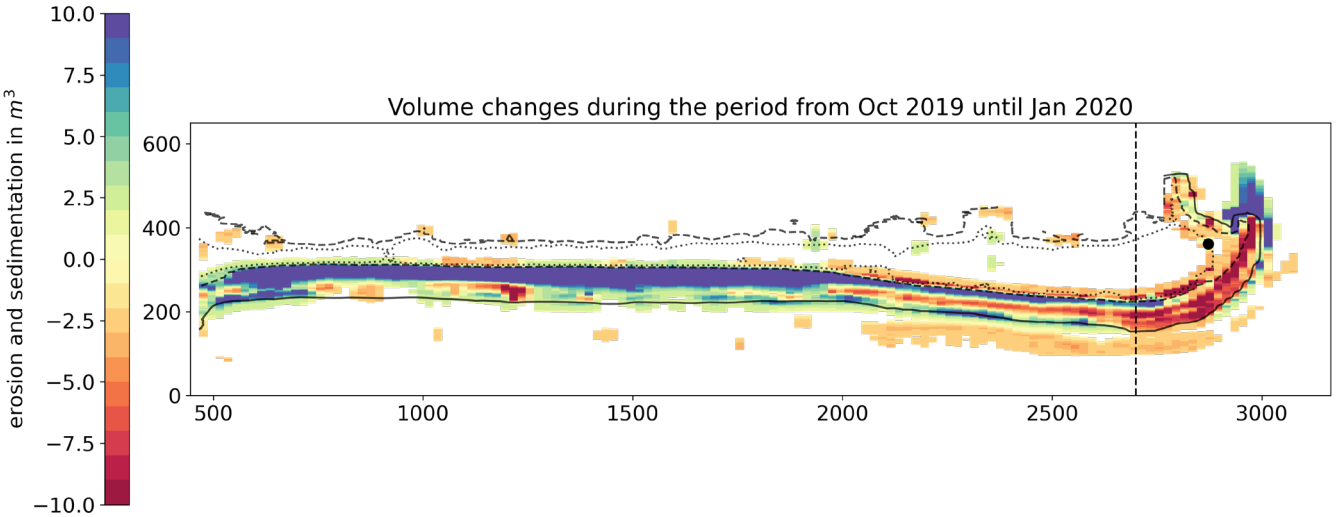
Volume changes during the period from Oct 2019 until Jan 2020
erosion and sedimentation in m^3
10.0
7.5
5.0
2.5
0.0
−2.5
−5.0
−7.5
−10.0
600
400
200
0
500
1000
1500
2000
2500
3000

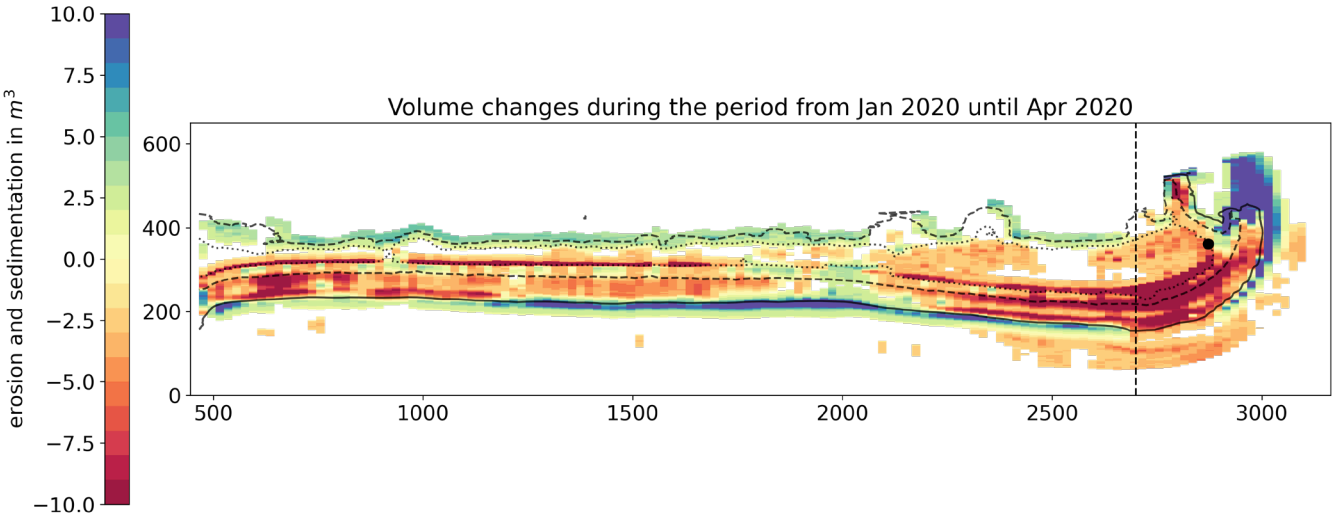
Volume changes during the period from Jan 2020 until Apr 2020
erosion and sedimentation in m^3
10.0
7.5
5.0
2.5
0.0
−2.5
−5.0
−7.5
−10.0
600
400
200
0
500
1000
1500
2000
2500
3000

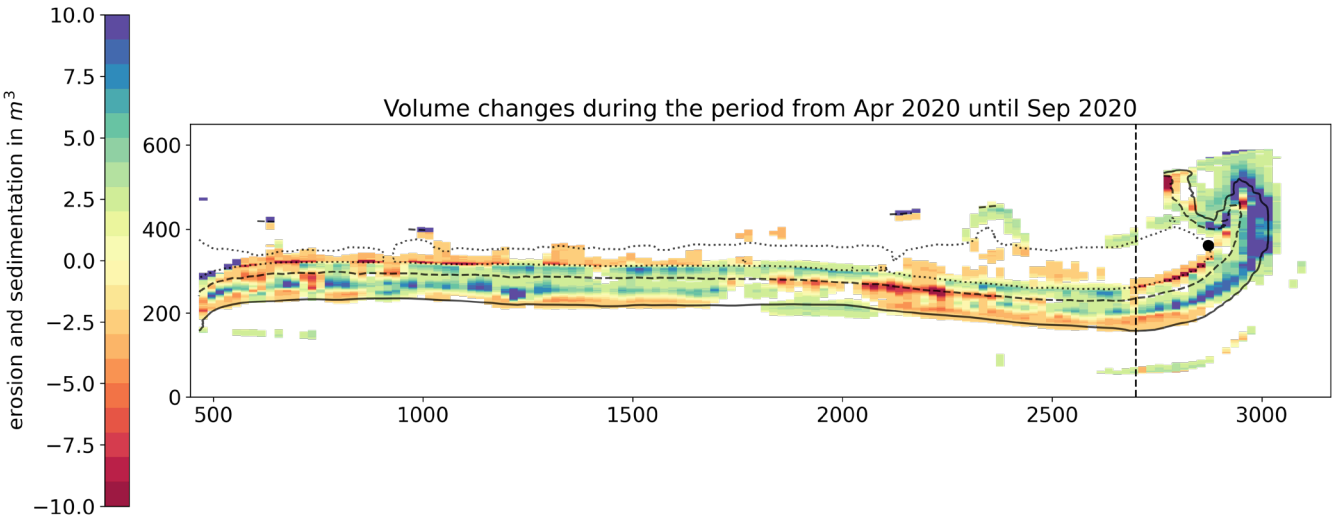
Volume changes during the period from Apr 2020 until Sep 2020
erosion and sedimentation in m^3
10.0
7.5
5.0
2.5
0.0
−2.5
−5.0
−7.5
−10.0
600
400
200
0
500
1000
1500
2000
2500
3000

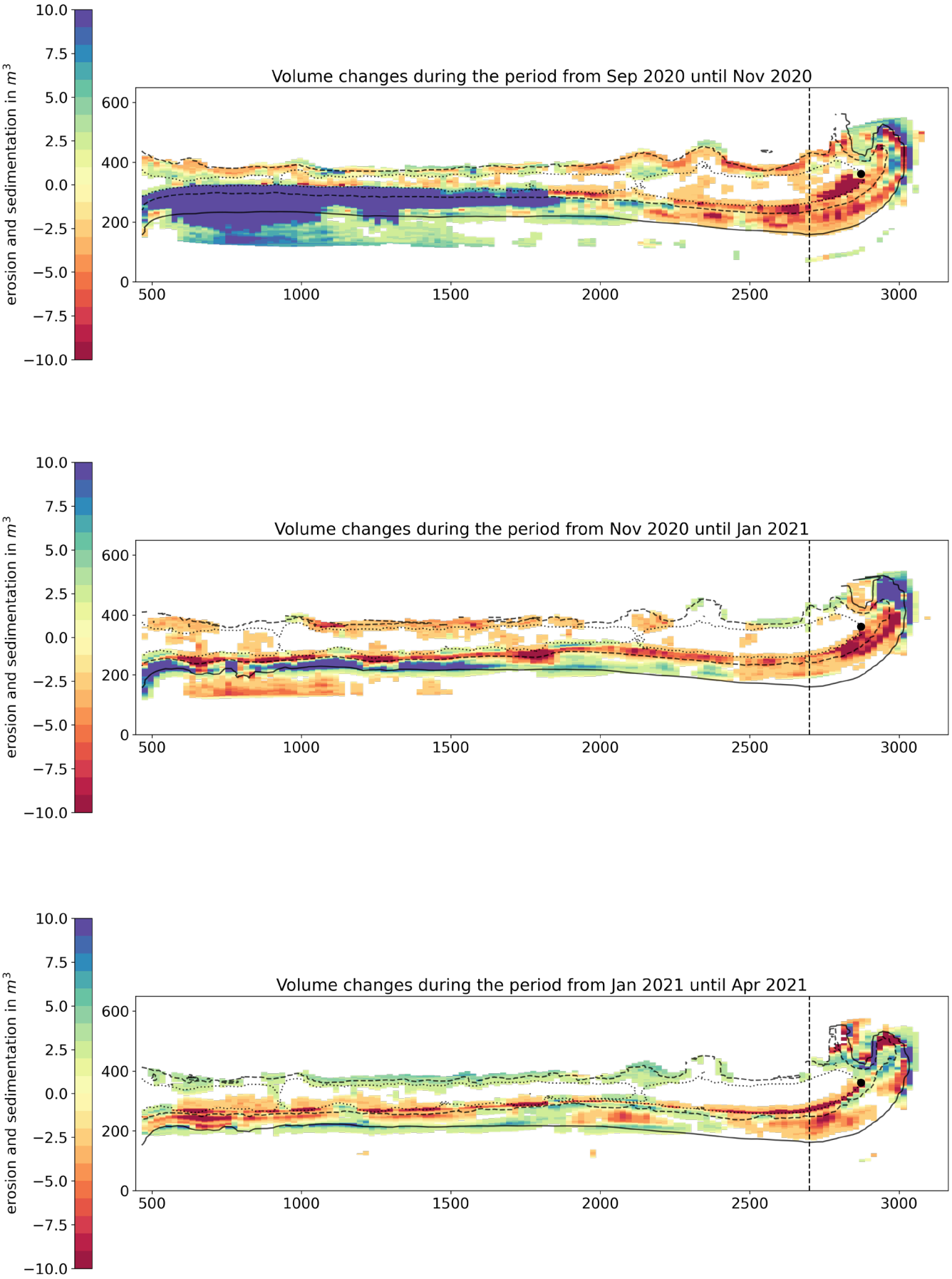

Figure 1. Volume maps of the entire Zuidstrand for every period

From these maps the sediment sources (clear erosion locations) can be identified as:

Zuidstrand:
- Small scarps at the storm set-up level (around 0,3 m NAP)
- Coastline
- Protrusions created by nourishments

Spit:
- Large scarp proximal end
- Coastline proximal end

Sediment sinks (clear sedimentation locations) can be identified as:

Zuidstrand:
- Around/below the platform boundary
- (Sometimes around the waterline)
- The spit (material eroded from the Zuidstrand is transported to the spit)

Spit:
- Platform level at the distal end
- Sub-platform level at the distal end
- The Zuidstrand (material eroded at the proximal end can be transported to the Zuidstrand)

Besides these clear sources and sinks it can also be seen that sometimes sedimentation occurs on some places on the platform and on other times erosion occurs on some locations on the platform. This can more clearly be seen around the spit where there is a sand bar like sedimentation on the platform near the proximal end (Apr 2020 – Sep 2020), but more often there seems to be erosion at this location on the platform level.

Quantification of erosion and sedimentation

With the volume maps also the volumes are known of the erosion and sedimentation on the Zuidstrand, and the erosion and sedimentation on the spit. With these volumes it can be investigated how much material that is eroded, is lost from the system and what the interaction is between the Zuidstrand and the spit (Table 1). In Table 1 there are periods where there is more erosion than sedimentation. This is physically possible because in this case material gets lost from the system and is for example sucked into the sand mining pits around the whole Zuidstrand. However, there are also periods, periods with nourishments not included, where there is generally more sedimentation than erosion. This is physically impossible as the material must originate from somewhere.

The best explanation is that there are sand bars on the platform that store sediment in between periods. But these sand bars cannot be observed and quantified in the volume maps because the interpolation of the platform, that gives the pointcloud of the platform, is relatively inaccurate compared to the other pointclouds sources (Appendix B). There are a couple of reasons why these sand bars are the most likely explanation for the appearance of sediment in a period:

- Sand bars are observed during fieldwork on the platform but these cannot be seen on the pointclouds.
- Periods where sediment ‘appears’ often come after periods where there was significantly more erosion than sedimentation. So, the material came free during an erosion period and accreted on the platform as a sand bar which could not be registered in the pointcloud. And in the subsequent period the sediment from the bar moved to the platform boundary for example where it can be registered, thus suddenly sediment ‘appears’.

- Storage of sediment on top of the platform is also already described by Ton et al. (2021).
- Most importantly, over the whole measured timespan (from September 2018 until April 2021) the net sediment balance is very balanced. If all the net total volumes are added for every period, the sediment surplus is 690.000 m^3 and the total nourished volume is around 700.000 m^3. This is well within the margin of what can be observed with the pointclouds and makes it likely that there is some form of sediment storage in the system.

So eventually it seems that almost no sediment gets lost to sand mining pits for example but practically all the material stays within the system. Also, from Table 1 it turns out that the spit is often in balance. In most periods the amount of sedimentation is in the same order of magnitude as the erosion at the spit. This means that indeed the proximal end of the spit, and its scarp, is the most important sediment supplier for spit growth. And there is little interaction of sediment between the beach and the spit.

In summary, the bulk of the material that is eroded from the Zuidstrand (beach) eventually ends up at the platform boundary and is used to extend the platform. This is in accordance with the findings of Ton et al. (2021). And the bulk of the sediment that is eroded at the proximal end of the spit ends up at the distal ends and allows for the spit to grow. Almost no material gets lost from the whole Zuidstrand system.

Period	Sed beach	Erosion beach	Net beach	Sed spit	Erosion spit	Net spit	Net total	Vol error/cm
Sep 2018-Jan 2019	418781	-74373	344408	17578	-11881	5696	350104	2787
Jan 2019-May 2019	44333	-21548	22784	14220	-13469	750	23534	3038
May 2019-Aug 2019	174221	-14831	159390	49274	-534	48740	208130	3468
Aug 2019-Oct 2019	6911	-73864	-66952	4870	-12593	-7722	-74675	849
Oct 2019-Jan 2020	50477	-12090	38386	9657	-10908	-1251	37134	2200
Jan 2020-Apr 2020	25230	-40138	-14907	25277	-22635	2642	-12265	2452
Apr 2020-Sep 2020	43450	-13707	29742	15279	-2604	12675	42418	2273
Sep 2020-Nov 2020	147080	-18826	128254	7939	-14543	-6604	121649	3655
Nov 2020-Jan 2021	22457	-29530	-7072	9972	-8115	1857	-5214	1476
Jan 2021-Apr 2021	19926	-18395	1530	7899	-10123	-2224	-693	2255

Table 1. Sediment balance for every period with the balance of the Zuidstrand on the left and the balance of the spit on the right. The total net sediment exchange over all periods is around 690.000 m^3 of surplus sedimentation.

Bibliography

Kraus, N. C., & Asce, M. (1999). *ANALYTICAL MODEL OF SPIT EVOLUTION AT INLETS*. ASCE.

Ton, A. M., Vuik, V., & Aarninkhof, S. G. J. (2021). Sandy beaches in low-energy, non-tidal environments: Linking morphological development to hydrodynamic forcing. *Geomorphology*, *374*. https://doi.org/10.1016/j.geomorph.2020.107522